COLLOQUIUM 620

EXTREME DISSIPATION AND INTERMITTENCY IN TURBULENCE
17 May – 19 May 2021, Delft, The Netherlands

Significant thin shear layers in high Reynolds number turbulence

Takashi Ishihara,
Gerrit E. Elsinga, &
Julian C. R. Hunt

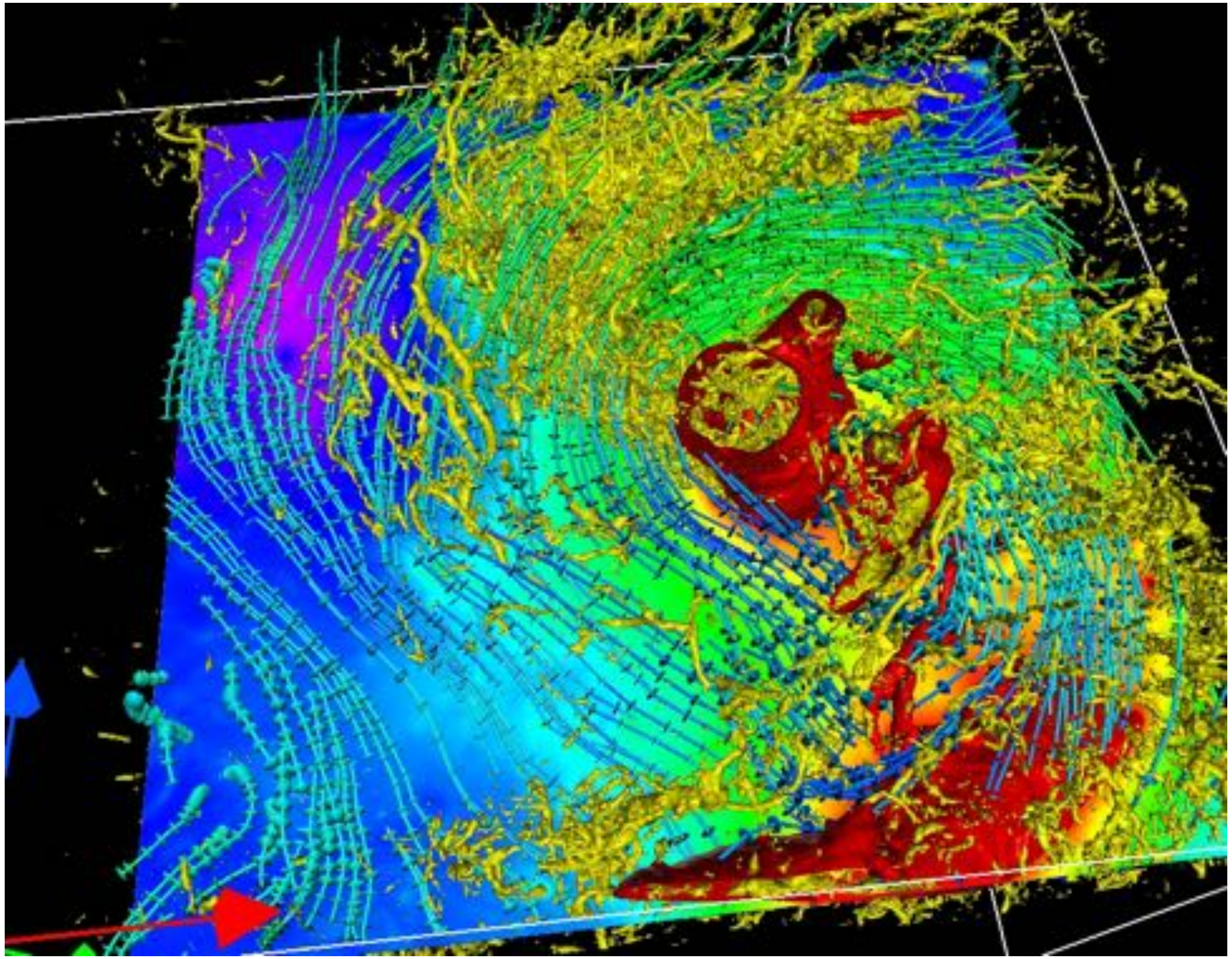

Extreme events in real geophysical flows

Typhoon No. 5 in 2017

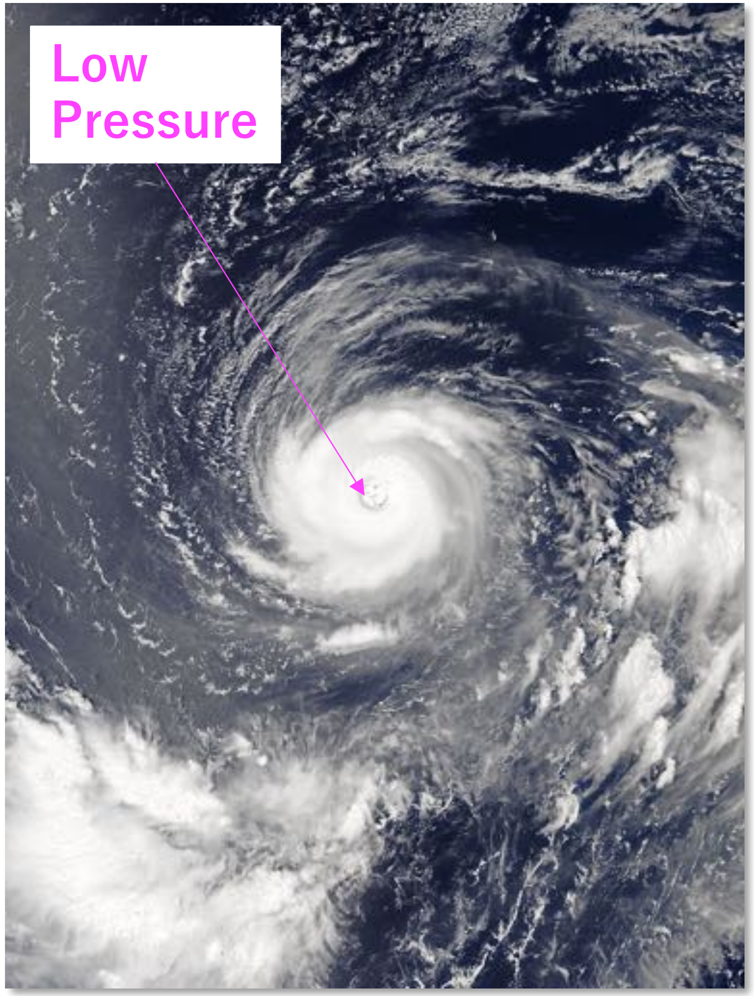

MODIS image captured by NASA’s Aqua satellite

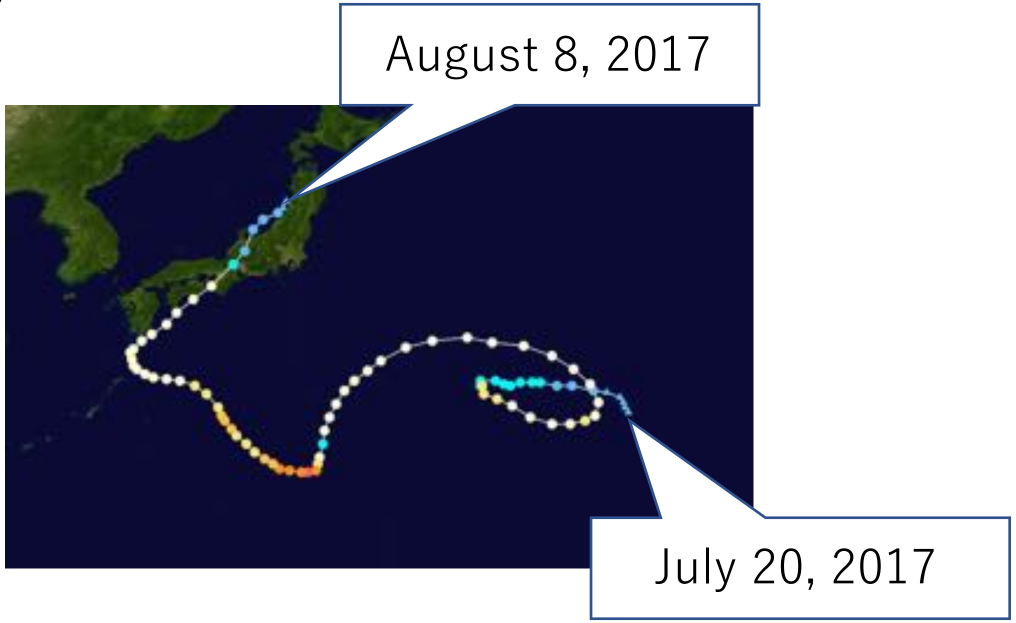

The longest lifetime: 456 hours

Typhoon track prediction

13 models failed to predict

各国の予想13パターン、意見割れる（7/31）

7月31日3時時点

This case was difficult to predict.

Precipitation

Typhoon No. 5 in 2017

spiral rainband

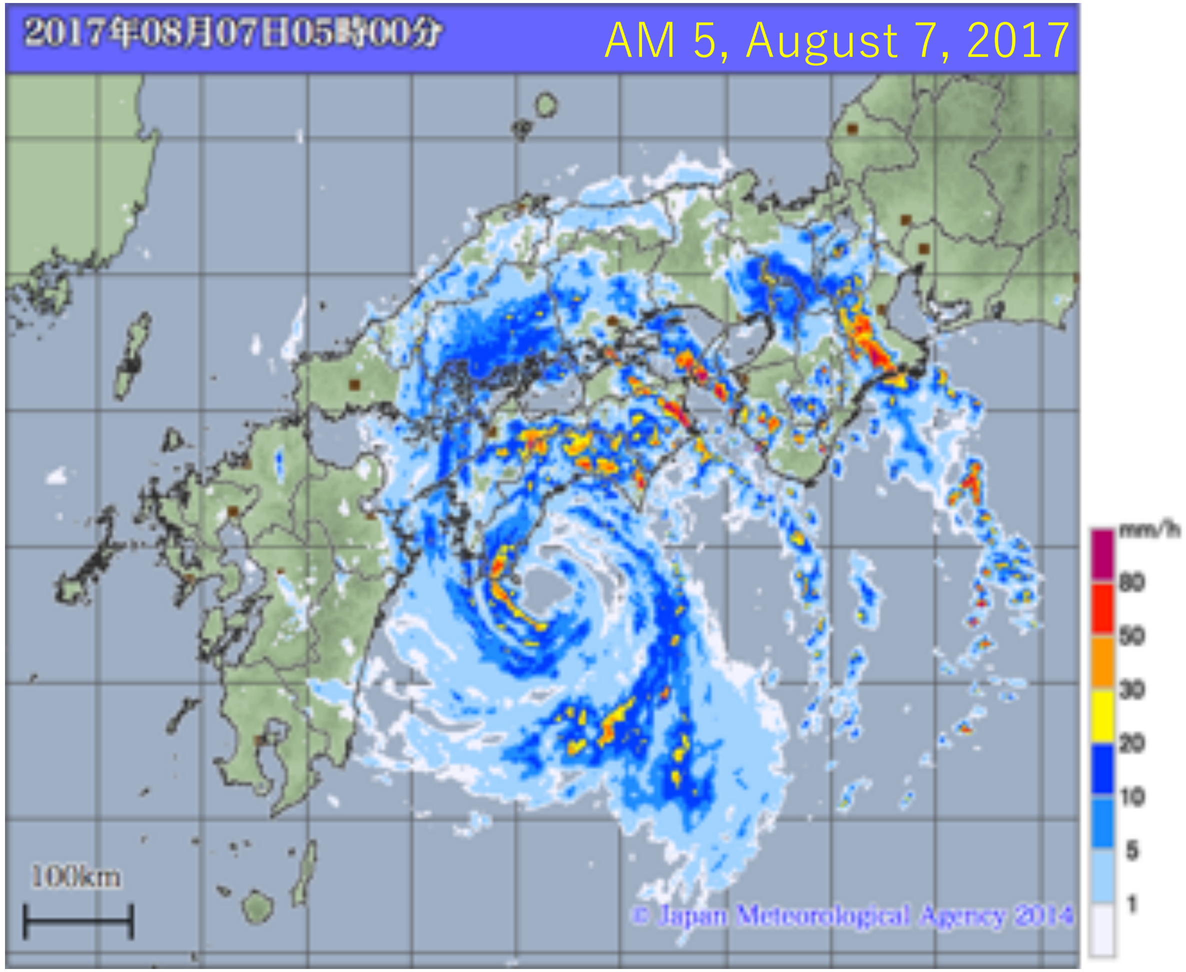

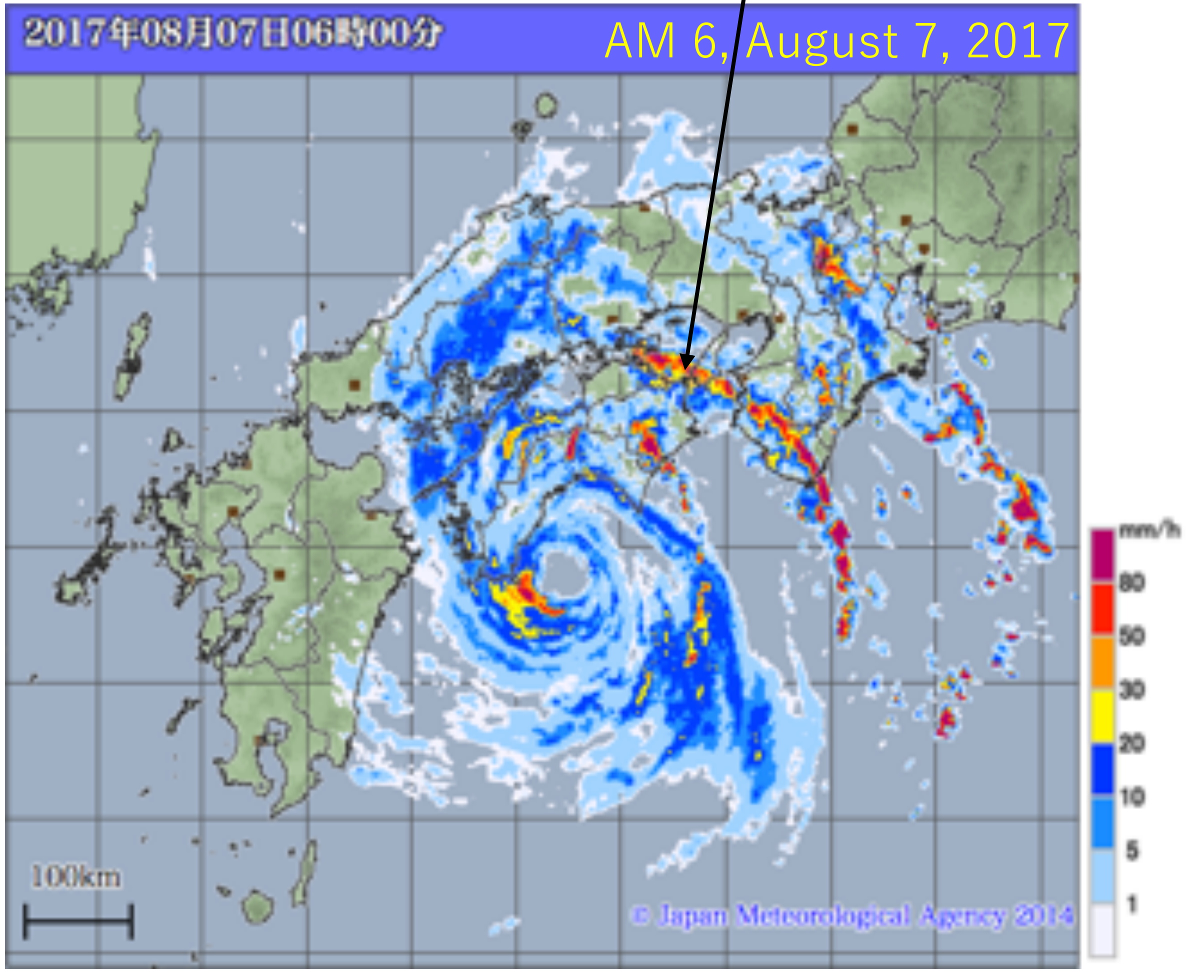

日テレNEWS24

豊橋市“竜巻”電柱９本倒れる　ケガ人も

ツイートする　シェアする

2017年8月7日 22:28

Tornado in Toyohashi city
Nine power poles toppled　Injured people
(caused by Typhoon No. 5)

Overturned trucks

【台風５号上陸】あすは関東地方を通過か…今後の進路は？

要約

７日午後、愛知県豊橋市で、竜巻とみられる突風が発生し、トラックが横転するなどの被害が出た。市内では子どもなど３人がけがをしている。

Extreme events in real flow phenomena

- Extreme events in real flow phenomena are often caused by vortex motions
- Most of the real flow phenomena are high Reynolds number turbulence

Vortex motions in high Reynolds number turbulence may be the key to understand real flow phenomena such as those in geophysical flows

Computational Science of turbulence

- Study of high–Reynolds number isotropic turbulence by direct numerical simulation, Ishihara, Gotoh, Kaneda, Ann. Rev. Fluid Mech. (2009)

DNS of turbulence with 4096^3 grid points on ES

Kaneda et al (2003)

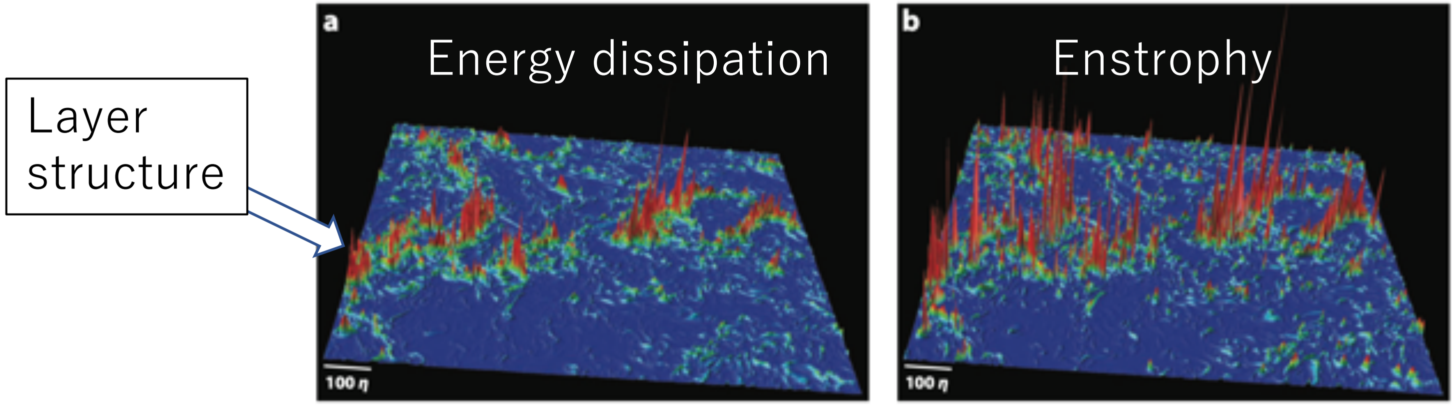

Figure 4

Snapshot of the intensity distributions of (*a*) the energy-dissipation rate $\tilde{\varepsilon} = \varepsilon/(2\nu)$ and (*b*) the enstrophy $\Omega = \omega^2/2$ on a cross section in DNS-ES at $R_\lambda = 675$ in arbitrary units.

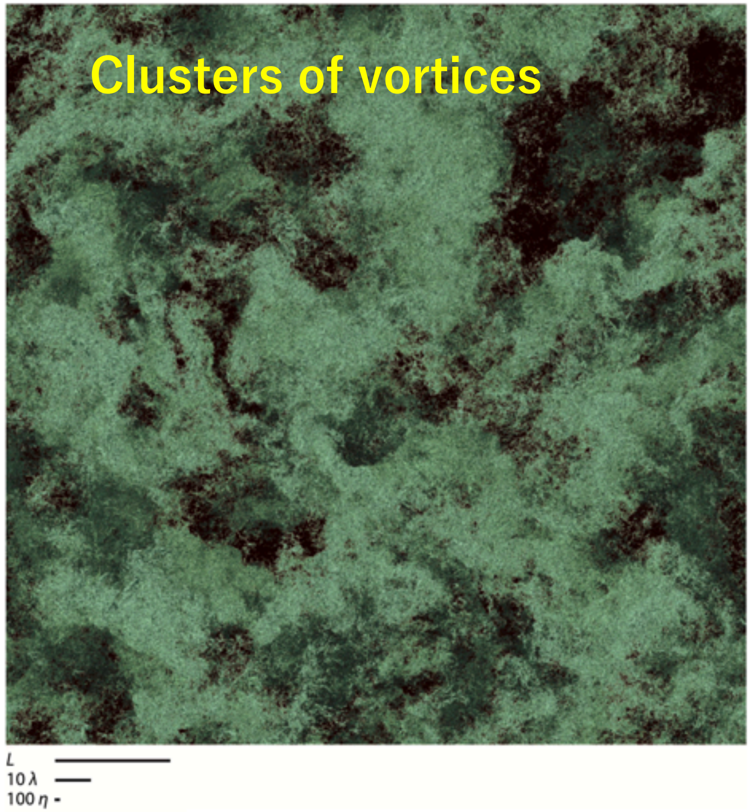

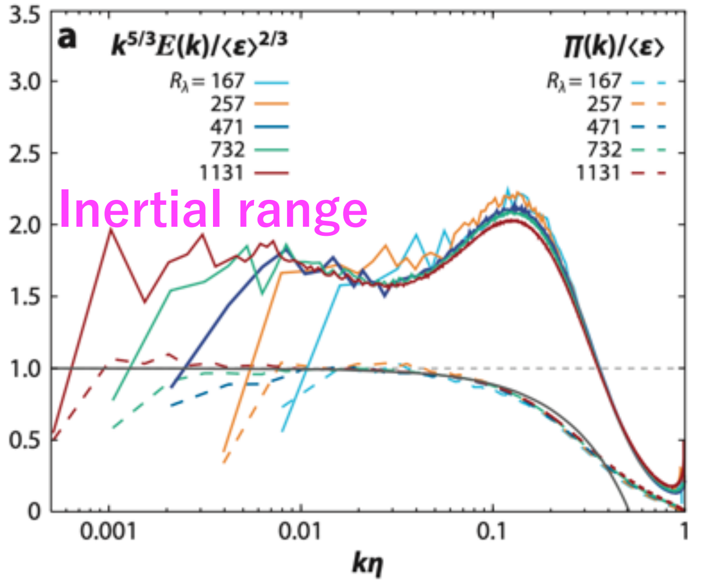

Thin shear layers in turbulence

- Thin shear layers in high Reynolds number turbulence—DNS results, Ishihara, Kaneda, Hunt, Flow, Turbulence and Combustion, (2013)
- Thin shear layer structures in high Reynolds number turbulence, Hunt, I, Worth, Kaneda, Flow, Turbulence and Combustion, (2014)

Sharp interface of high vorticity regions

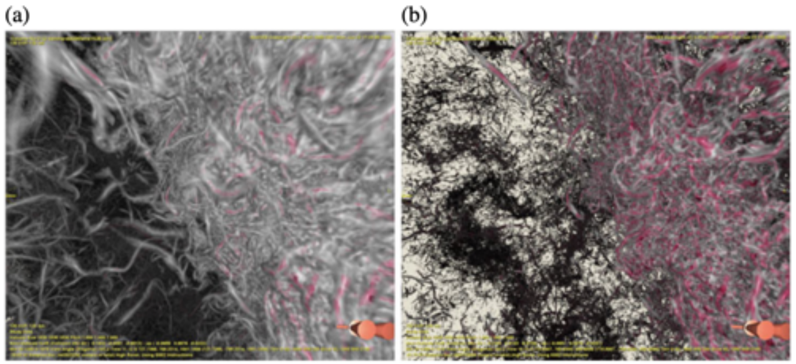

Fig. 3 Iso-surfaces of vorticity amplitude, showing vortices near the interface of the significant thin shear layer. Threshold values are set to $|\omega| = \alpha\langle\omega^2\rangle^{1/2}$. **a** $\alpha = 6$ (*pink*), $\alpha = 2$ (*grey*); **b** $\alpha = 6$ (*pink*), $\alpha = 4$ (*grey*). In this graphics the brightness of the iso-surface is decreased due to the distance from view point, so that the far objects look dark. Also, the white color is used as the background color, so that the white parts in (**b**) indicate that the visualized data (of finite size) do not have the iso-surfaces in that directions

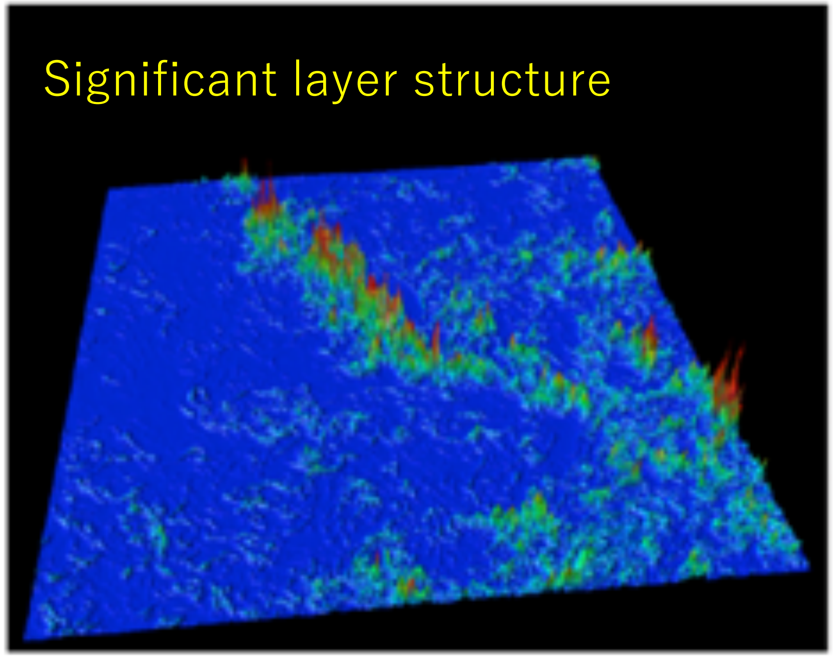

Not observed in low Re

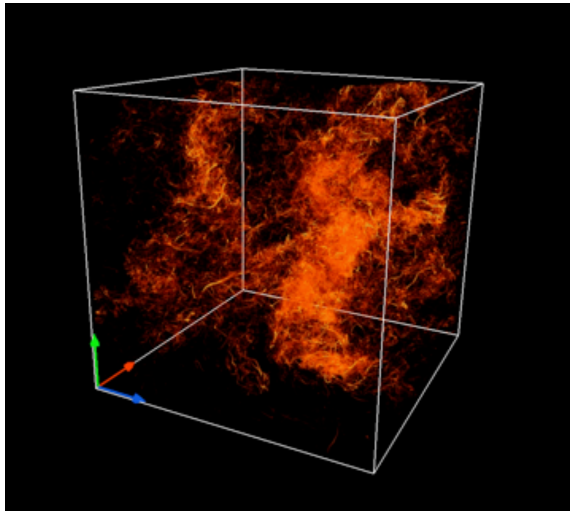

The scaling of straining motions in turbulence

- The scaling of straining motions in homogeneous isotropic turbulence, Elsinga, Ishihara, Goudar, Da Silva, Hunt, J. Fluid Mech. (2017)

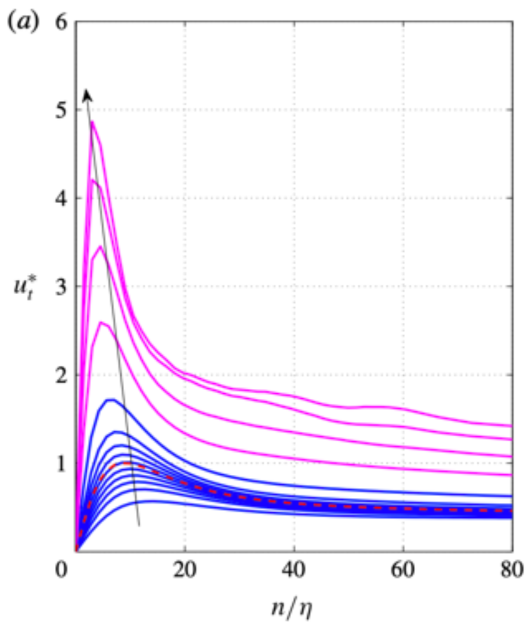

Re transitions in flow structure

Extreme dissipation is connected with strong shear at small scales and with large tangential velocity at large scales

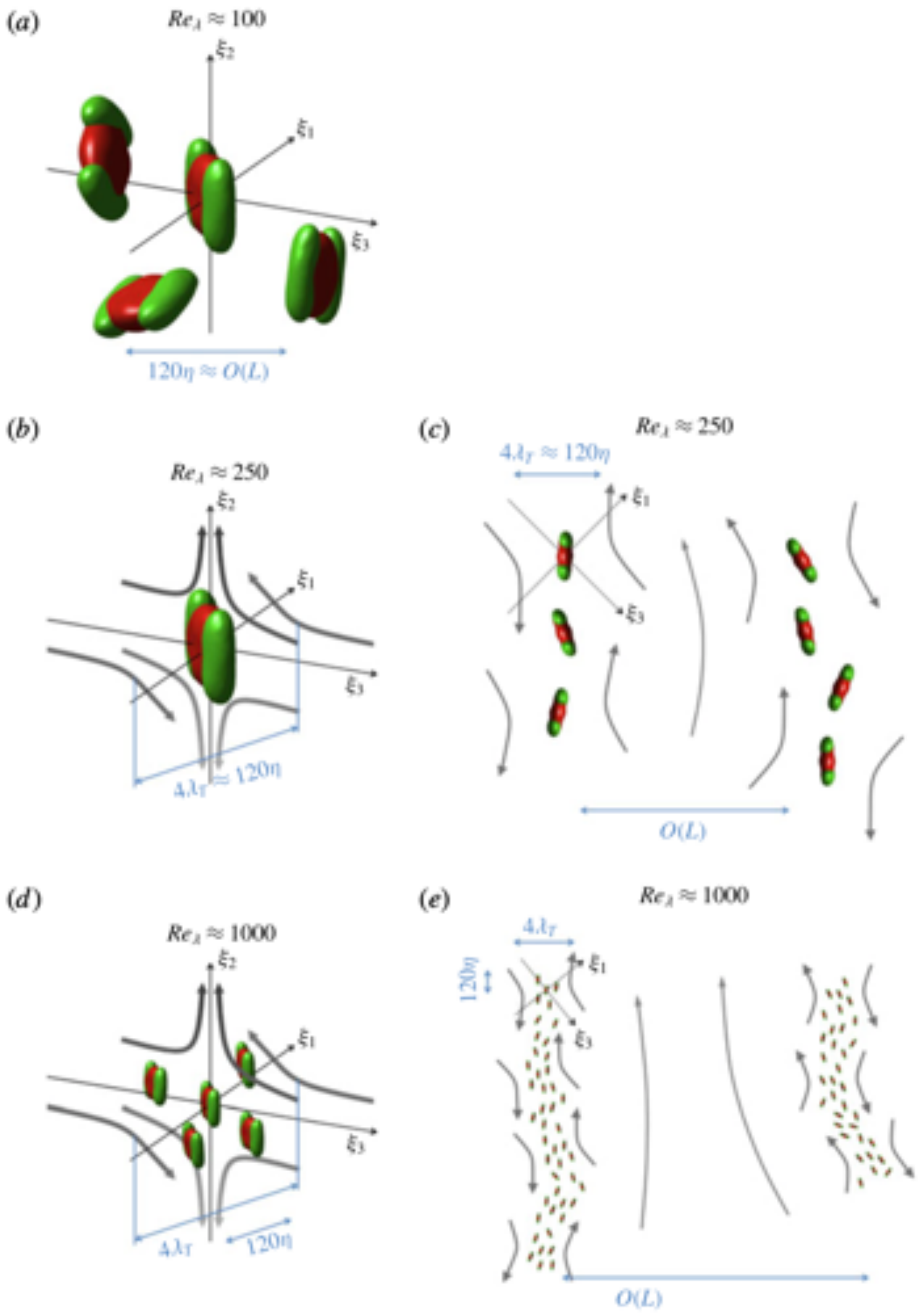

Extreme dissipation in high Re turbulence

- Extreme dissipation and intermittency in turbulence at very high Reynolds numbers, Elsinga, Ishihara, Hunt, Proceedings of the Royal Society A, (2020)

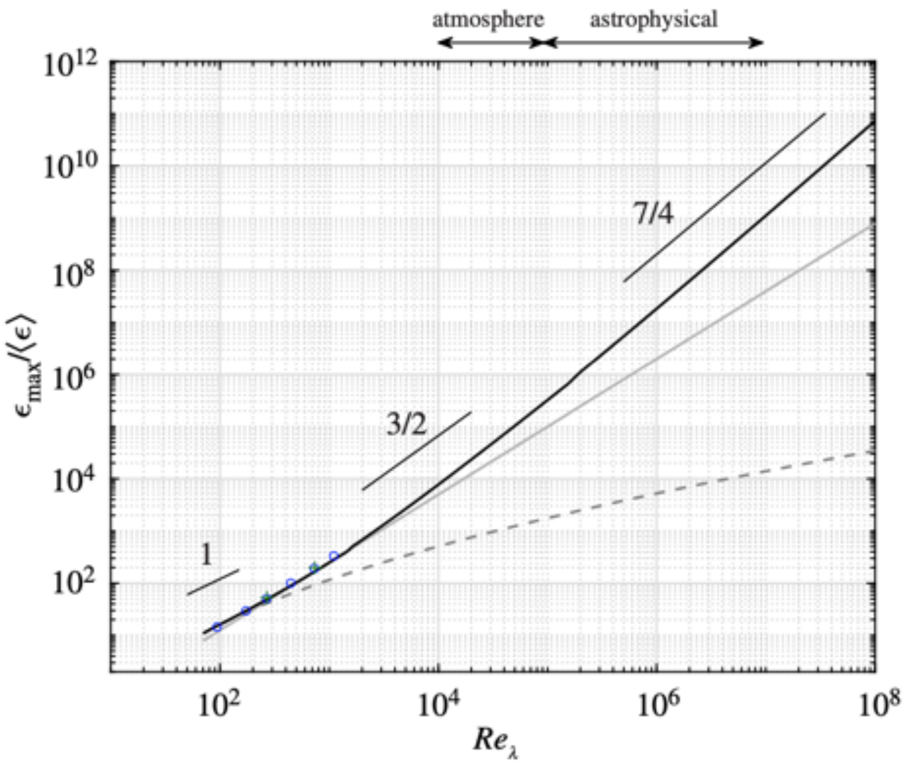

A model based on the DNS of turbulence which explains and predicts extreme dissipation in high Re turbulence

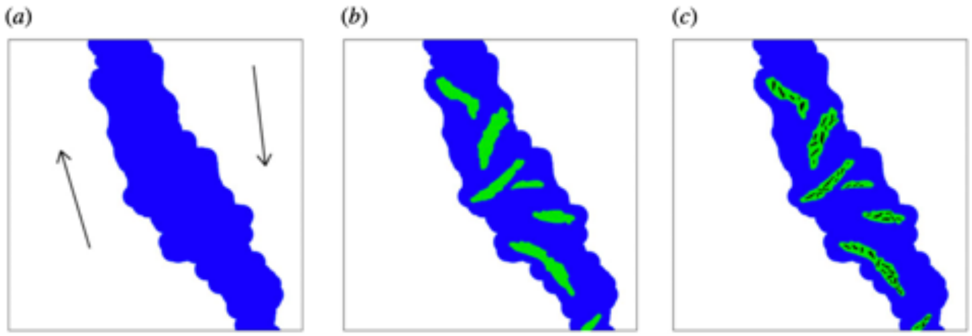

Figure 2. (*a*) Significant shear layer structure (blue) within a part of the flow domain ($Re_\lambda > 150$). (*b*) Significant shear layer structure with sublayers in green ($Re_\lambda > 1560$). (*c*) Significant shear layer structure with sub-sublayers in black ($Re_\lambda > 1.8 \times 10^5$). For illustration purposes only, layers are not to scale. (Online version in colour.)

In this talk

- DNSs of high Re turbulence
  - Energy spectrum and vortical structures
- Significant vortical structure in high Re turbulence – DNS results
  - Properties
  - Flow structure around the layer
  - Distribution
  - Time evolution and lifetime
- Significant layer in real geophysical flow
- Summary
- (Vortical structures in higher Re turbulence)

Direct Numerical Simulations (DNSs) of turbulence

- Solve incompressible NS equations
  - No model, no numerical viscosity
- Resolve not only large scales but also small scales (↔ LES)
- Simple geometry and simple forcing (negative viscosity)
- High accuracy, high resolution and high precision
  - e.g., Spectral method
    - To avoid extra uncertainties
- High performance (and many steps)
  - Reynolds number as high as possible

Computer resource is finite,
↓
We have to sacrifice some of these.

To explore Universality of Turbulence
To understand the nature of high Re turbulence

Reynolds Number & Development of Supercomputer

$$Re = Lu'/\nu$$

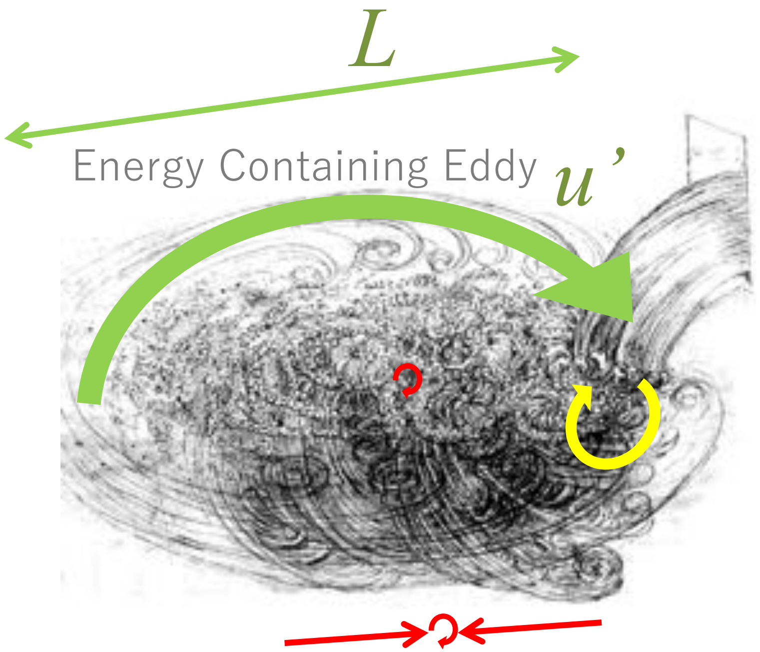

$\eta = (\nu^3/\varepsilon)^{1/4}$: Smallest eddy

Kolmogorov length scale

$(\varepsilon \sim u'^3/L)$

Kolmogorov (1941)

Scale ratio $L/\eta \propto \mathrm{Re}^{3/4}$

Degree of Freedom $(L/\eta)^3 \propto \mathrm{Re}^{9/4}$

Computational Cost $\propto \mathrm{Re}^3$

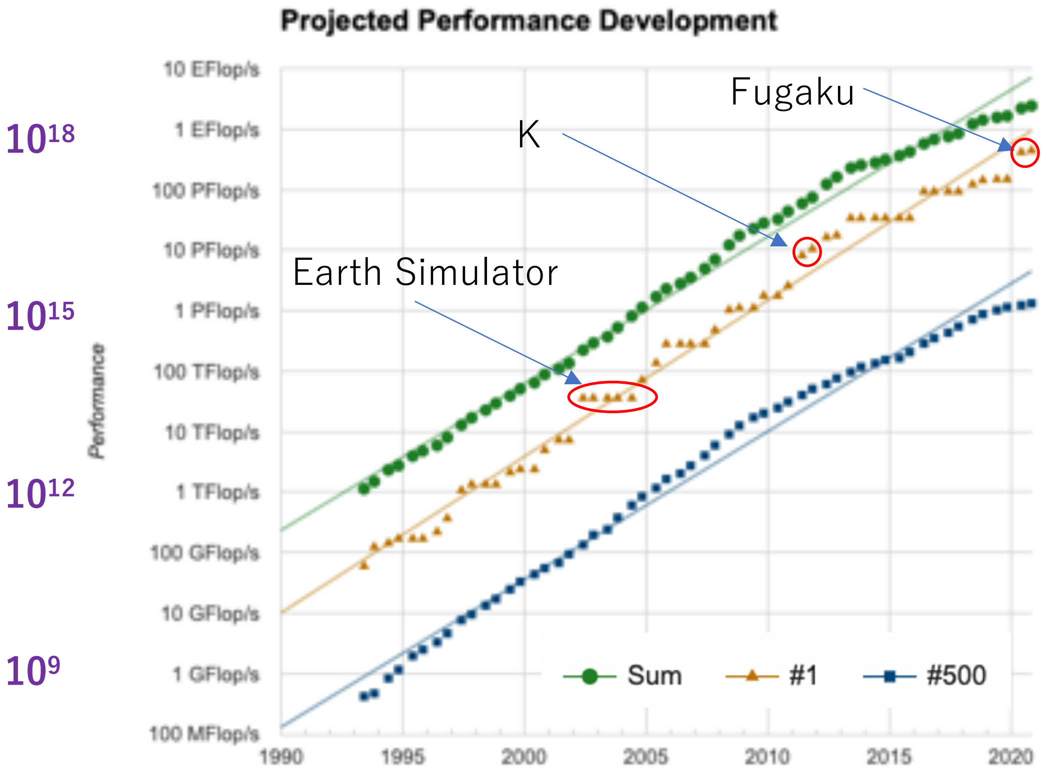

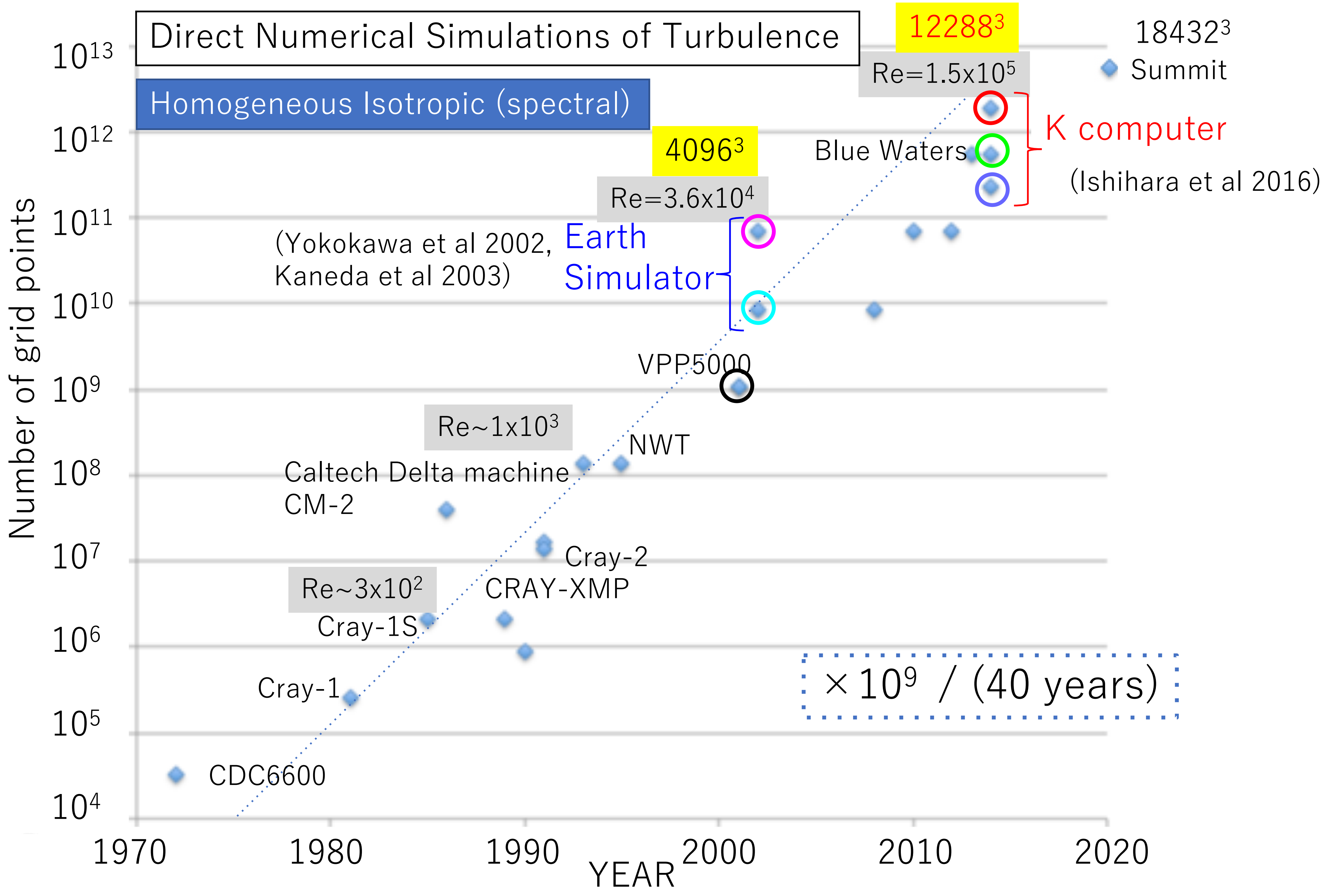

Direct Numerical Simulations of Turbulence
Homogeneous Isotropic (spectral)
12288^3
$Re=1.5x10^5$
18432^3
Summit
K computer
(Ishihara et al 2016)
Blue Waters
4096^3
$Re=3.6x10^4$
(Yokokawa et al 2002,
Kaneda et al 2003)
Earth
Simulator
VPP5000
$Re\sim1x10^3$
NWT
Caltech Delta machine
CM-2
Cray-2
CRAY-XMP
$Re\sim3x10^2$
Cray-1S
Cray-1
CDC6600
$\times 10^9$ / (40 years)
Number of grid points
10^{13}
10^{12}
10^{11}
10^{10}
10^9
10^8
10^7
10^6
10^5
10^4
1970
1980
1990
2000
2010
2020
YEAR

Energy Spectrum and Vortex Structures

- Low Re

  $Re<10^3$

  Inertial Range?
  Vortex Tubes!

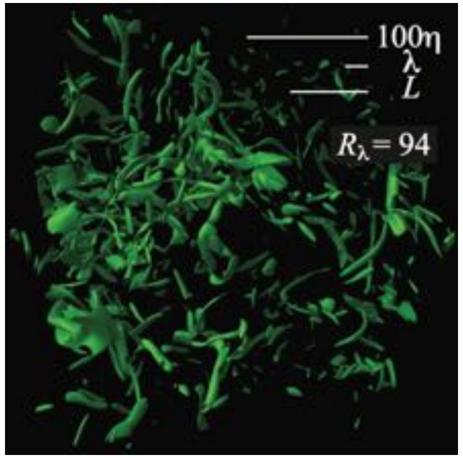

- High Re

  $Re>10^4$

  Wide IR !
  Vortex Clusters!

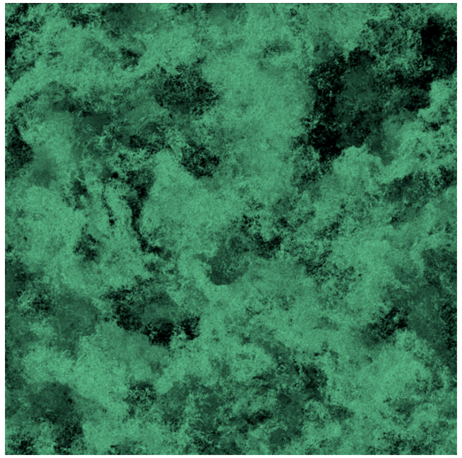

$\epsilon^{-\frac{2}{3}} k^{\frac{5}{3}} E(k)$ Jimenez et al (1993) 512^3

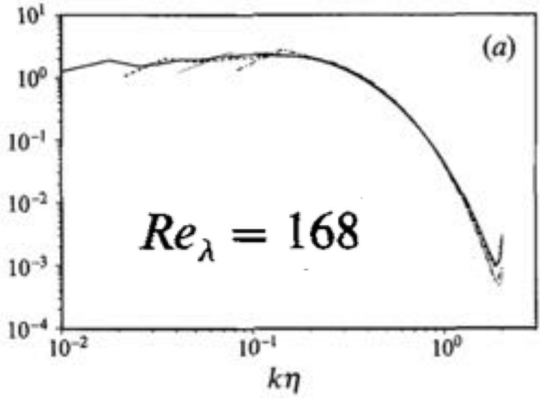

$E(k) \propto k^{-5/3-m}$ (m~0.1)

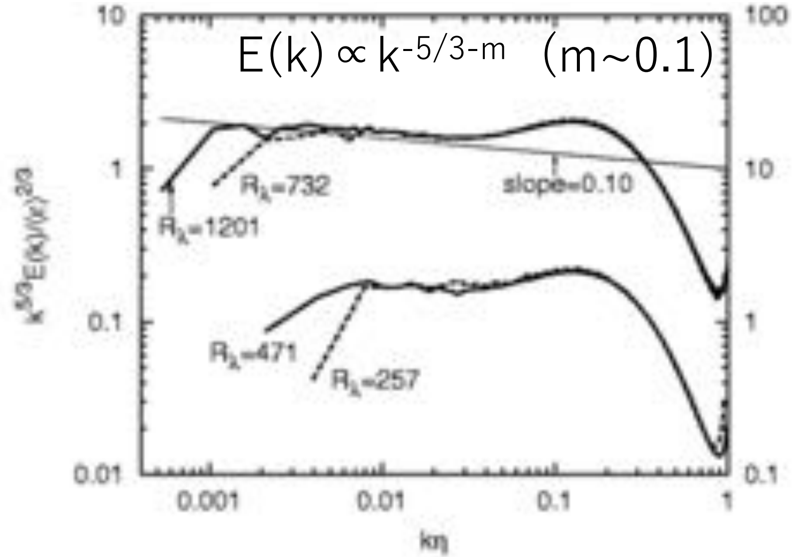

Kaneda et al (2003)

4096^3

Energy Spectrum & Vortex Structures

Re>10^5

DNSs on K **Wider IR**

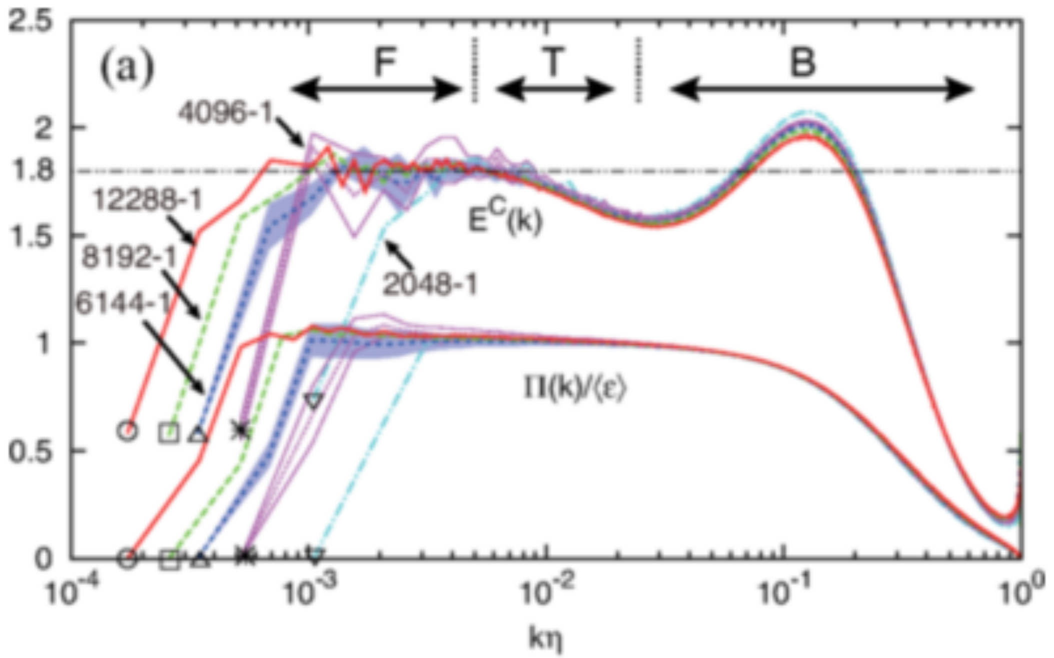

Ishihara et al PRF (2016, 2020)

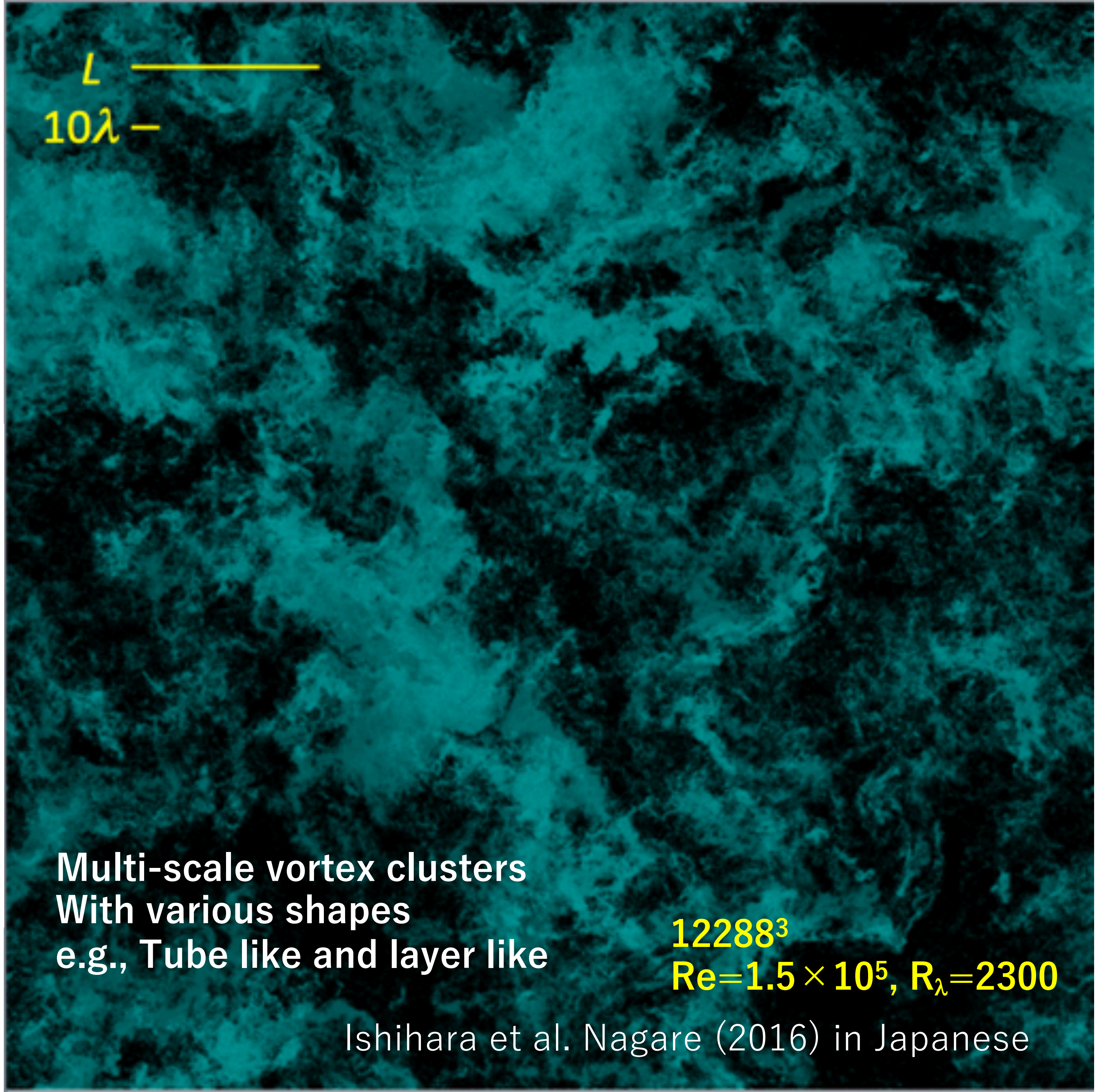

Ishihara et al. Nagare (2016) in Japanese

Significant vortical structures in turbulence

Transition in the forms of the significant, high vorticity, intermittent structures:

from tube-like isolated vortices at $R_\lambda<100$

to complex thin-shear layers at $R_\lambda >1000$

Significant, high vorticity, intermittent structure

Ishihara, Kaneda, Hunt FTAC (2013), Hunt, Ishihara, Worth, Kaneda FTAC (2014)

$R_\lambda = 1131$

$\lambda/\eta = 66$
$L/\lambda = 32$

$Re = (10^4)$

ARF2009

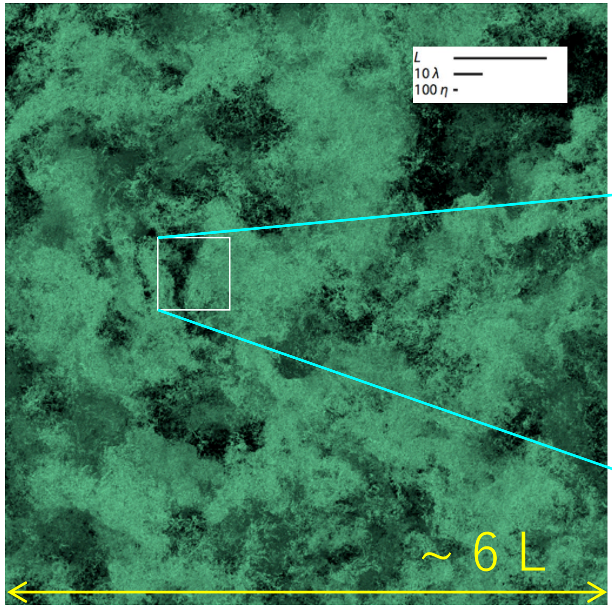

… Complex thin-shear layers

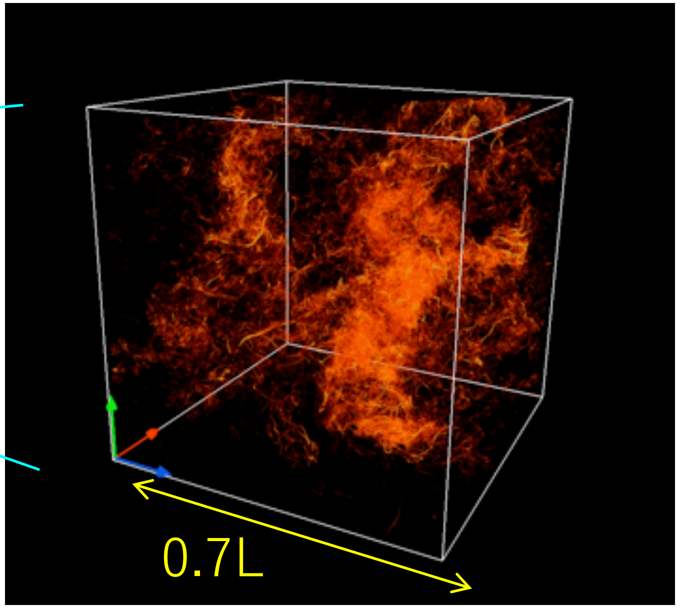

Transition is consistent with quantitative results by Elsinga et al 2017

Width ~ O(L), Thickness ~ O(λ) >> η

… Isolated vortices

$R_\lambda = 94$

$\lambda/\eta = 20$
$L/\lambda = 3$

$Re = (10^2)$

JFM2007

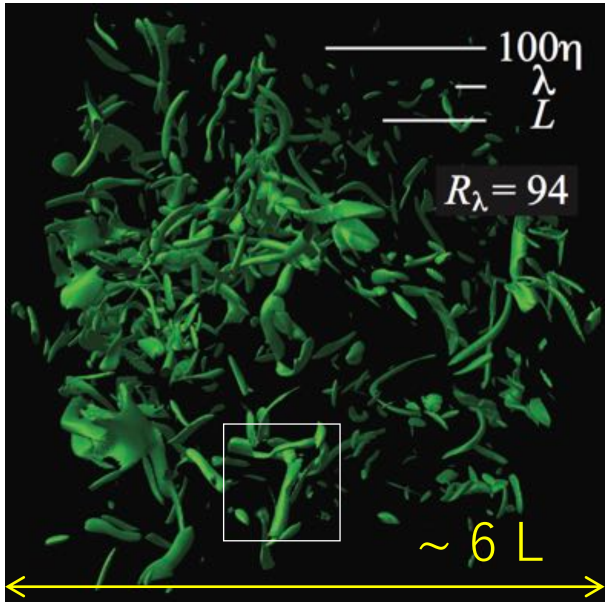

Length ~ O(L)
Thickness ~ O(10η)
~ O(λ)

$\lambda \sim L\, Re^{-1/2}$

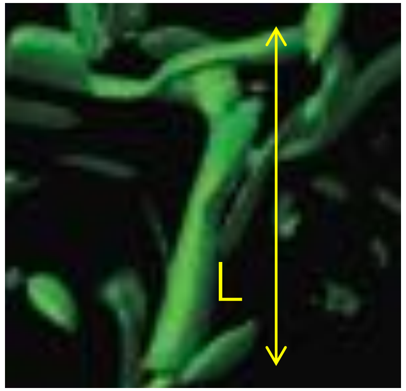

A slice of a strong layer-like cluster

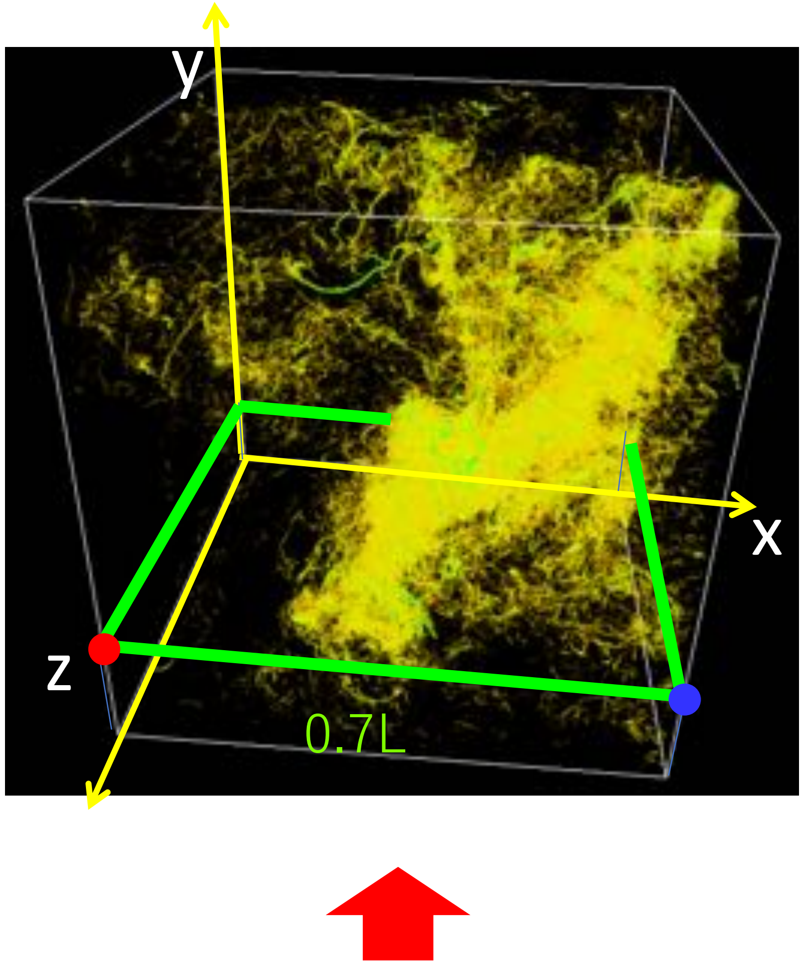

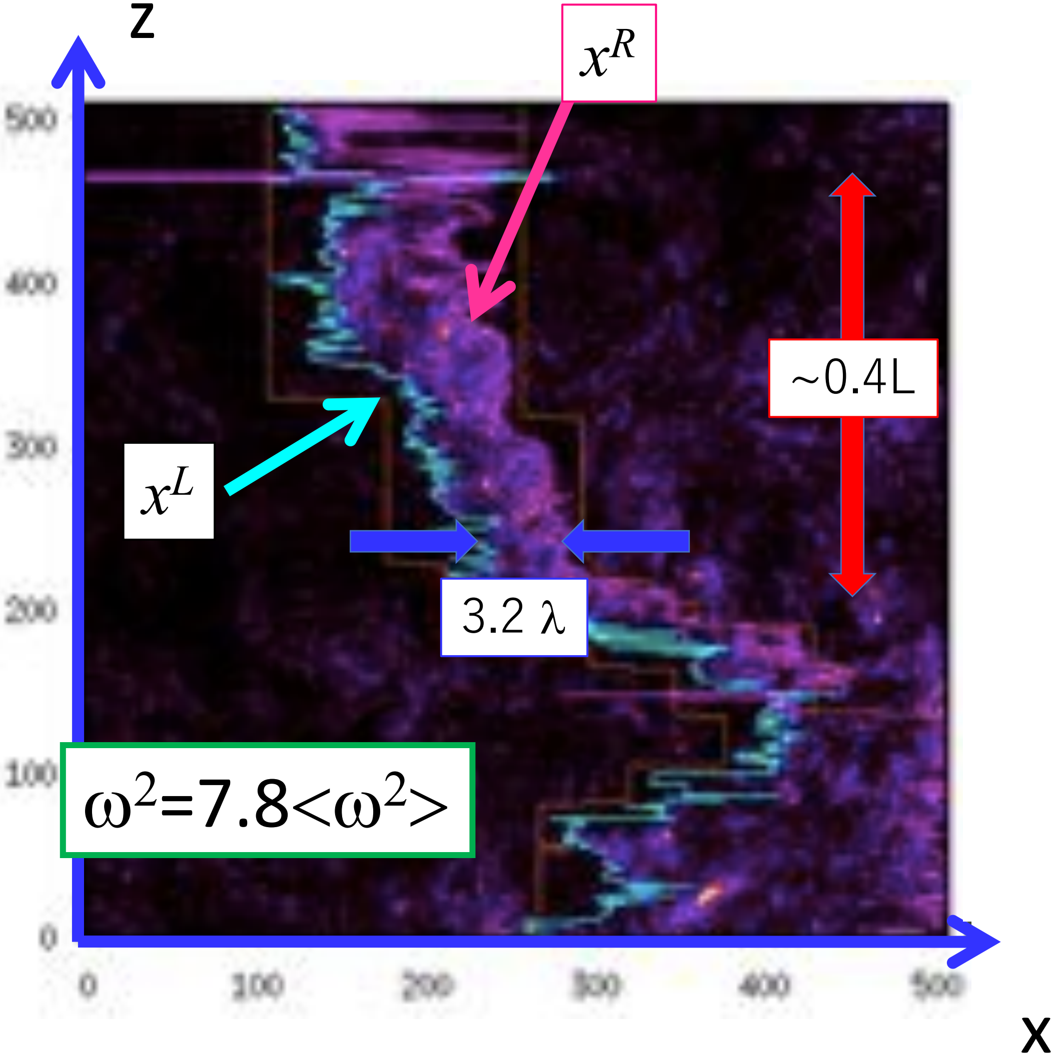

Thin Shear Layers in Homogeneous Isotropic Turbulence

(FTAC 2013, 2014)

Thickness ~ 4 λ

High enstrophy, high dissipation

Averages over z in a certain range conditioned on the distance from the Right interface

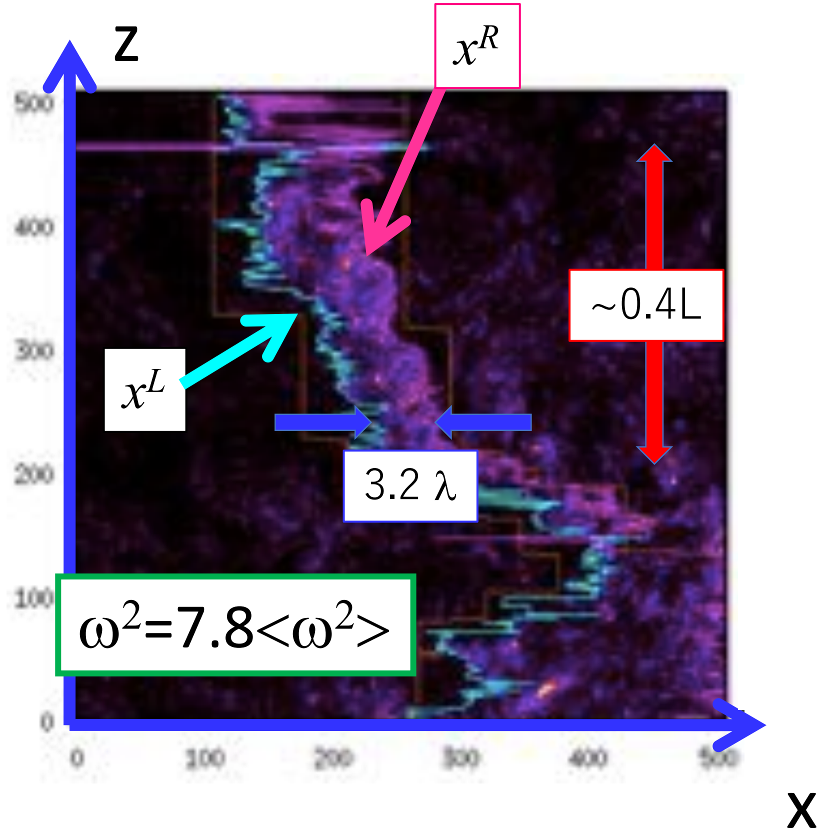

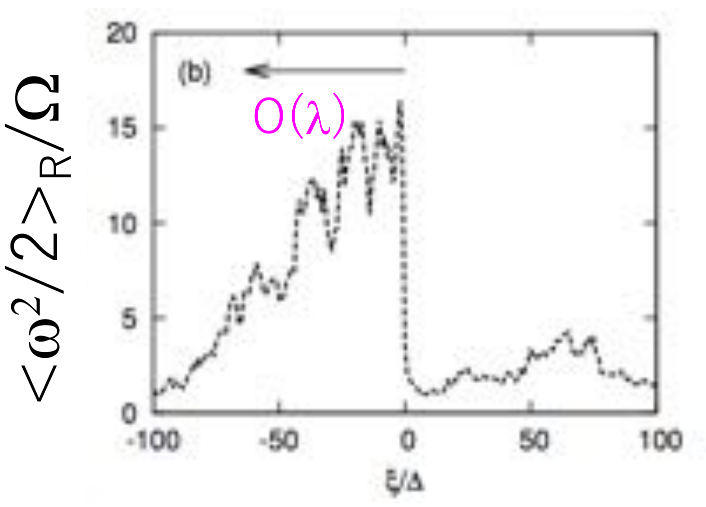

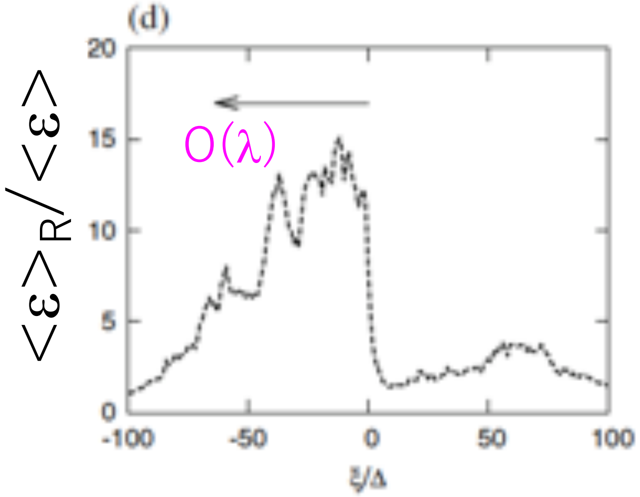

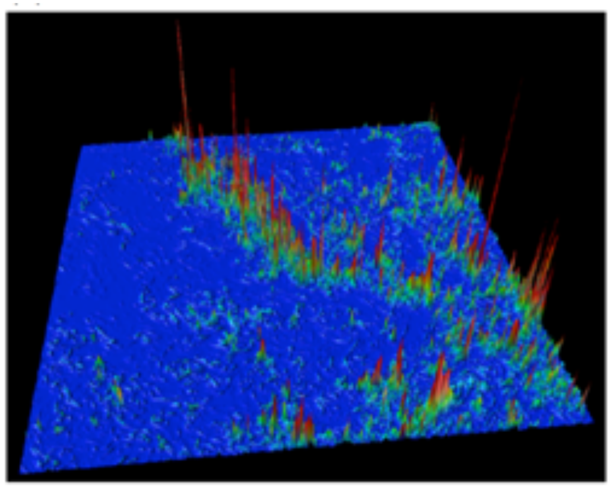

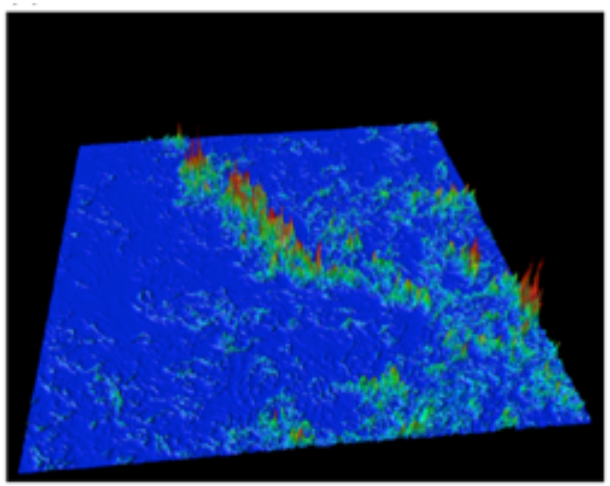

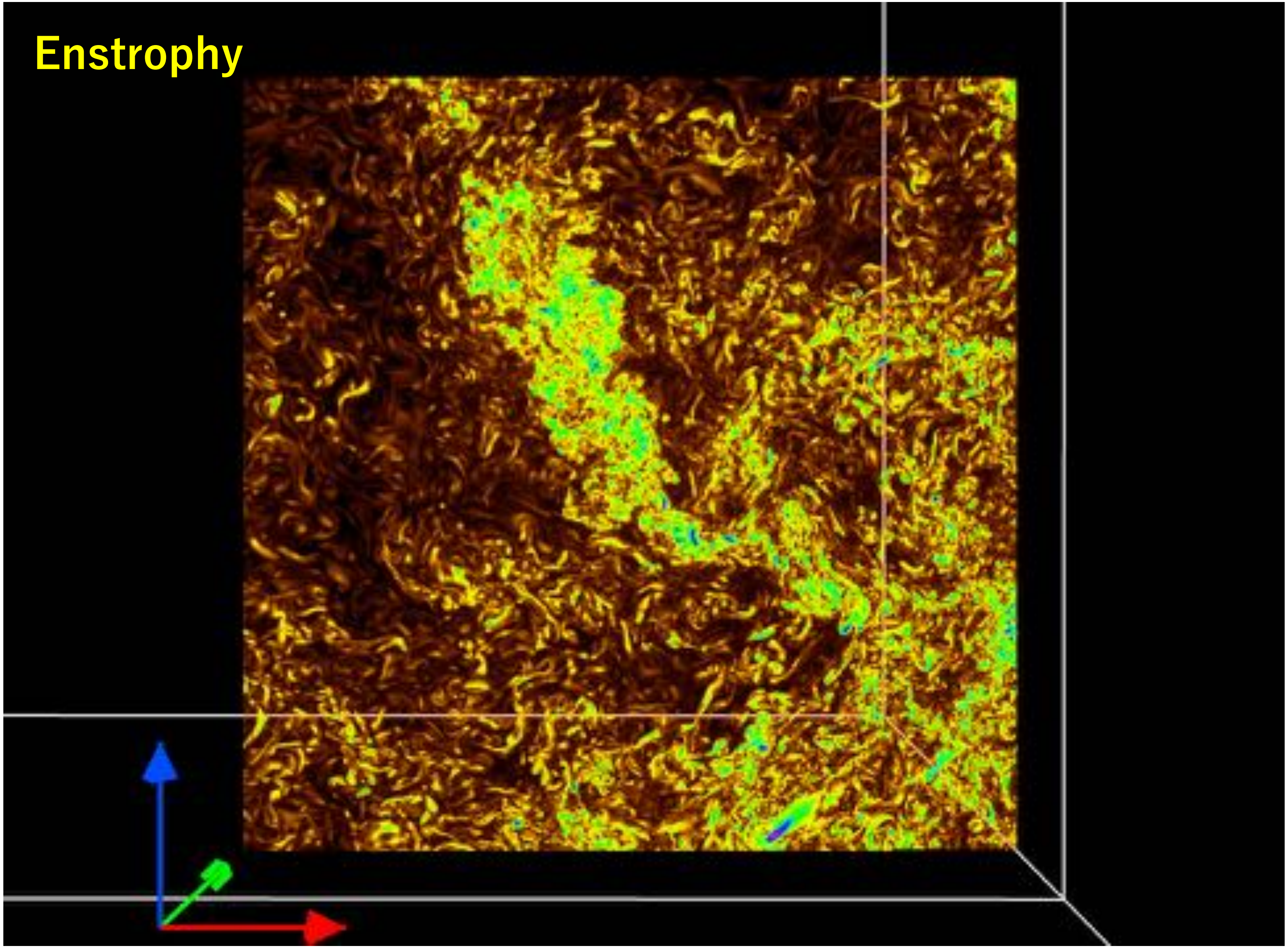
Enstrophy

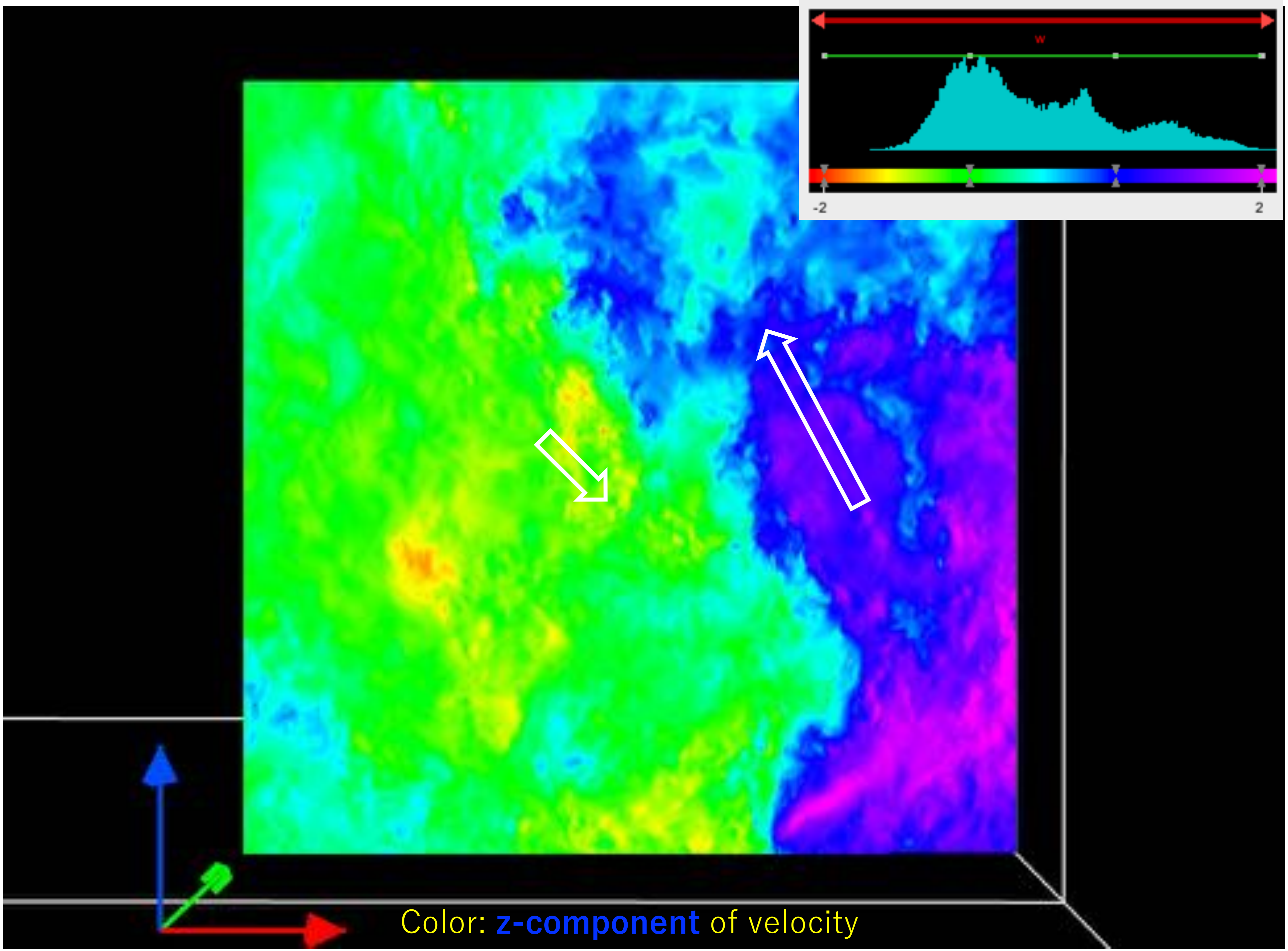

Color: z-component of velocity

Positive y direction

Negative y direction

$$\langle \boldsymbol{\omega} \rangle_{Inside} / \omega' = (-0.15, -0.54, -0.54),$$
$$\langle \boldsymbol{\omega} \rangle_{Left} / \omega' = (-0.07, -0.01, 0.06),$$
$$\langle \boldsymbol{\omega} \rangle_{Right} / \omega' = (-0.08, -0.16, -0.09),$$

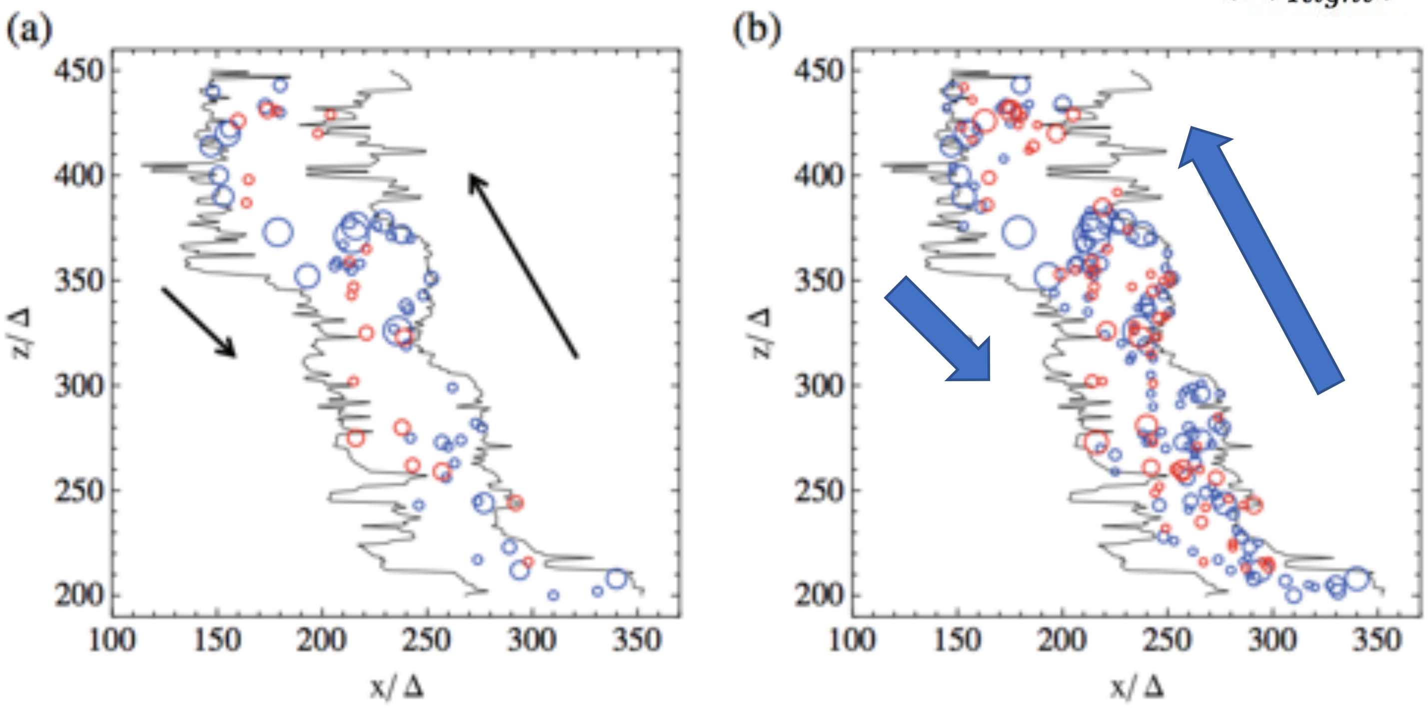

Fig. 17 Distribution of the high $|\omega_y|$ peaks (isolated regions) that satisfy $|\omega_y| > \gamma\omega_{\text{Inside}}$; **a** $\gamma = 2.0$, **b** $\gamma = 1.5$. *Red circles* are for $\omega_y > 0$ and *blue* ones are for $\omega_y > 0$. Circle size is determined as the area is proportional to the circulation intensity of each peak. The *right* and *left side arrows* represent the directions of $\langle \mathbf{u} \rangle_{\text{Right}} - \langle \mathbf{u} \rangle_{\text{Inside}}$ and $\langle \mathbf{u} \rangle_{\text{Left}} - \langle \mathbf{u} \rangle_{\text{Inside}}$ projected onto the xz-plane, respectively

Thin Shear Layers in High Re Homogeneous Isotropic Turbulence

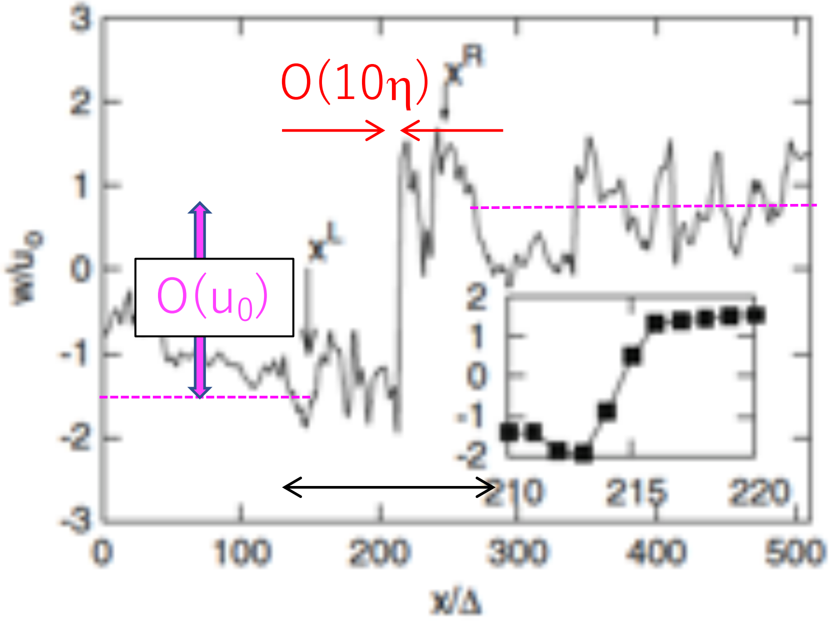

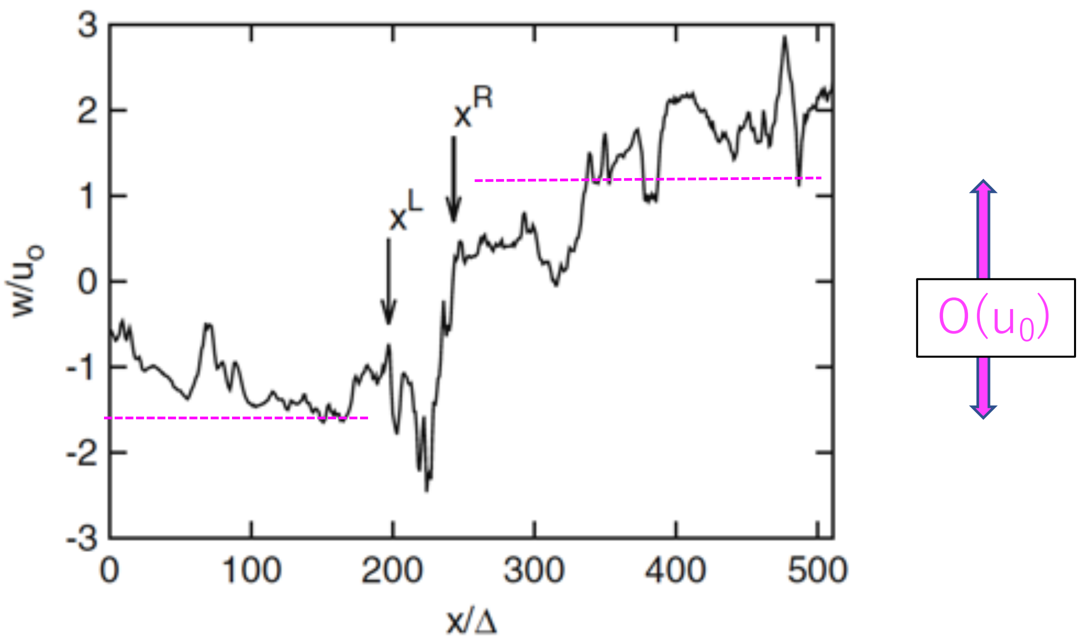

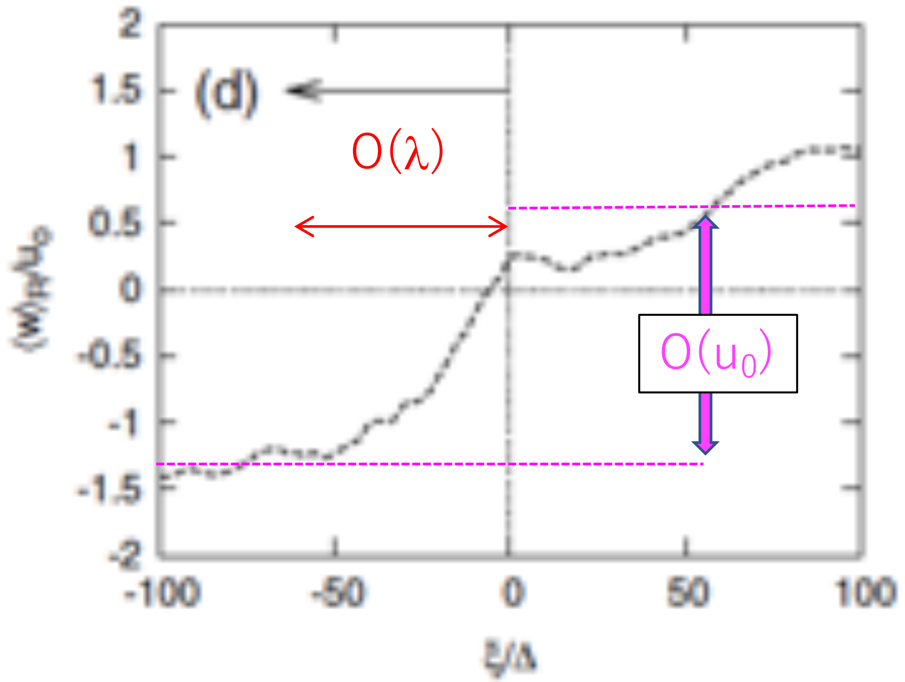

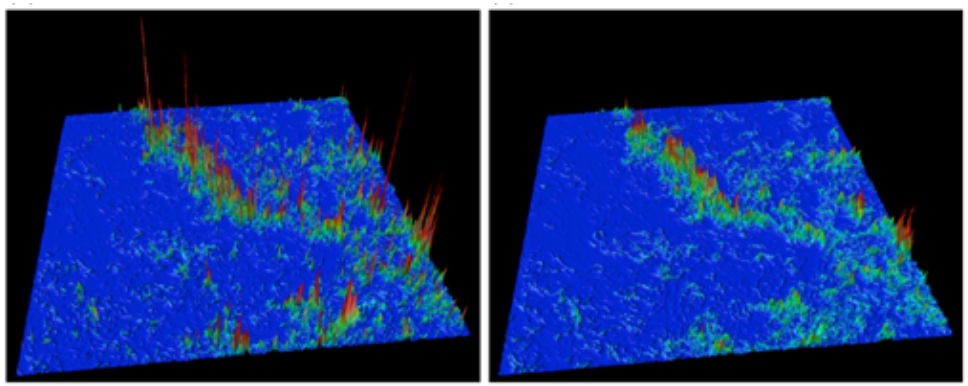

Large-scale velocity jumps generate Lambda-scale shear (on average) and Spikes of energy dissipation

Inside structure of the shear layers

Distribution of the strong vortices inside the layer

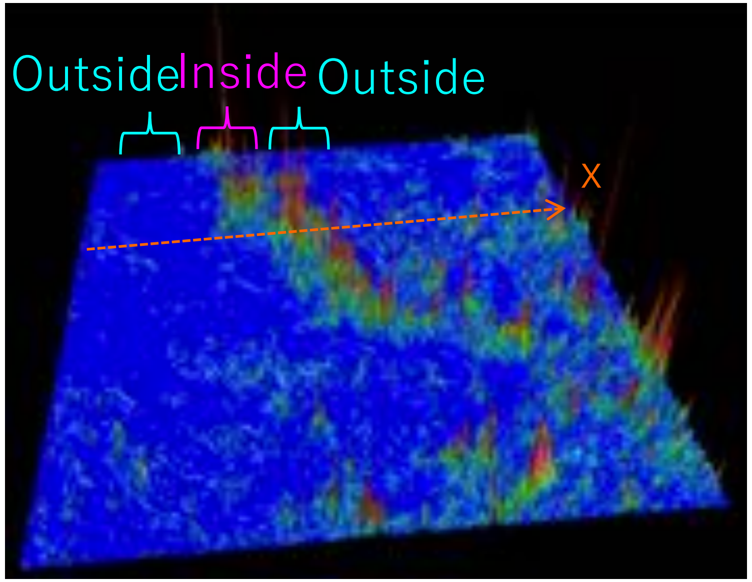

($\Delta = 2\pi/4096 \sim 3\eta$: grid spacing)

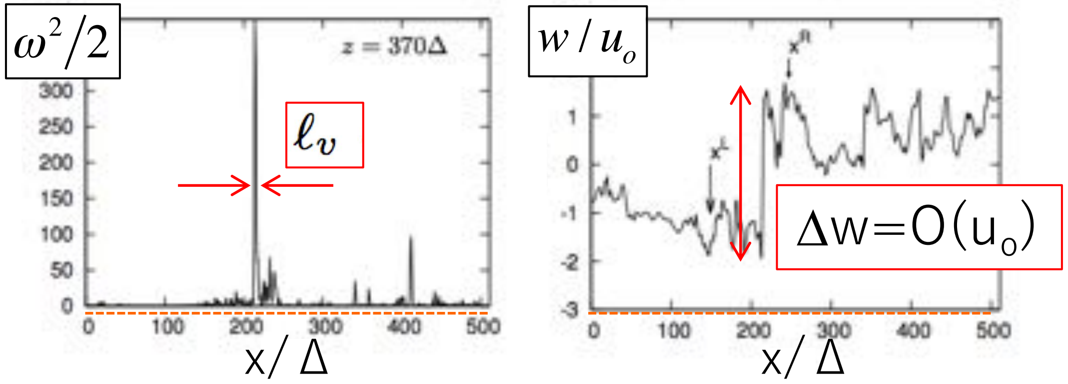

Thickness of the micro-scale vortices: $\ell_v \sim 10\eta$
(insensitive to their strength)

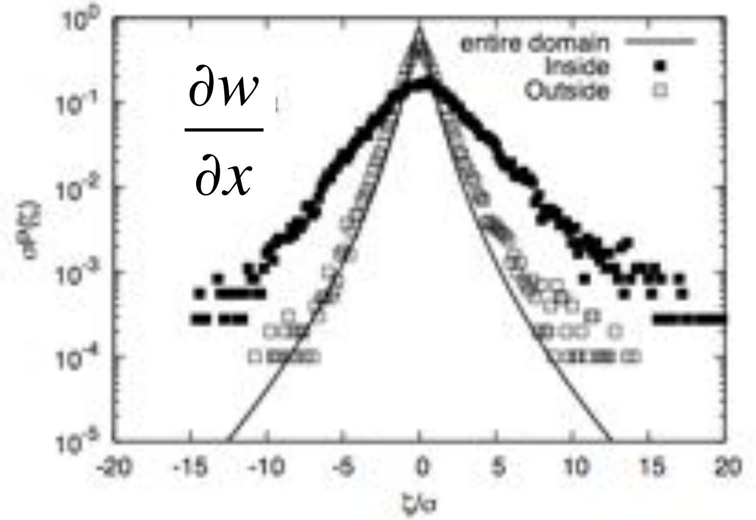

Very strong vorticity of $O(u_o/10\eta)$

$>> u_{Kol}/\eta = 1/\tau_{Kol}$ (K41)

Velocity jump of $O(u_o)$ over distances of $O(10\eta)$

$>> u_{Kol} \sim u_o Re^{-1/4}$ (K41)

The layers may dominate the extreme point values of the statistical distributions of dissipation, velocity and vorticity fluctuations

Strong vortices within strong layers (much stronger than K41)

Enstrophy

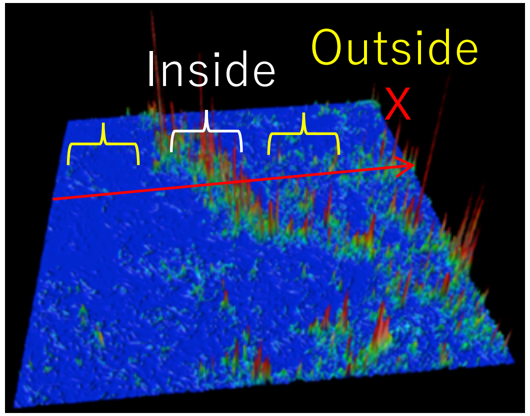

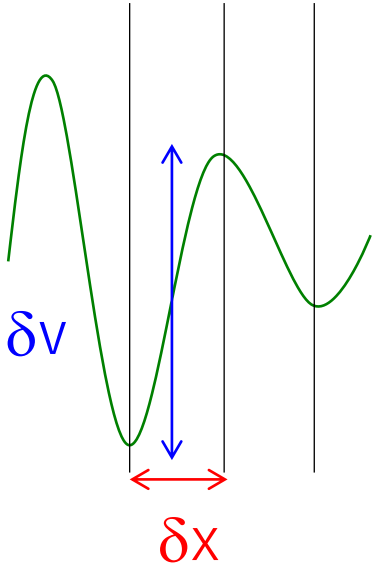

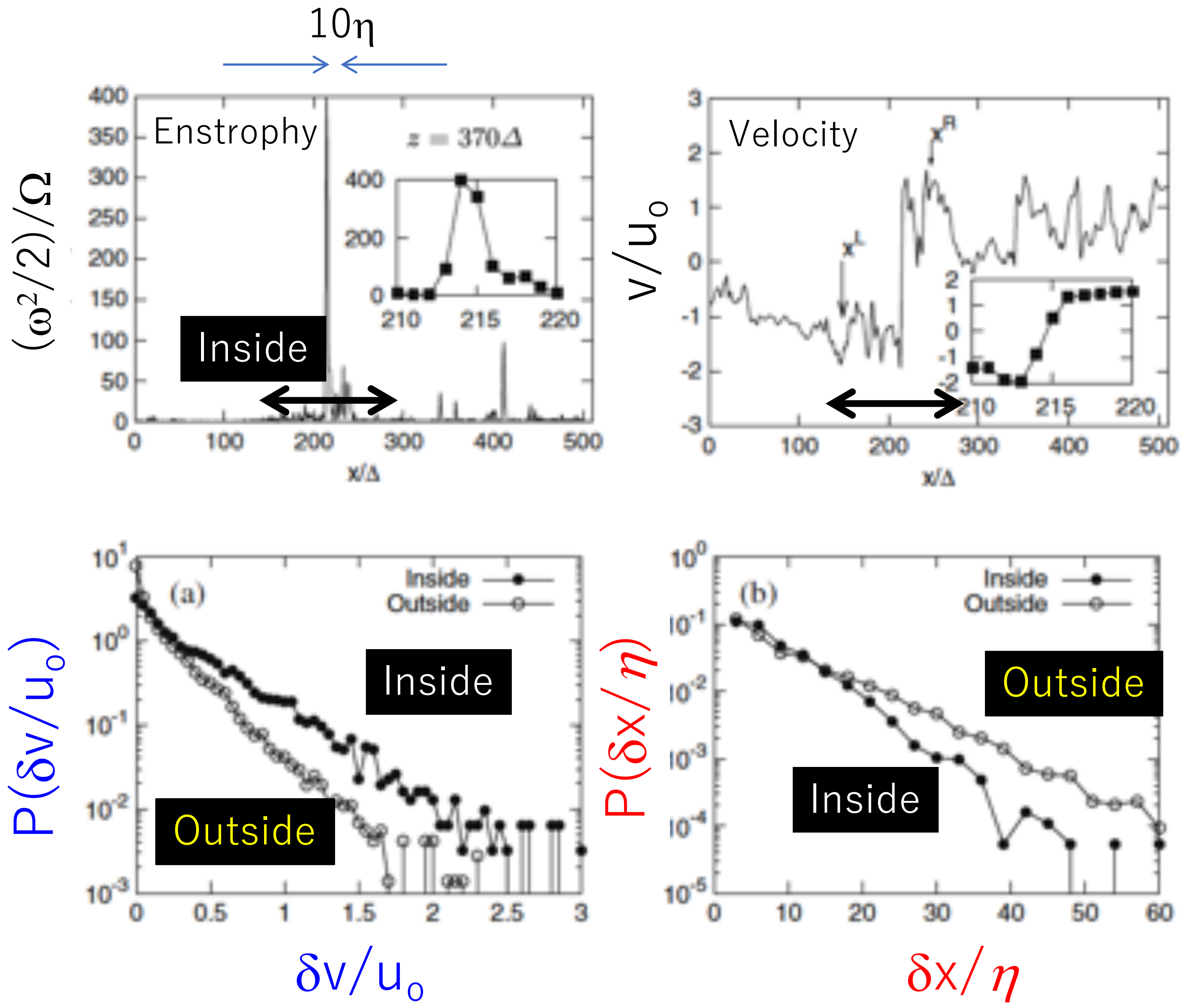

Thin shear layer & Energy transfer

- Let $\overline{\quad}$ be the filtering operation to remove all the Fourier modes with wavenumbers higher than k, then

$$T(\mathbf{x}, k) \equiv \sum_{ij} (\overline{u_i u_j} - \bar{u}_i \bar{u}_j) \bar{S}_{ij}$$

is the energy transfer at $\boldsymbol{x}$ across the wave number k

(e.g. Domaradzki et al 1990, Cerutti & Meneveau 1998, Chen et al 2003, Aoyama et al 2005)

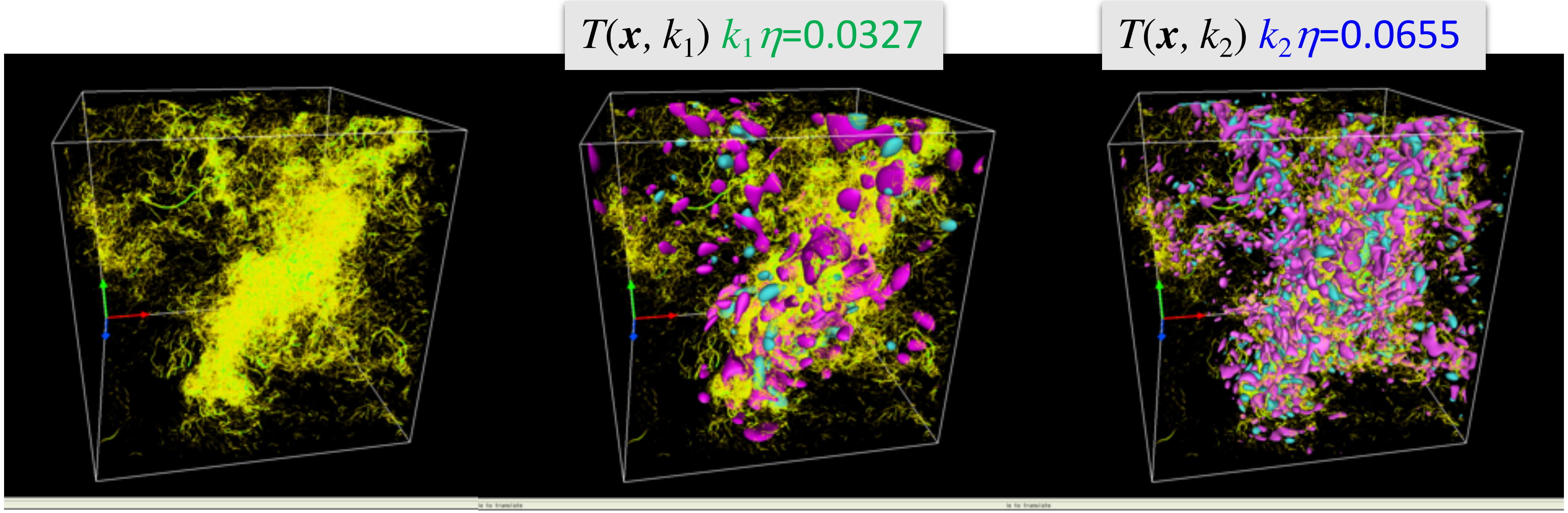

T>0 downscale (from large to small) ,T<0 upscale (from small to large)

Energy transfer $\boldsymbol{T(x, k)}$ and energy dissipation $\boldsymbol{\varepsilon}$ near the layer

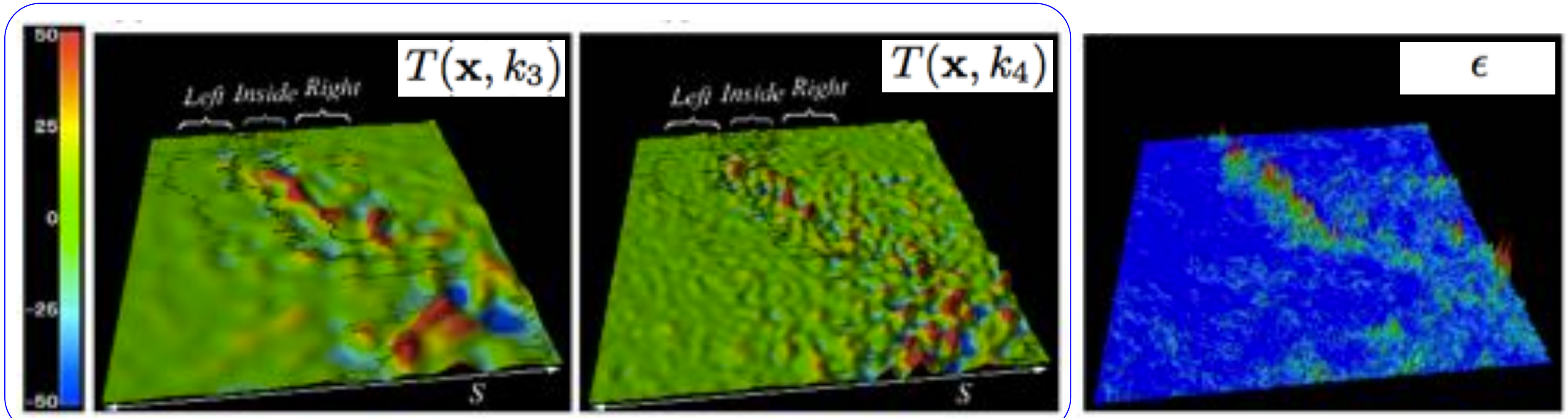

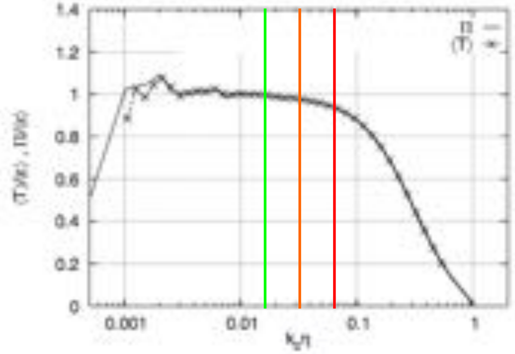

Large amplitude positive/negative (i.e. downscale/upscale) fluctuations of T near the thin layer

$<T(x,k)>_{Inside} = <\varepsilon>_{Inside} \sim 10 <\varepsilon>$ for $k > \pi / l$

l :thickness of the layer

$10 \sim L/ l \sim R_\lambda/100$

A net energy flux from the larger scale motions from outside

A		$\langle A\rangle/\langle\epsilon\rangle$	$\langle A\rangle_{Left}/\langle\epsilon\rangle$	$\langle A\rangle_{Inside}/\langle\epsilon\rangle$	$\langle A\rangle_{Right}/\langle\epsilon\rangle$
$T(\mathbf{x}, k_2)$	$\pi/k_2 \approx 2.9\lambda$	0.99(3.86)	3.76(5.99)	3.9(12.4)	1.2(19.7)
$T(\mathbf{x}, k_3)$	$\pi/k_3 \approx 1.4\lambda$	0.98(4.24)	0.36(2.17)	10.7(22.5)	5.7(18.5)
$T(\mathbf{x}, k_4)$	$\pi/k_4 \approx 0.7\lambda$	0.94(4.93)	1.03(3.55)	10.2(24.6)	4.0(13.6)
ϵ	—	1	0.88(1.40)	10.2(11.9)	2.44(3.49)

Histograms of velocity components normalized by rms

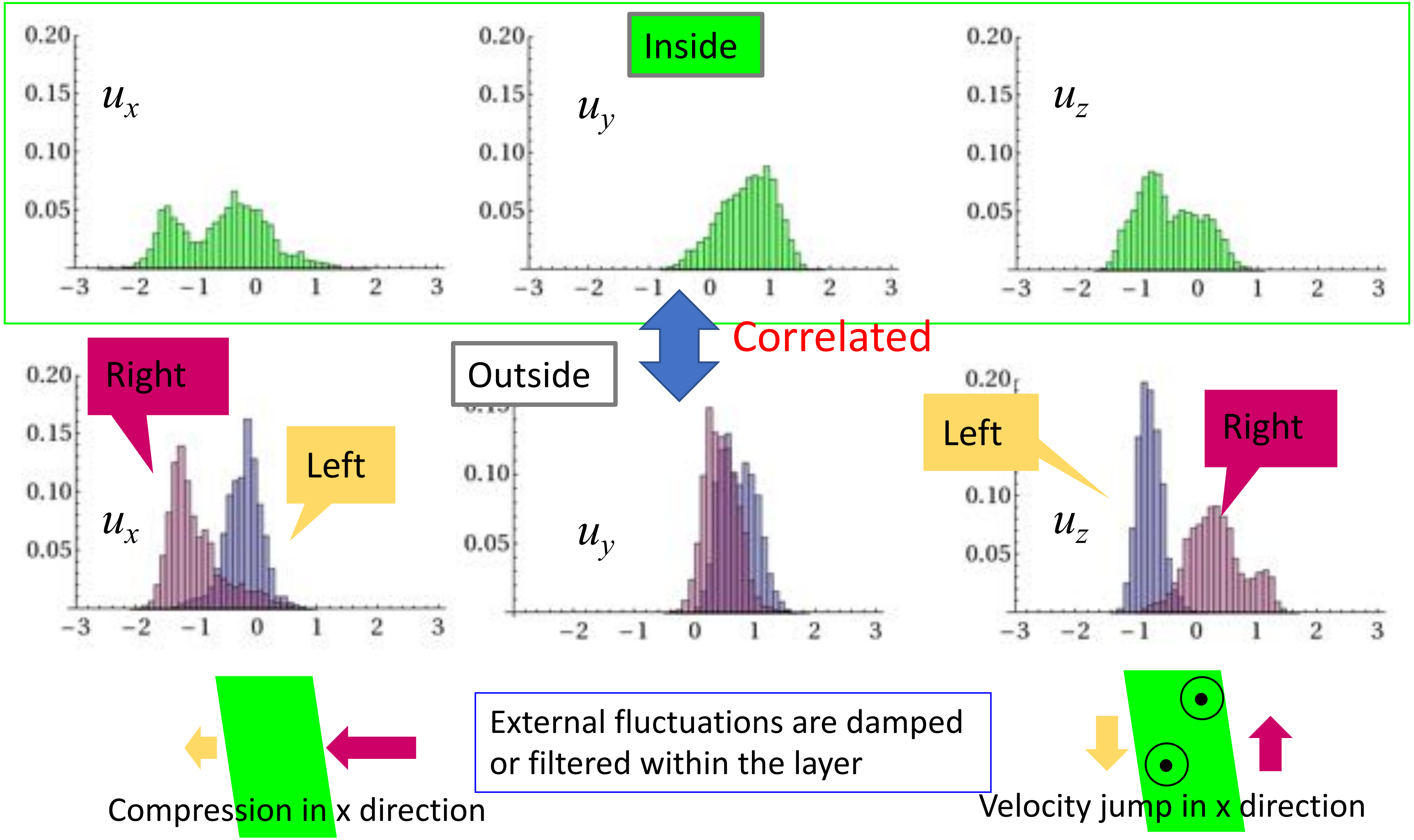

Flow structure around the layer

Layers as edged of large-scale motions

Velocity vector directions

Number density of velocity vector directions in 465

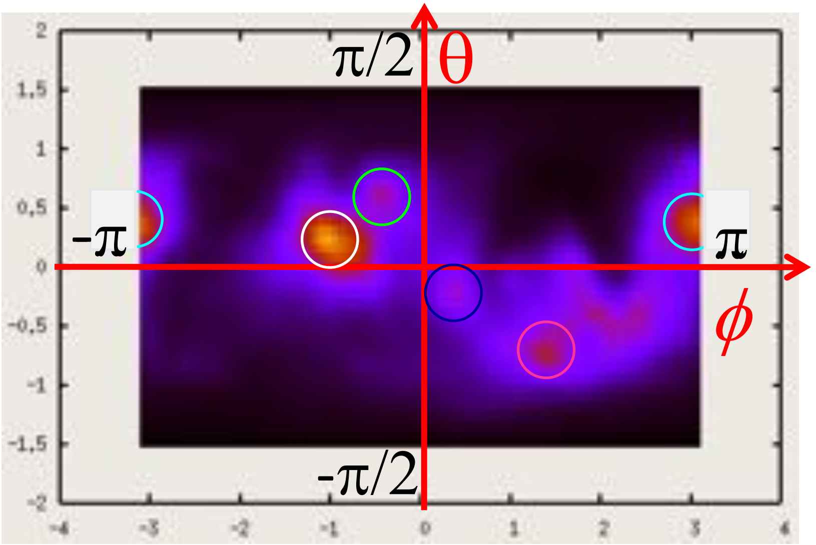

Elsinga and Marusic, JFM 2010

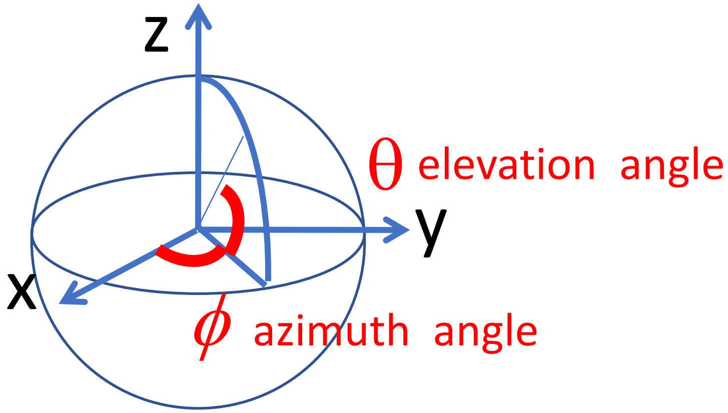

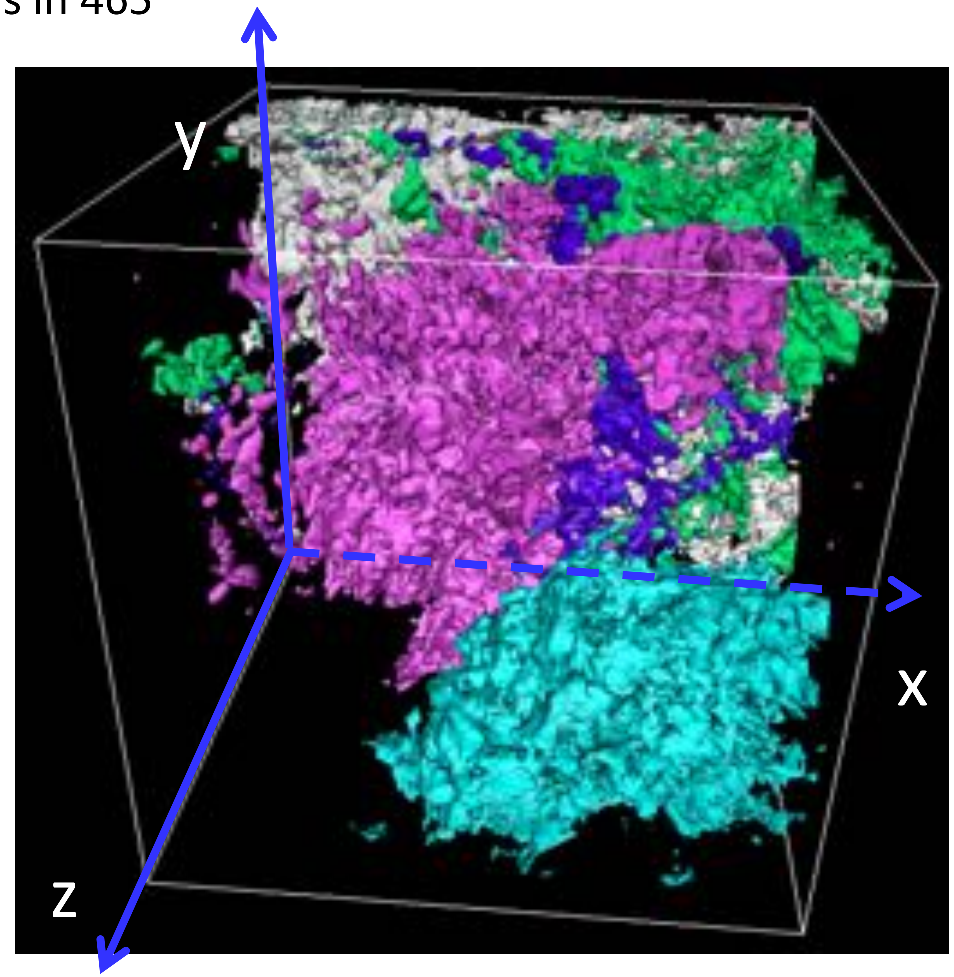

Uniform velocity zones

Velocity vector directions

Number density of velocity vector directions in 465

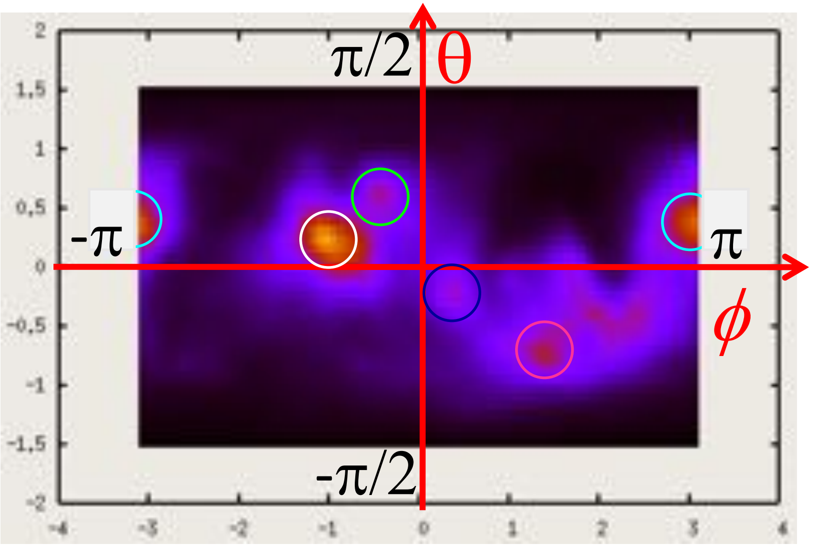

Elsinga and Marusic, JFM 2010

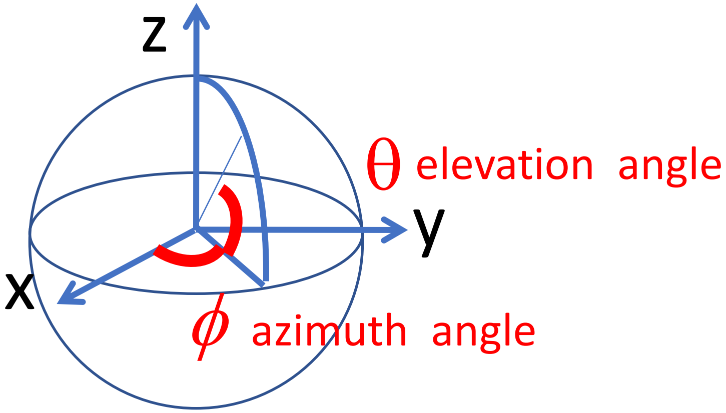

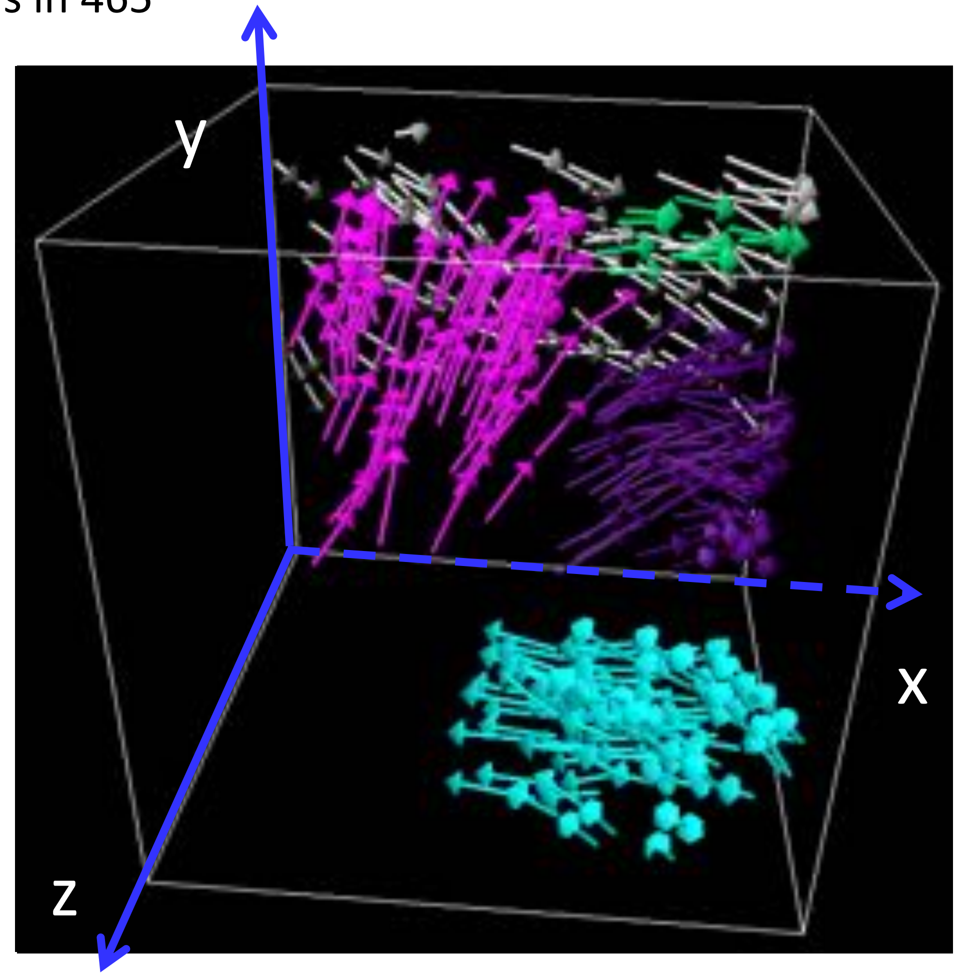

Flow directions

Uniform velocity zones & high vorticity regions

Number density of velocity vector directions in 465

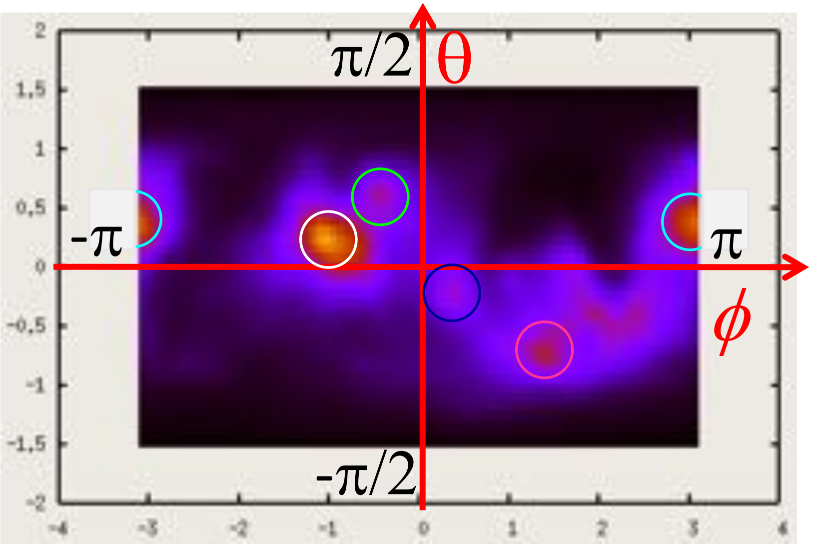

Elsinga and Marusic, JFM 2010

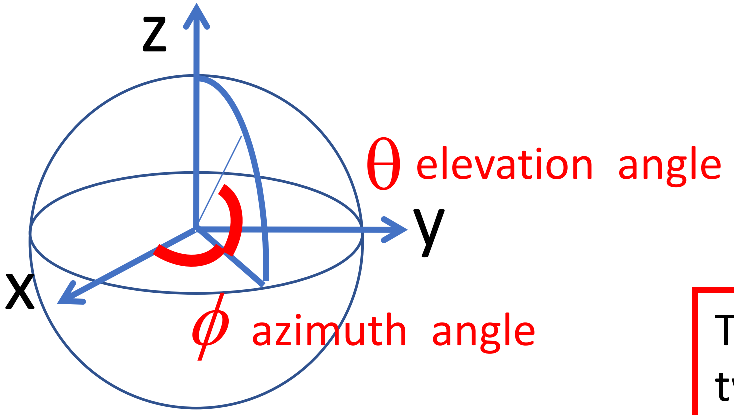

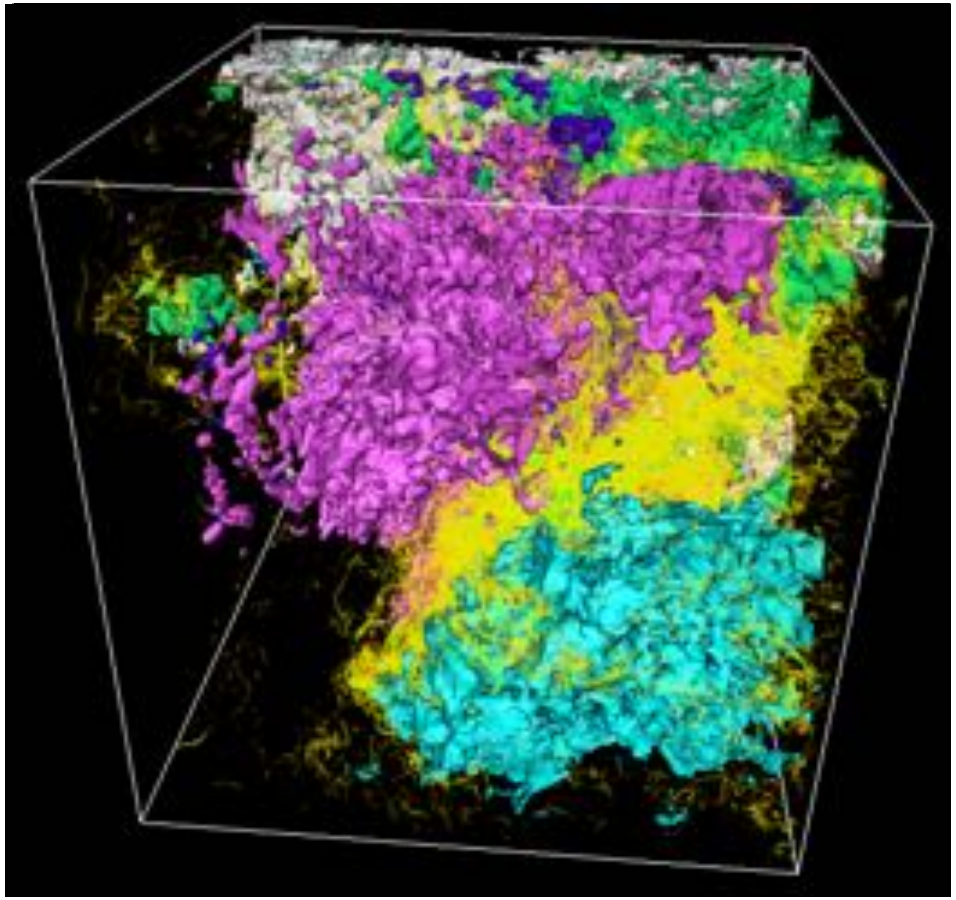

The high vorticity regions are in between two different velocity zones and form a shear layer

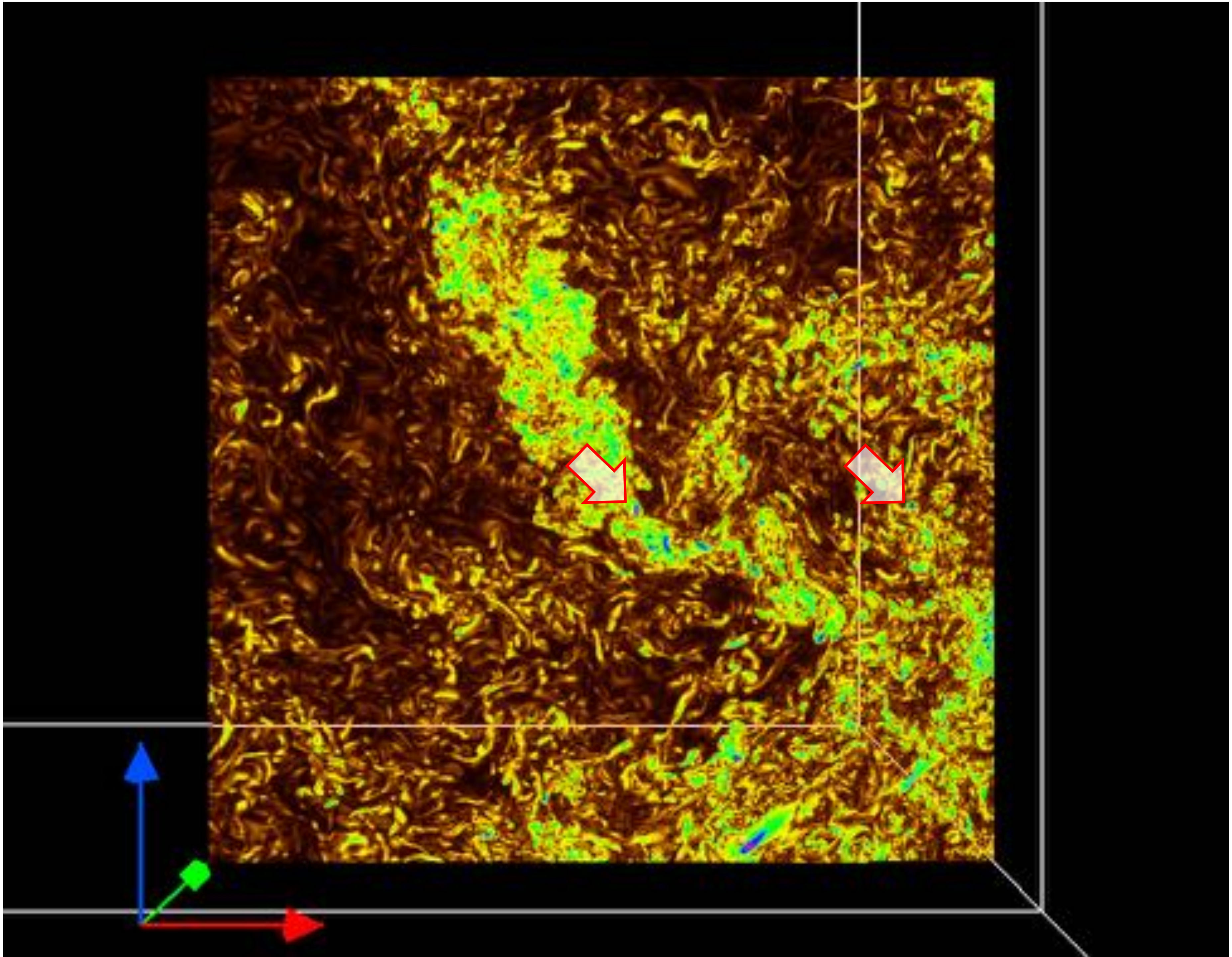

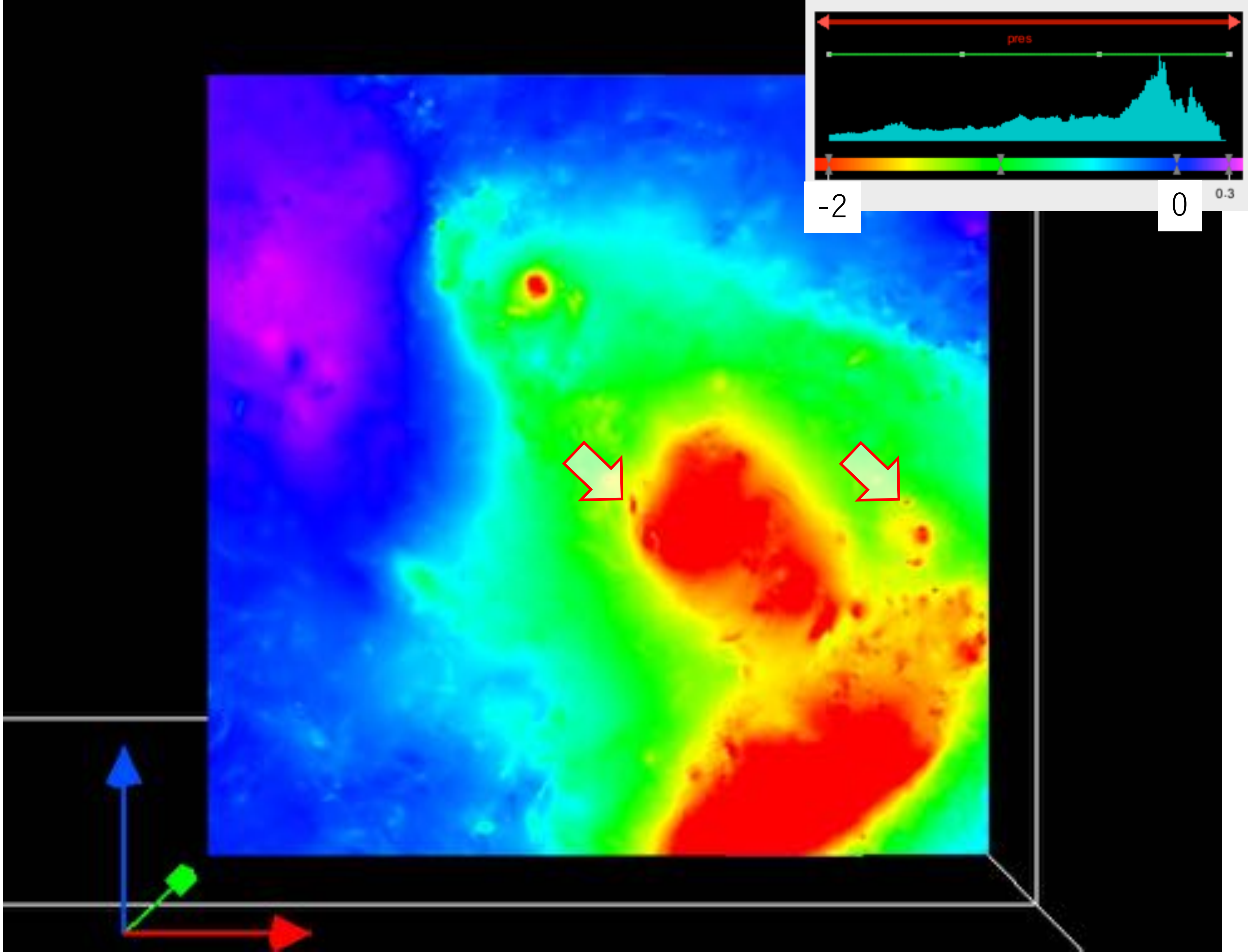
pres
-2
0
0.3

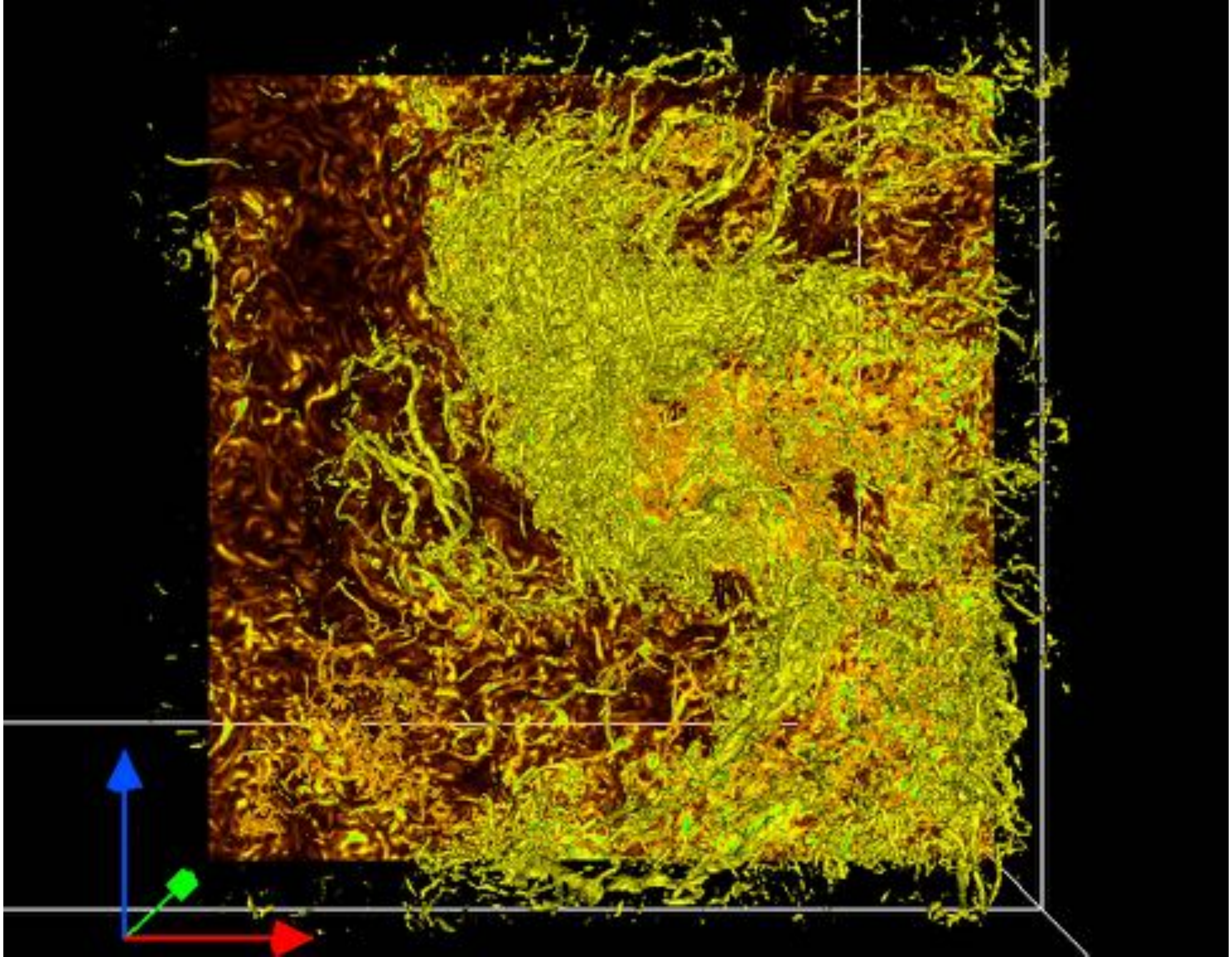

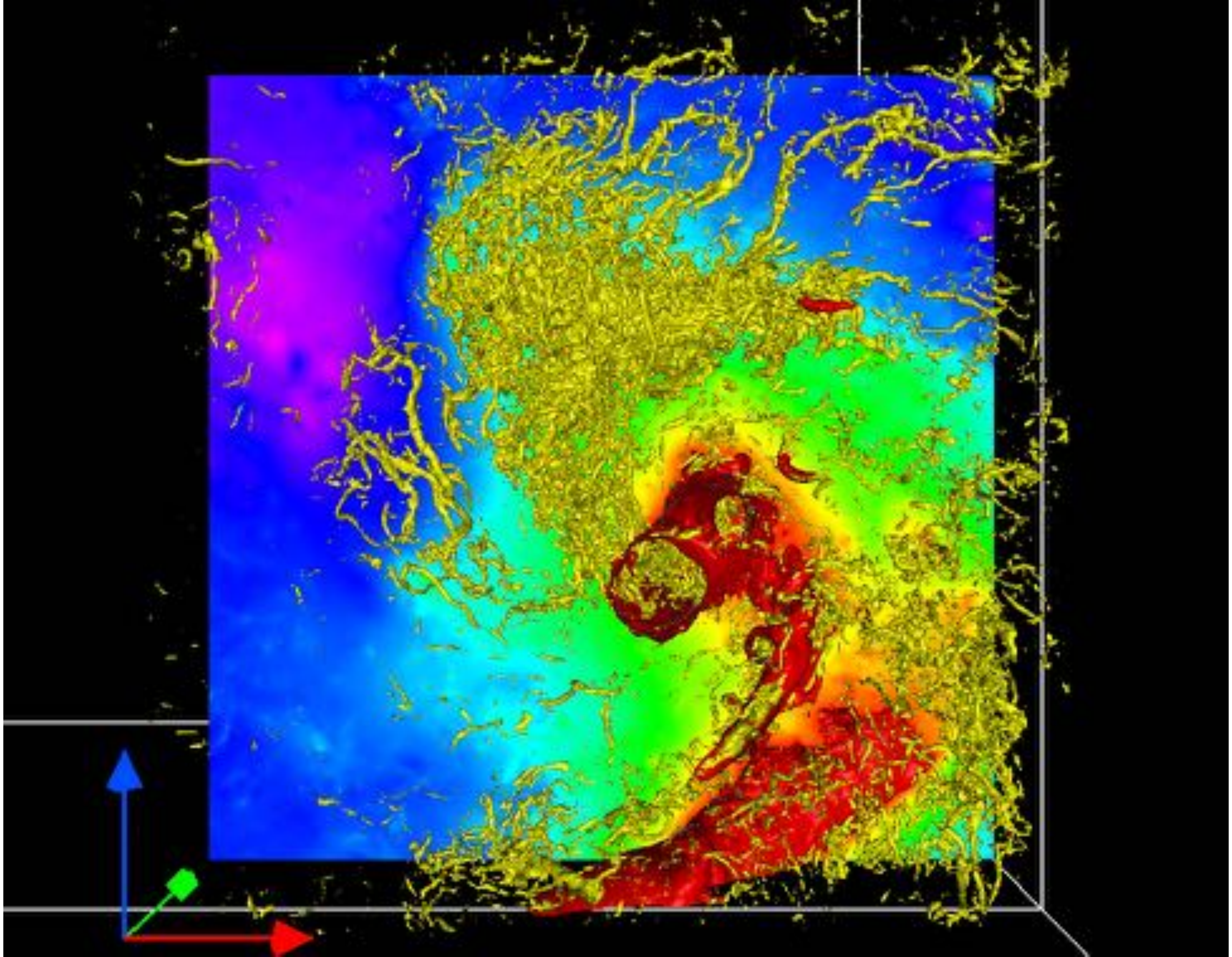

Flow around a large-scale low-pressure tubular vortex

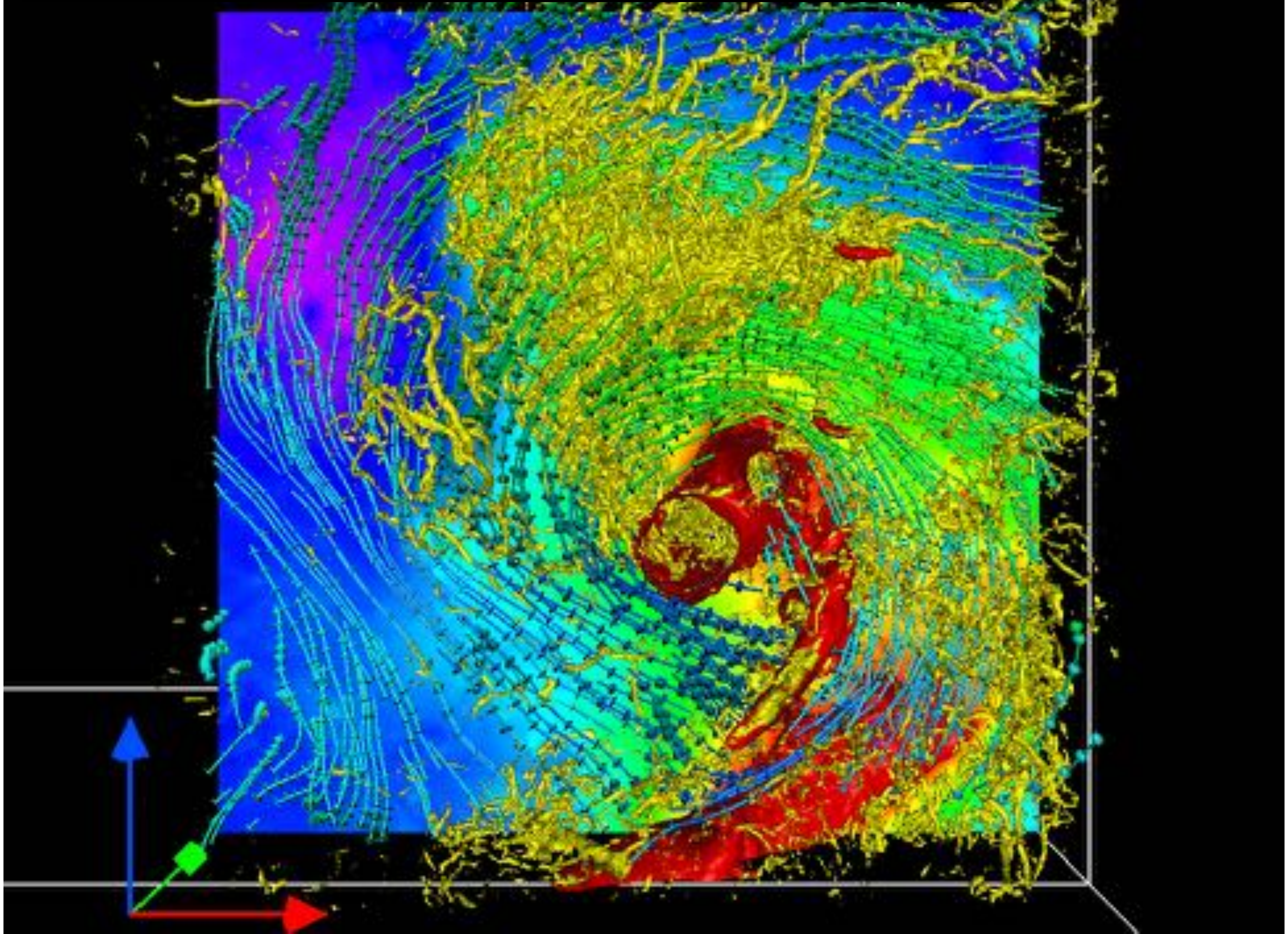

Flow around a large-scale low-pressure tubular vortex

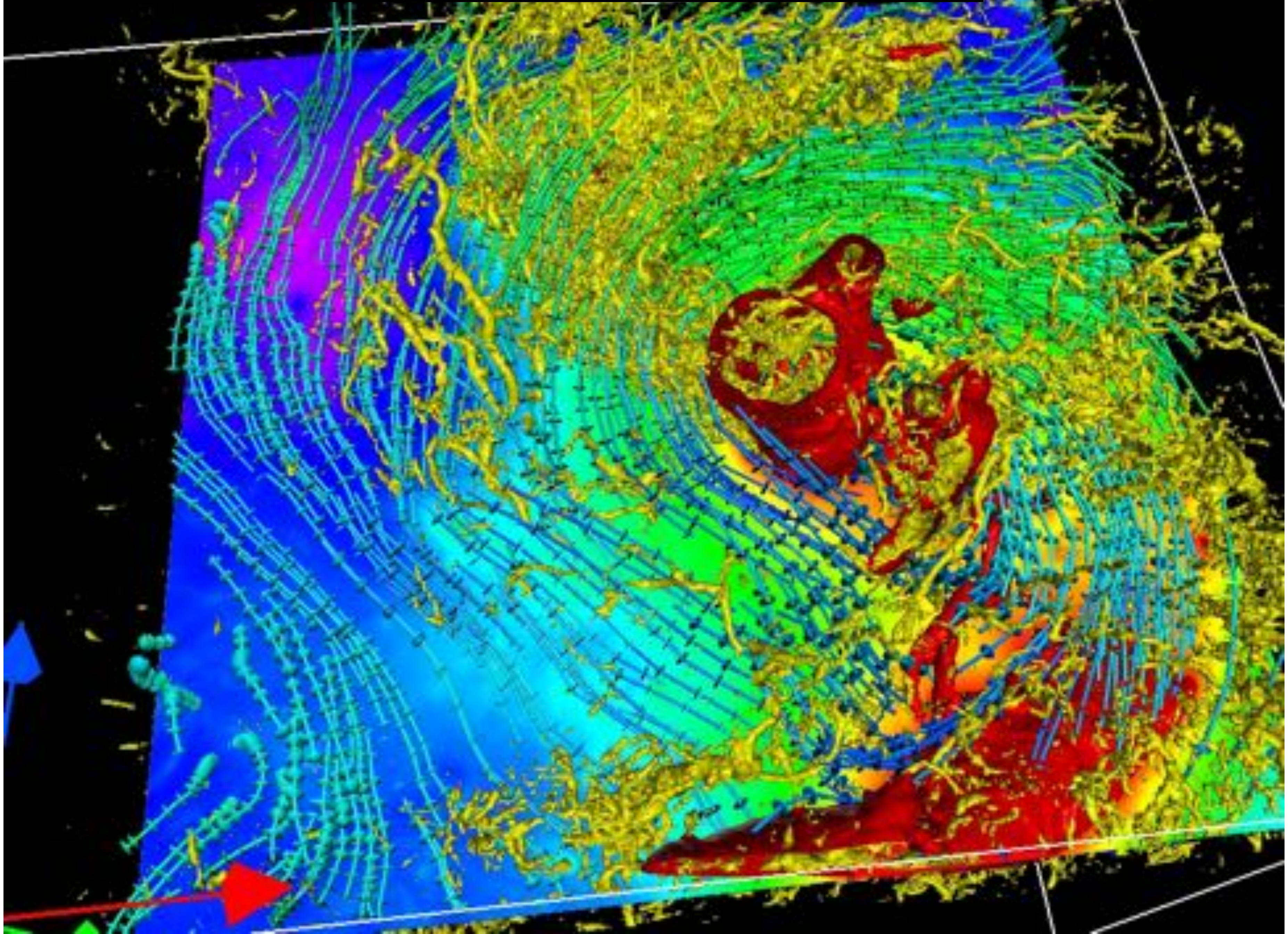

Flow around a large-scale low-pressure tubular vortex

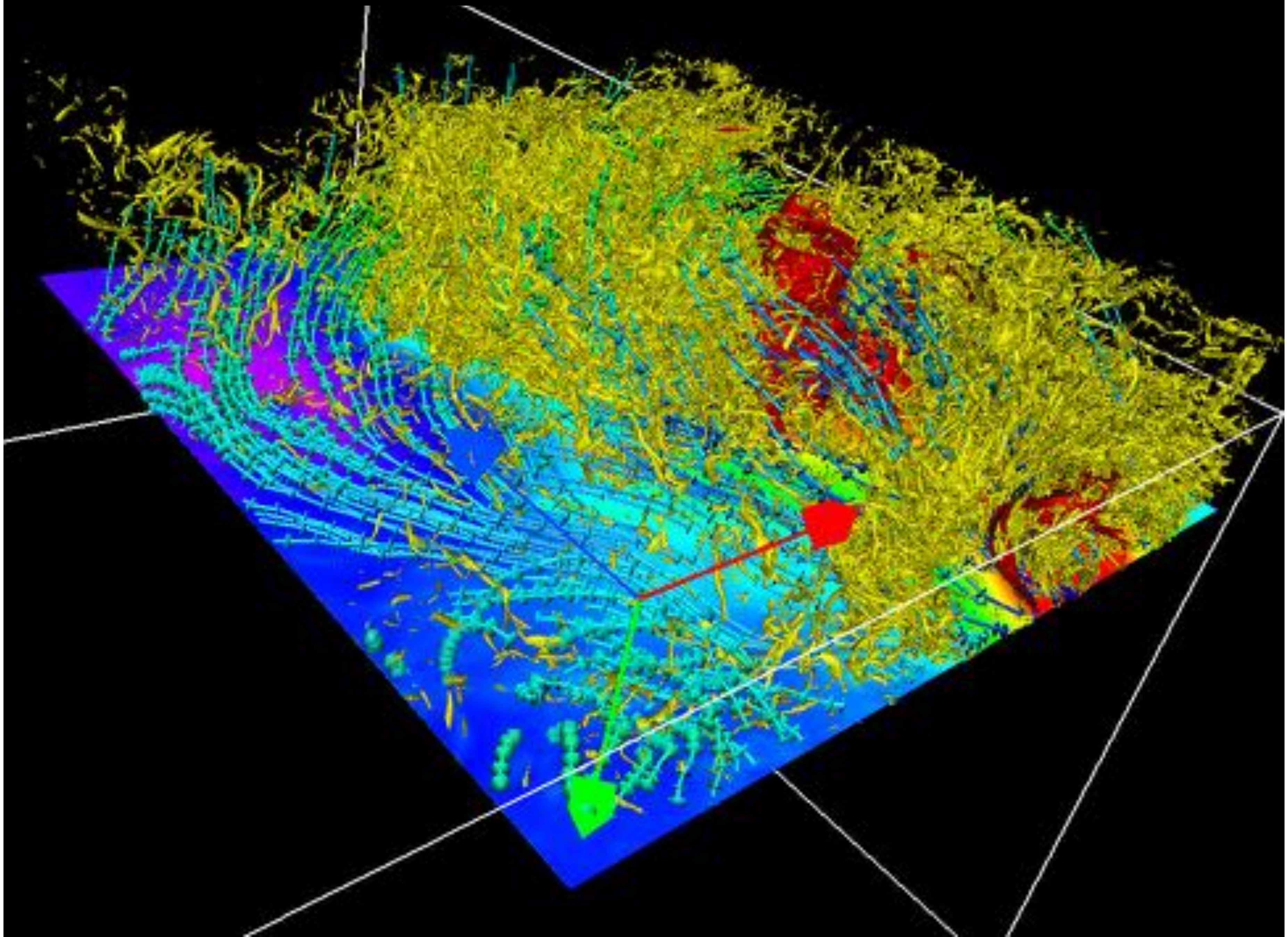

Journal of the Physical Society of Japan
Vol. 69, No. 10, October, 2000, pp. 3466-3467

Double Spirals around a Tubular Vortex in Turbulence

Shigeo KIDA and Hideaki MIURA

decaying Re_λ is 106

c.f.

Lundgren (1982)
Kawahara (2005)
Horiuti & Fujisawa (2008)
Horiuti & Ozawa (2011)

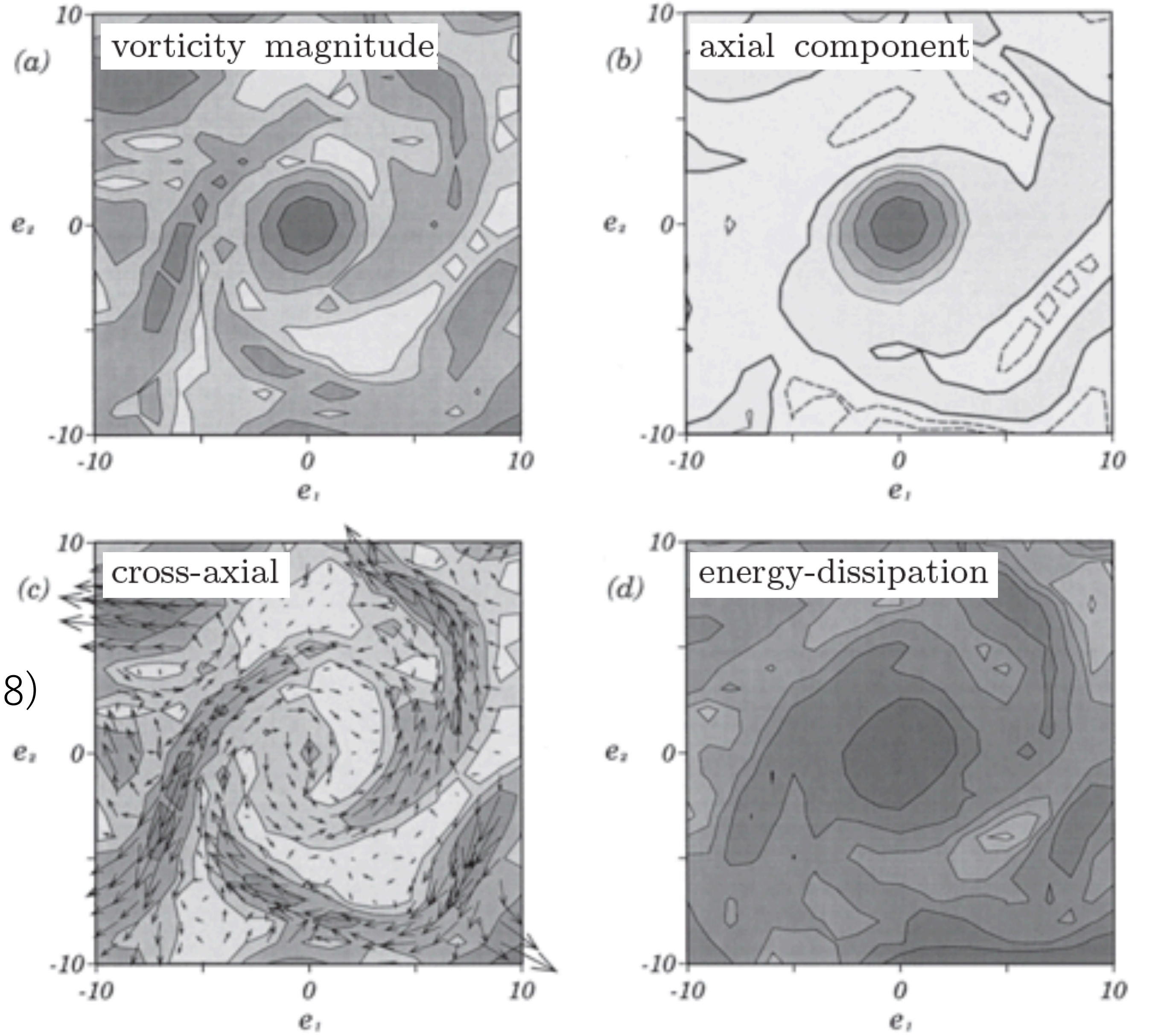

Fig. 1. Double spiral structure. Contours of (a) vorticity magnitude, (b) the axial component, (c) magnitude of the cross-axial component, and (d) energy-dissipation rate on a cross-section of a low-pressure vortex in isotropic turbulence. Darker shade implies larger values in (a), (c) and (d). Vorticity is pointed into (or out of) the paper in gray (or white) area in (b). Vorticity vectors at every grid point are shown by arrows in (c). The coordinates of the cross-section, e_1 and e_2, are measured in the unit of the grid width Δx taken in the numerical simulation. The Kolmogorov length is $2.0\Delta x$. The levels of contours are 0, $\pm 10^{-2+n/4}$ ($n = 1 \sim 5$) in (a)–(c), $\pm 10^{-8+n/4}$ ($n = 2 \sim 8$) in (d).

Velocity & vorticity near the layer

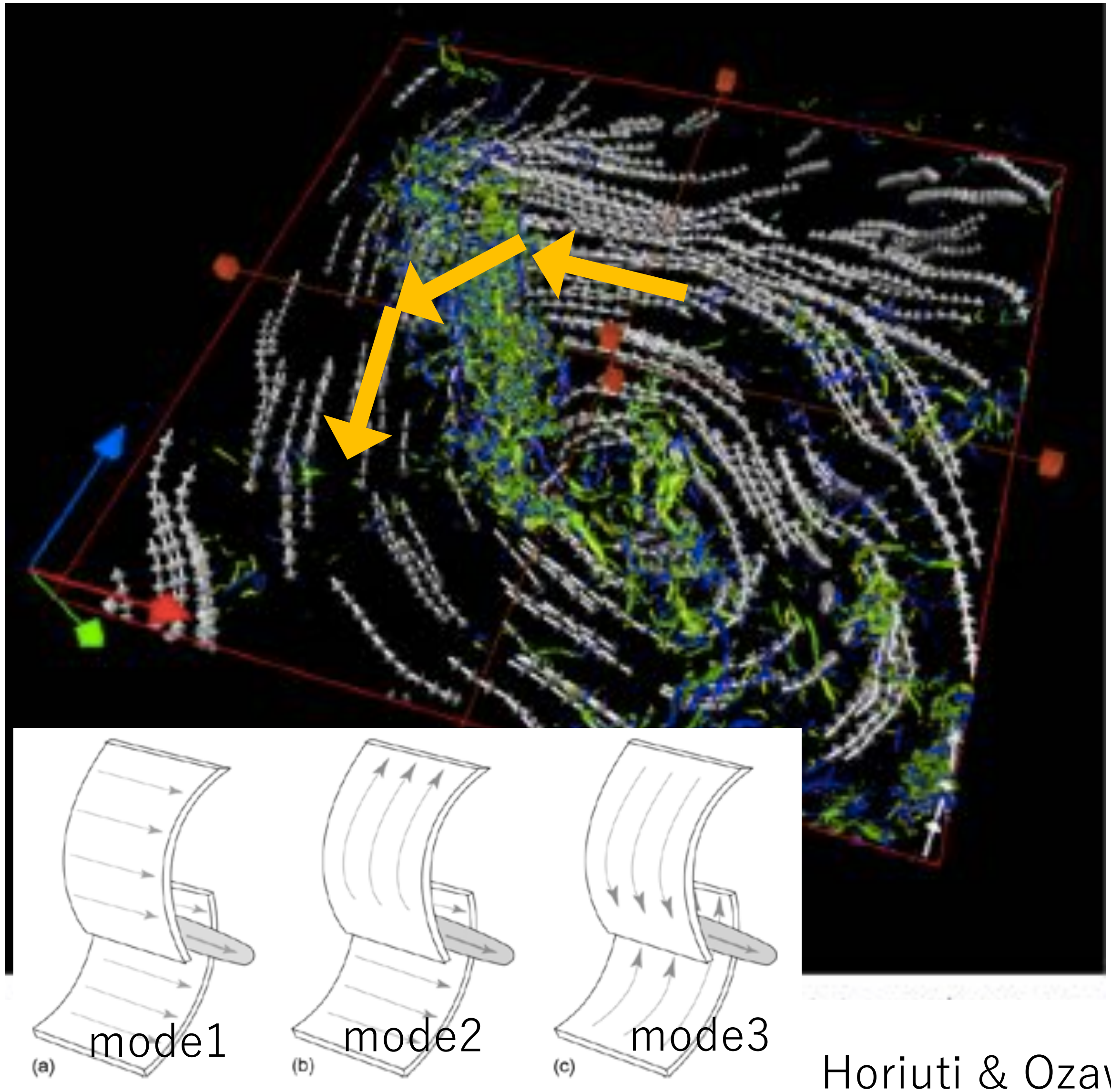

FIG. 2. Schematics of three modes of vorticity vector alignment along the vortex tube and dual sheets. The gray arrows denote vorticity vectors. (a) Mode 1, (b) Mode 2, (c) Mode 3.

$$\langle \mathbf{u} \rangle_{Inside}/u' = (-0.94,\ 1.07,\ -0.80),$$
$$\langle \mathbf{u} \rangle_{Left}/u' = (-0.39,\ 1.25,\ -1.32),$$
$$\langle \mathbf{u} \rangle_{Right}/u' = (-1.74,\ 0.77,\ 0.58),$$

$$\delta \mathbf{U} \equiv \langle \mathbf{u} \rangle_{Left} - \langle \mathbf{u} \rangle_{Right} = (1.35, 0.47, -1.90)u'$$

$$|\delta \mathbf{U}| \approx 2.4u'$$

$$\langle \boldsymbol{\omega} \rangle_{Inside}/\omega' = (-0.15, -0.54, -0.54),$$
$$\langle \boldsymbol{\omega} \rangle_{Left}/\omega' = (-0.07, -0.01, 0.06),$$
$$\langle \boldsymbol{\omega} \rangle_{Right}/\omega' = (-0.08, -0.16, -0.09),$$

$$|\langle \boldsymbol{\omega} \rangle_{Inside}| = 0.78\omega'$$

Horiuti & Ozawa 2011

$$\Omega = (3/2)\omega'^2$$

Distribution of the vortical clusters

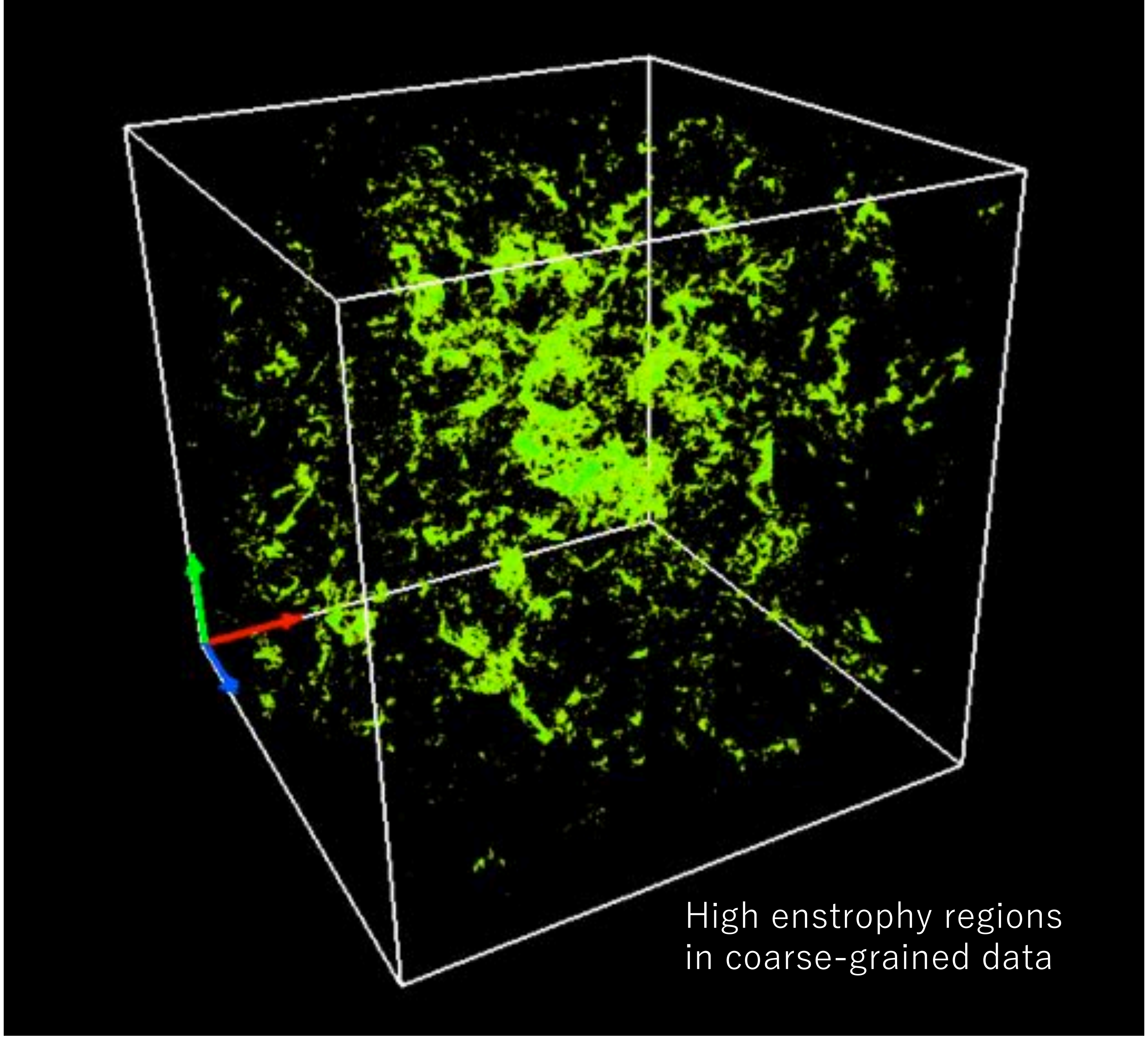
High enstrophy regions
in coarse-grained data

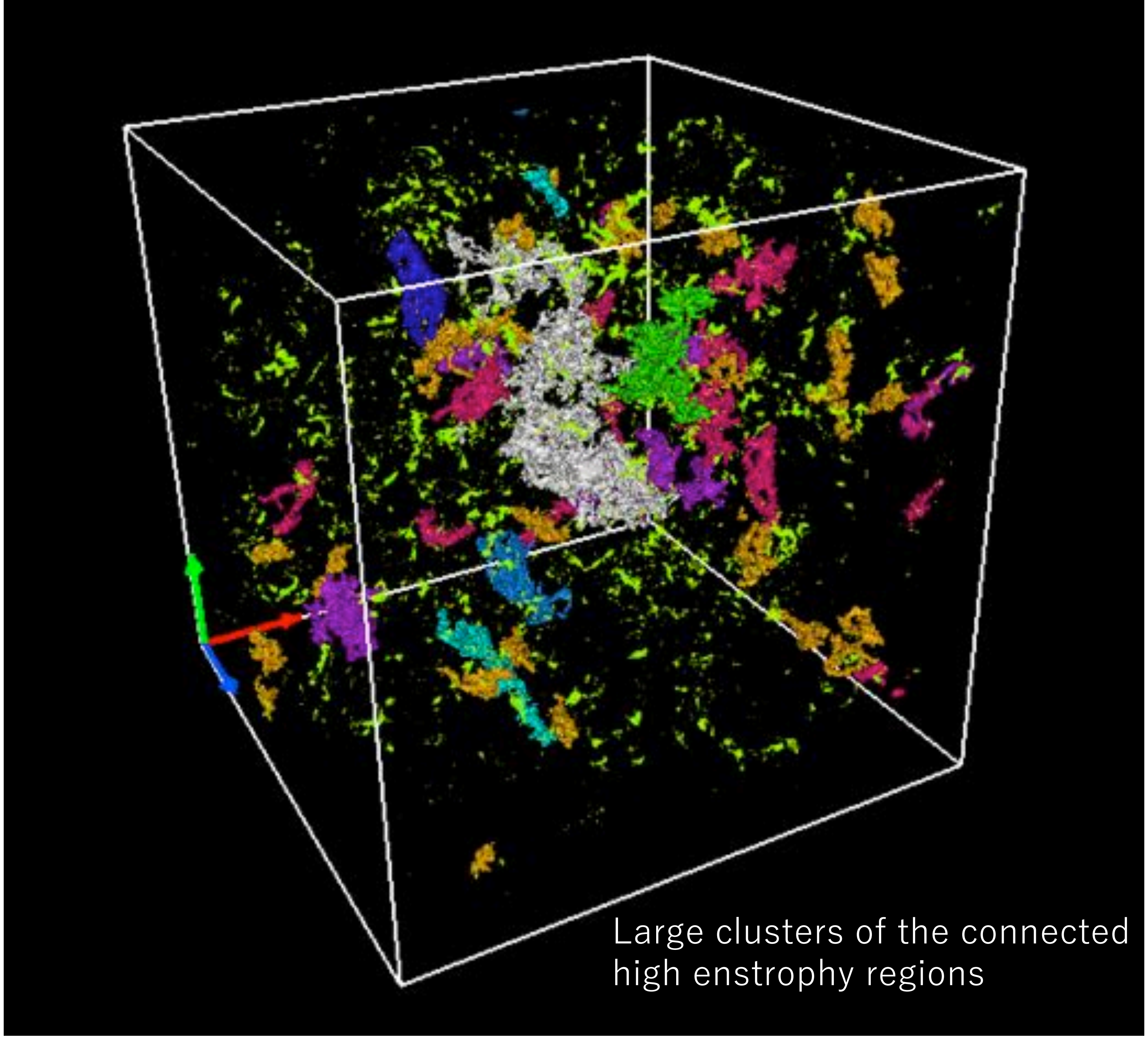
Large clusters of the connected
high enstrophy regions

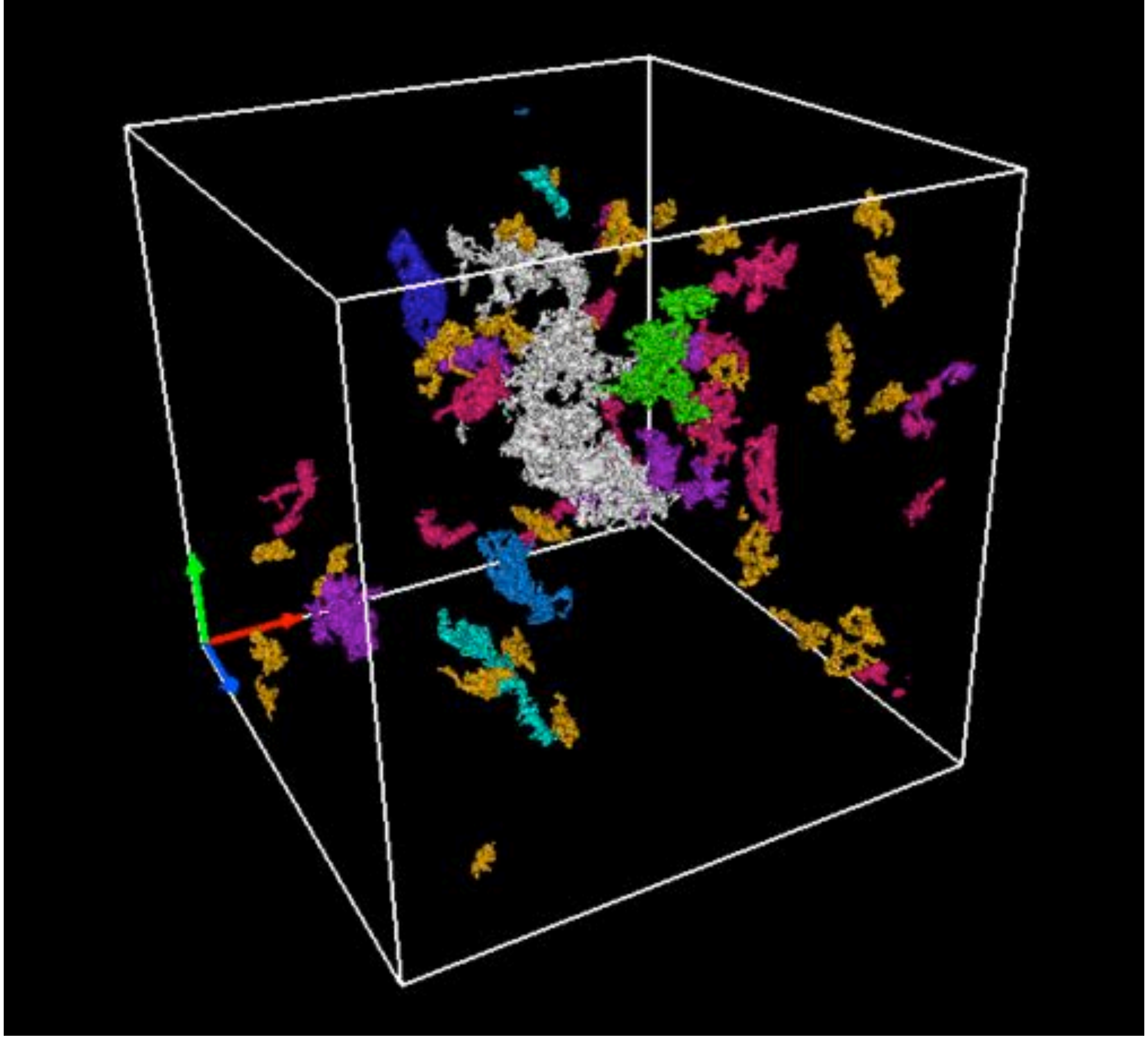

Data handling

DNS with 4096^3 grid points
(Kaneda et al, Phys. Fluids, 2003)

$k_{max}\eta=1$, $R_\lambda=1131$(at a statistically steady state)

Divide a 4096^3 box into
512(=8x8x8) boxes

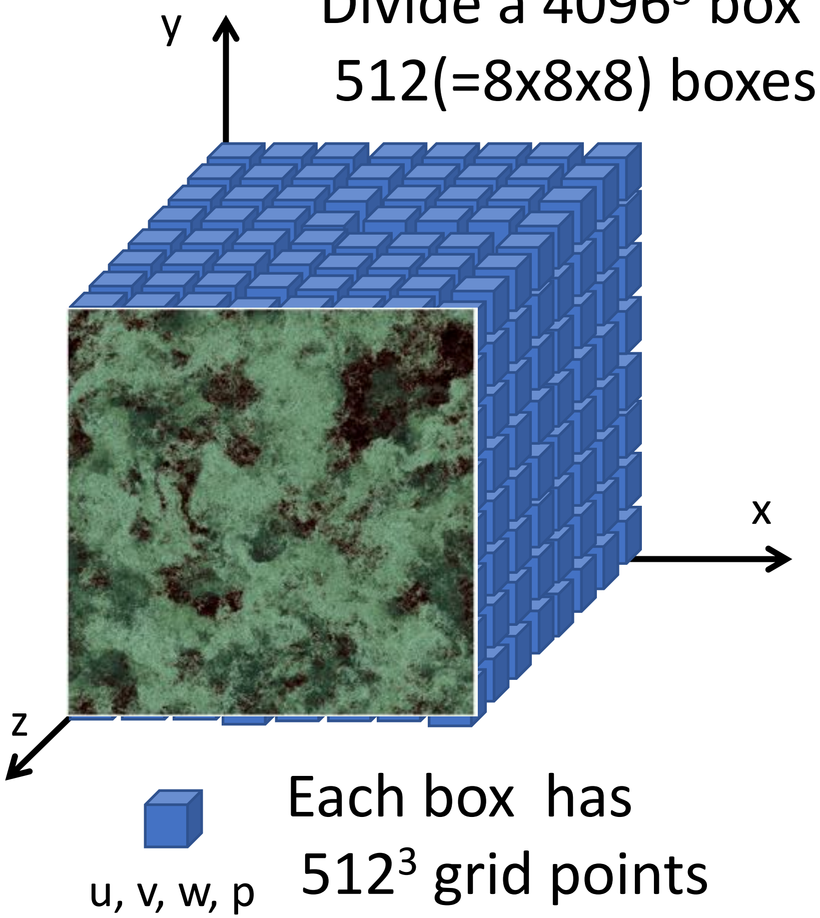

Each box has
512^3 grid points

$\Omega=2174$

High Enstrophy ranking

RANKING(new)	nx	ny	nz	Ω box
1	4	5	5	6127
2	5	6	5	5850
3	4	6	5	5828
4	5	4	5	5639
5	6	6	5	5360
6	5	5	5	5091
7	4	7	5	5036
509	2	7	1	796
510	3	8	8	746
511	2	7	7	690
512	2	7	8	623

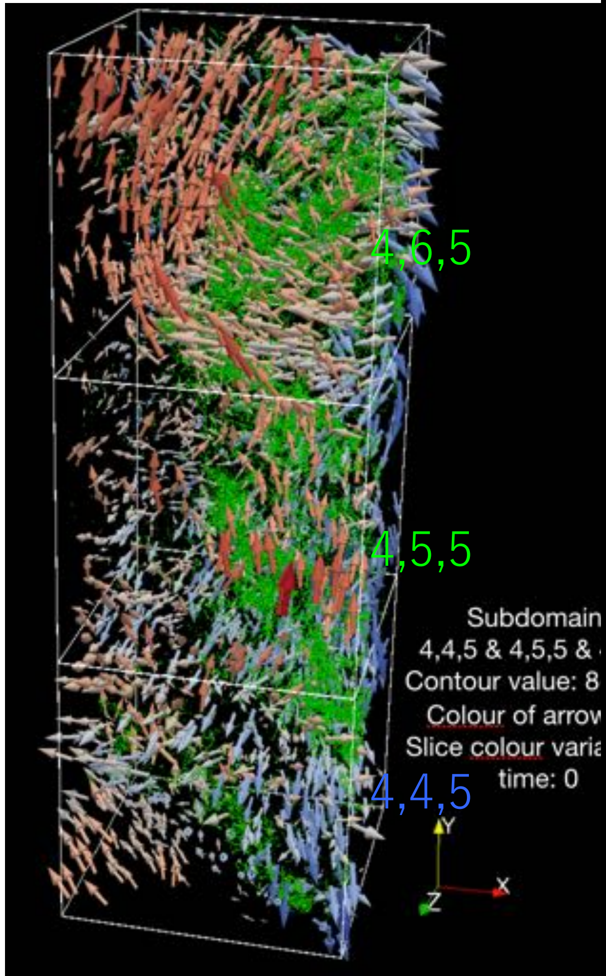
4,6,5
4,5,5
Subdomain
4,4,5 & 4,5,5 &
Contour value: 8
Colour of arrow
Slice colour varia
time: 0
4,4,5
Y
Z
X

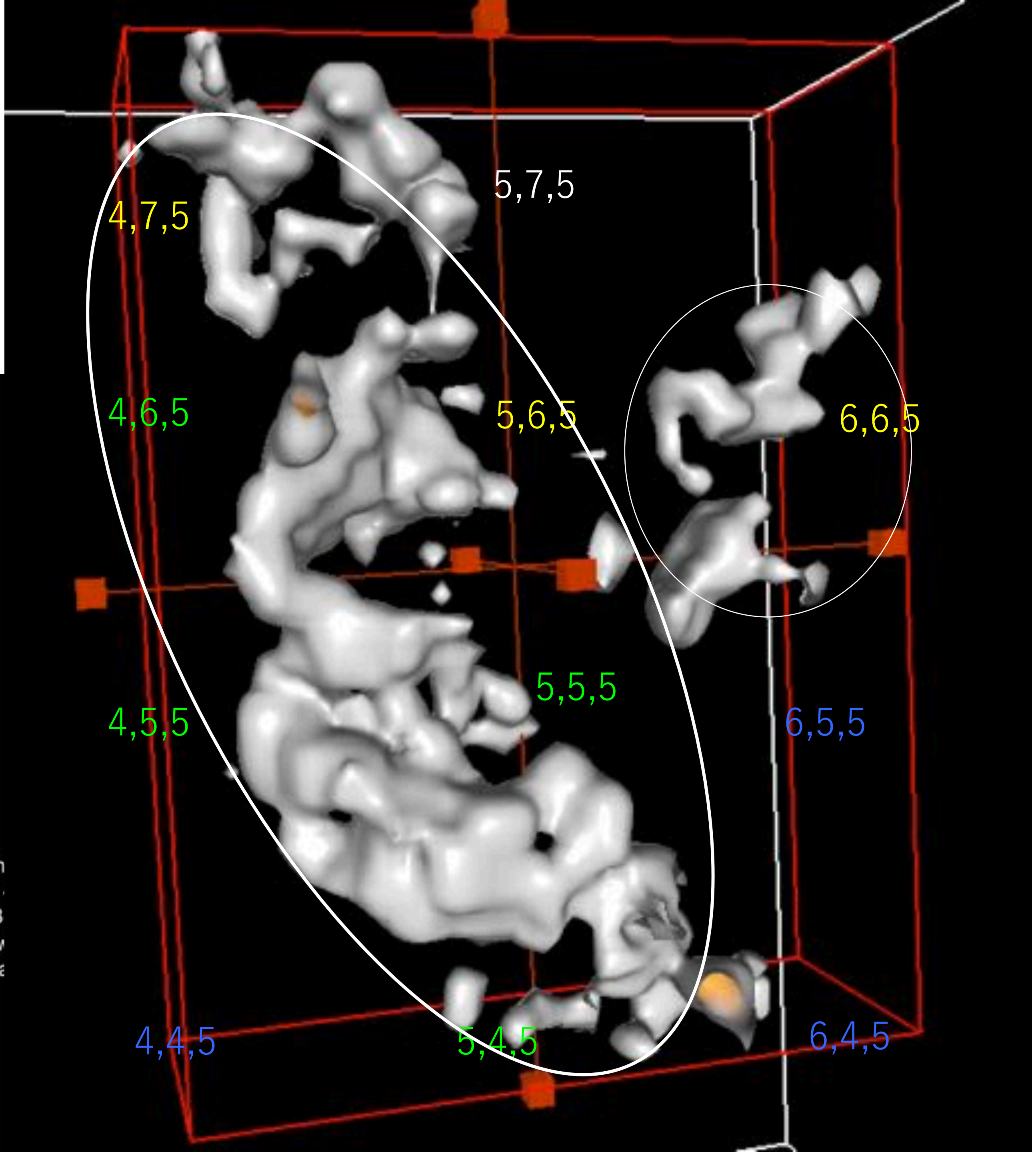
4,7,5
5,7,5
4,6,5
5,6,5
6,6,5
5,5,5
4,5,5
6,5,5
4,4,5
5,4,5
6,4,5

Top10 Enstrophy subdomains

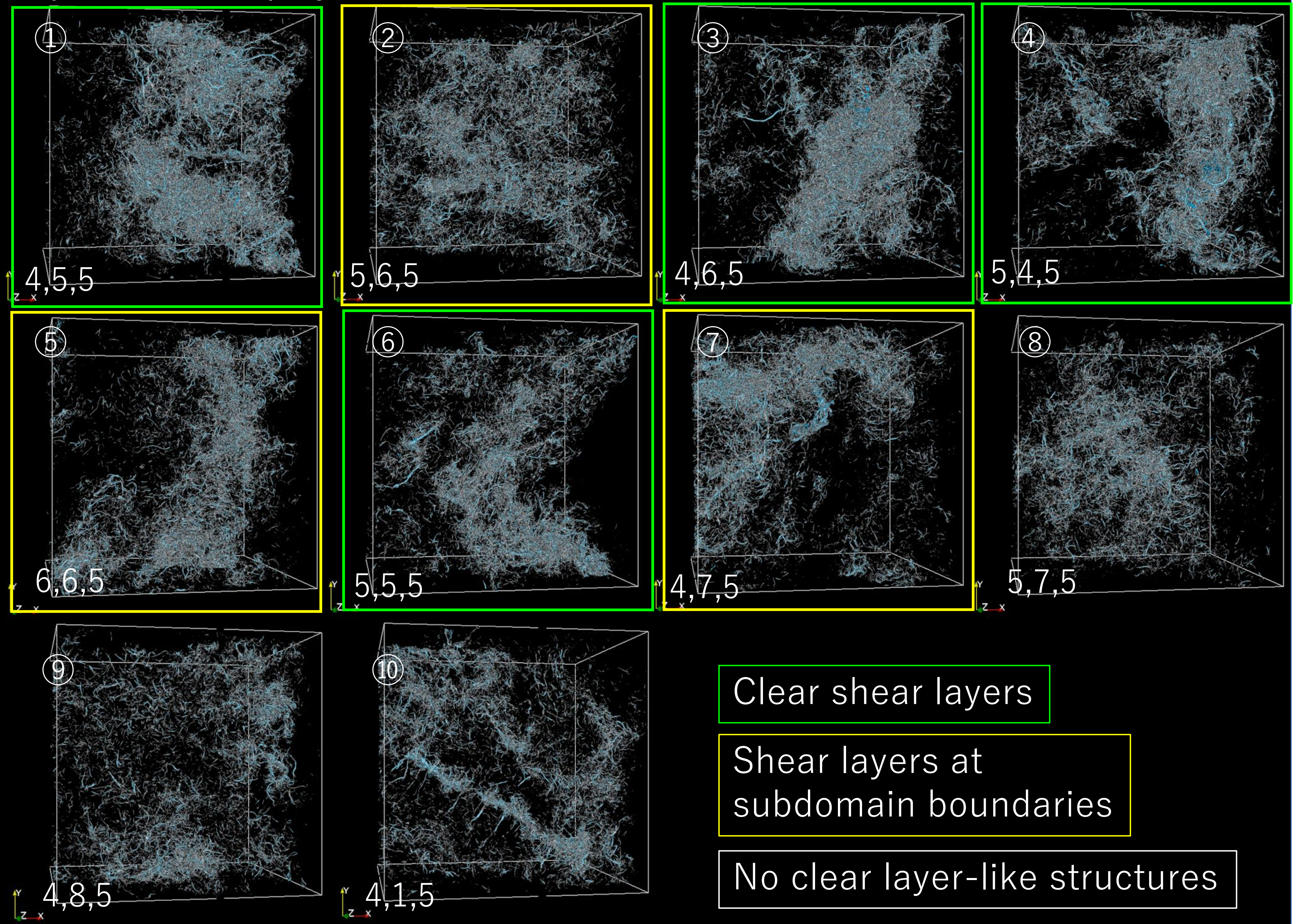

Time evolution and lifetime

The most significant shear layer (at $t = t_0$)

(In the most active subdomain of the 4096^3 DNS)

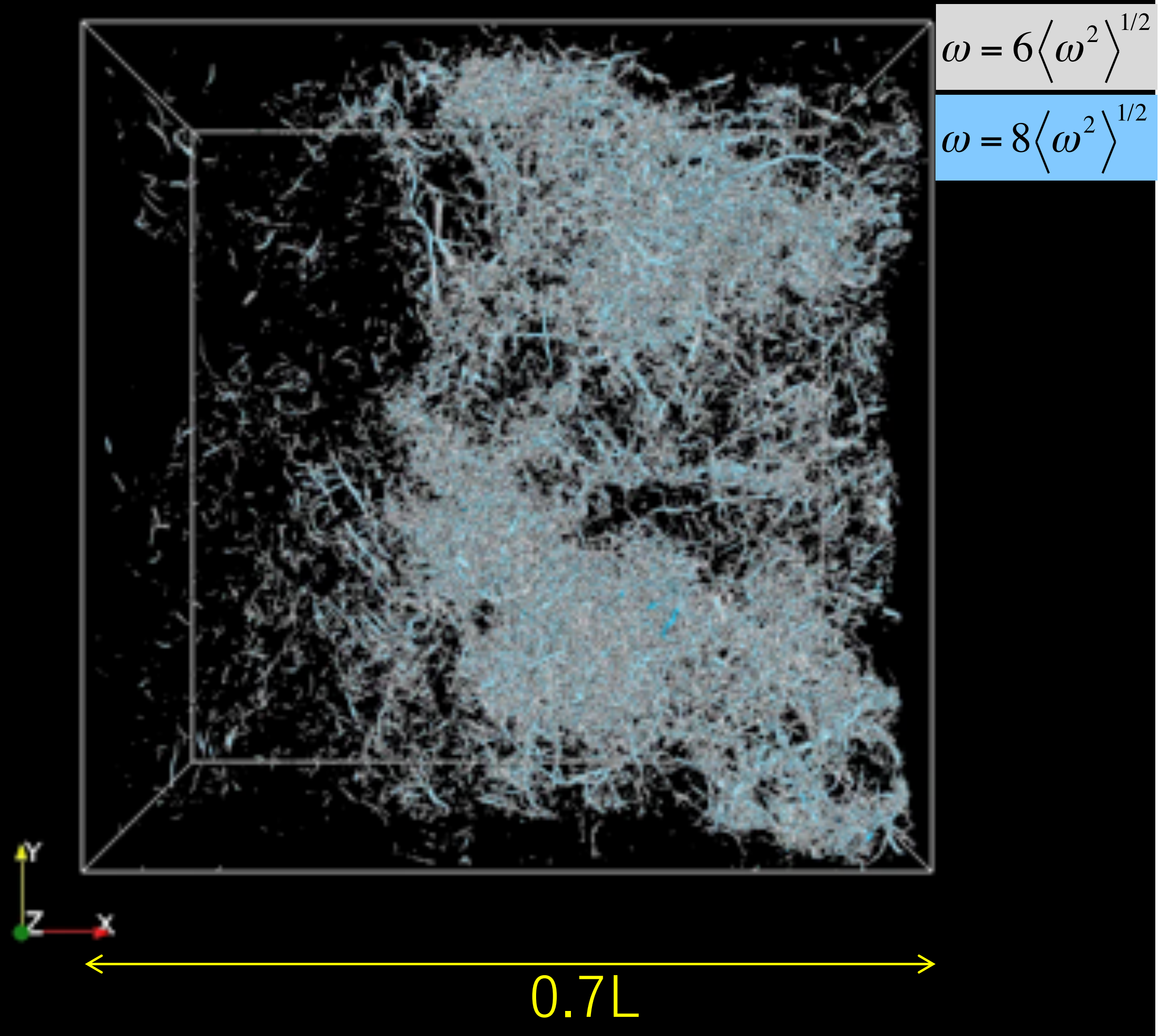

The most significant shear layer from $t = t_0$ to $t_0+10\tau$ $(=t_0+2.55\lambda/u_o)$

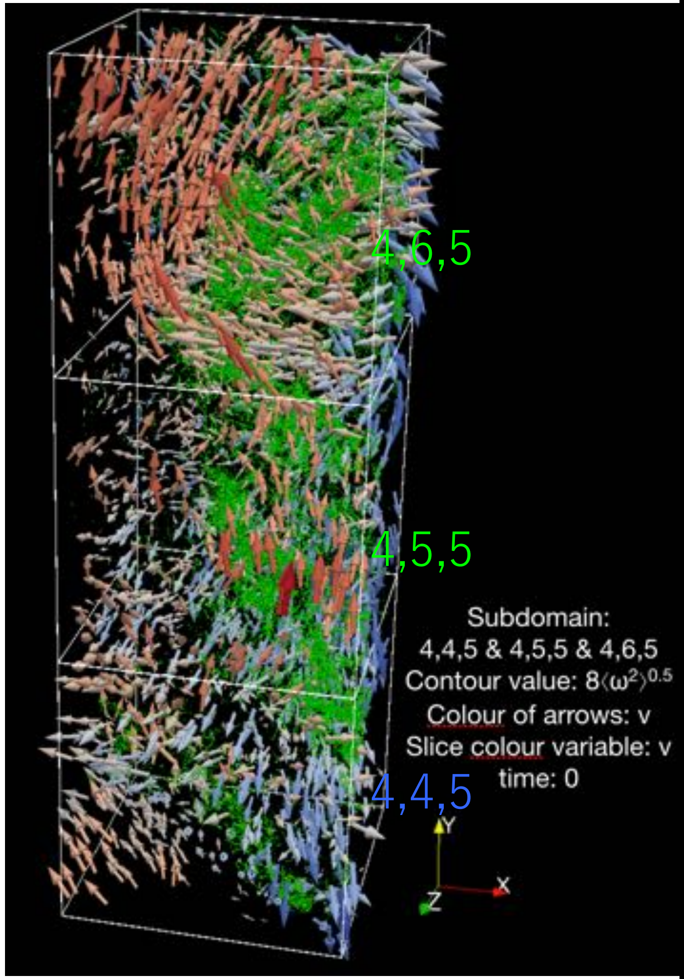

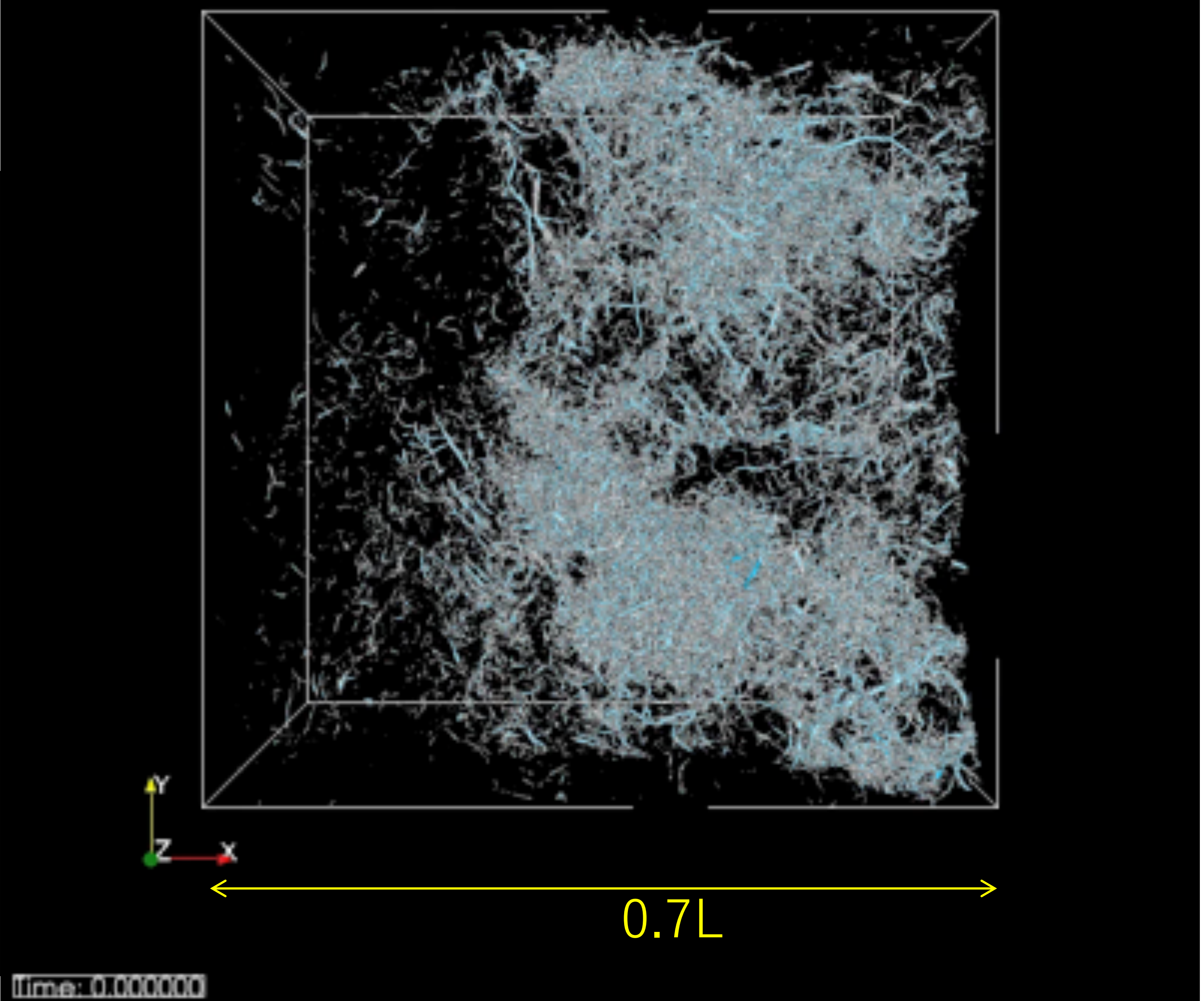

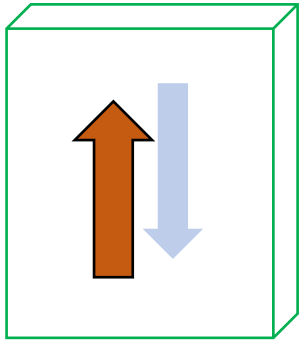

The extreme points ($\omega > 20\langle\omega^2\rangle^{1/2}$) in the most active subdomain

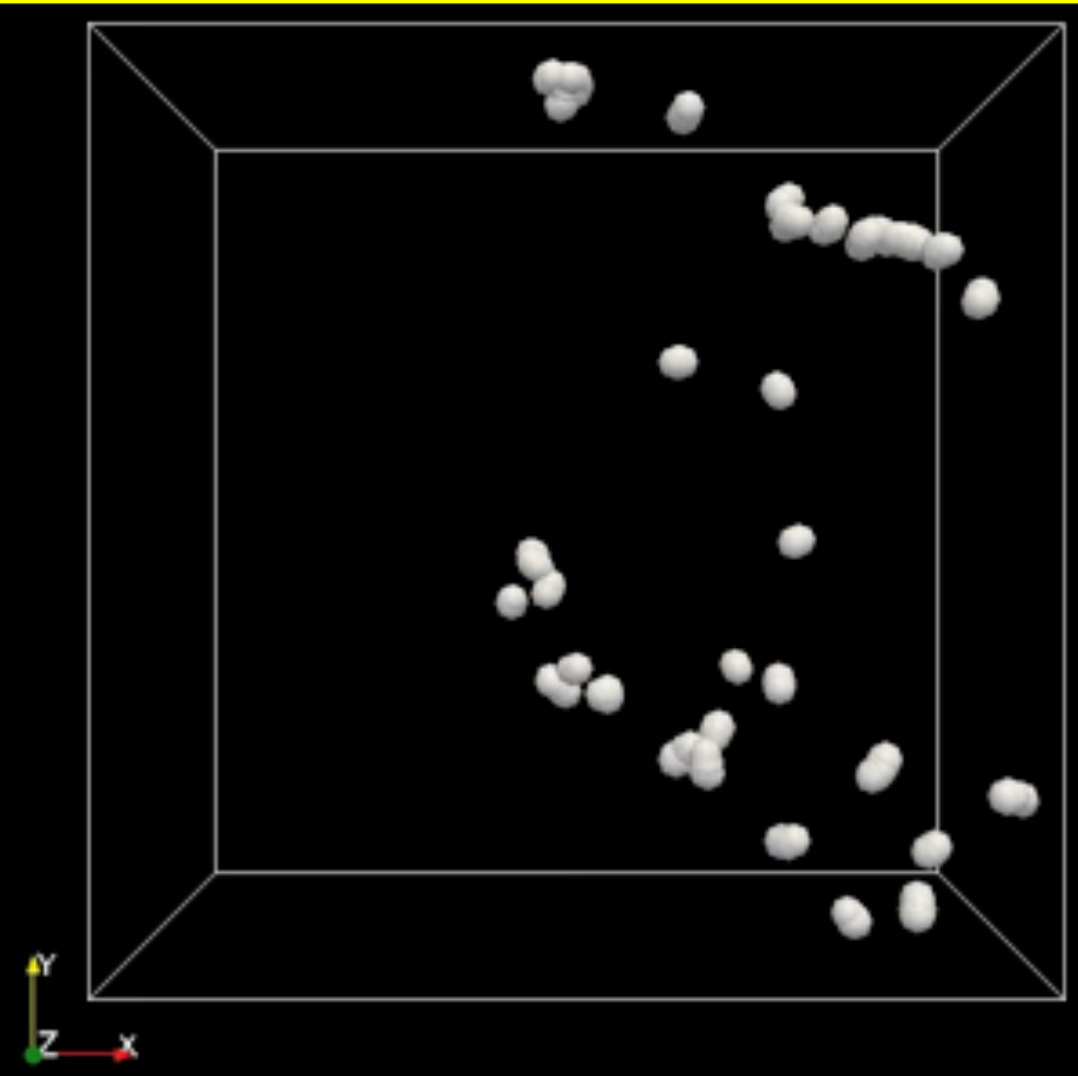

Generation of
Spikes of enstrophy

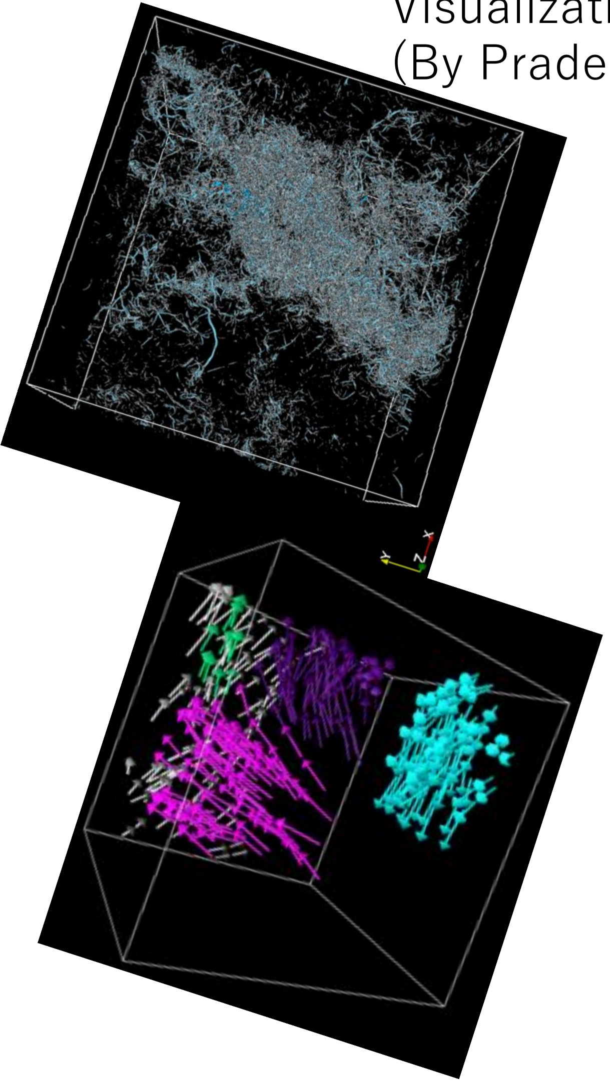

Visualization
(By Pradeep Jha)

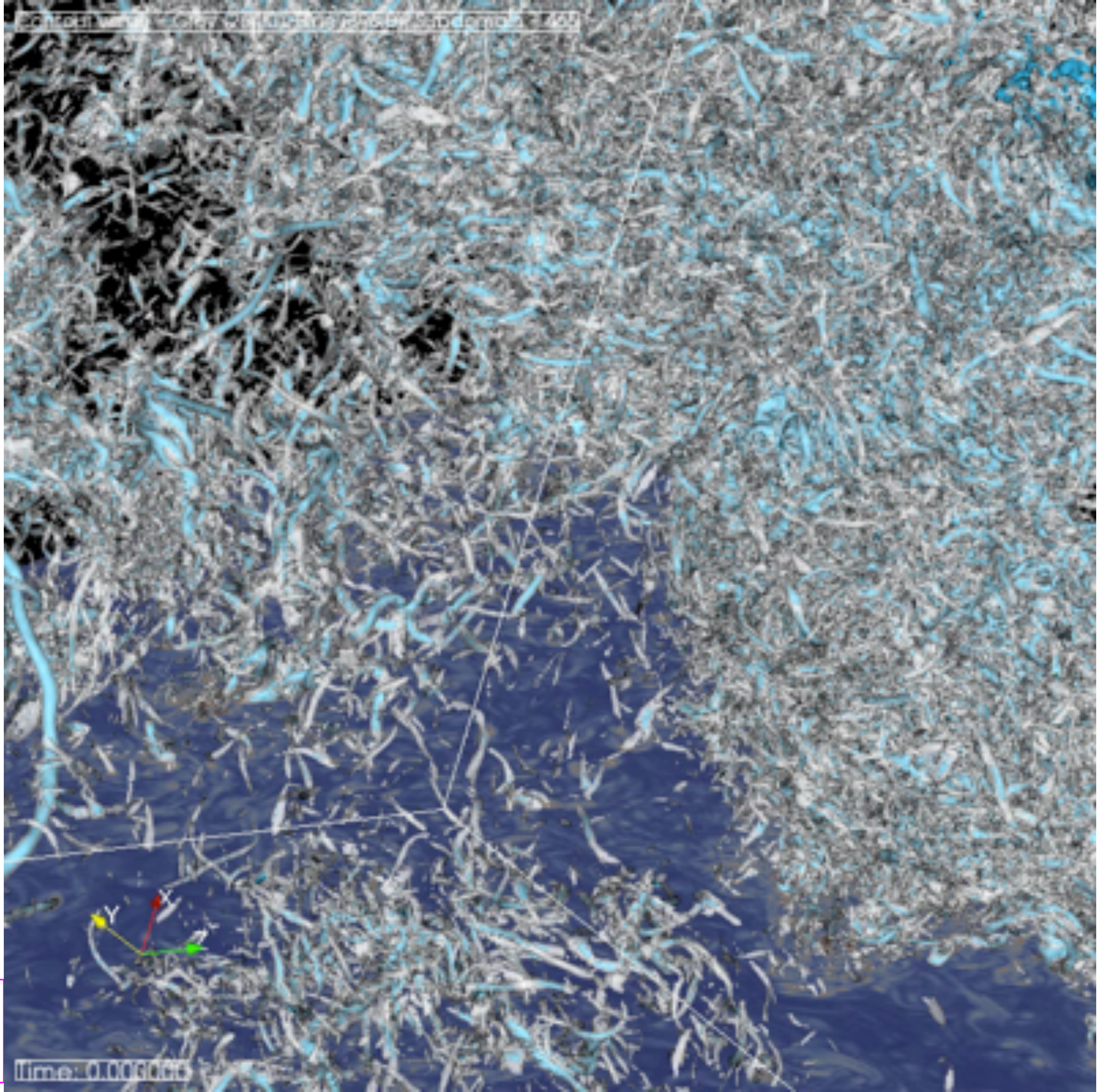

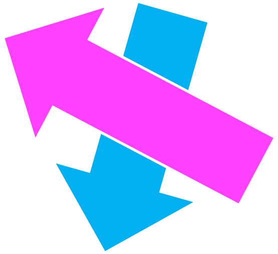

Large-scale shear
persists

Layer is deformed
Interface become less remarkable

465

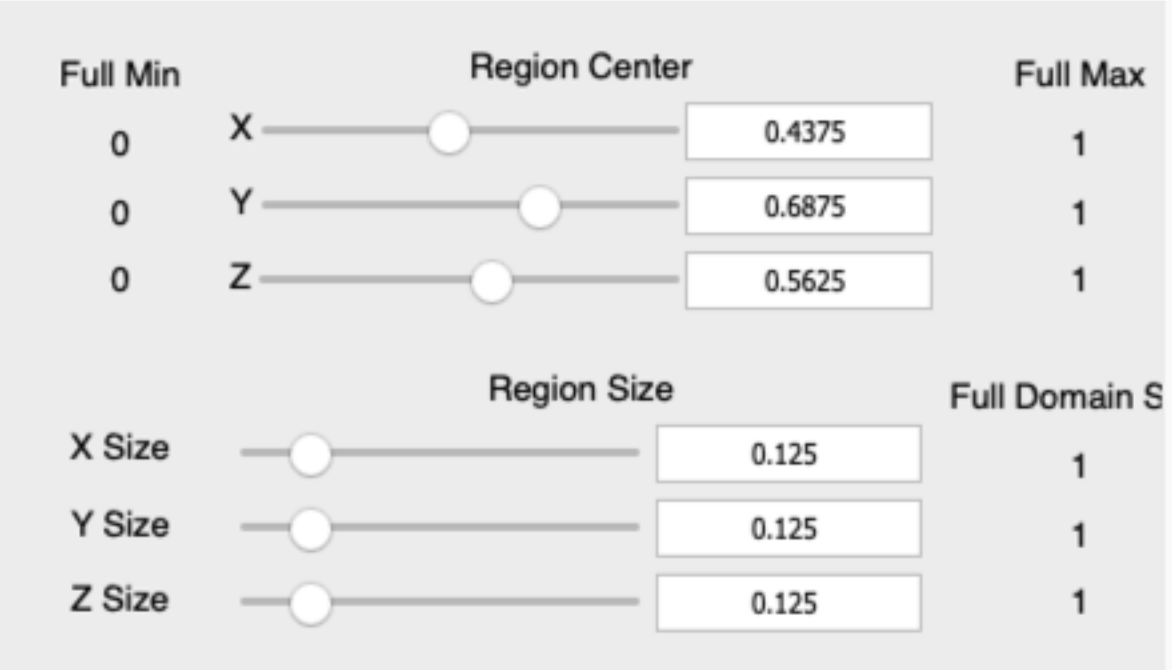

Full Min
Region Center
Full Max
X
Y
Z
0
0
0
0.4375
0.6875
0.5625
1
1
1
Region Size
Full Domain S
X Size
Y Size
Z Size
0.125
0.125
0.125
1
1
1

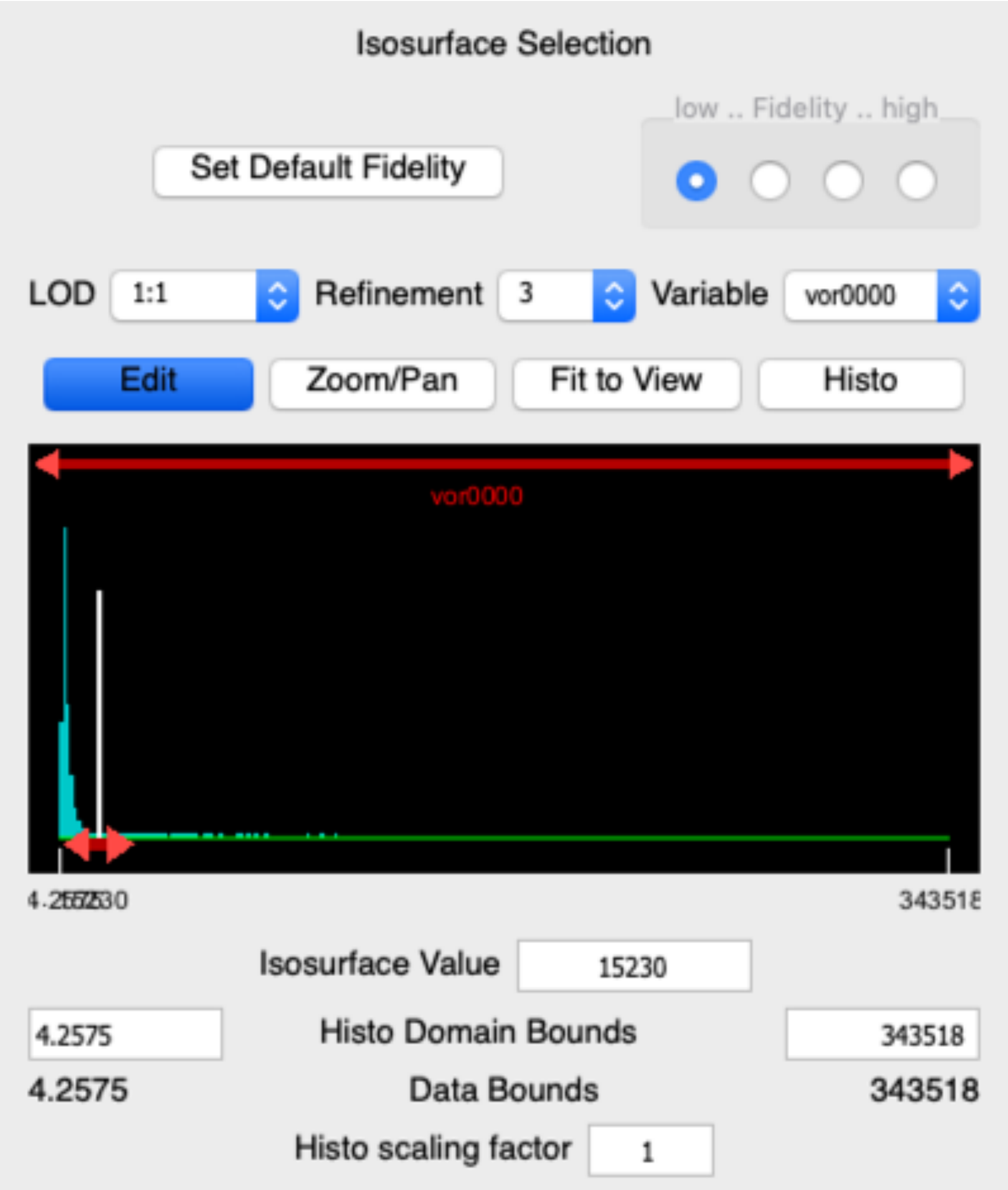

Isosurface Selection
low .. Fidelity .. high
Set Default Fidelity
LOD
1:1
Refinement
3
Variable
vor0000
Edit
Zoom/Pan
Fit to View
Histo
vor0000
343518
Isosurface Value
15230
4.2575
Histo Domain Bounds
343518
4.2575
Data Bounds
343518
Histo scaling factor
1

0

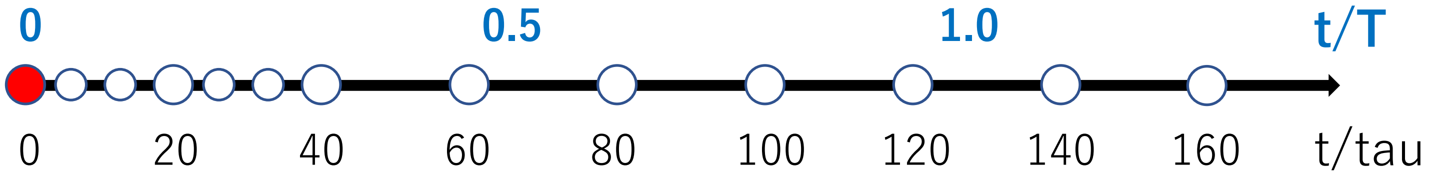

t/tau=0

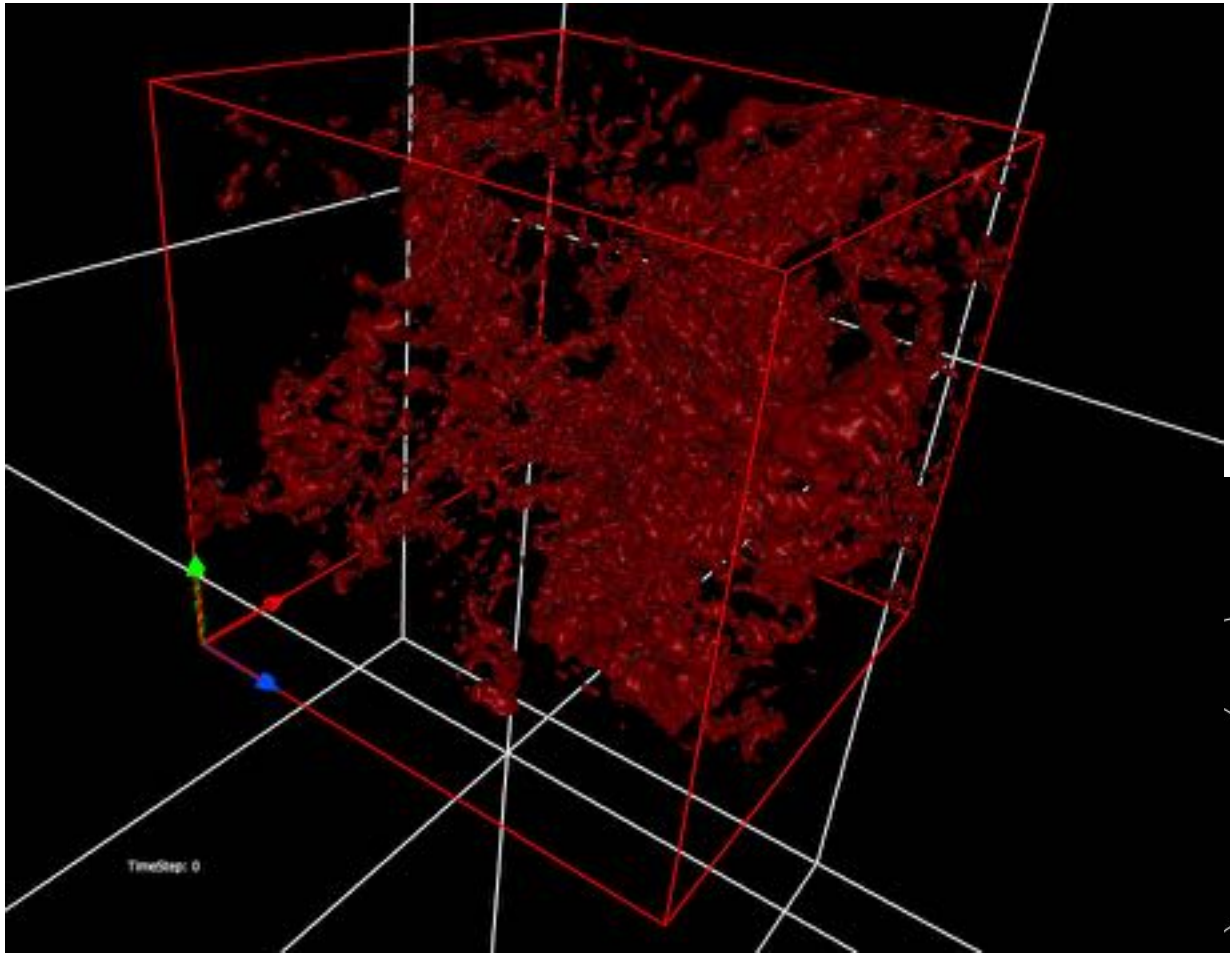

$\langle \omega^2/2 \rangle_{8\Delta x} > 7\Omega$

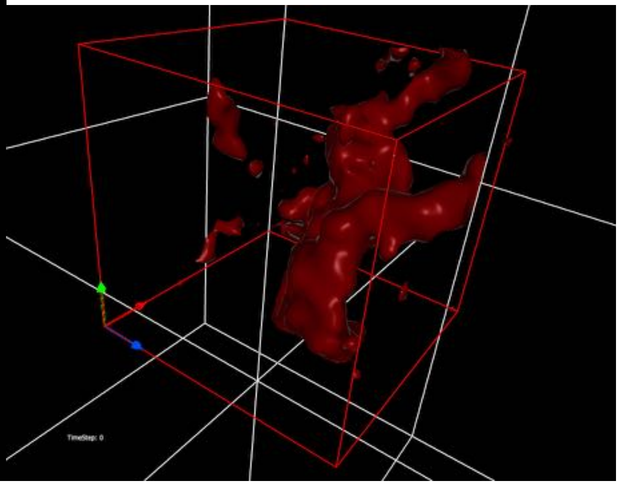

$\langle \omega^2/2 \rangle_{32\Delta x} = \langle \omega^2/2 \rangle_{1.4\lambda} > 7\Omega$

400

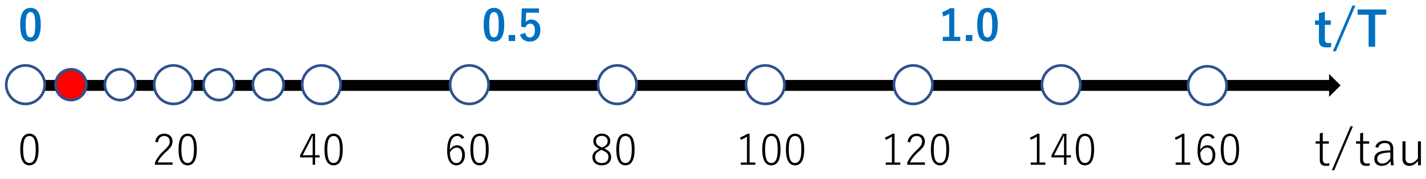

t/tau=6.7

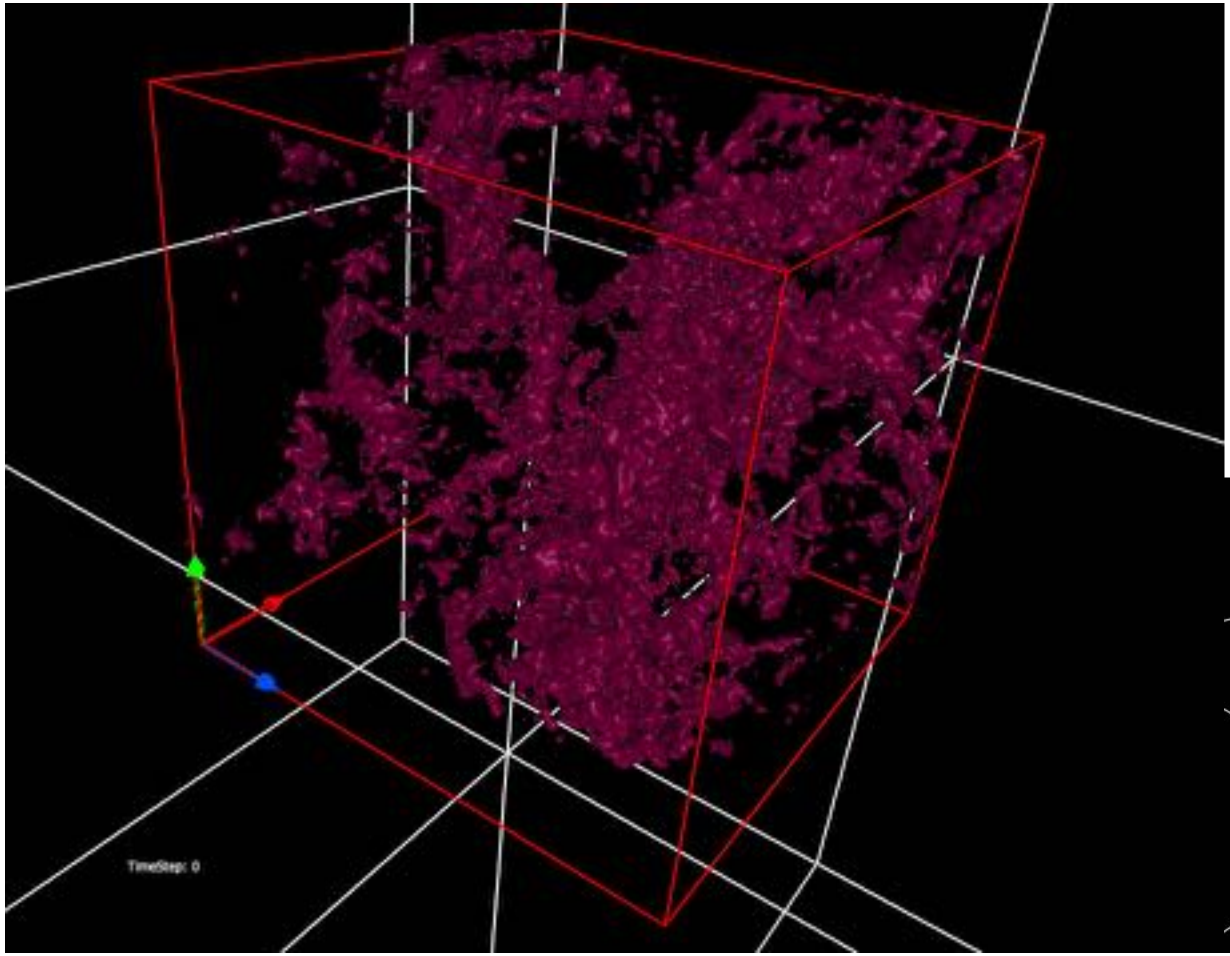

$\langle \omega^2/2 \rangle_{8\Delta x} > 7\Omega$

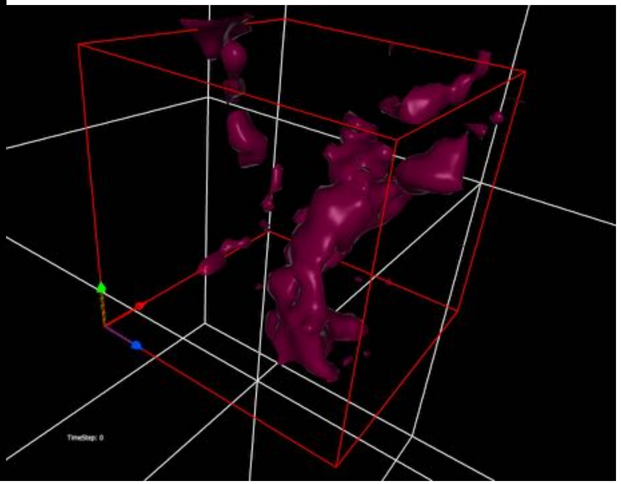

$\langle \omega^2/2 \rangle_{32\Delta x} = \langle \omega^2/2 \rangle_{1.4\lambda} > 7\Omega$

800

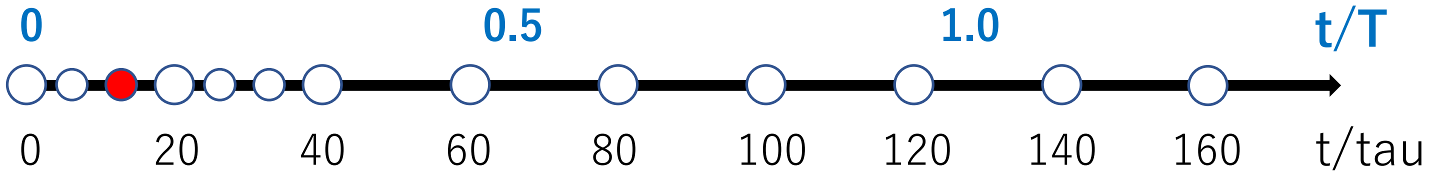

t/tau=13.3

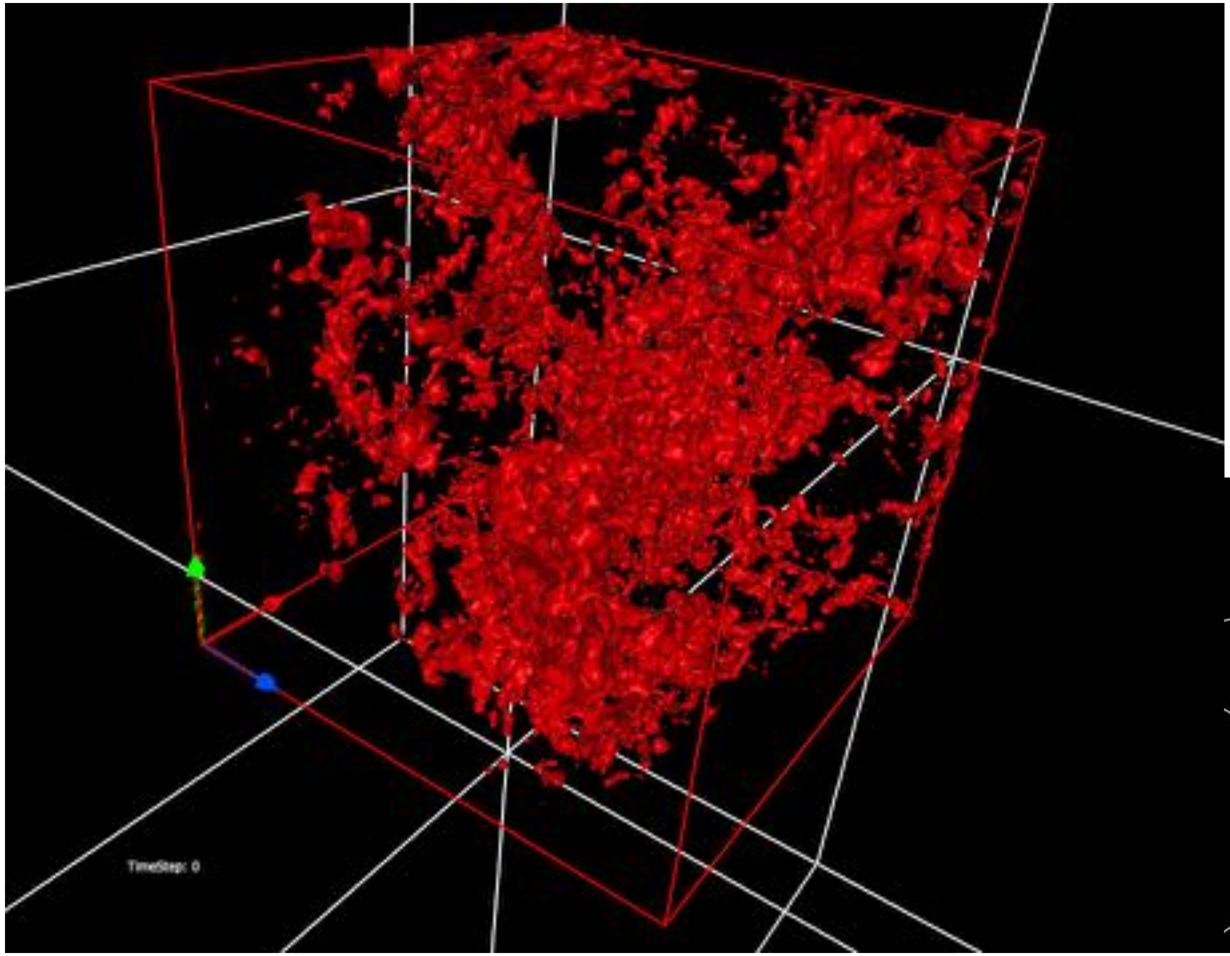

$\langle \omega^2/2 \rangle_{8\Delta x} > 7\Omega$

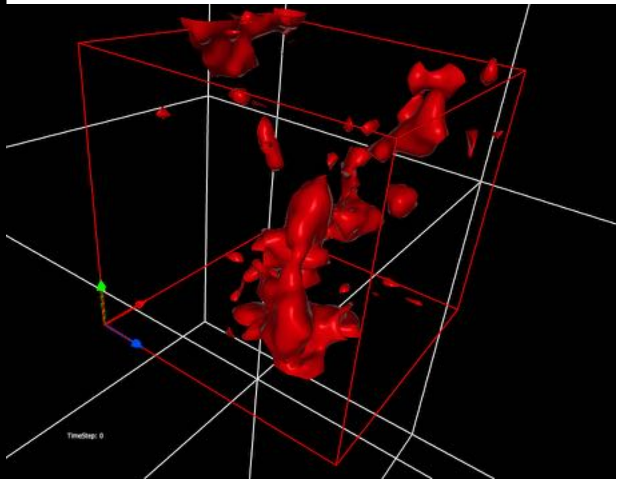

$\langle \omega^2/2 \rangle_{32\Delta x} = \langle \omega^2/2 \rangle_{1.4\lambda} > 7\Omega$

1200

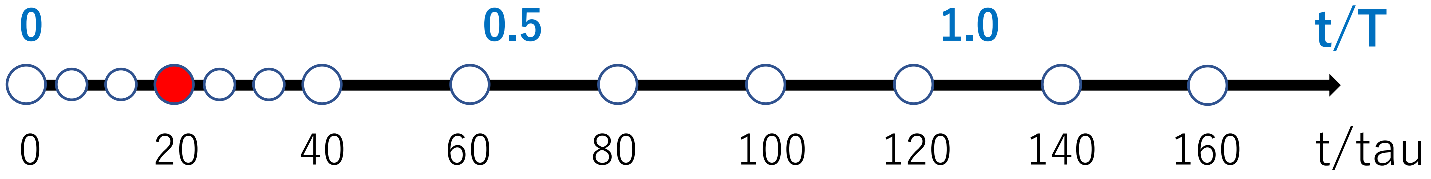

t/tau=20

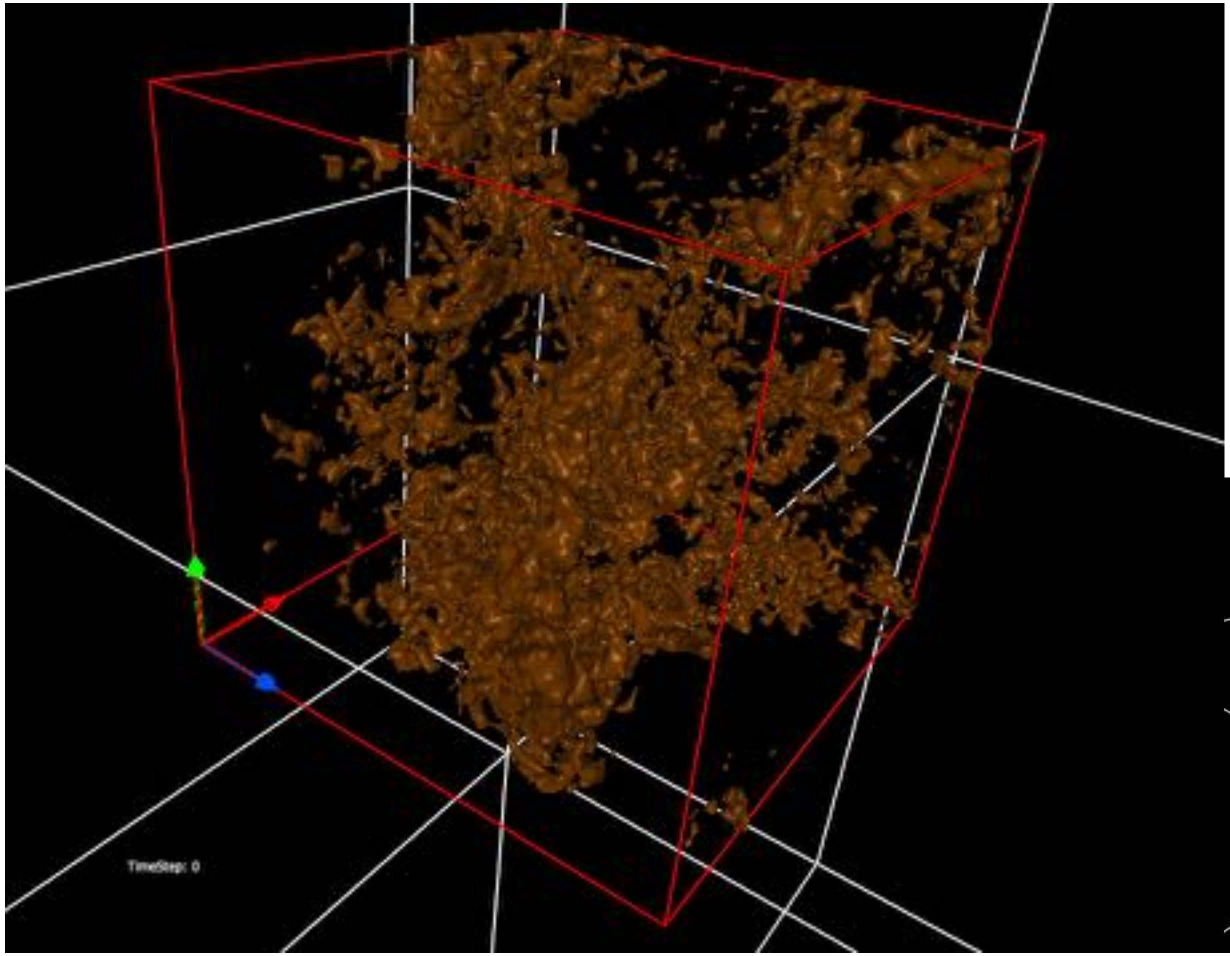

$\langle \omega^2/2 \rangle_{8\Delta x} > 7\Omega$

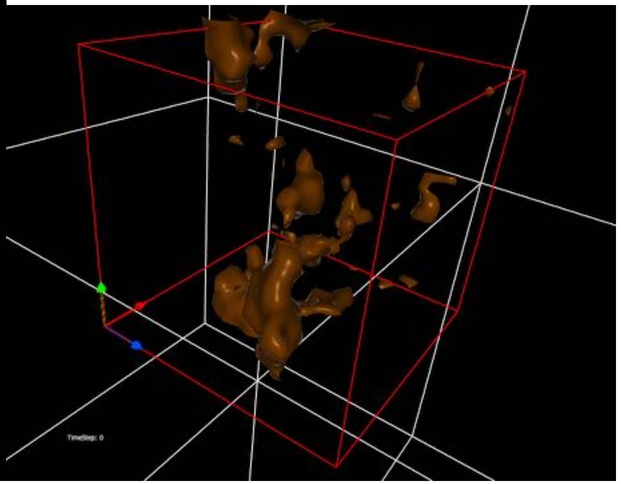

$\langle \omega^2/2 \rangle_{32\Delta x} = \langle \omega^2/2 \rangle_{1.4\lambda} > 7\Omega$

1600

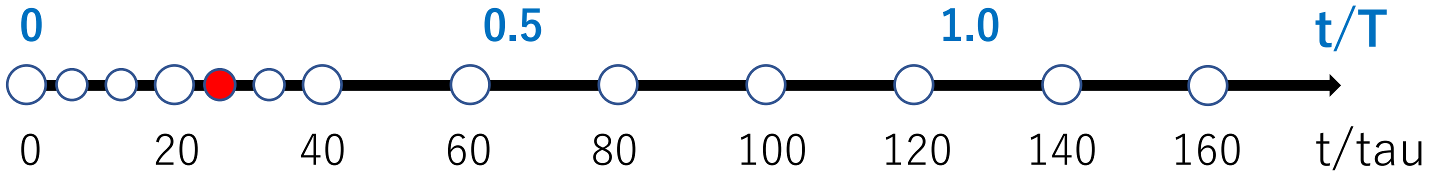

t/tau=26.7

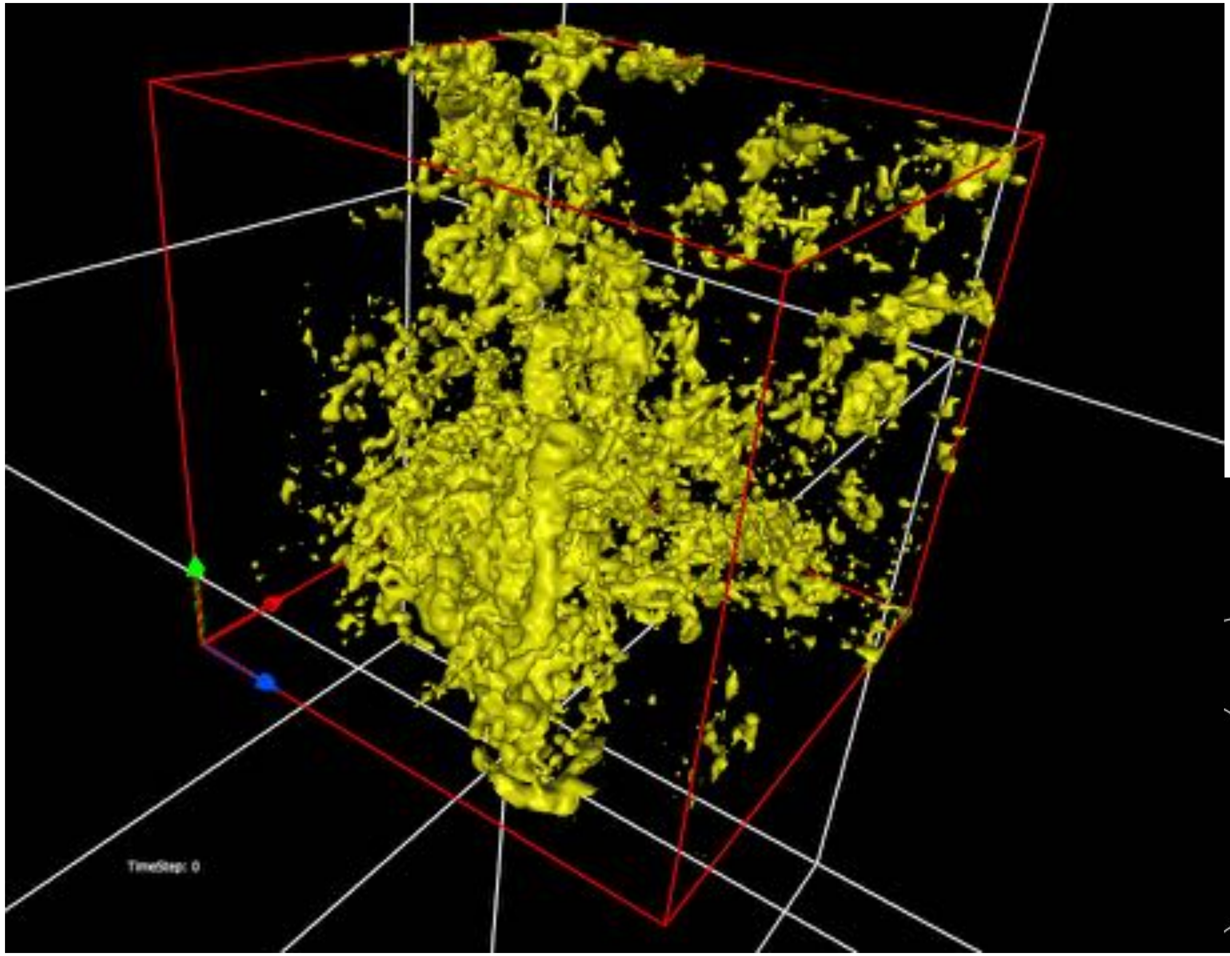

$\langle \omega^2/2 \rangle_{8\Delta x} > 7\Omega$

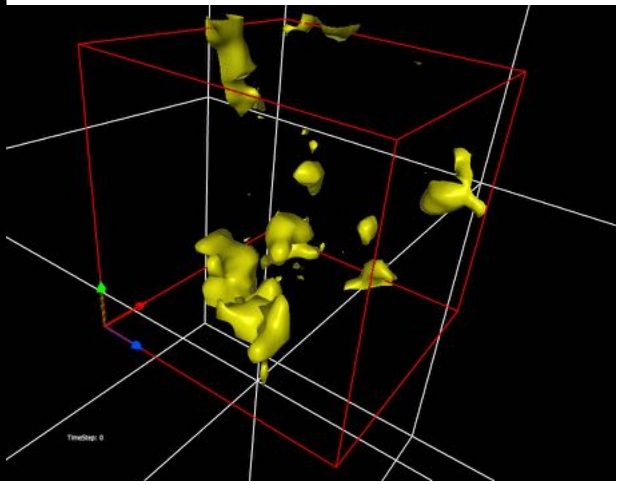

$\langle \omega^2/2 \rangle_{32\Delta x} = \langle \omega^2/2 \rangle_{1.4\lambda} > 7\Omega$

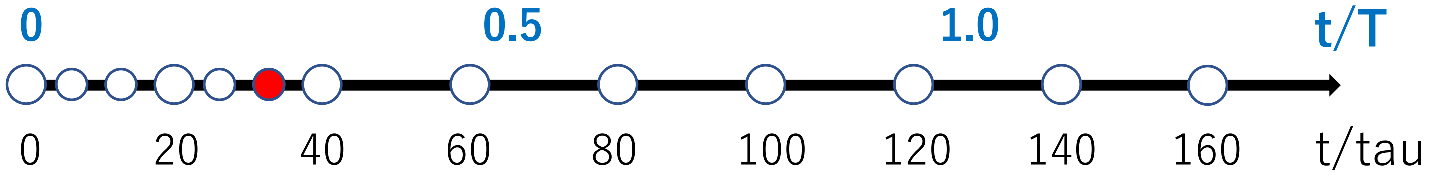

2000

t/tau=33.3

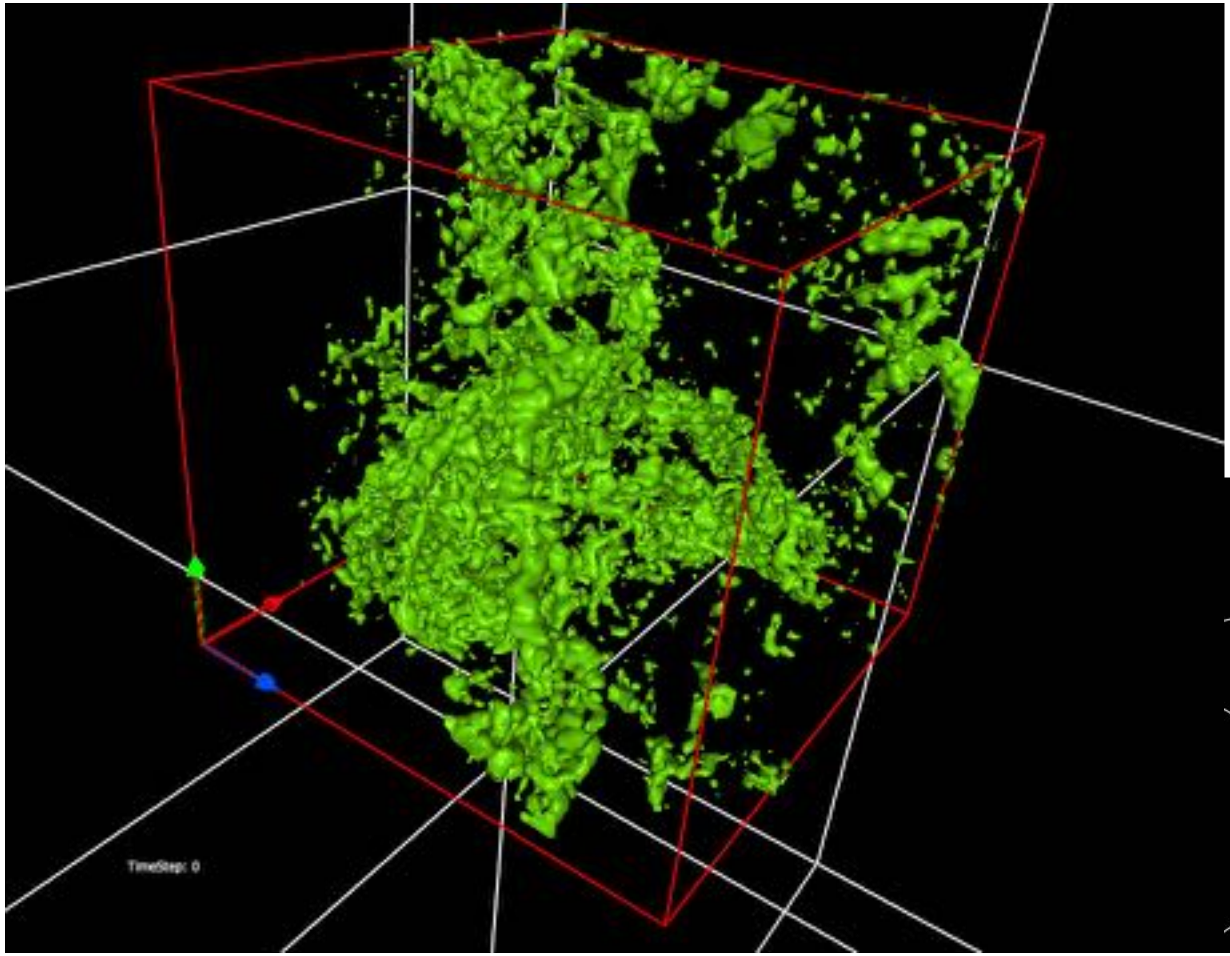

$\langle \omega^2/2 \rangle_{8\Delta x} > 7\Omega$

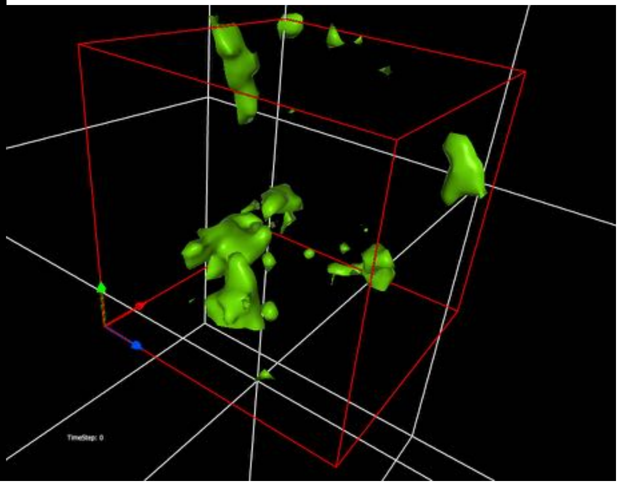

$\langle \omega^2/2 \rangle_{32\Delta x} = \langle \omega^2/2 \rangle_{1.4\lambda} > 7\Omega$

2400

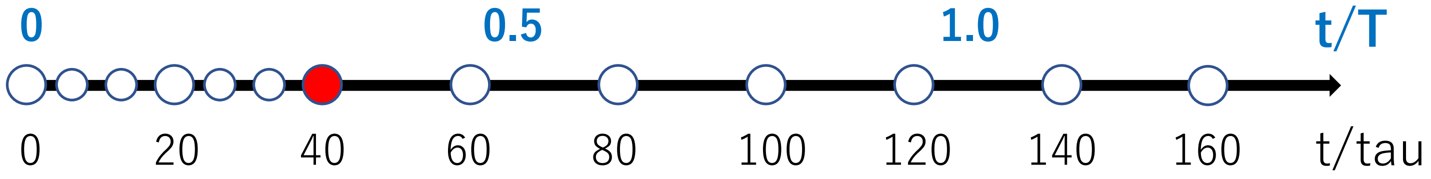

t/tau=40

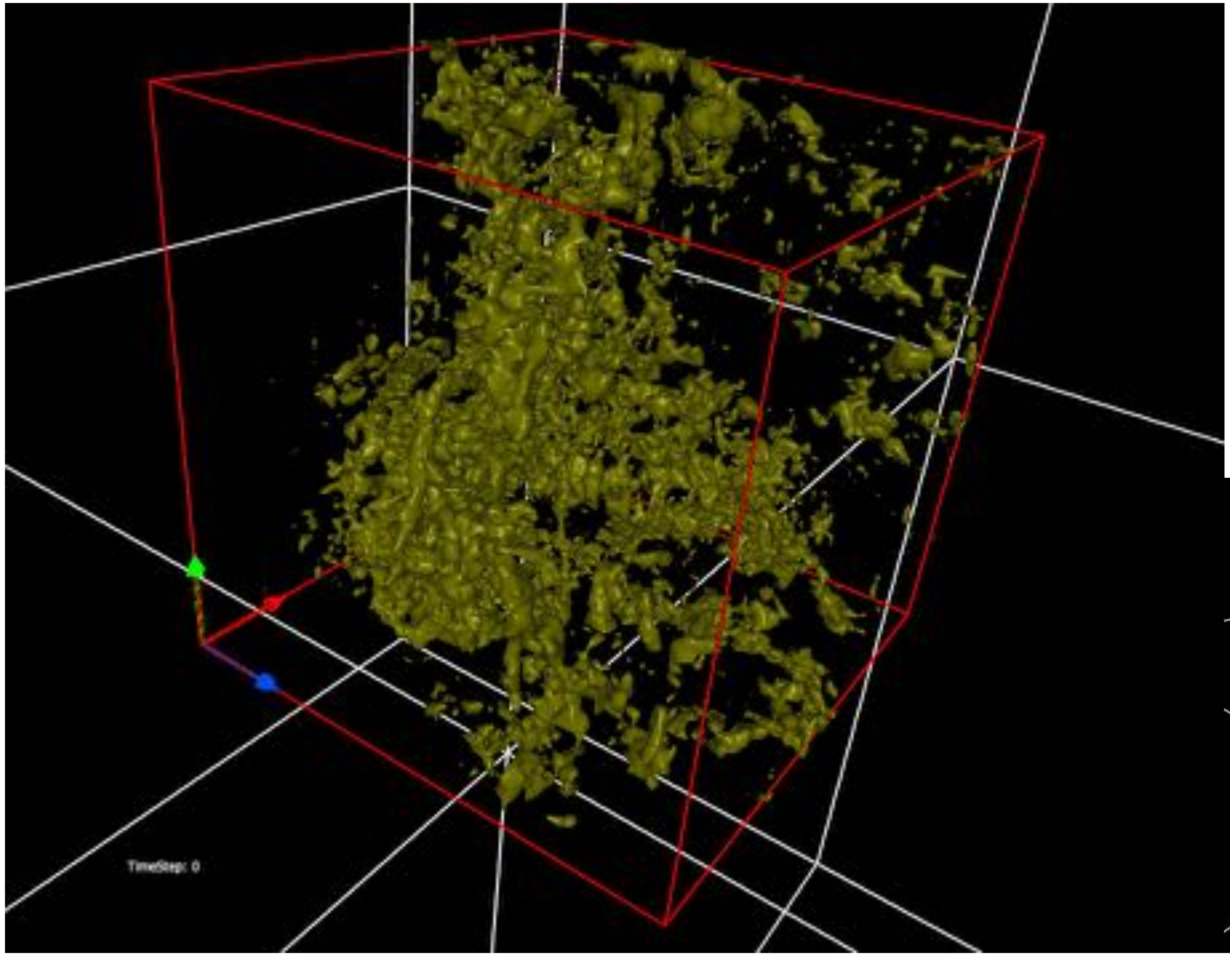

$\langle \omega^2/2 \rangle_{8\Delta x} > 7\Omega$

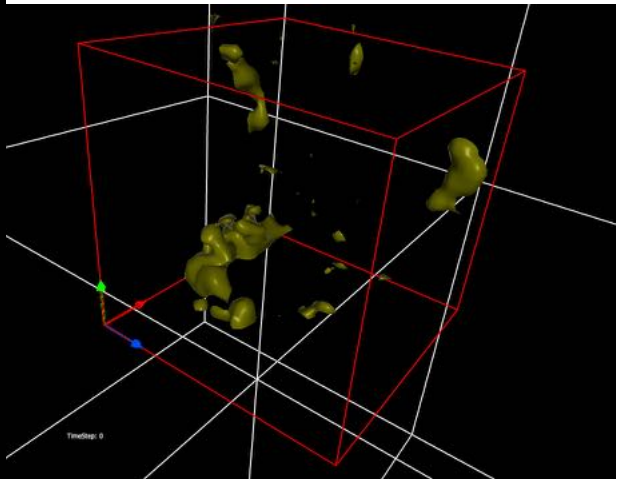

$\langle \omega^2/2 \rangle_{32\Delta x} = \langle \omega^2/2 \rangle_{1.4\lambda} > 7\Omega$

3600

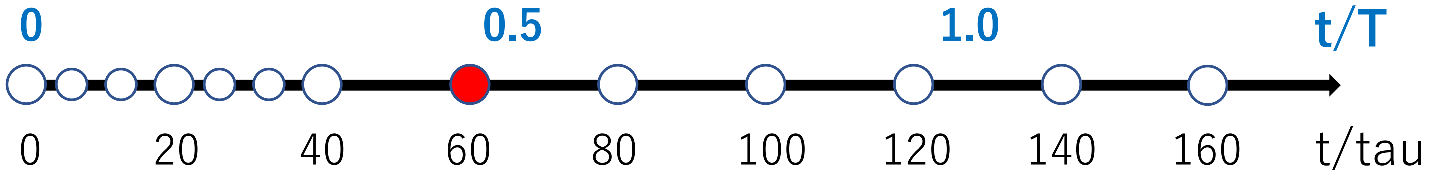

t/tau=60

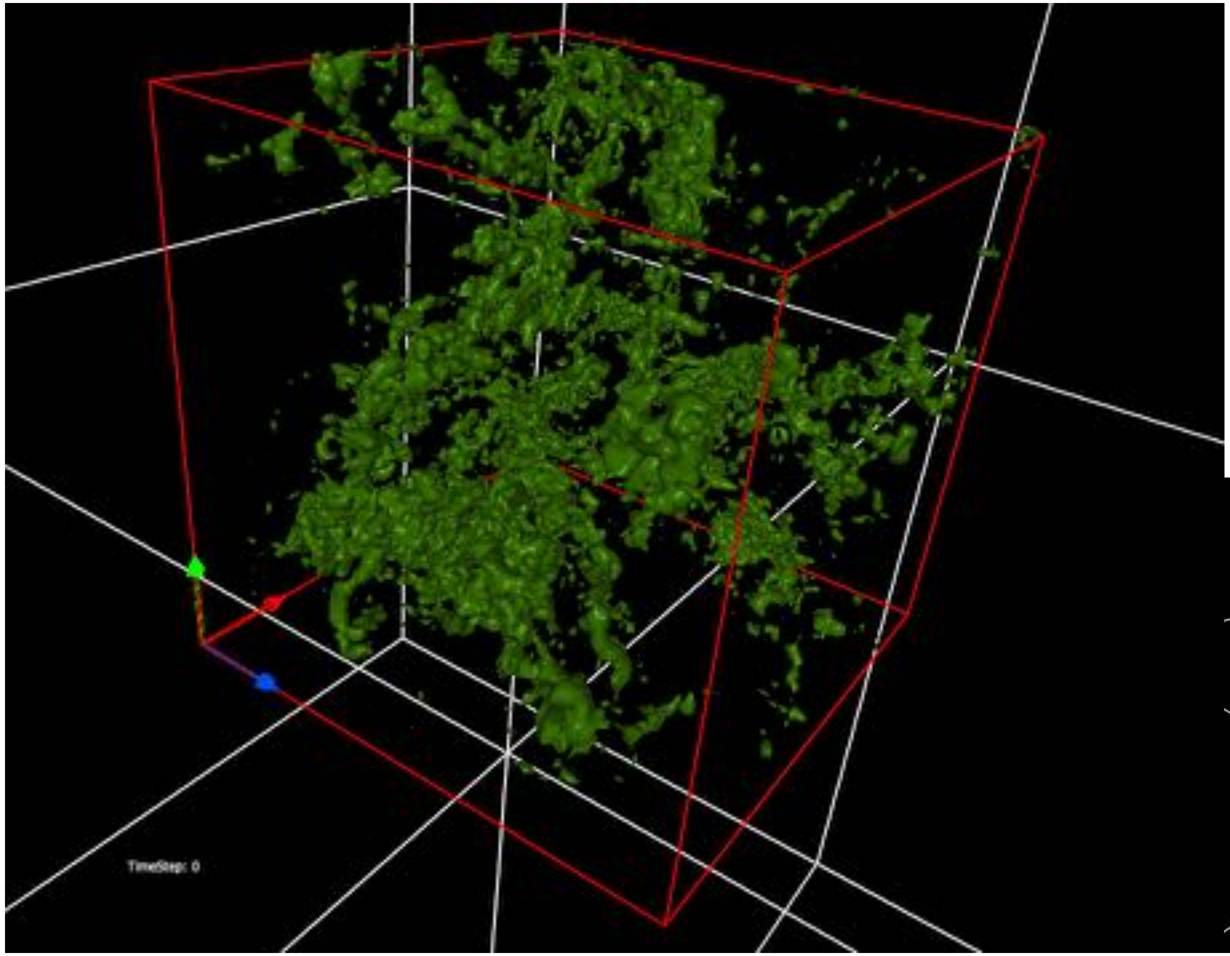

$\langle \omega^2/2 \rangle_{8\Delta x} > 7\Omega$

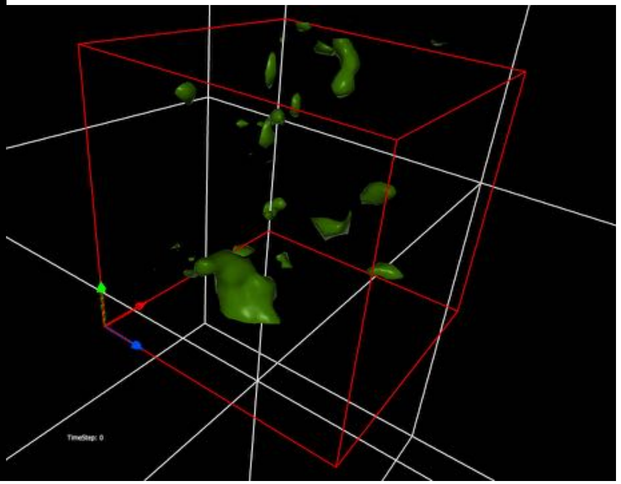

$\langle \omega^2/2 \rangle_{32\Delta x} = \langle \omega^2/2 \rangle_{1.4\lambda} > 7\Omega$

4800

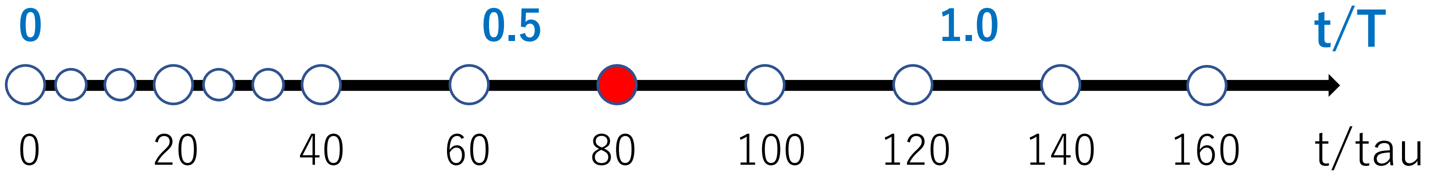

t/tau=80

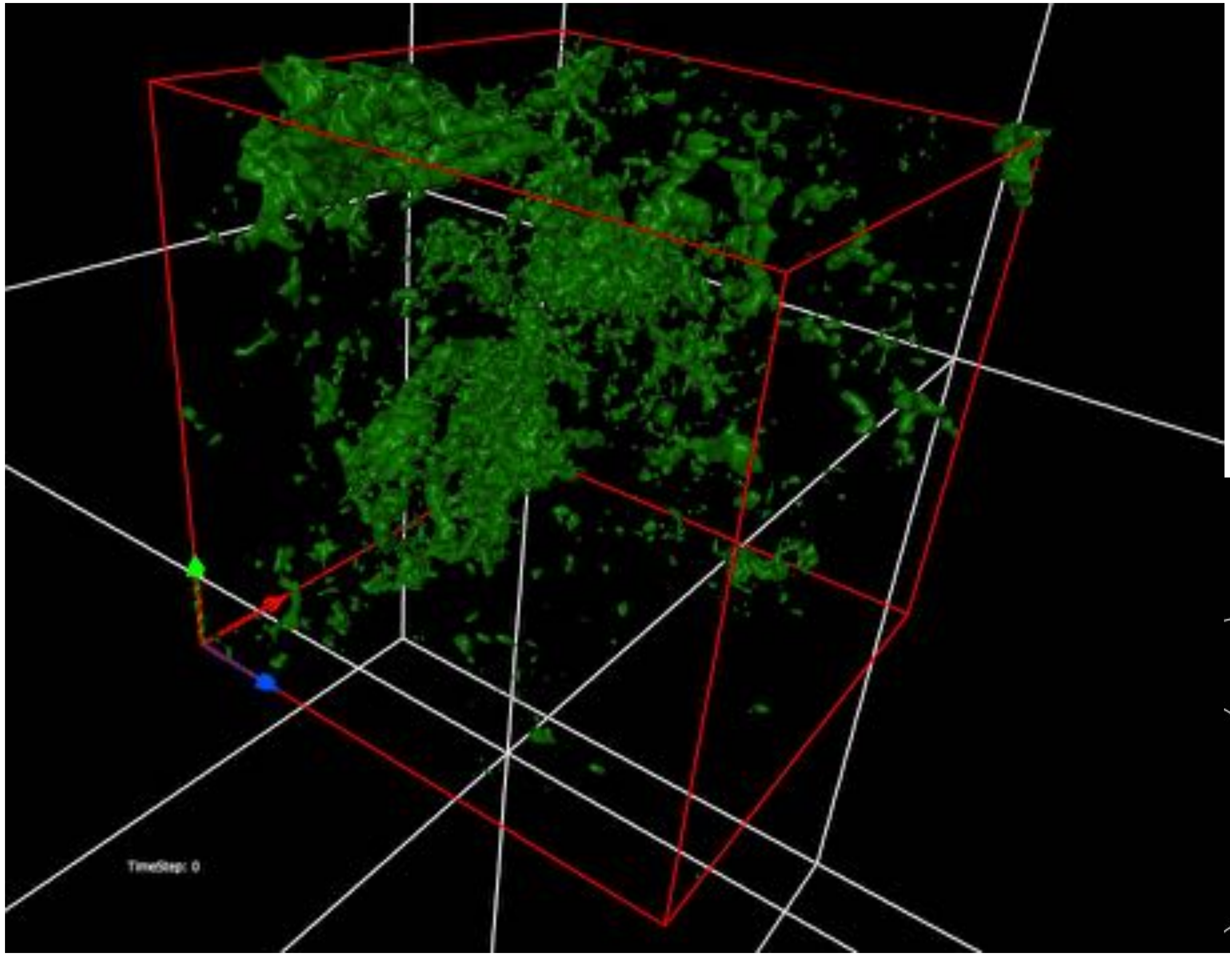

$\langle \omega^2/2 \rangle_{8\Delta x} > 7\Omega$

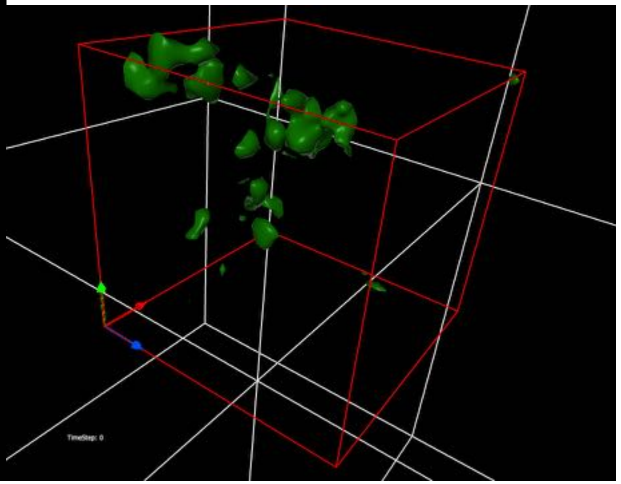

$\langle \omega^2/2 \rangle_{32\Delta x} = \langle \omega^2/2 \rangle_{1.4\lambda} > 7\Omega$

6000

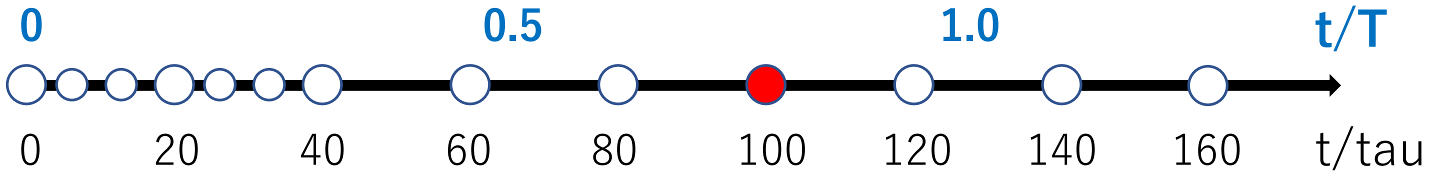

t/tau=100

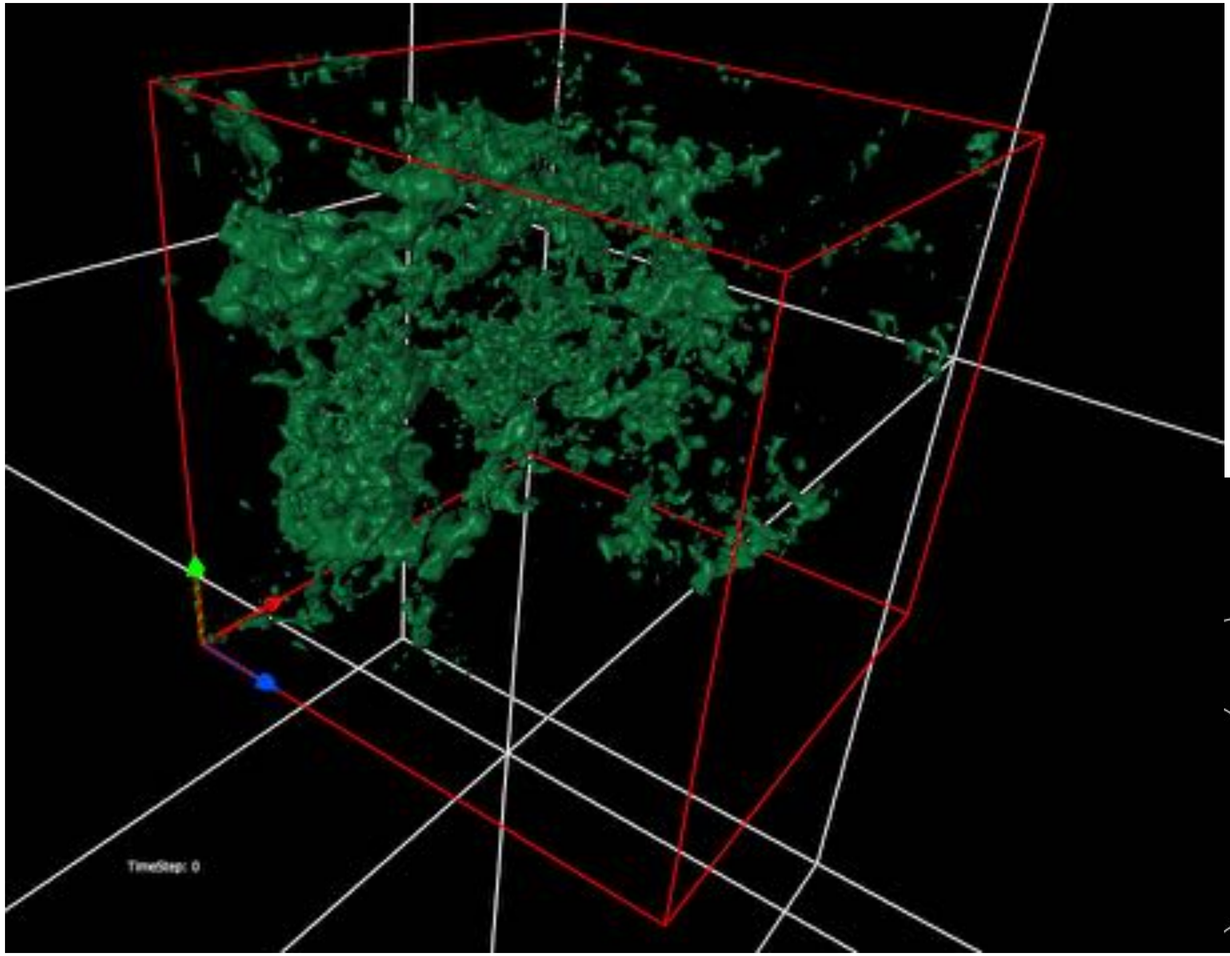

$\langle \omega^2/2 \rangle_{8\Delta x} > 7\Omega$

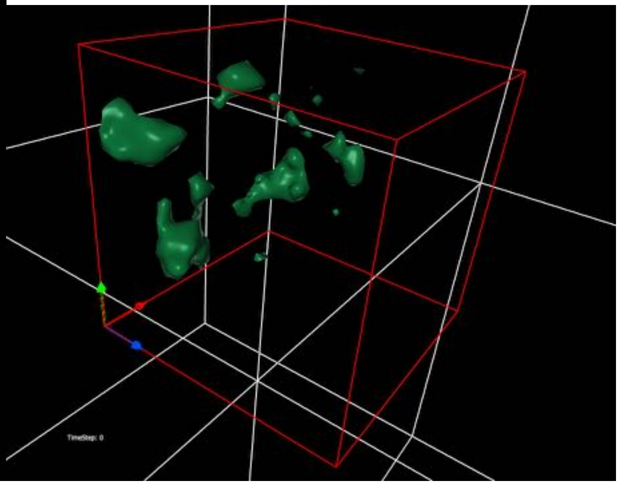

$\langle \omega^2/2 \rangle_{32\Delta x} = \langle \omega^2/2 \rangle_{1.4\lambda} > 7\Omega$

7200

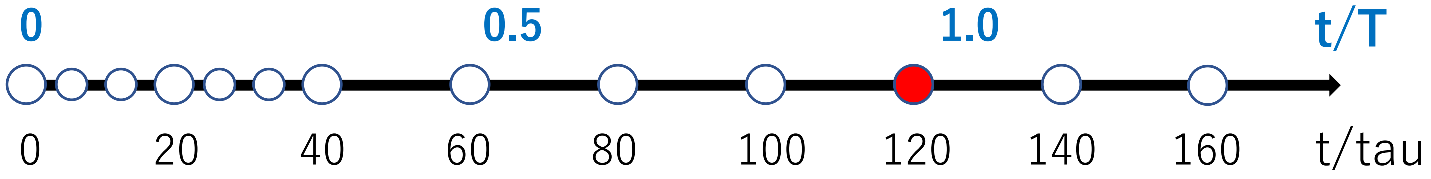

t/tau=120

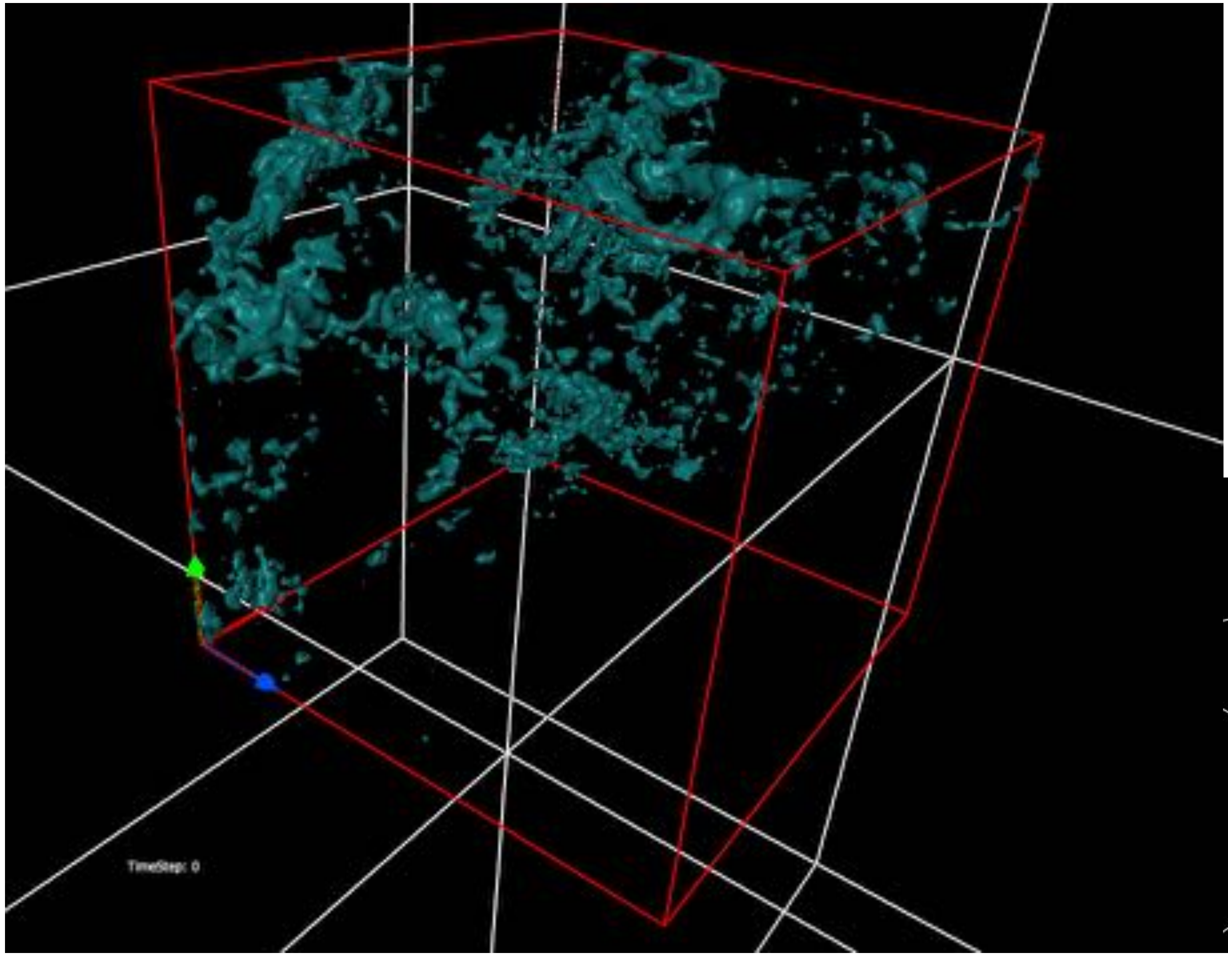

$\langle \omega^2/2 \rangle_{8\Delta x} > 7\Omega$

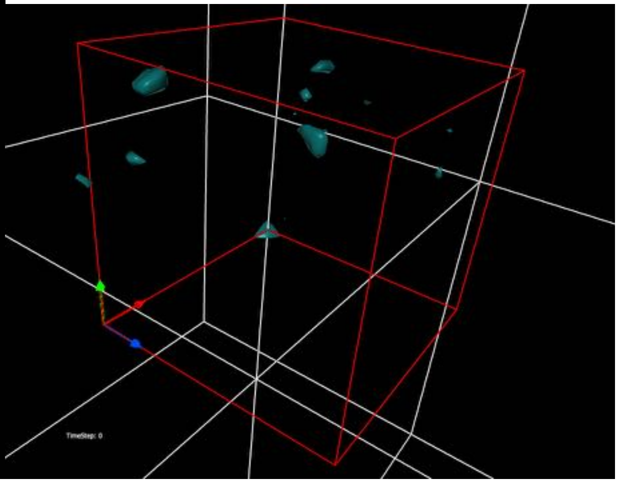

$\langle \omega^2/2 \rangle_{32\Delta x} = \langle \omega^2/2 \rangle_{1.4\lambda} > 7\Omega$

8400

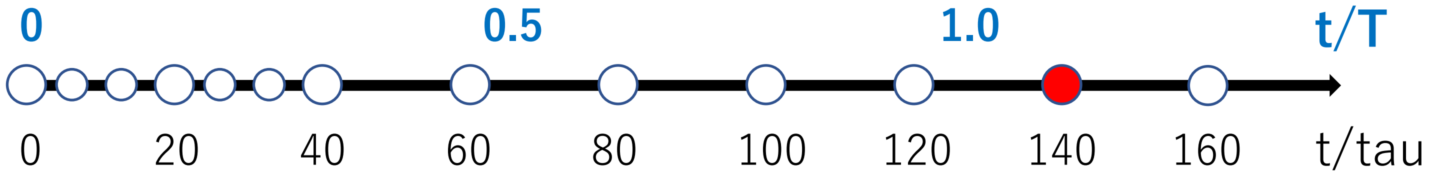

t/tau=140

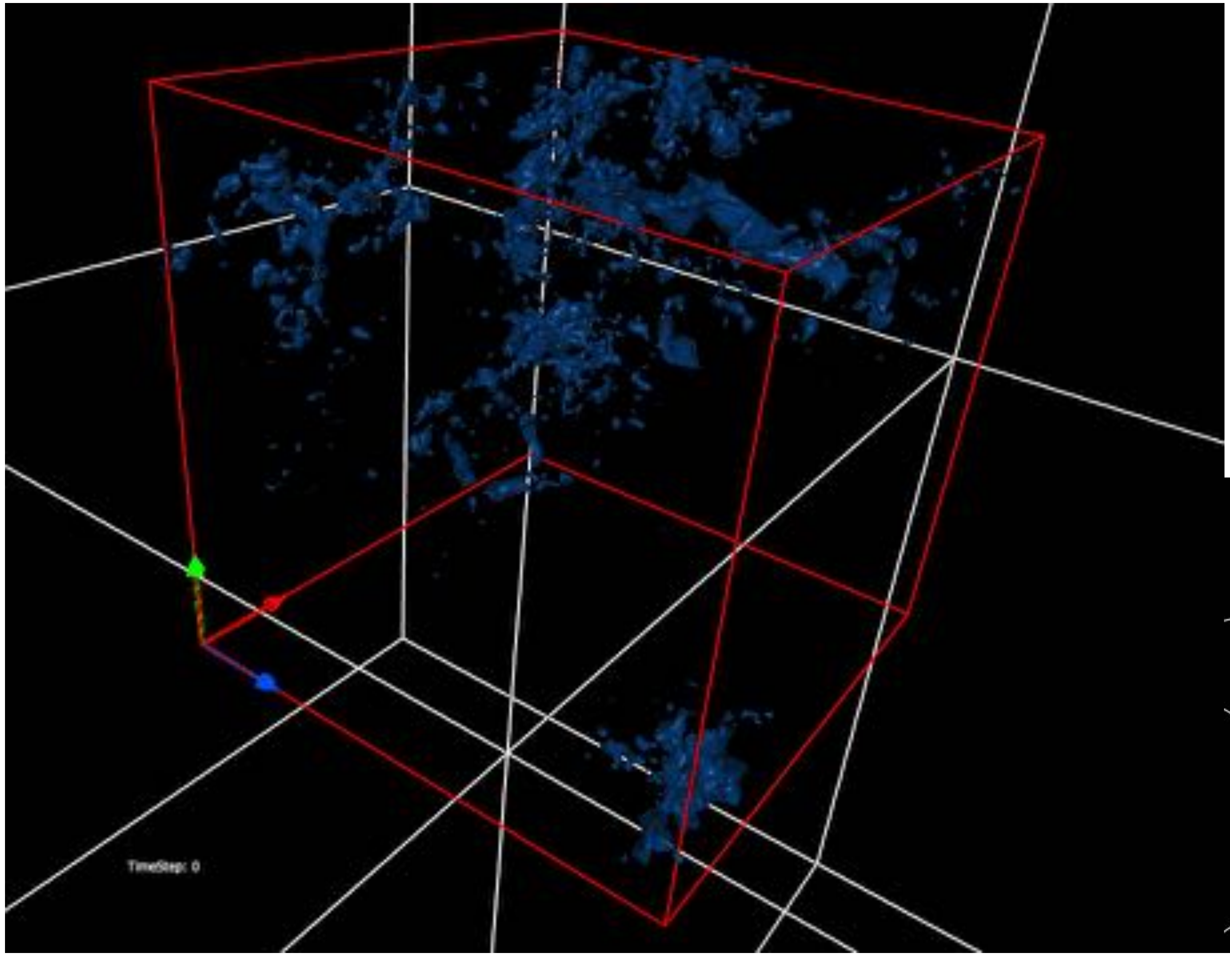

$\langle \omega^2/2 \rangle_{8\Delta x} > 7\Omega$

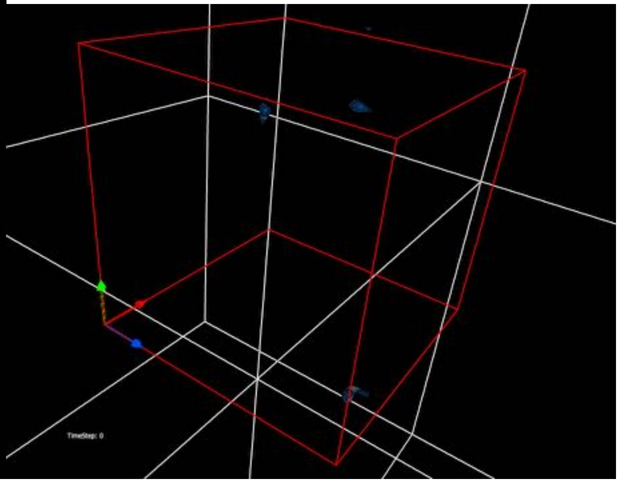

$\langle \omega^2/2 \rangle_{32\Delta x} = \langle \omega^2/2 \rangle_{1.4\lambda} > 7\Omega$

9600

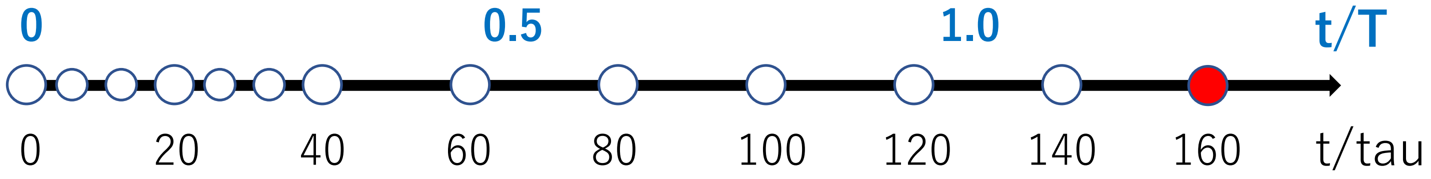

t/tau=160

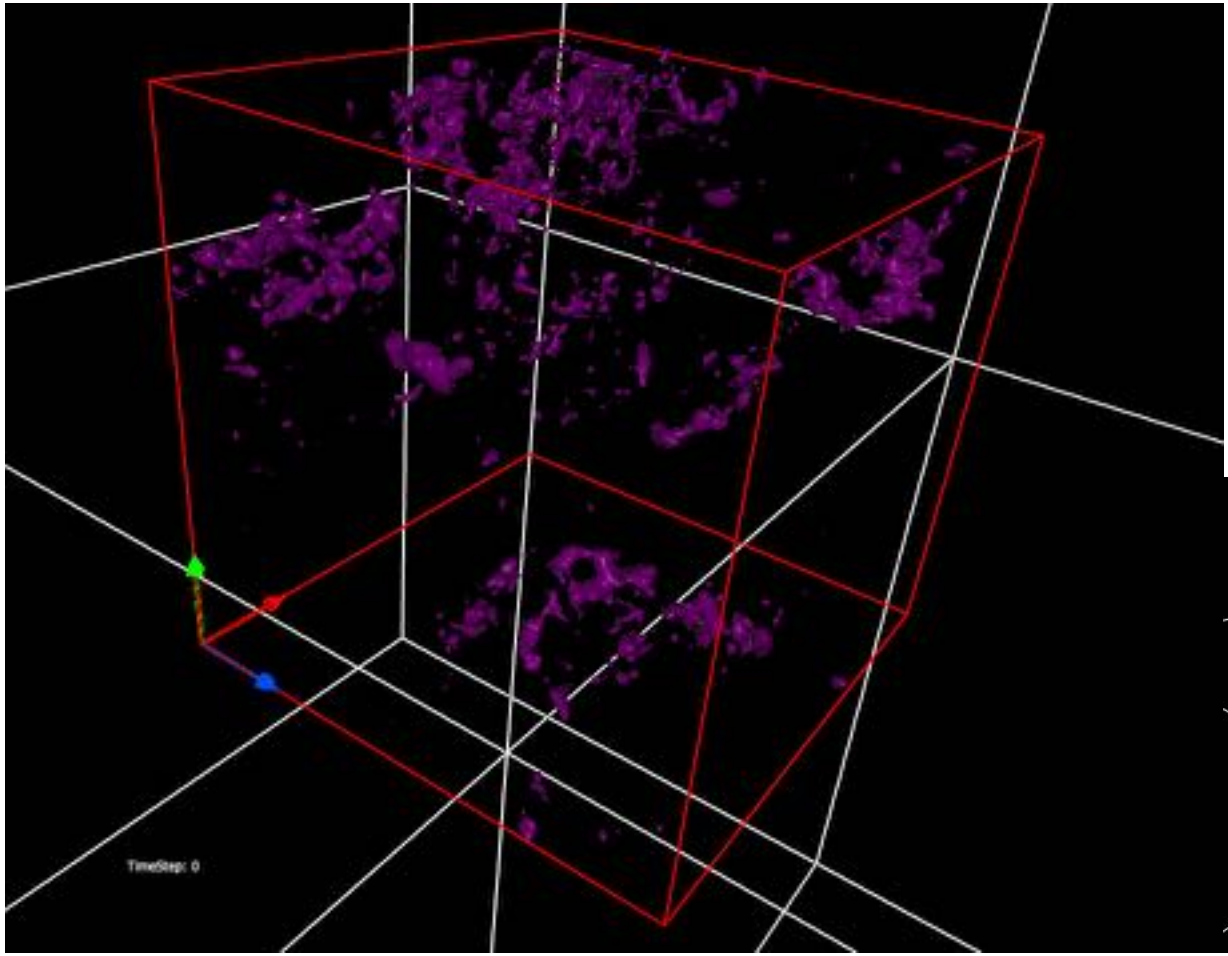

$\langle \omega^2/2 \rangle_{8\Delta x} > 7\Omega$

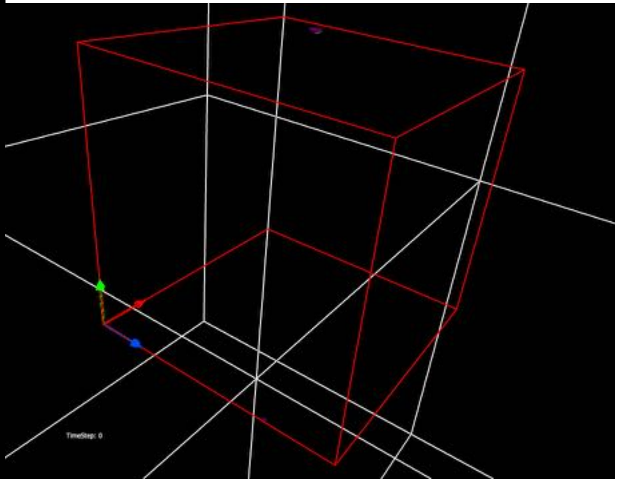

$\langle \omega^2/2 \rangle_{32\Delta x} = \langle \omega^2/2 \rangle_{1.4\lambda} > 7\Omega$

545

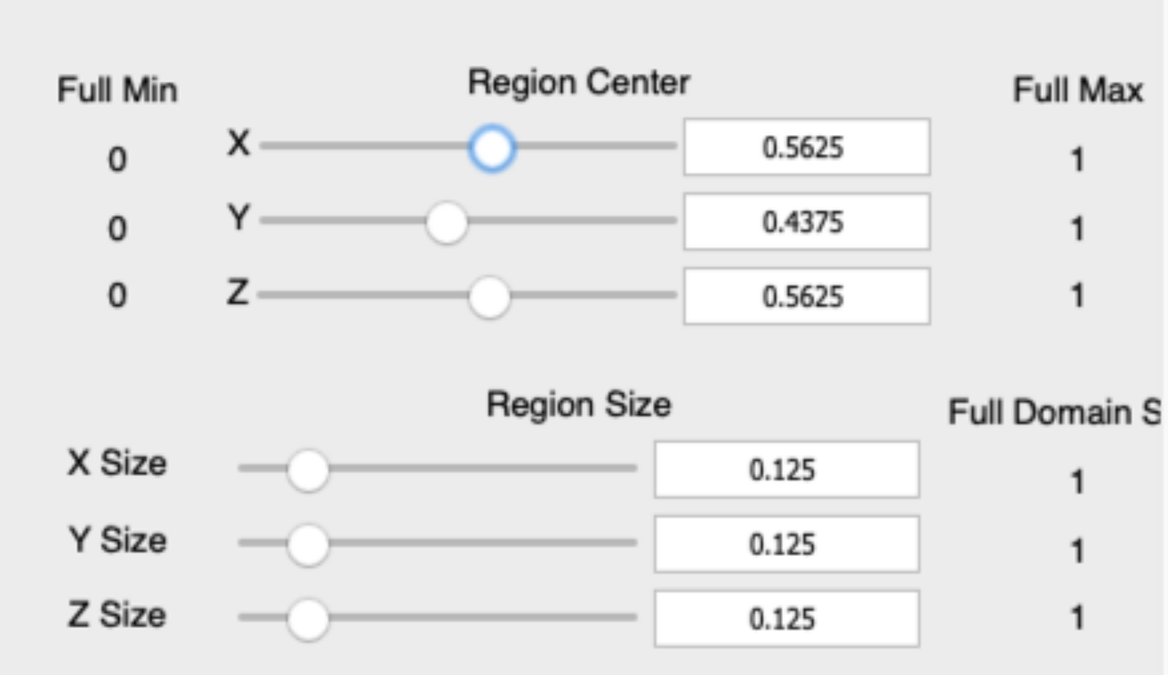
Full Min
Region Center
Full Max
X
Y
Z
0
0
0
0.5625
0.4375
0.5625
1
1
1
Region Size
Full Domain S
X Size
Y Size
Z Size
0.125
0.125
0.125
1
1
1

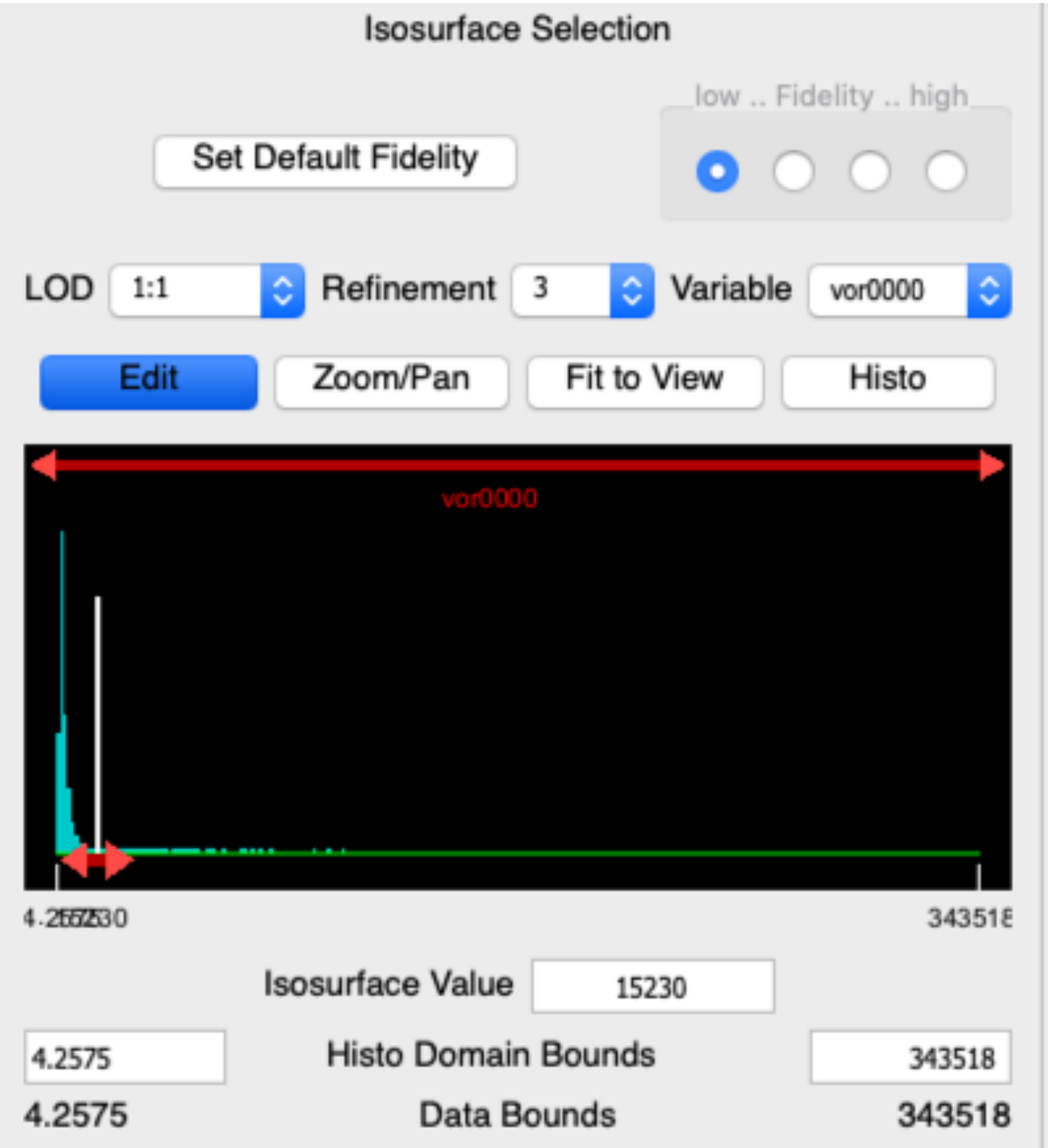
Isosurface Selection
low .. Fidelity .. high
Set Default Fidelity
LOD
1:1
Refinement
3
Variable
vor0000
Edit
Zoom/Pan
Fit to View
Histo
vor0000
343518
Isosurface Value
15230
4.2575
Histo Domain Bounds
343518
4.2575
Data Bounds
343518

0

t/tau=0

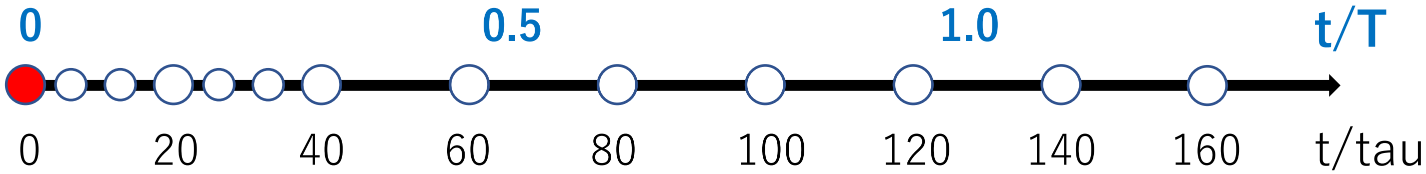

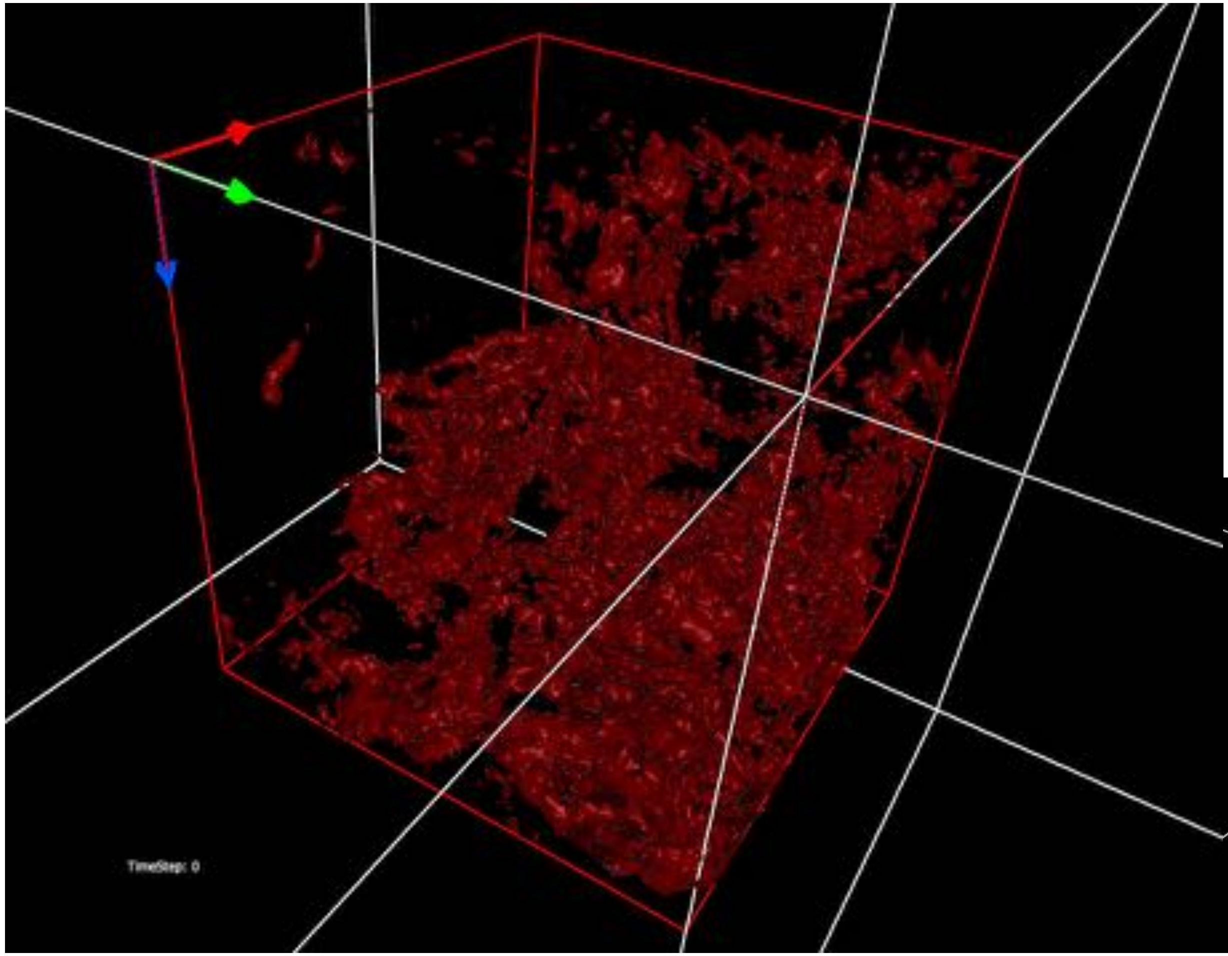

$\langle \omega^2/2 \rangle_{8\Delta x} > 7\Omega$

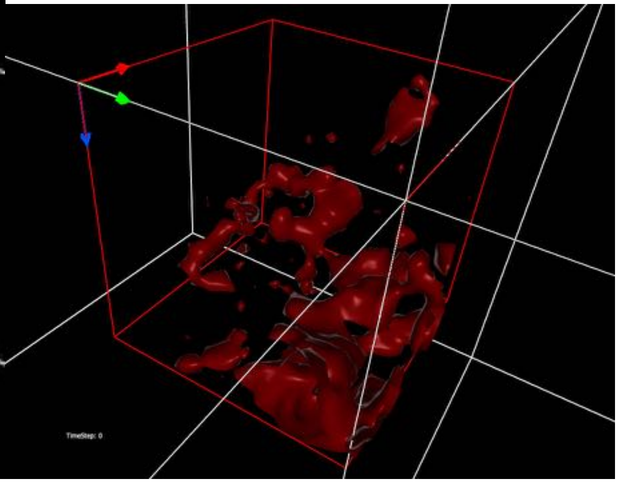

$\langle \omega^2/2 \rangle_{32\Delta x} = \langle \omega^2/2 \rangle_{1.4\lambda} > 7\Omega$

1200

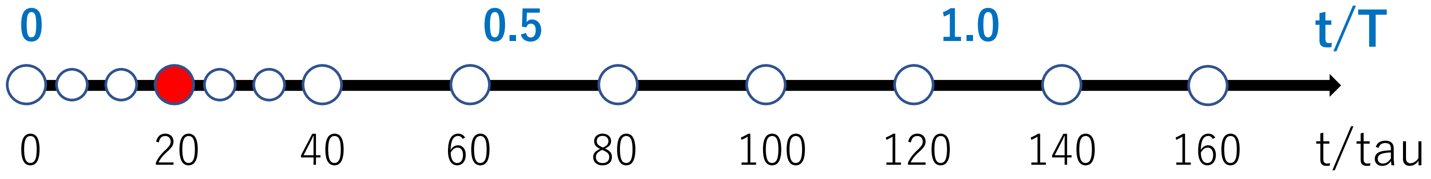

t/tau=20

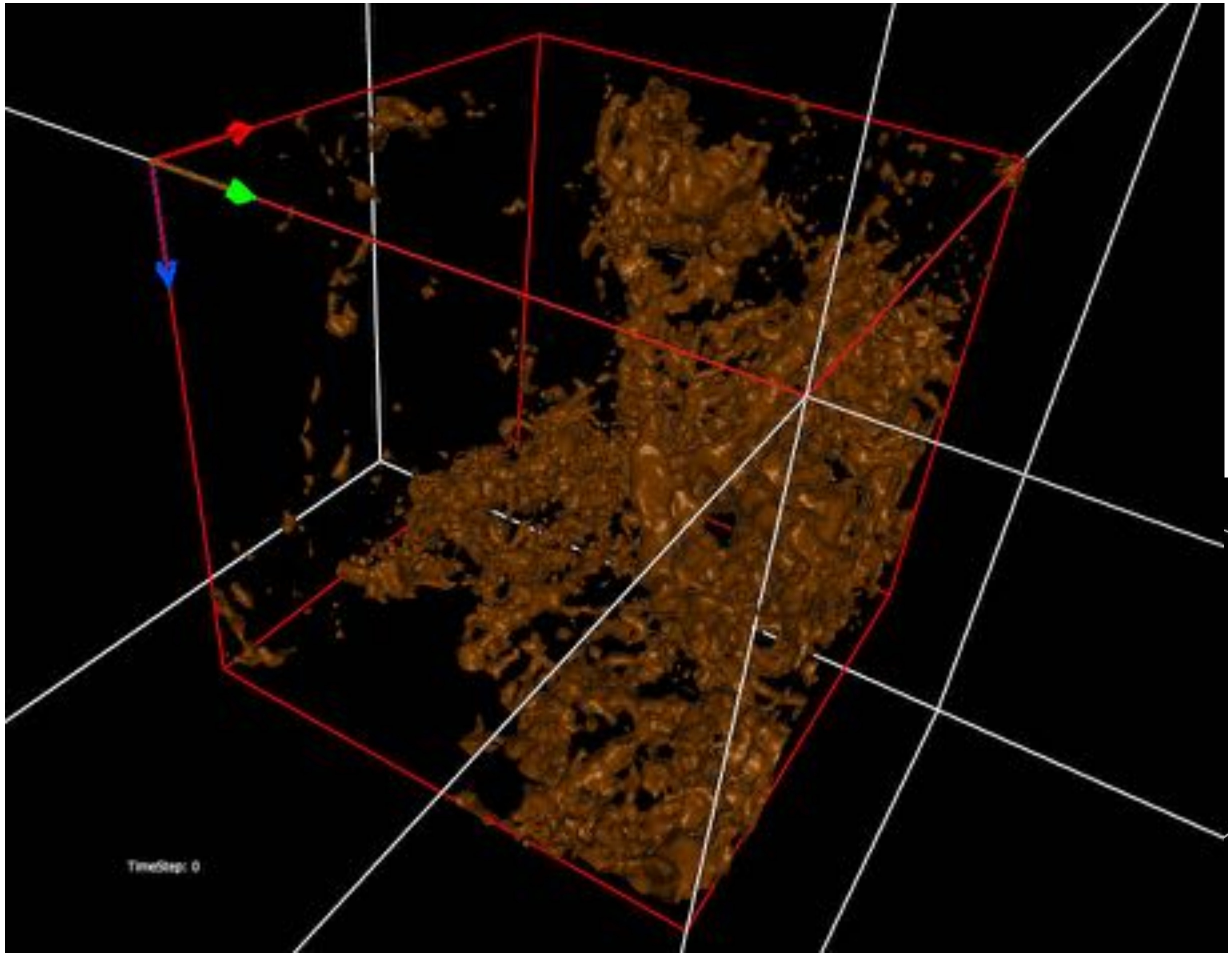

$\langle \omega^2/2 \rangle_{8\Delta x} > 7\Omega$

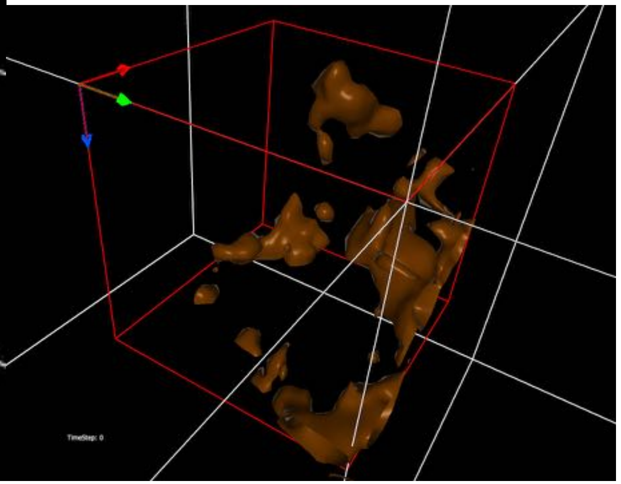

$\langle \omega^2/2 \rangle_{32\Delta x} = \langle \omega^2/2 \rangle_{1.4\lambda} > 7\Omega$

2400

t/tau=40

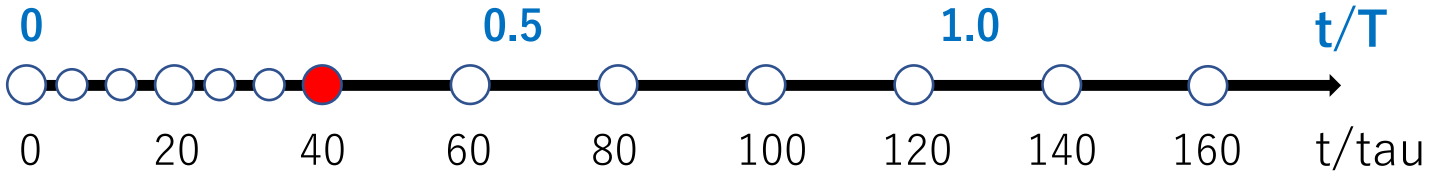

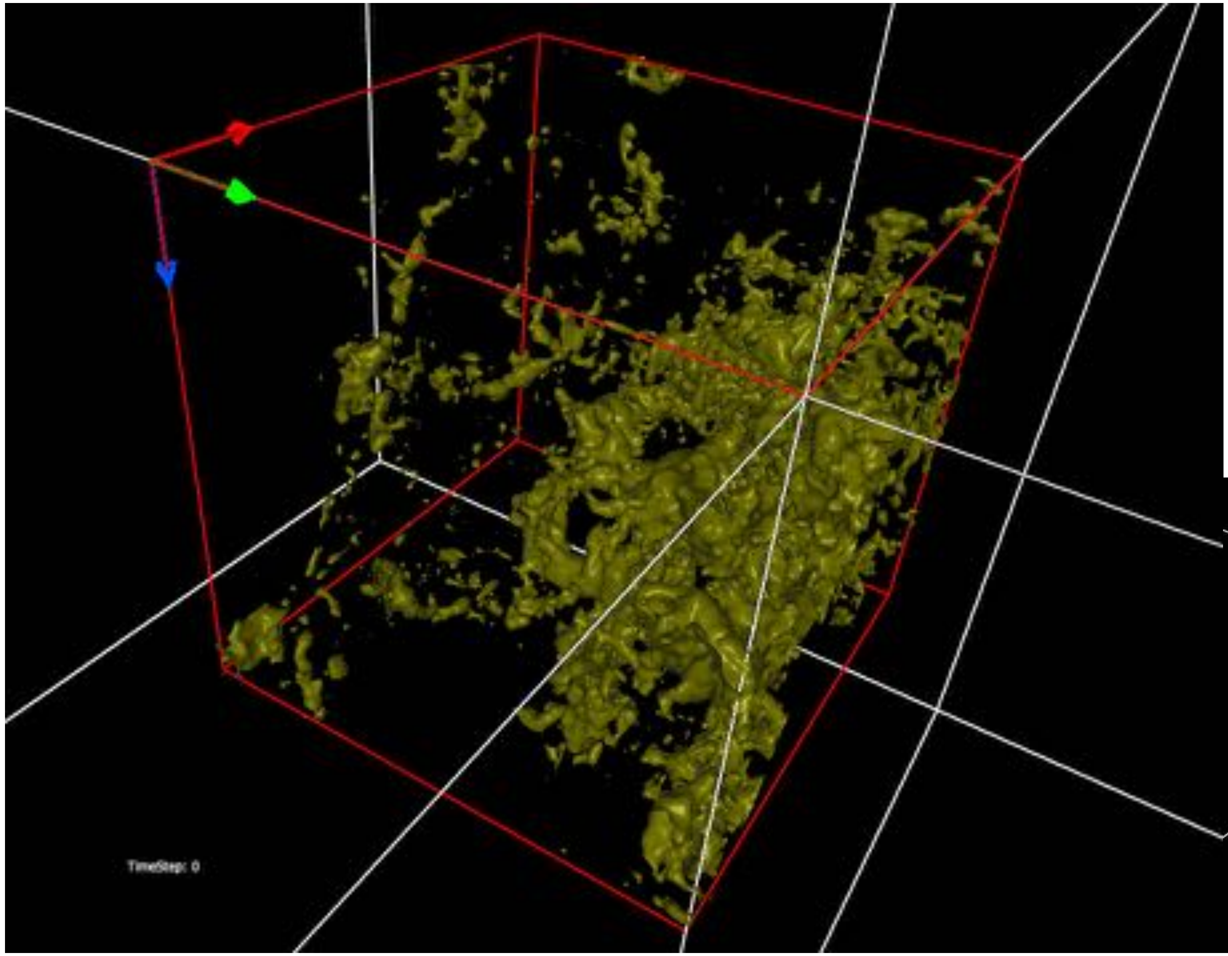

$\langle \omega^2/2 \rangle_{8\Delta x} > 7\Omega$

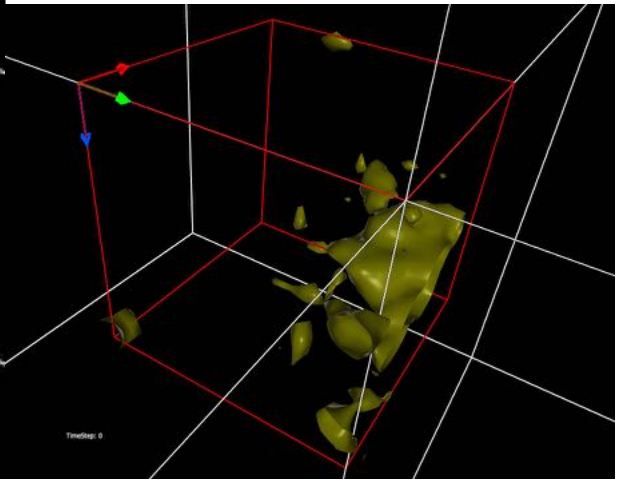

$\langle \omega^2/2 \rangle_{32\Delta x} = \langle \omega^2/2 \rangle_{1.4\lambda} > 7\Omega$

3600

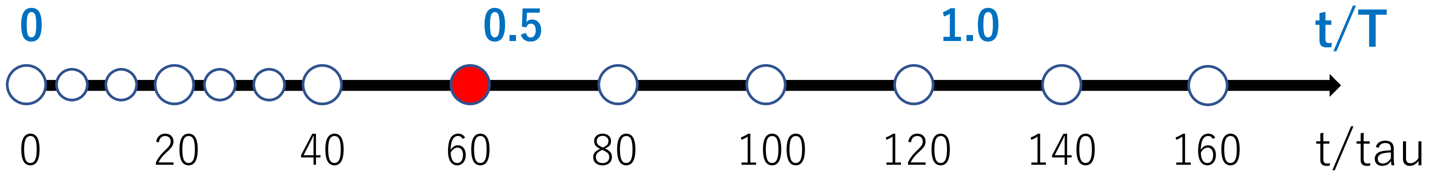

t/tau=60

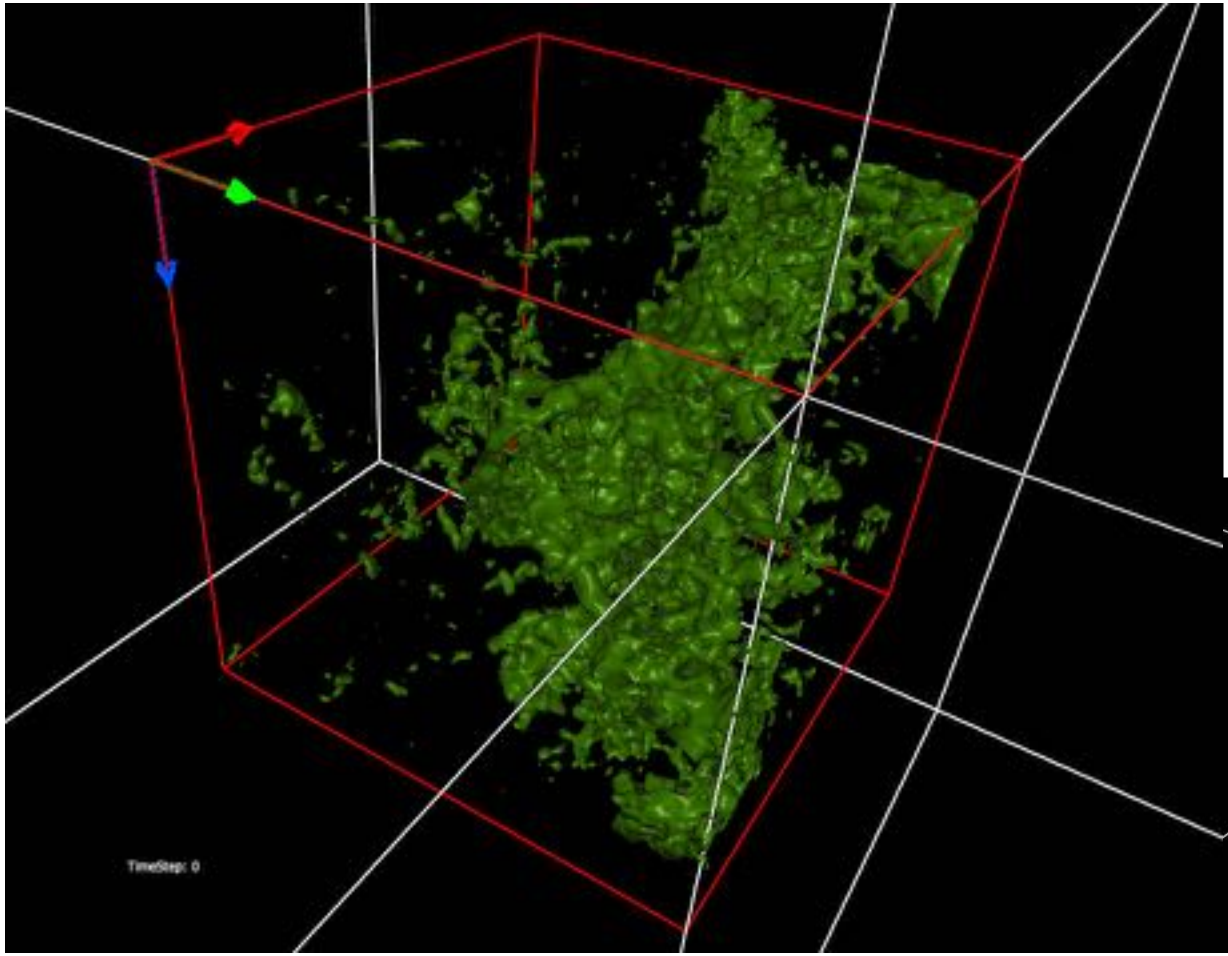

$\langle \omega^2/2 \rangle_{8\Delta x} > 7\Omega$

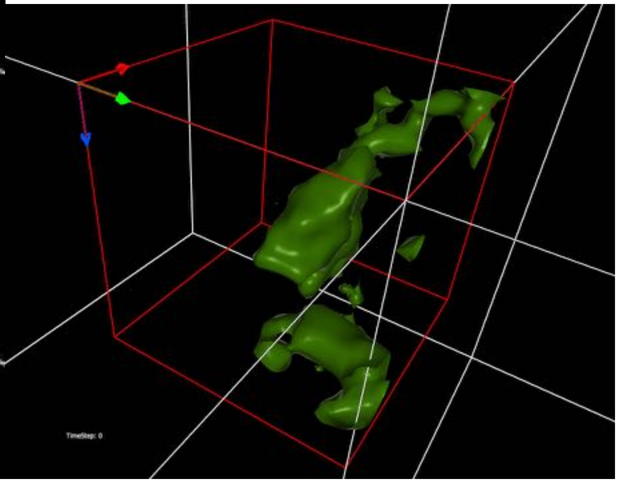

$\langle \omega^2/2 \rangle_{32\Delta x} = \langle \omega^2/2 \rangle_{1.4\lambda} > 7\Omega$

4800

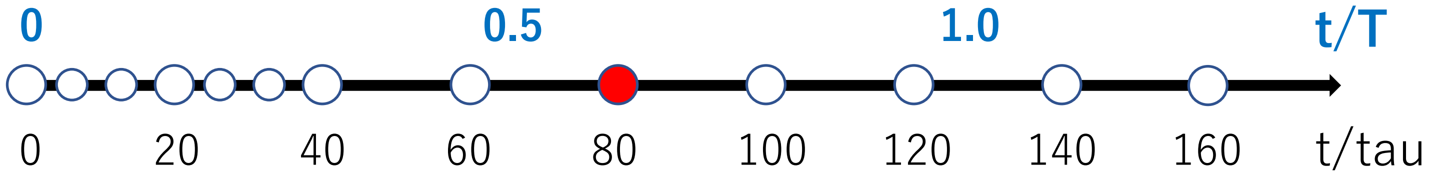

t/tau=80

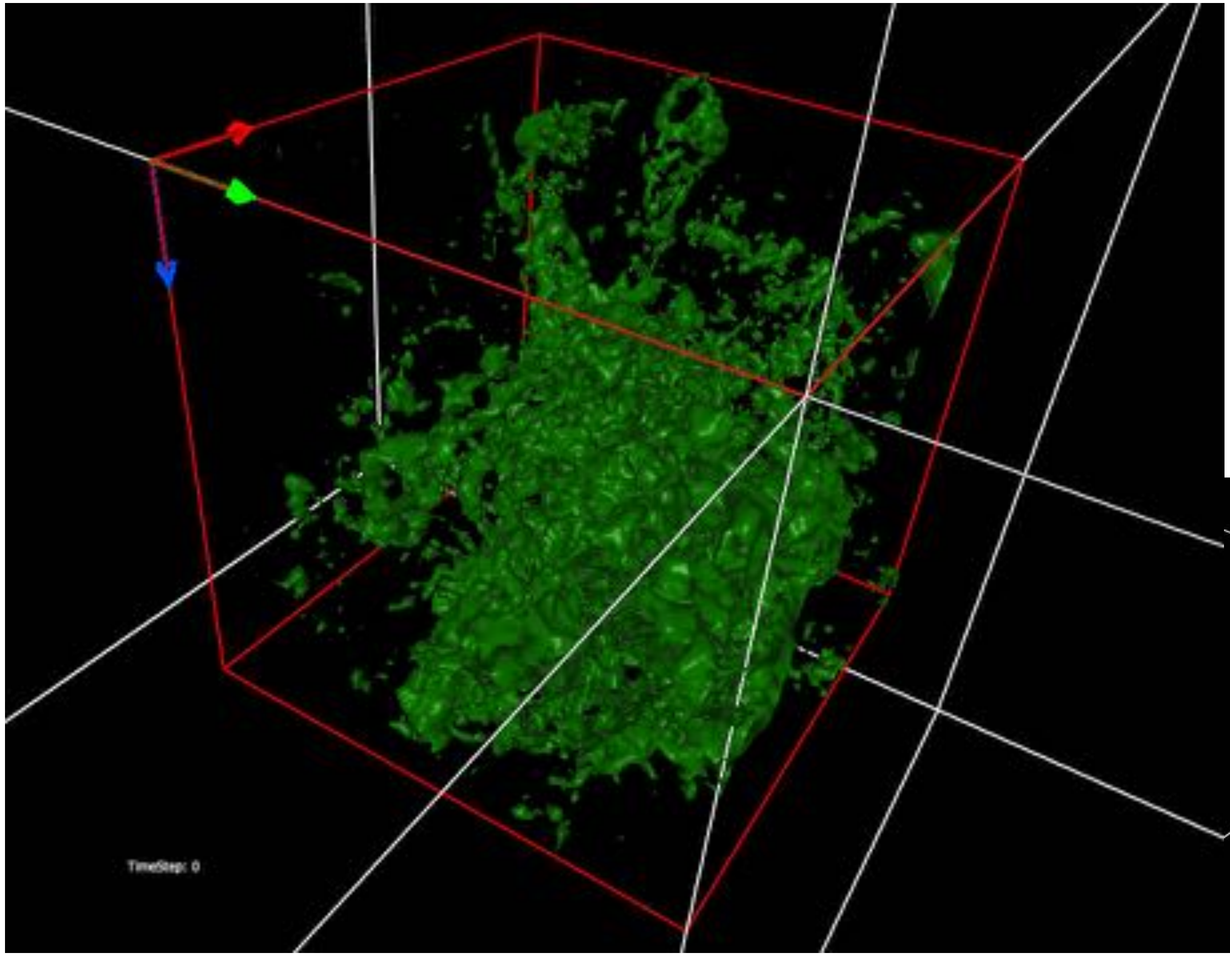

$\langle \omega^2/2 \rangle_{8\Delta x} > 7\Omega$

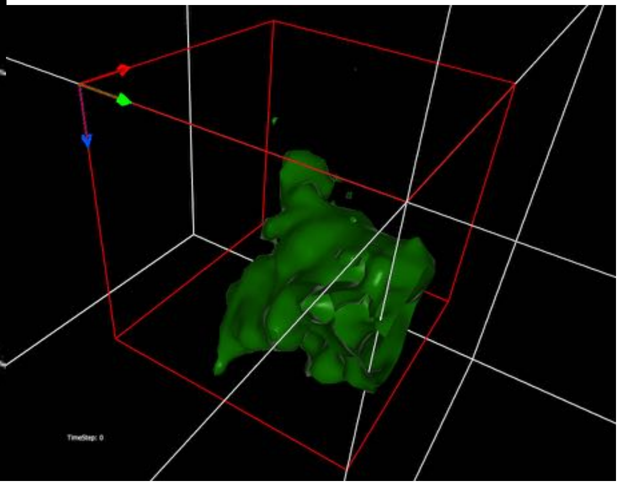

$\langle \omega^2/2 \rangle_{32\Delta x} = \langle \omega^2/2 \rangle_{1.4\lambda} > 7\Omega$

6000

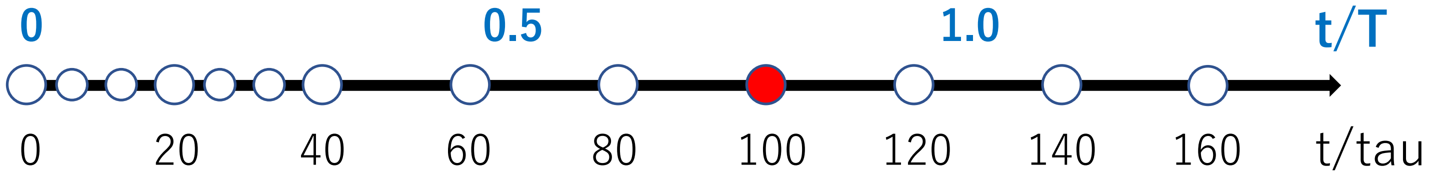

t/tau=100

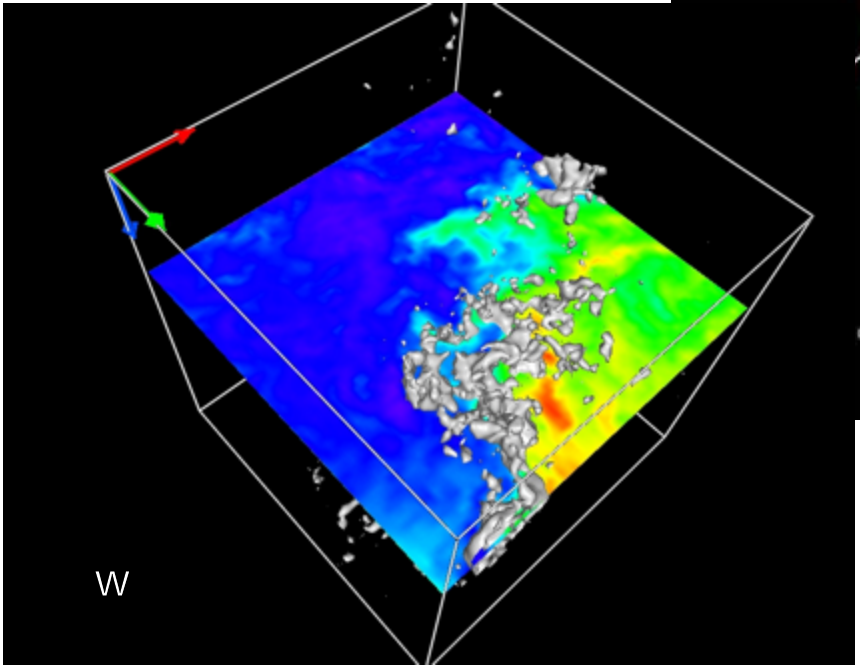

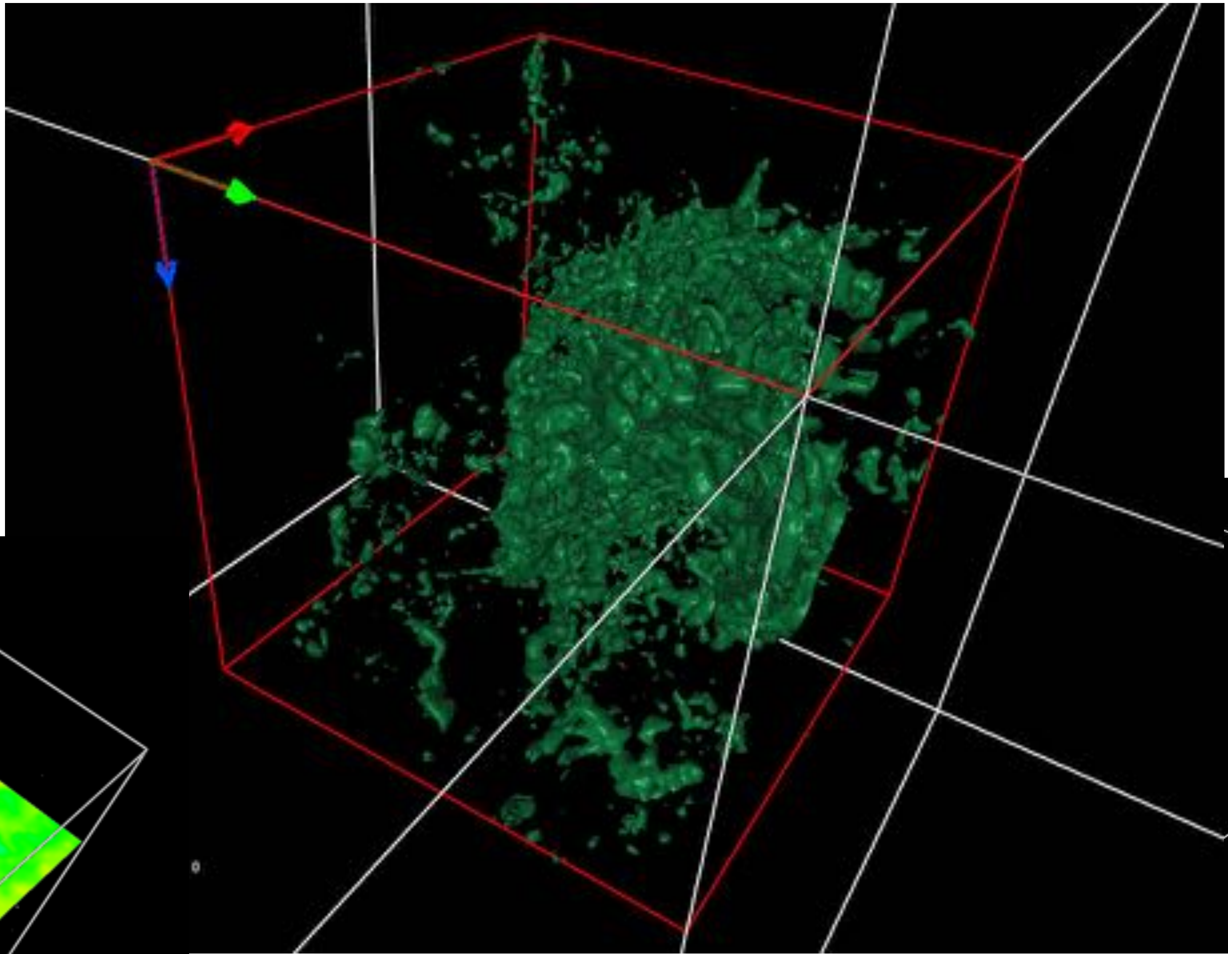

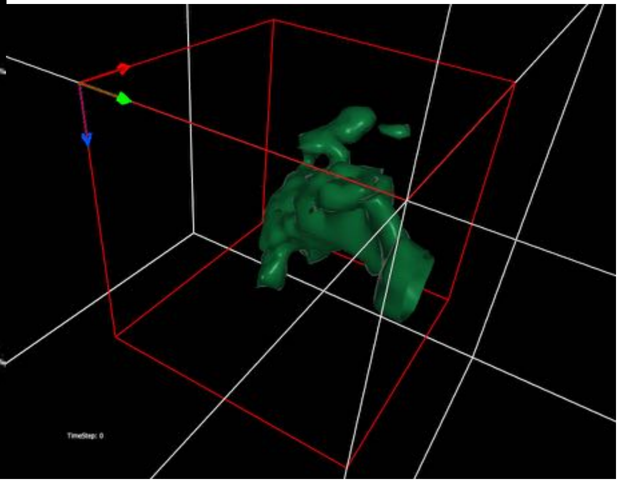

$\langle \omega^2/2 \rangle_{8\Delta x} > 7\Omega$

$\langle \omega^2/2 \rangle_{32\Delta x} = \langle \omega^2/2 \rangle_{1.4\lambda} > 7\Omega$

7200

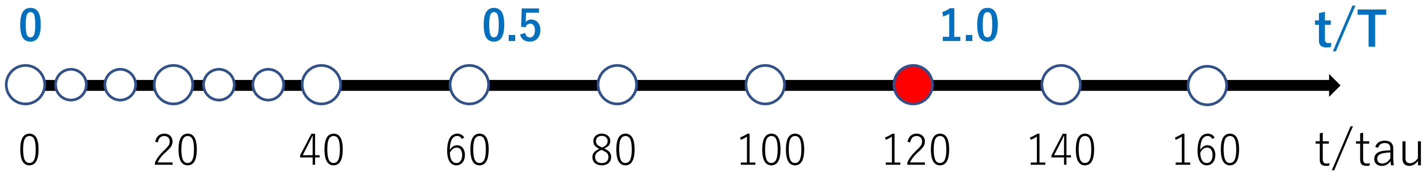

t/tau=120

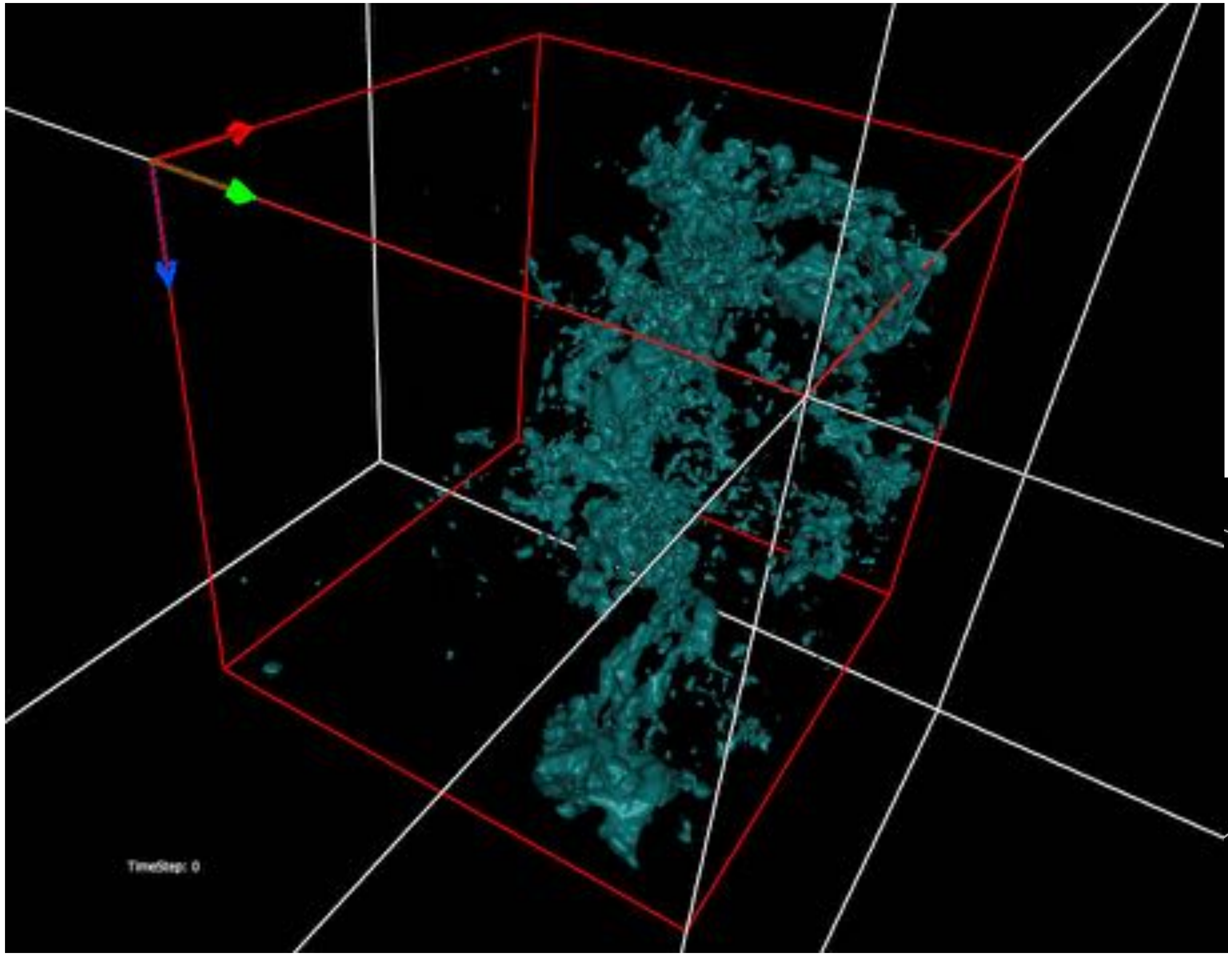

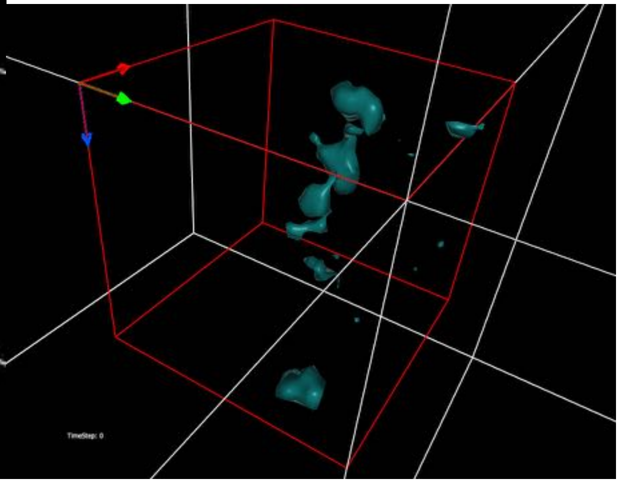

$\langle \omega^2/2 \rangle_{8\Delta x} > 7\Omega$

$\langle \omega^2/2 \rangle_{32\Delta x} = \langle \omega^2/2 \rangle_{1.4\lambda} > 7\Omega$

8400

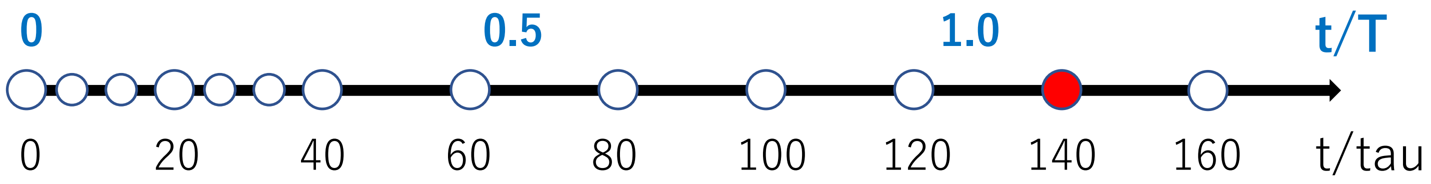

t/tau=140

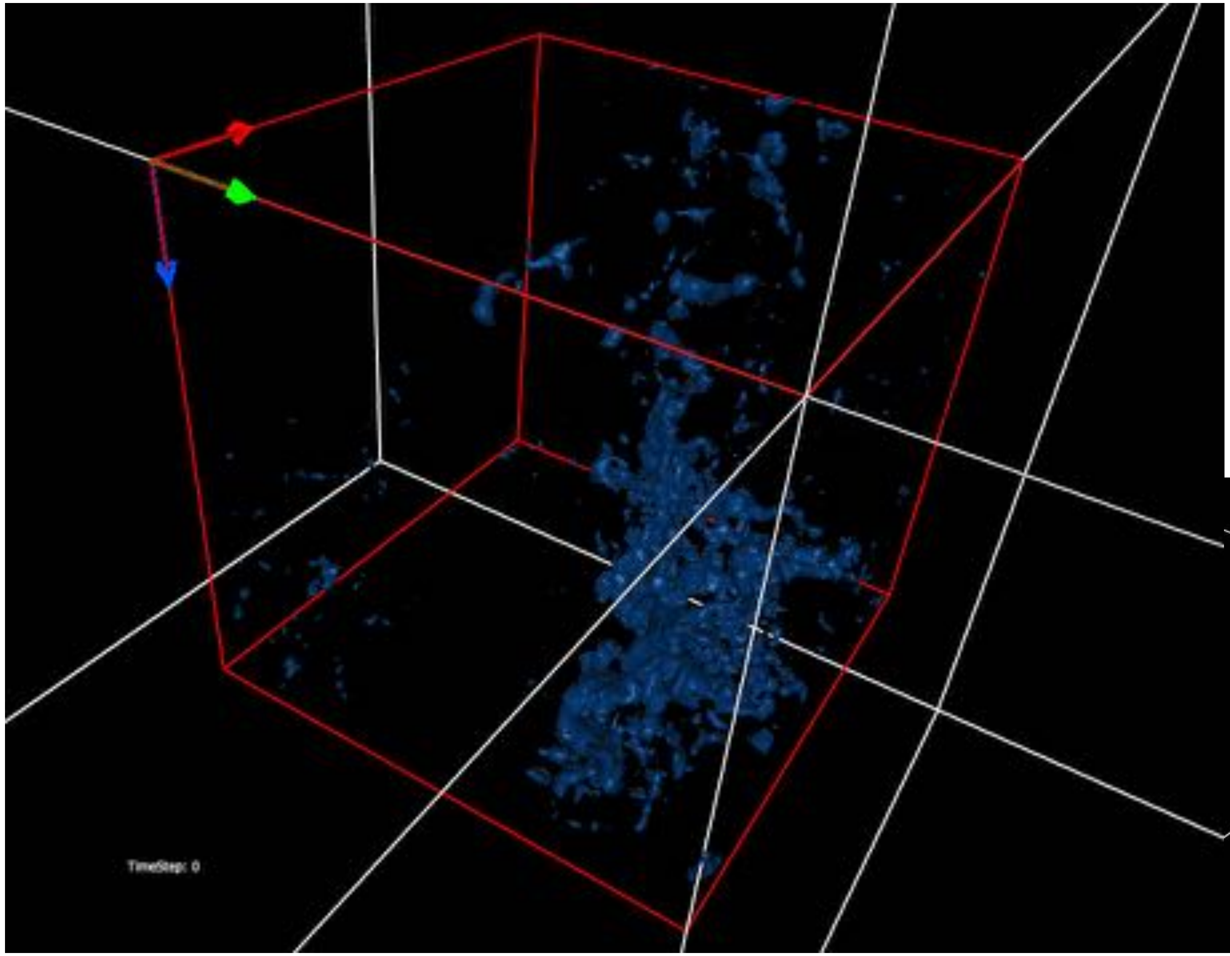

$\langle \omega^2/2 \rangle_{8\Delta x} > 7\Omega$

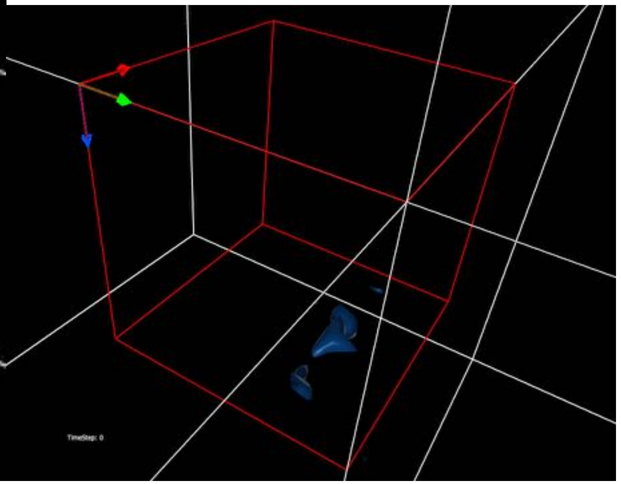

$\langle \omega^2/2 \rangle_{32\Delta x} = \langle \omega^2/2 \rangle_{1.4\lambda} > 7\Omega$

9600

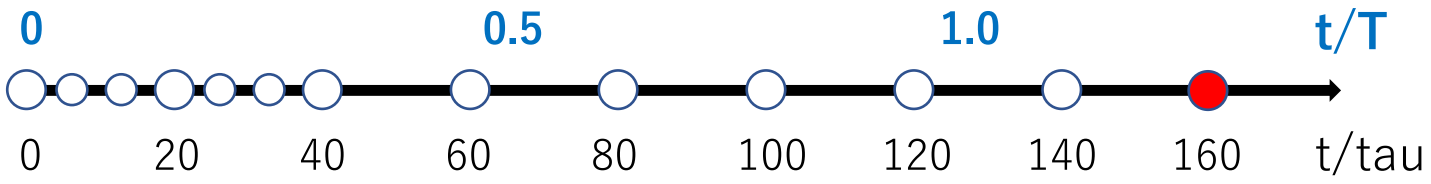

t/tau=160

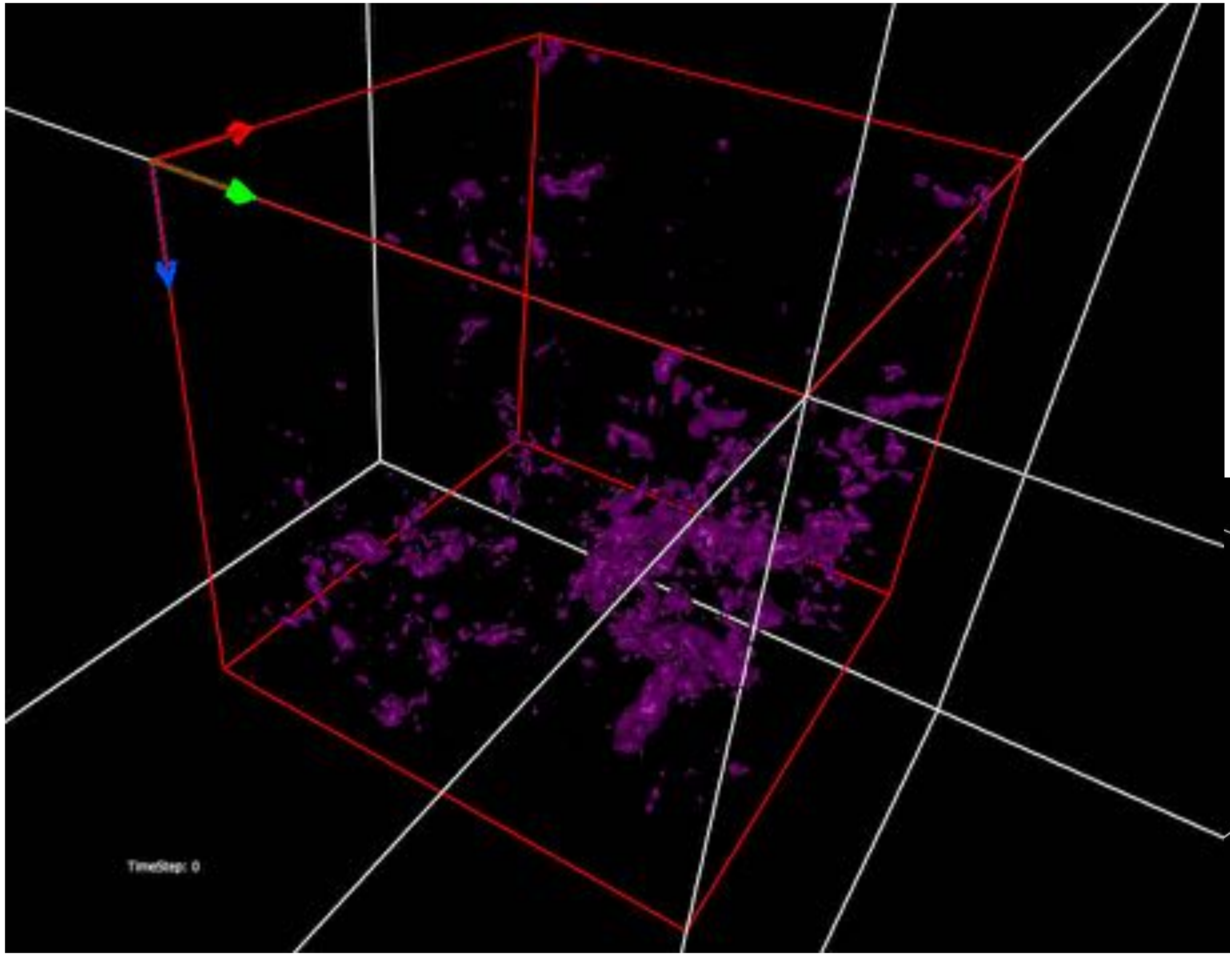

$\langle \omega^2/2 \rangle_{8\Delta x} > 7\Omega$

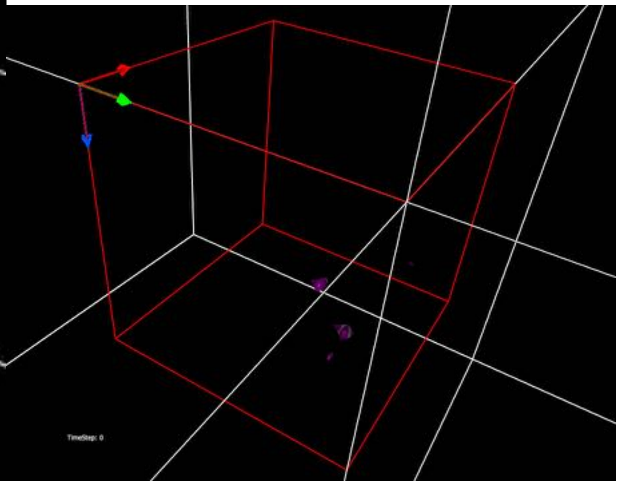

$\langle \omega^2/2 \rangle_{32\Delta x} = \langle \omega^2/2 \rangle_{1.4\lambda} > 7\Omega$

Significant layer in real geophysical flow

Layer structures associated with typhoon 5 in 2017

Precipitation

Typhoon No. 5 in 2017

AM 04:00

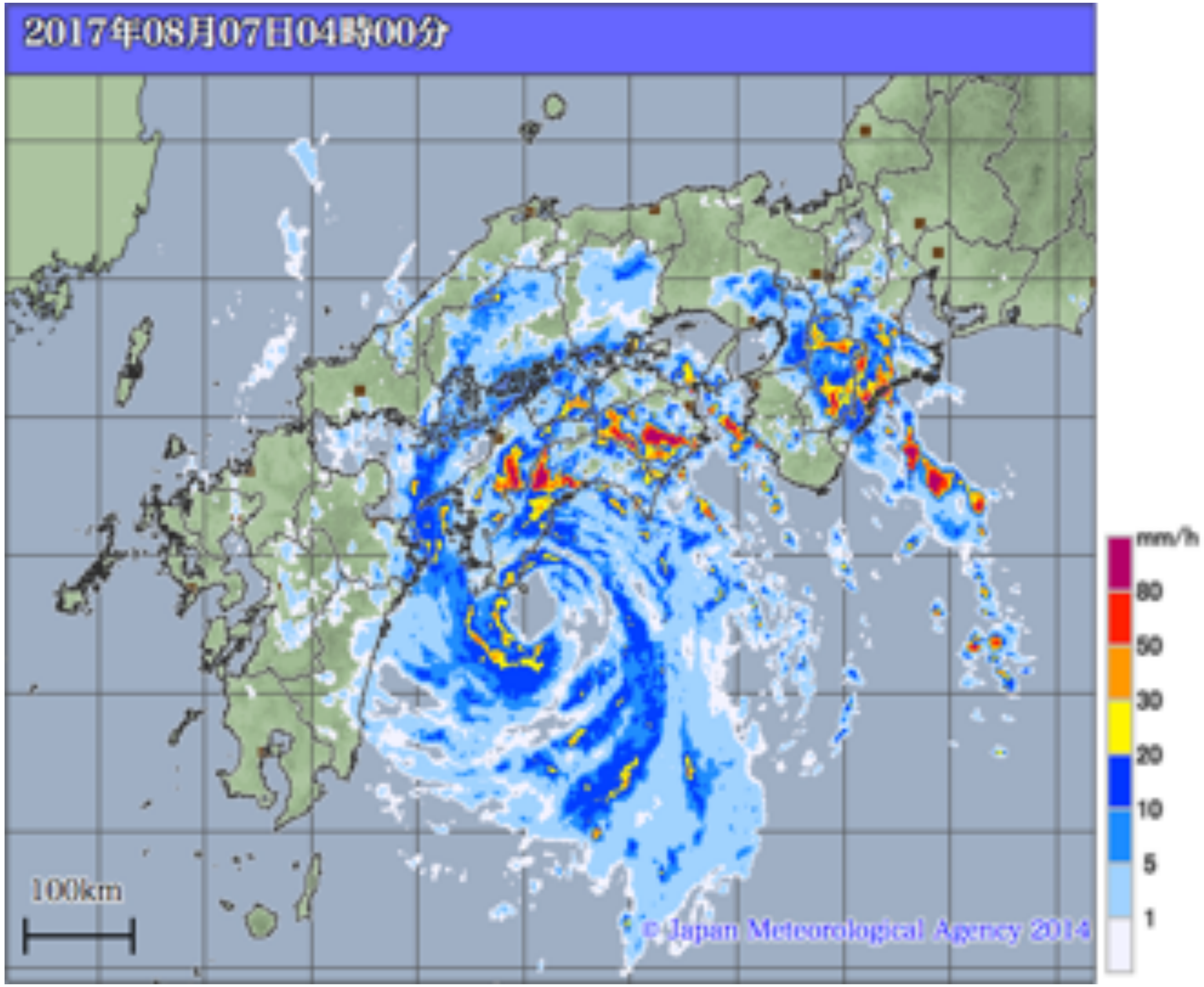

AM 04:05

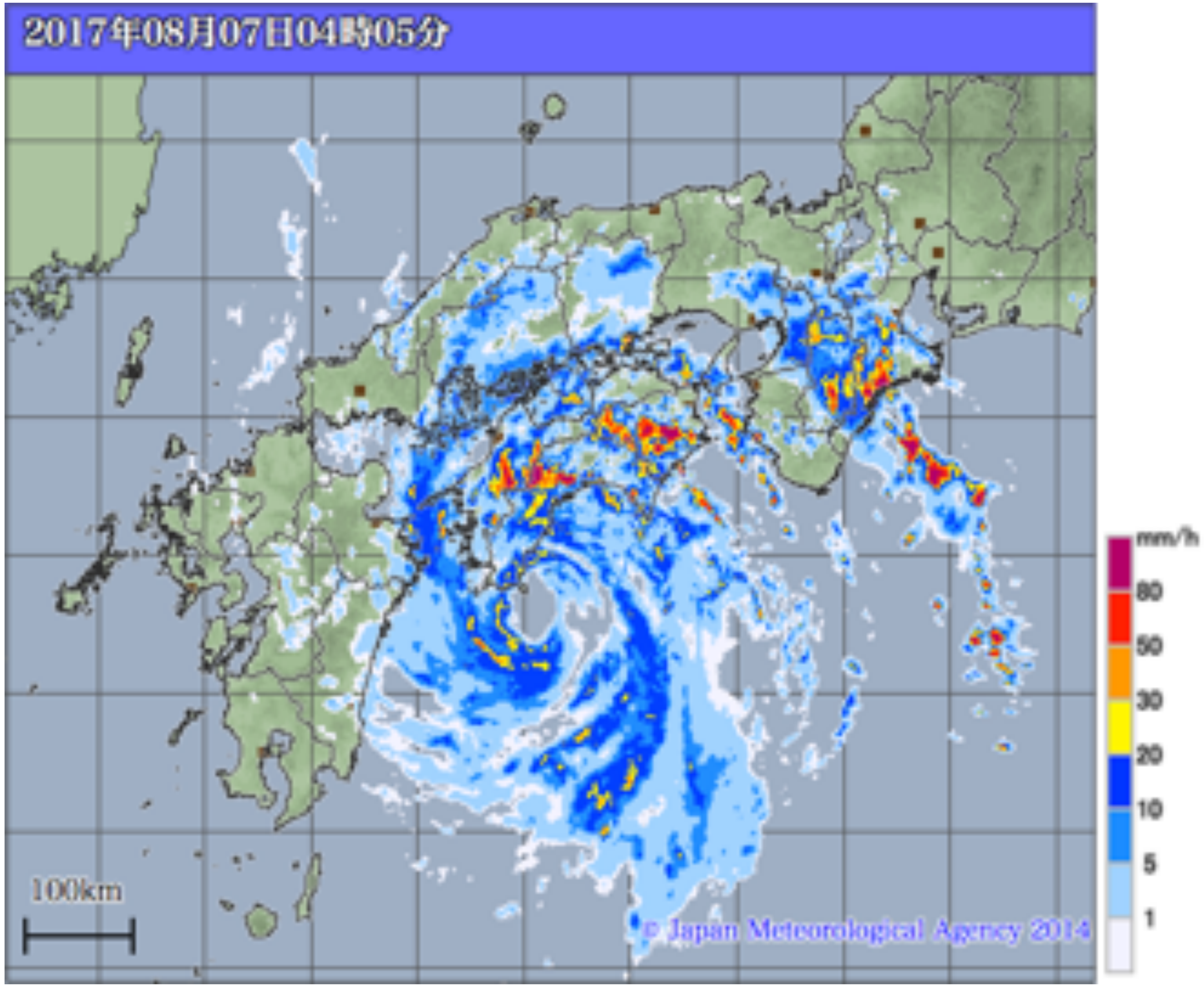

2017年08月07日04時05分
100km
© Japan Meteorological Agency 2014
mm/h
80
50
30
20
10
5
1

AM 04:10

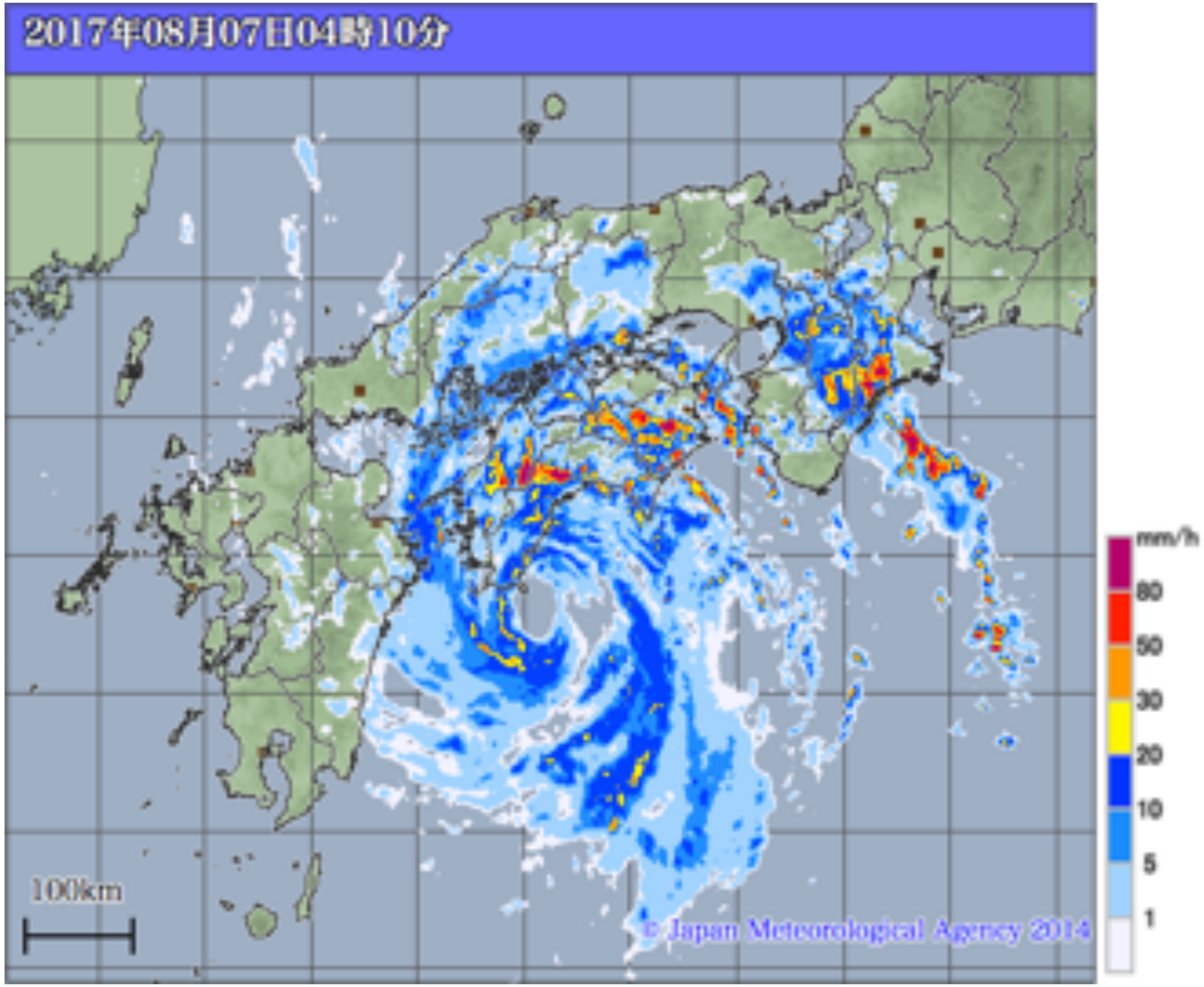

2017年08月07日04時10分
100km
© Japan Meteorological Agency 2014
mm/h
80
50
30
20
10
5
1

AM 04:15

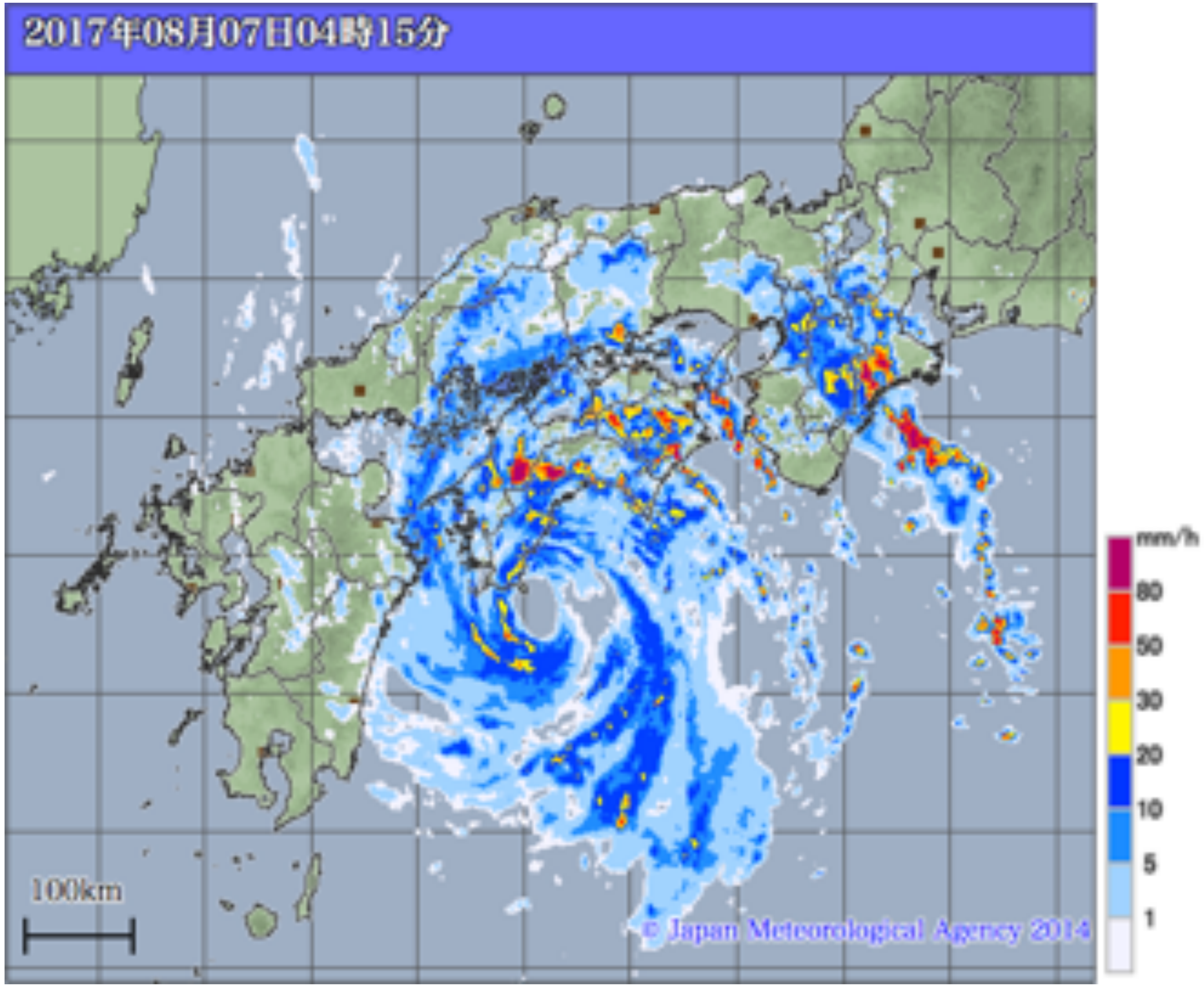
2017年08月07日04時15分
100km
© Japan Meteorological Agency 2014
mm/h
80
50
30
20
10
5
1

AM 04:20

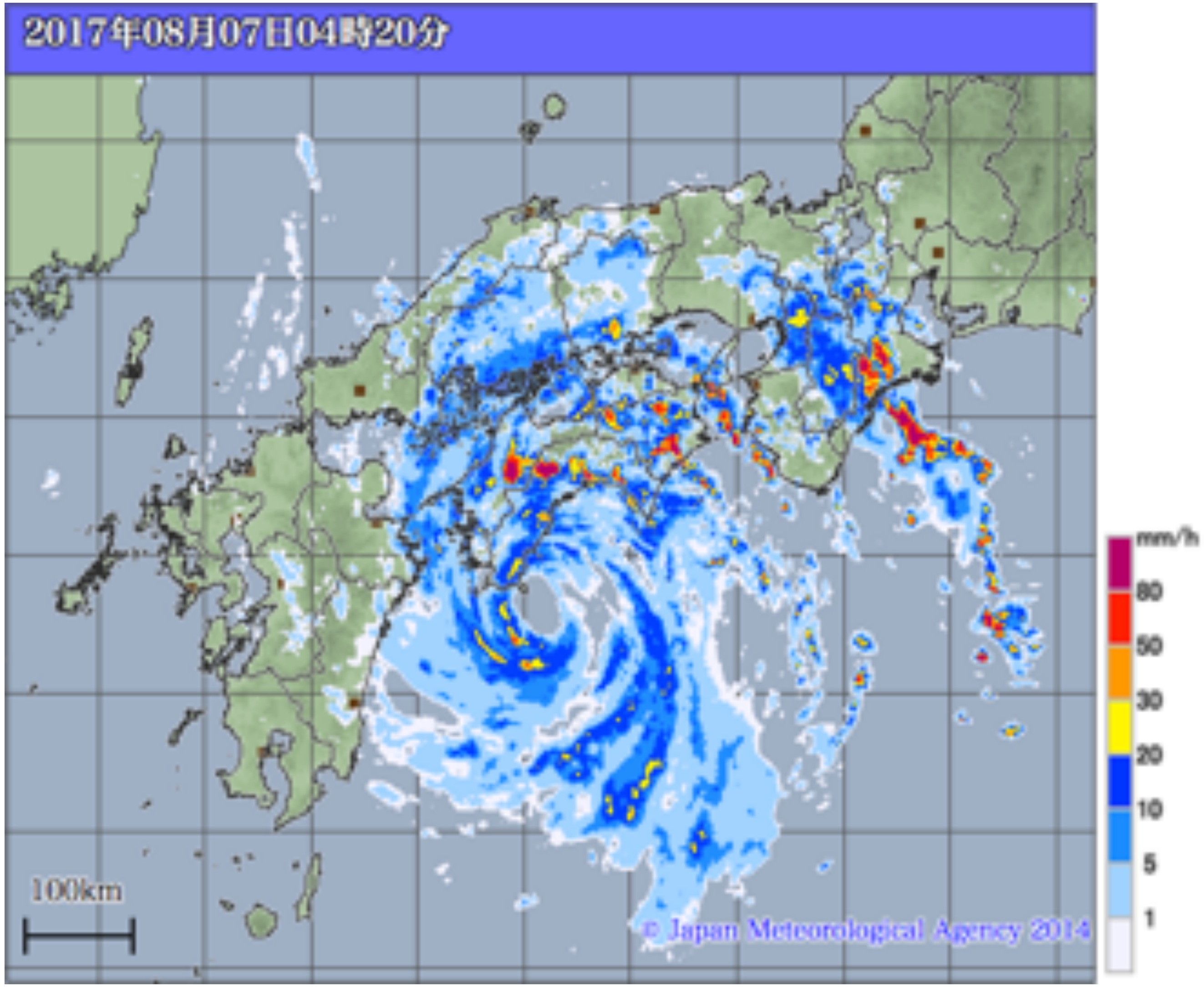

2017年08月07日04時20分
100km
© Japan Meteorological Agency 2014
mm/h
80
50
30
20
10
5
1

AM 04:25

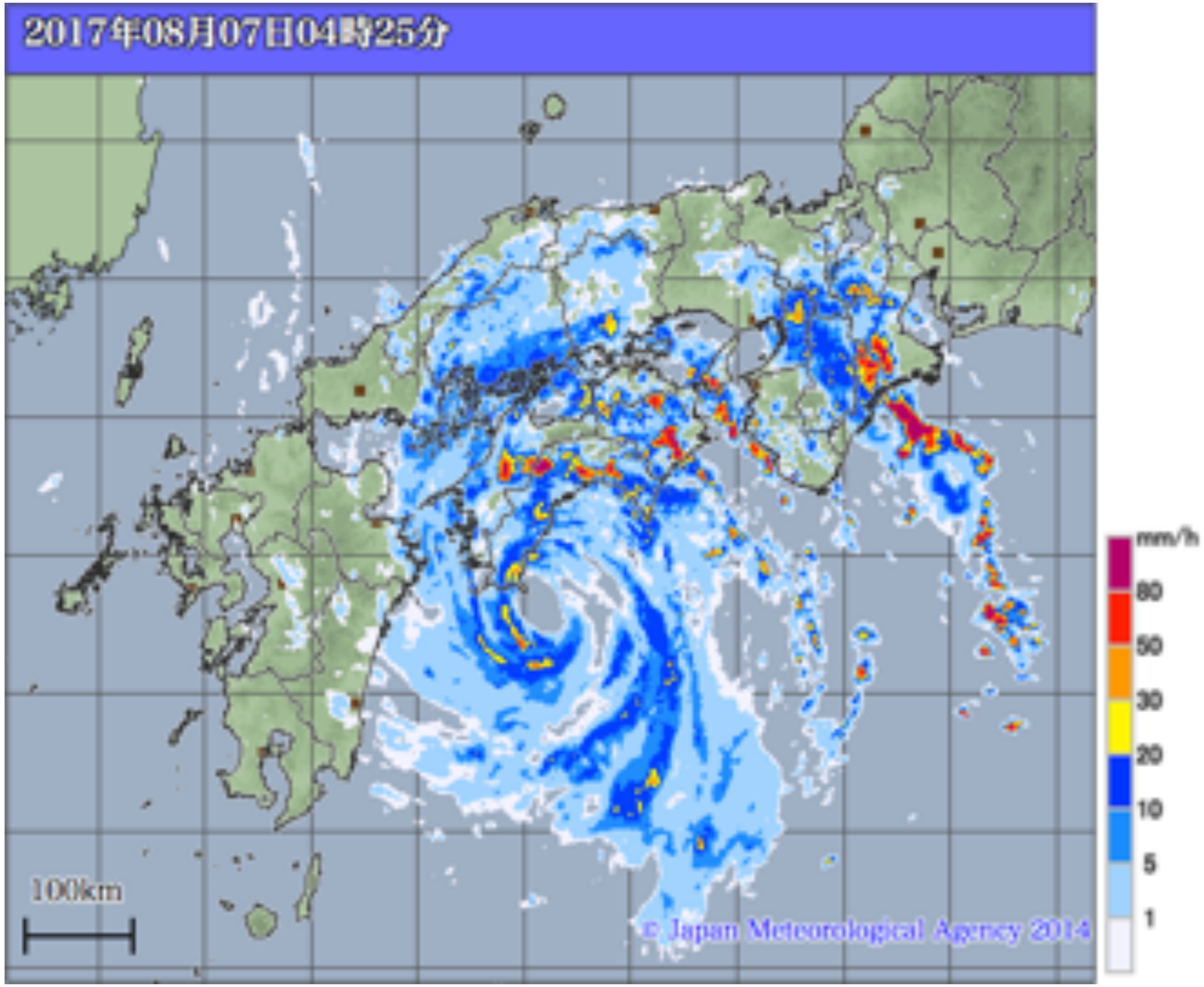
2017年08月07日04時25分
100km
© Japan Meteorological Agency 2014
mm/h
80
50
30
20
10
5
1

AM 04:30

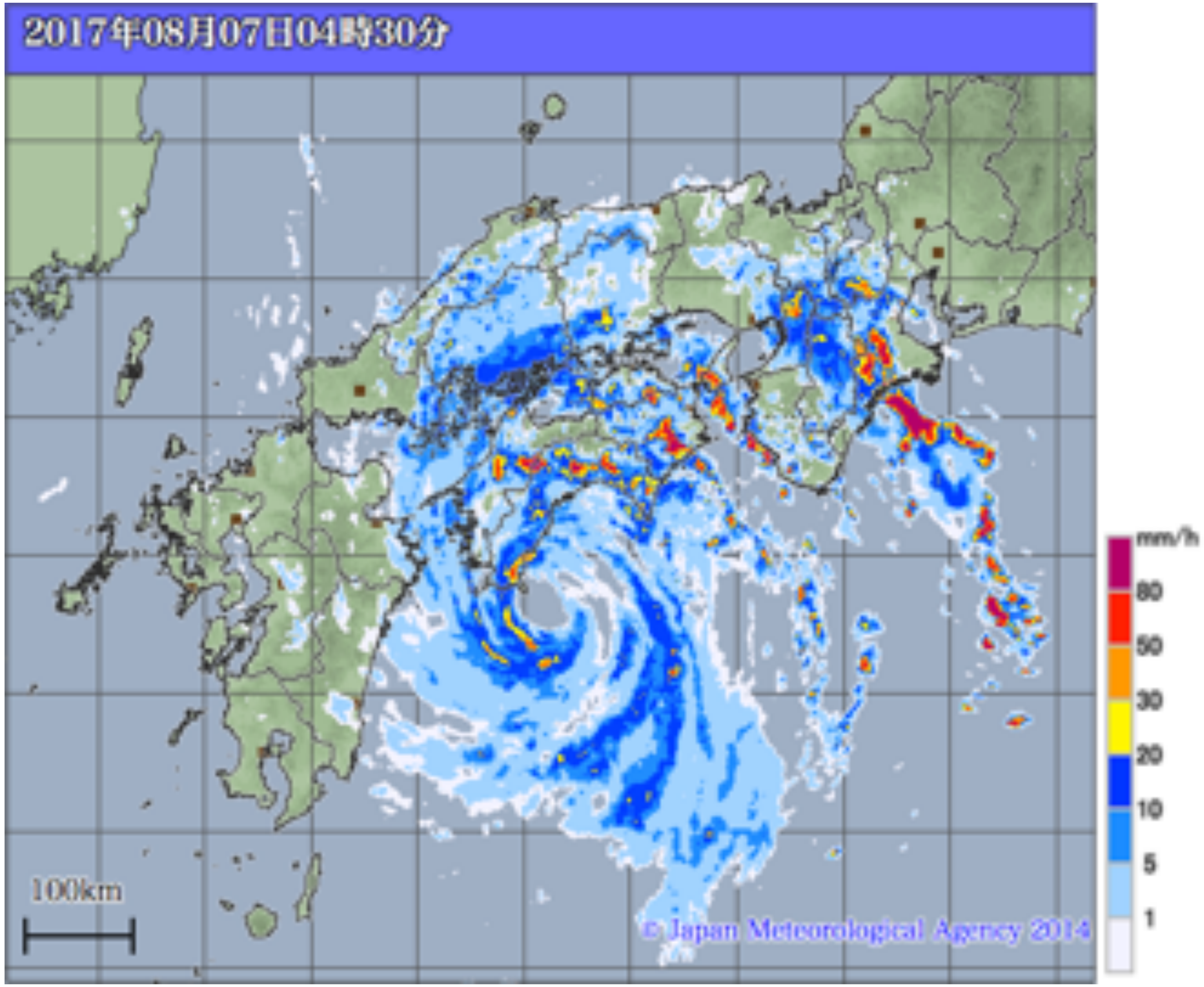

2017年08月07日04時30分
100km
© Japan Meteorological Agency 2014
mm/h
80
50
30
20
10
5
1

AM 04:35

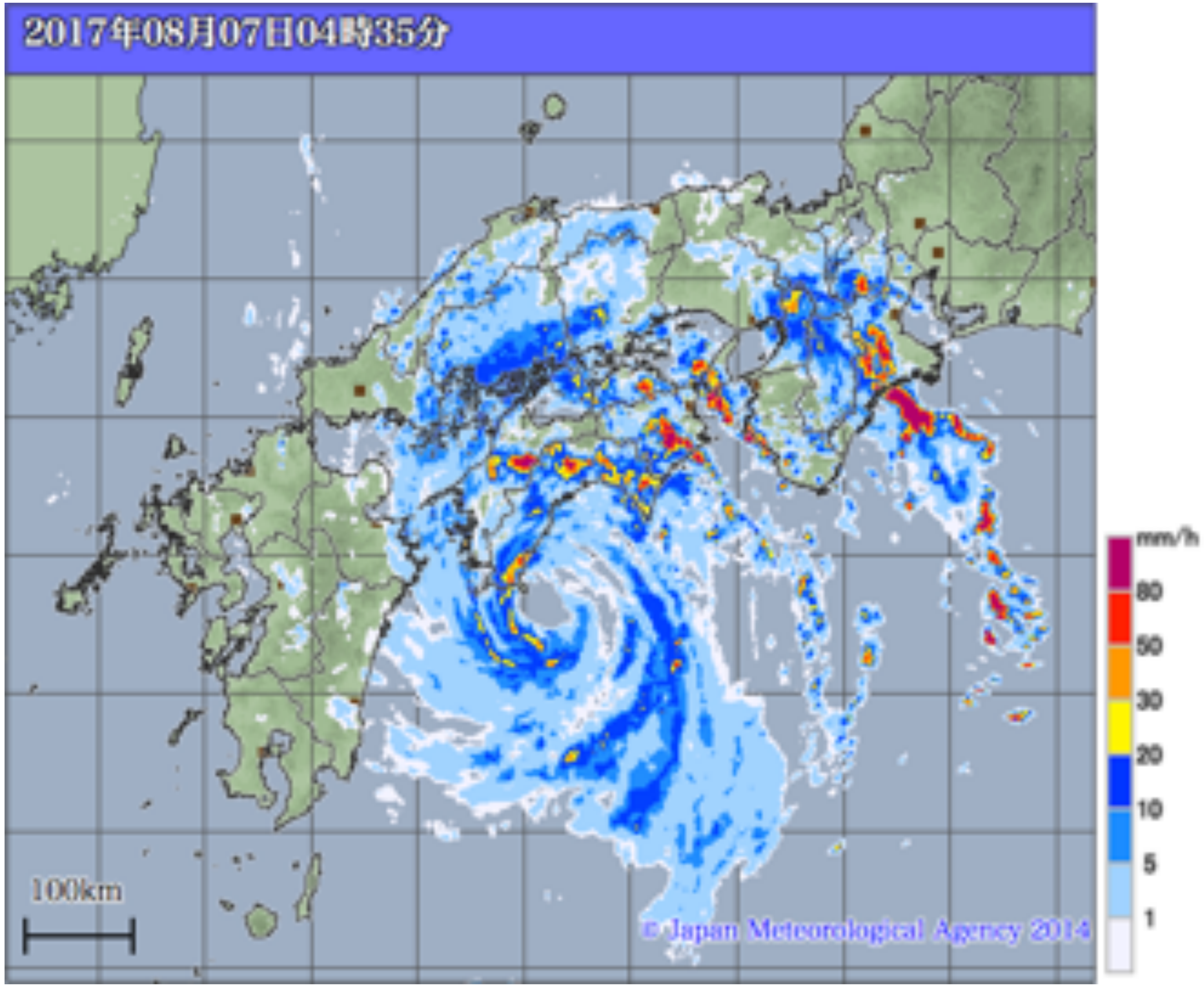

2017年08月07日04時35分
100km
© Japan Meteorological Agency 2014
mm/h
80
50
30
20
10
5
1

AM 04:40

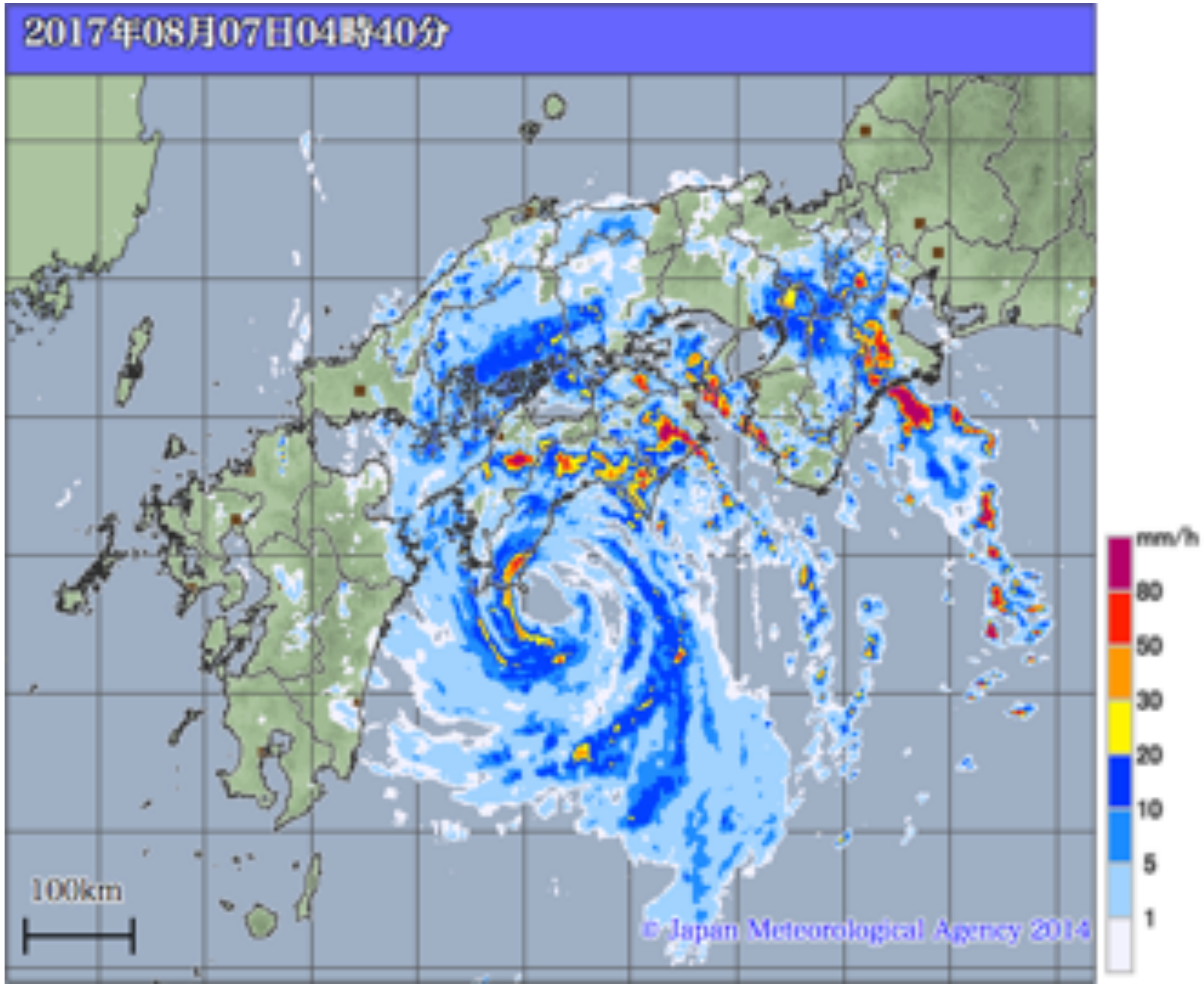
2017年08月07日04時40分
100km
© Japan Meteorological Agency 2014
mm/h
80
50
30
20
10
5
1

AM 04:45

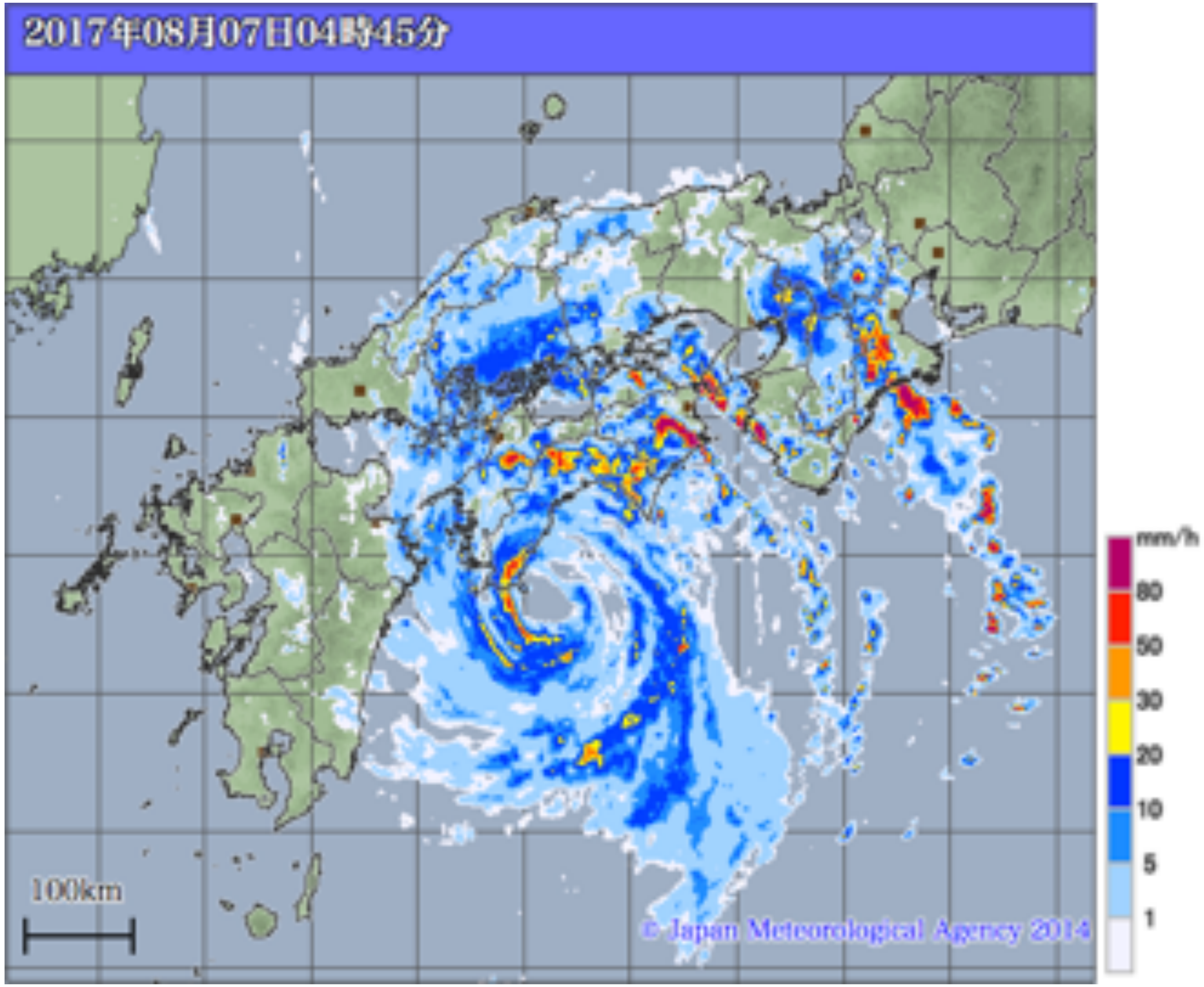

2017年08月07日04時45分
100km
© Japan Meteorological Agency 2014
mm/h
80
50
30
20
10
5
1

AM 04:50

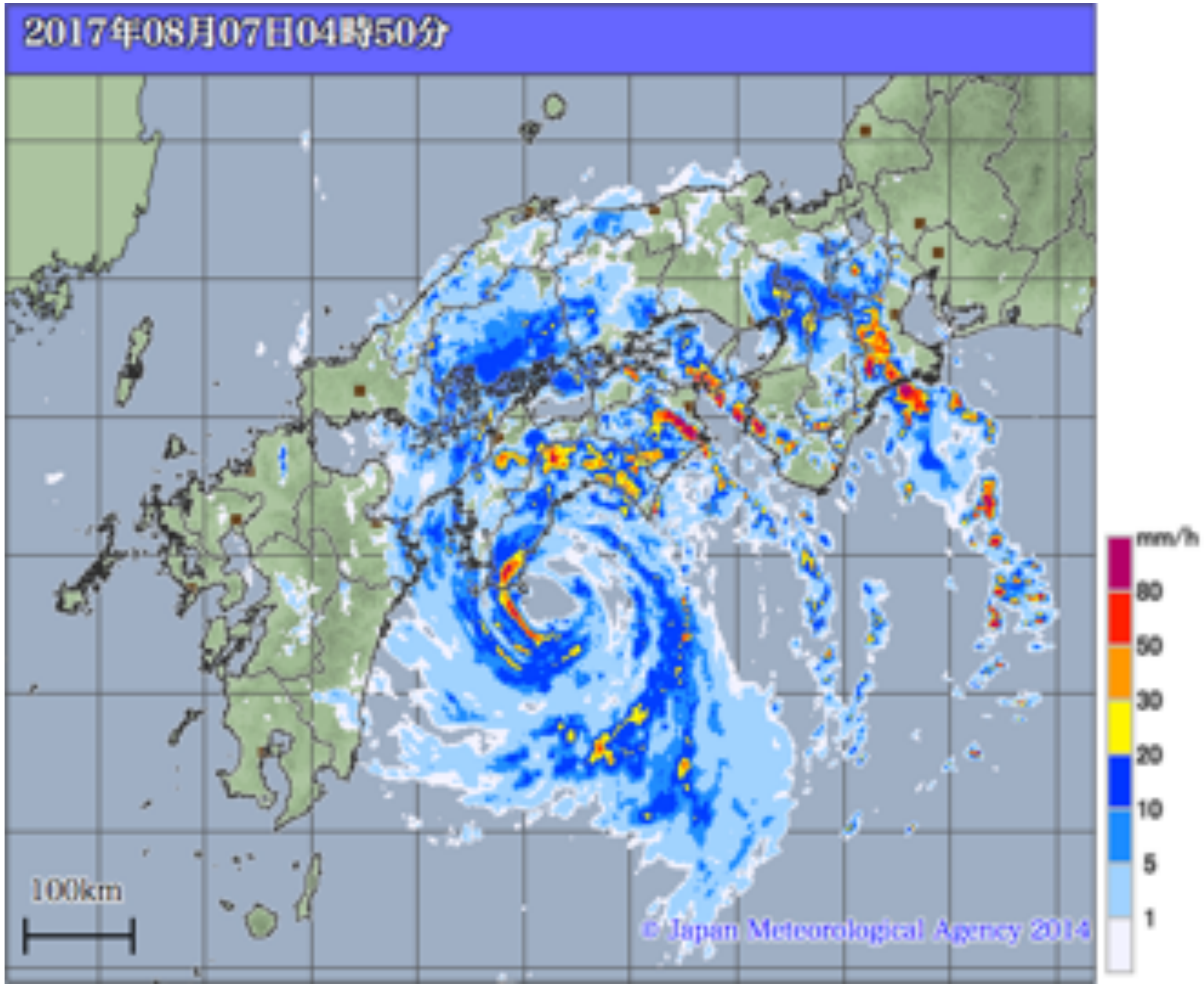
2017年08月07日04時50分
100km
© Japan Meteorological Agency 2014
mm/h
80
50
30
20
10
5
1

AM 04:55

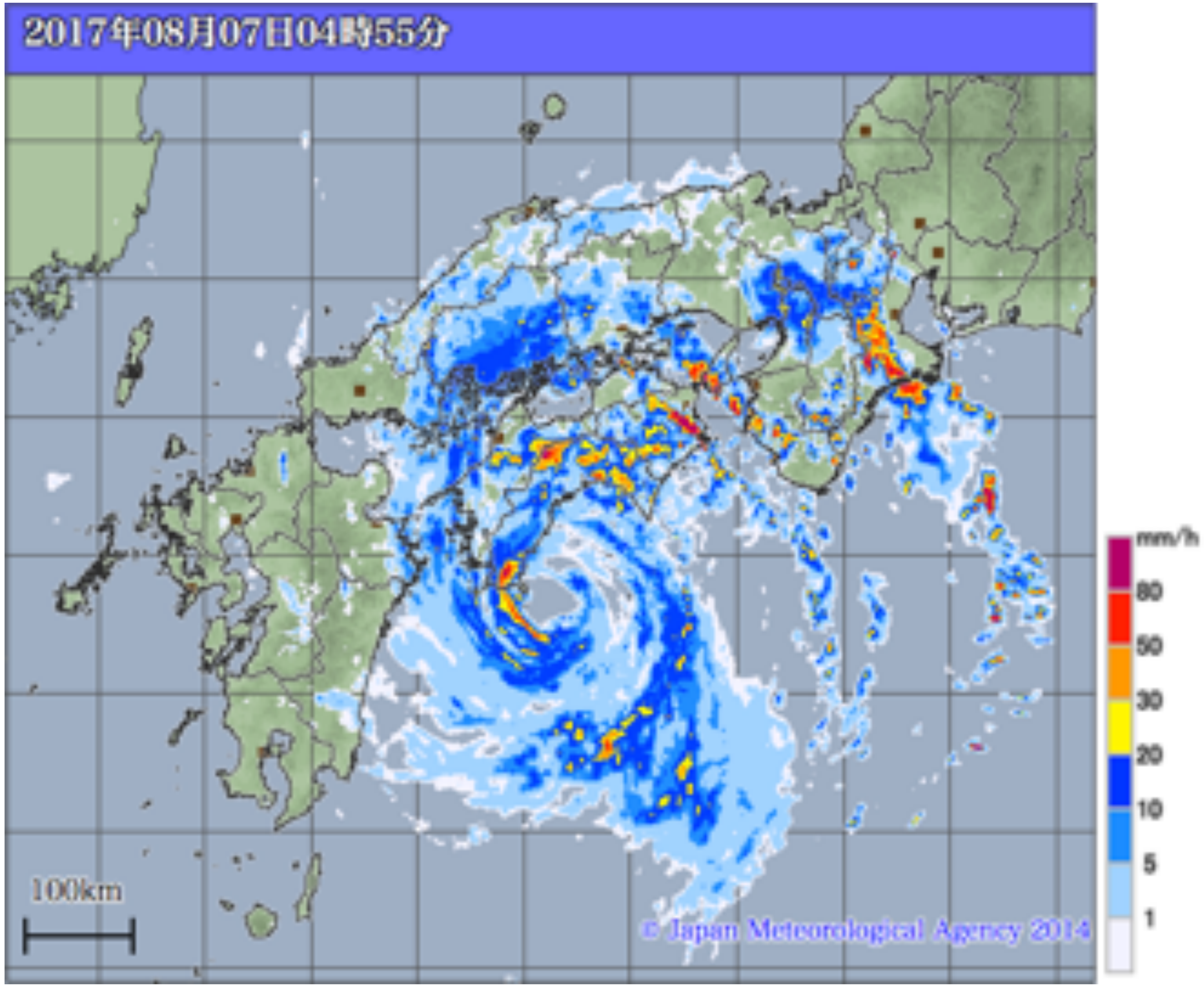

2017年08月07日04時55分
100km
© Japan Meteorological Agency 2014
mm/h
80
50
30
20
10
5
1

AM 05:00

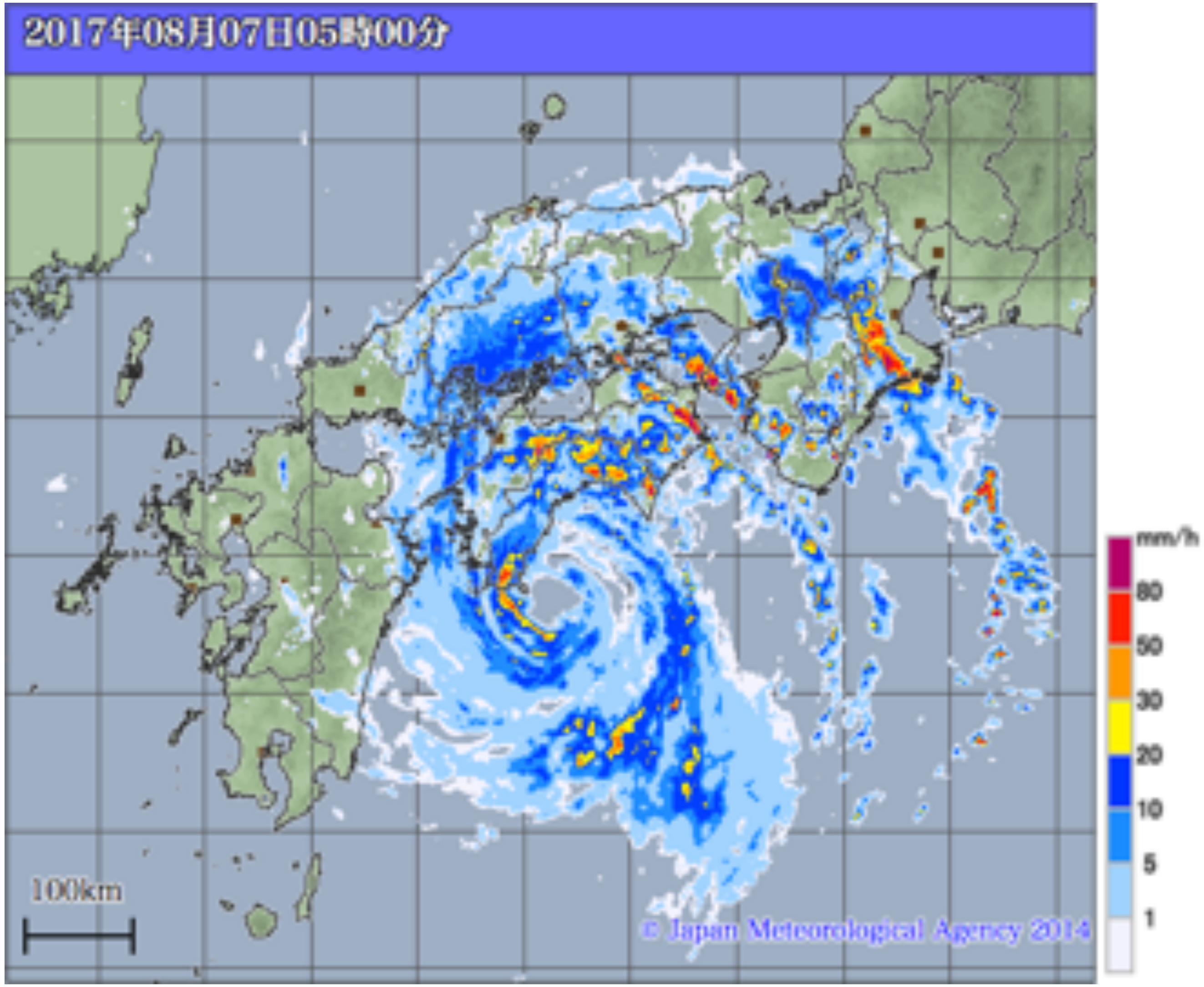
2017年08月07日05時00分
100km
© Japan Meteorological Agency 2014
mm/h
80
50
30
20
10
5
1

AM 05:05

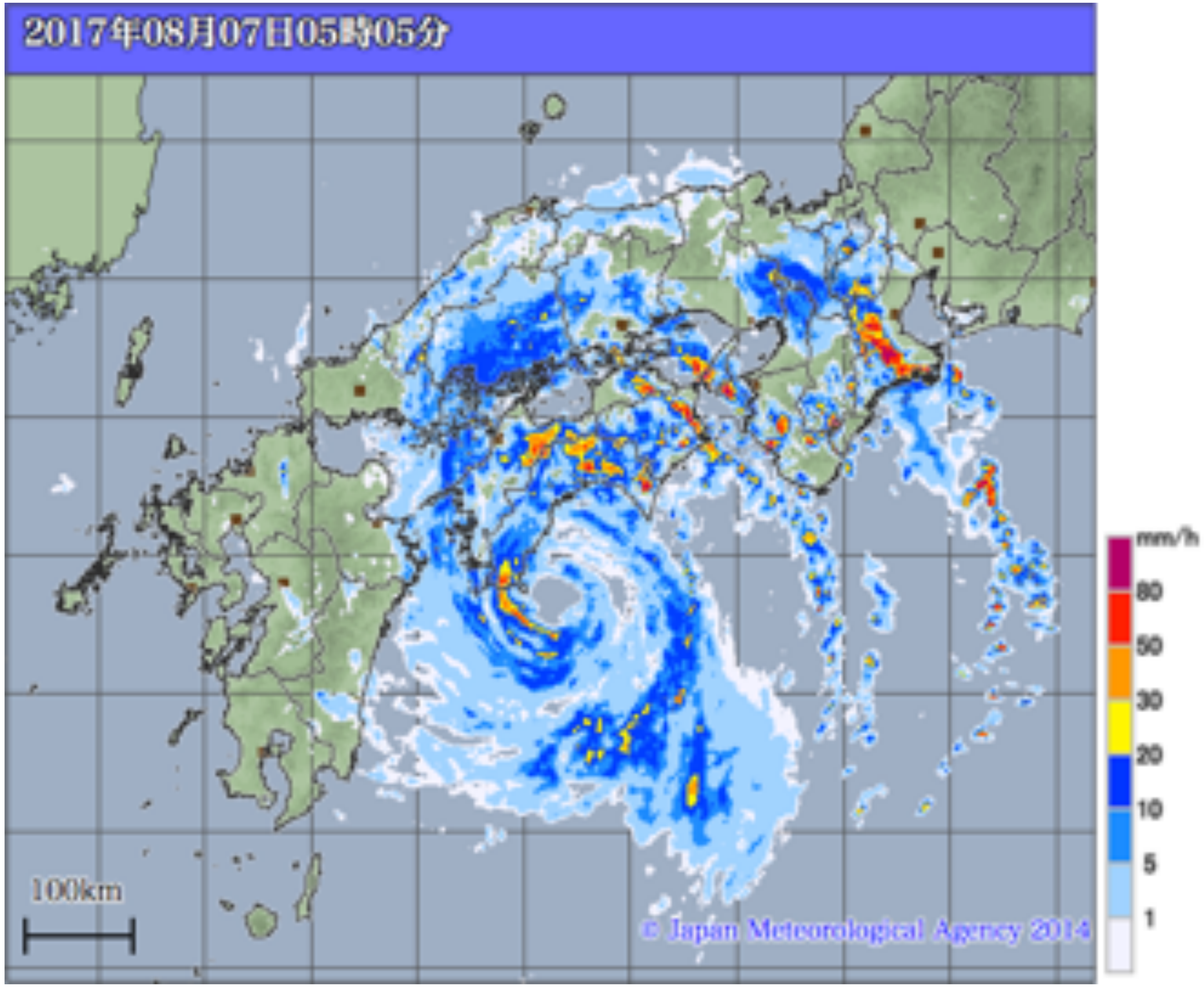
2017年08月07日05時05分
100km
© Japan Meteorological Agency 2014
mm/h
80
50
30
20
10
5
1

AM 05:10

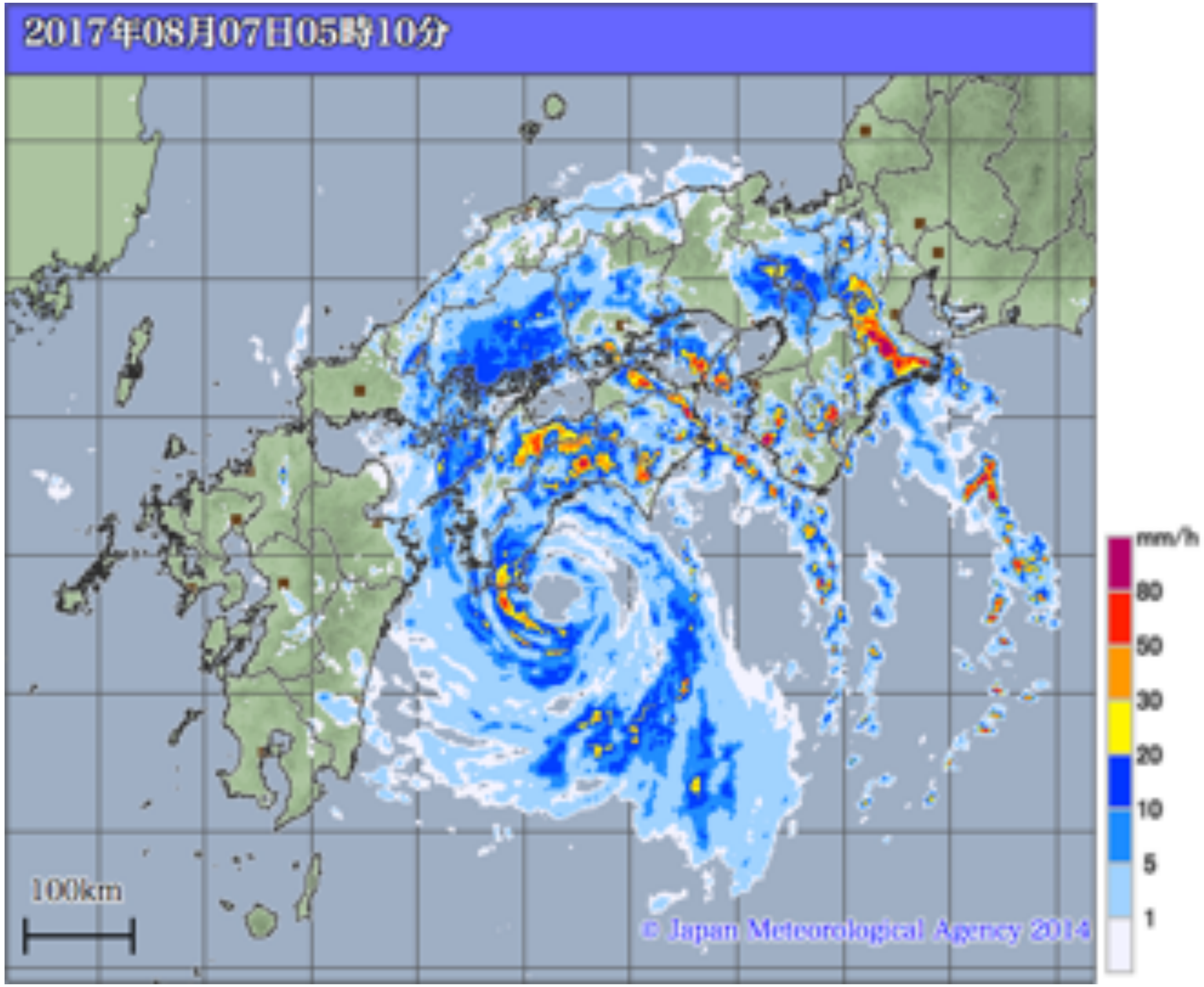
2017年08月07日05時10分
100km
© Japan Meteorological Agency 2014
mm/h
80
50
30
20
10
5
1

AM 05:15

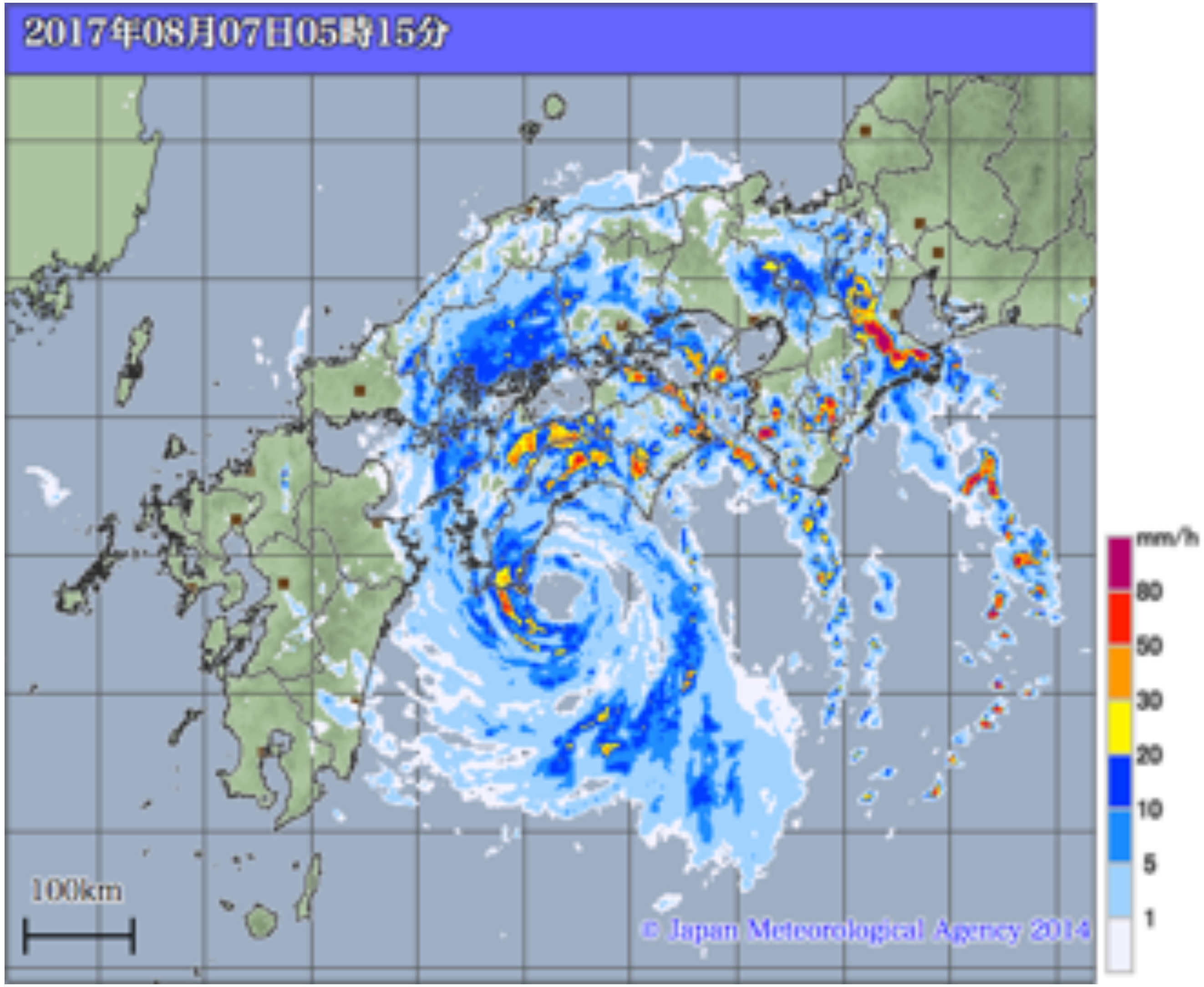
2017年08月07日05時15分
100km
© Japan Meteorological Agency 2014
mm/h
80
50
30
20
10
5
1

AM 05:20

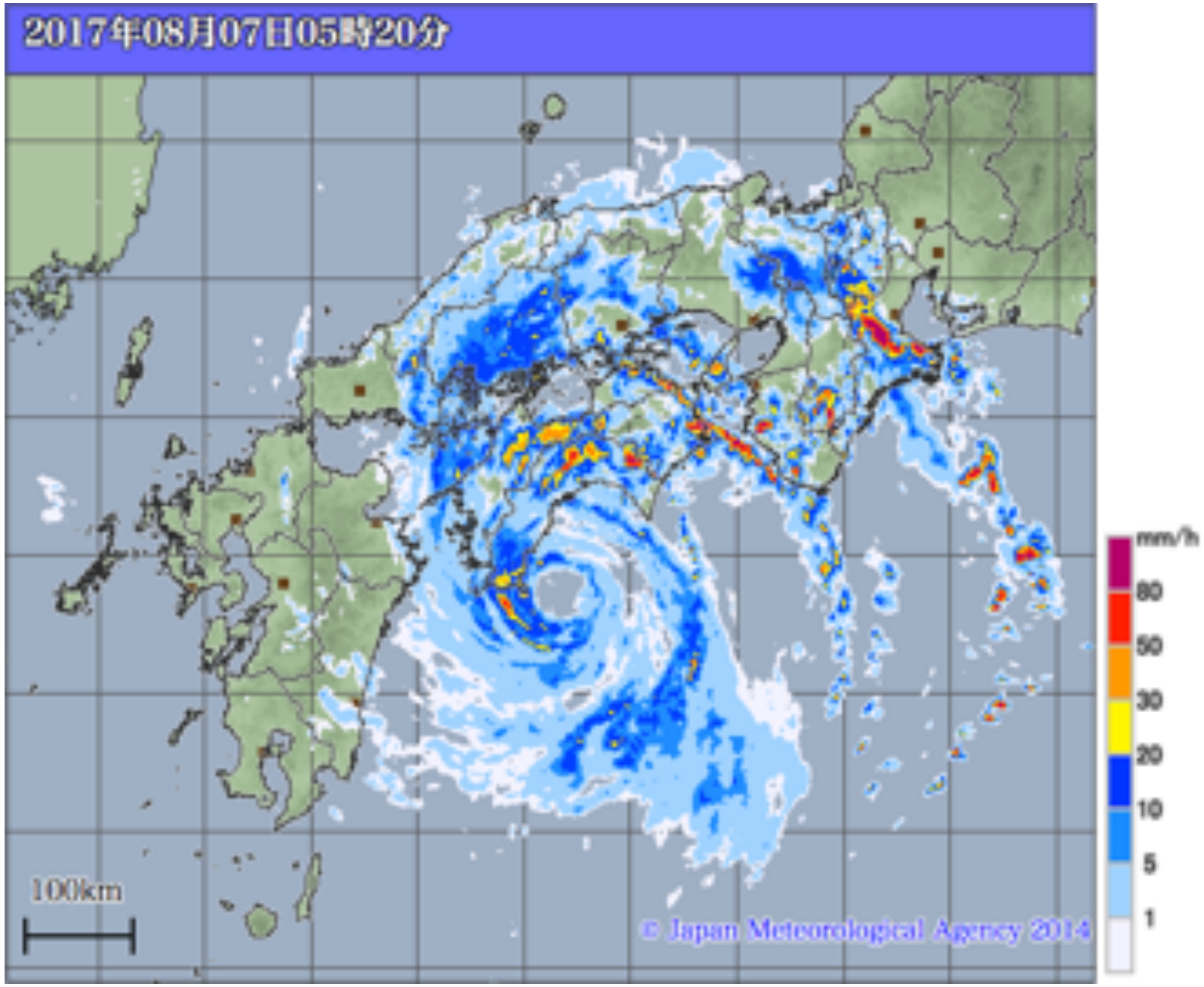

2017年08月07日05時20分
100km
© Japan Meteorological Agency 2014
mm/h
80
50
30
20
10
5
1

AM 05:25

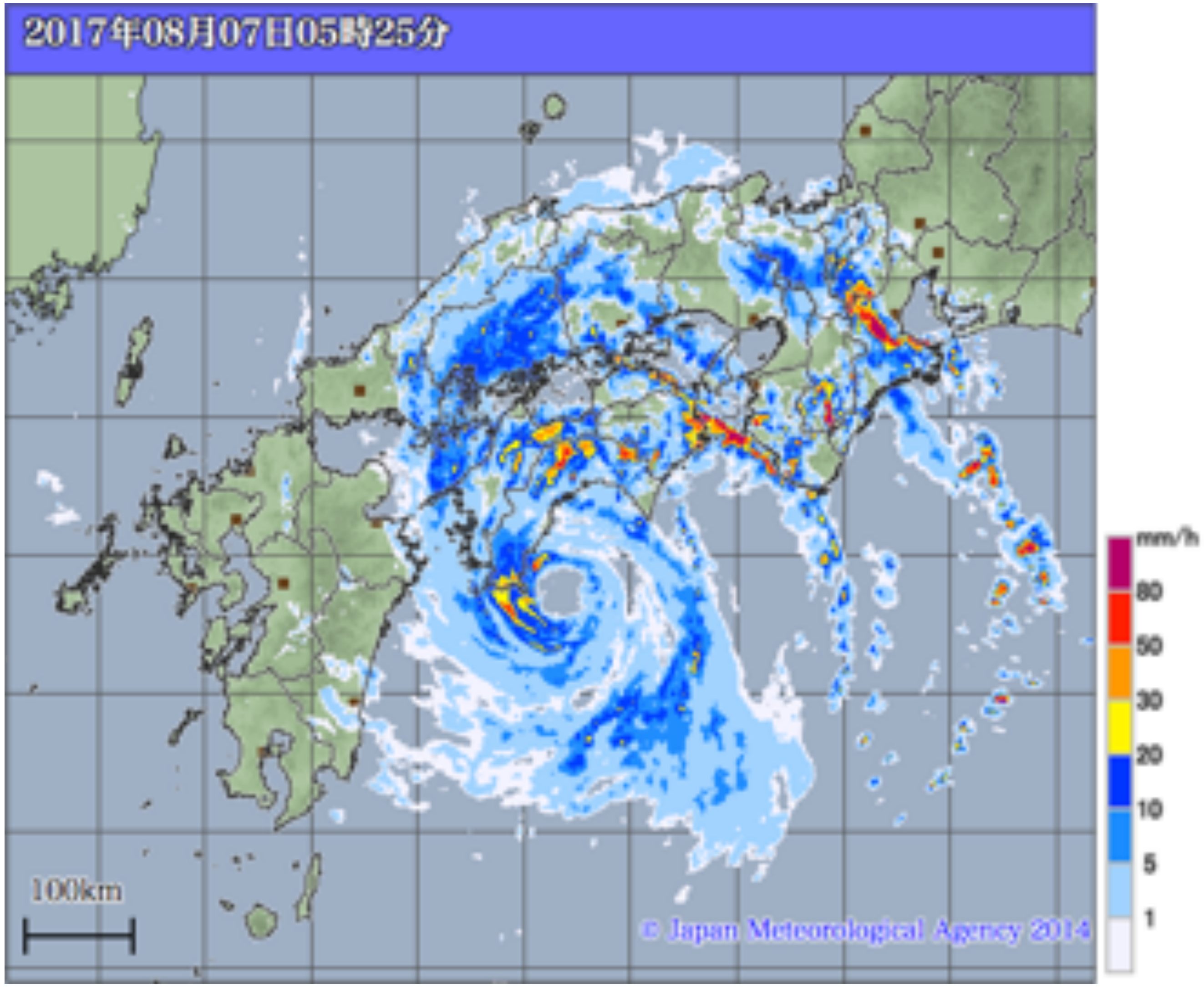
2017年08月07日05時25分
mm/h
80
50
30
20
10
5
1
100km
© Japan Meteorological Agency 2014

AM 05:30

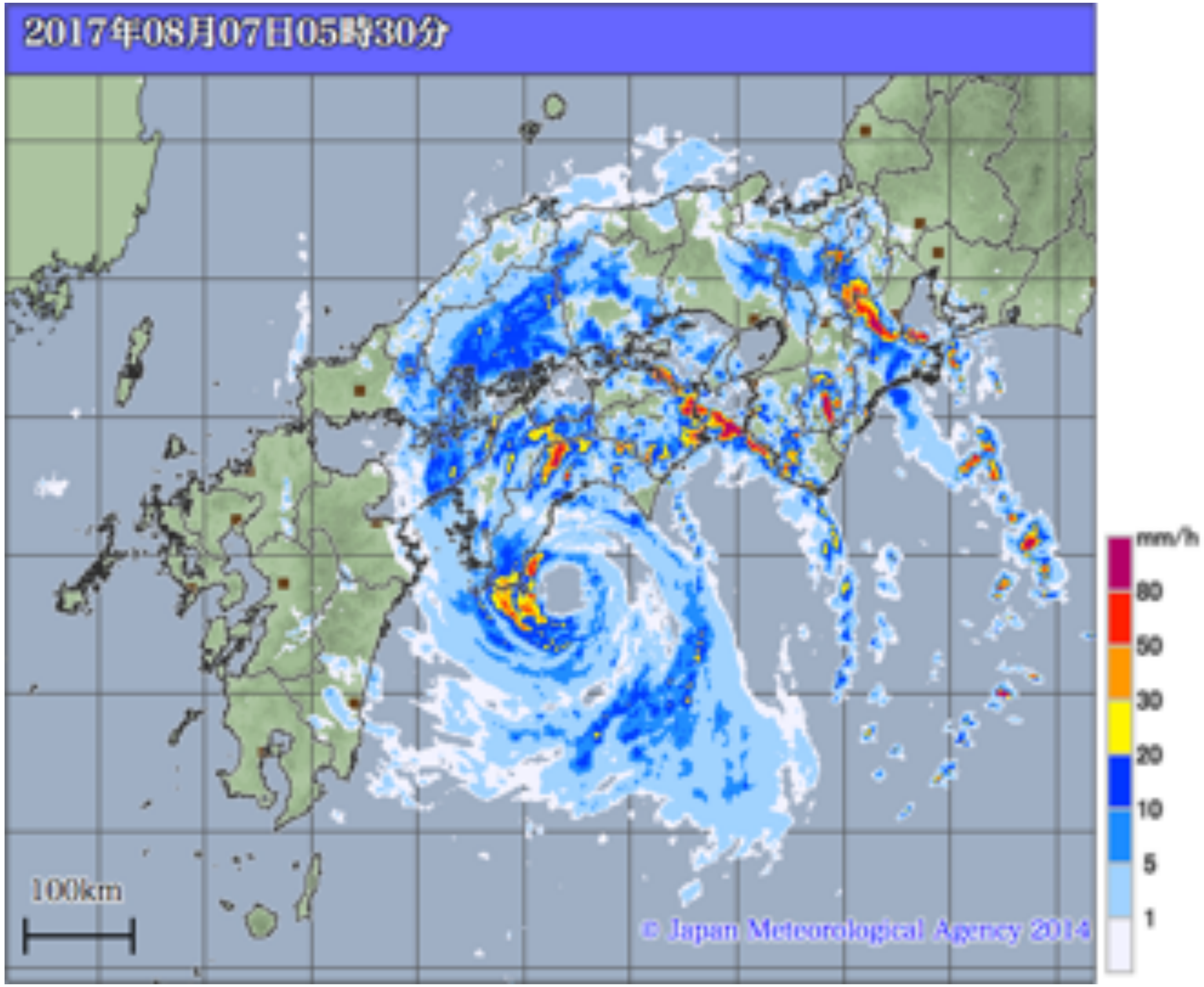
2017年08月07日05時30分
100km
© Japan Meteorological Agency 2014
mm/h
80
50
30
20
10
5
1

AM 05:35

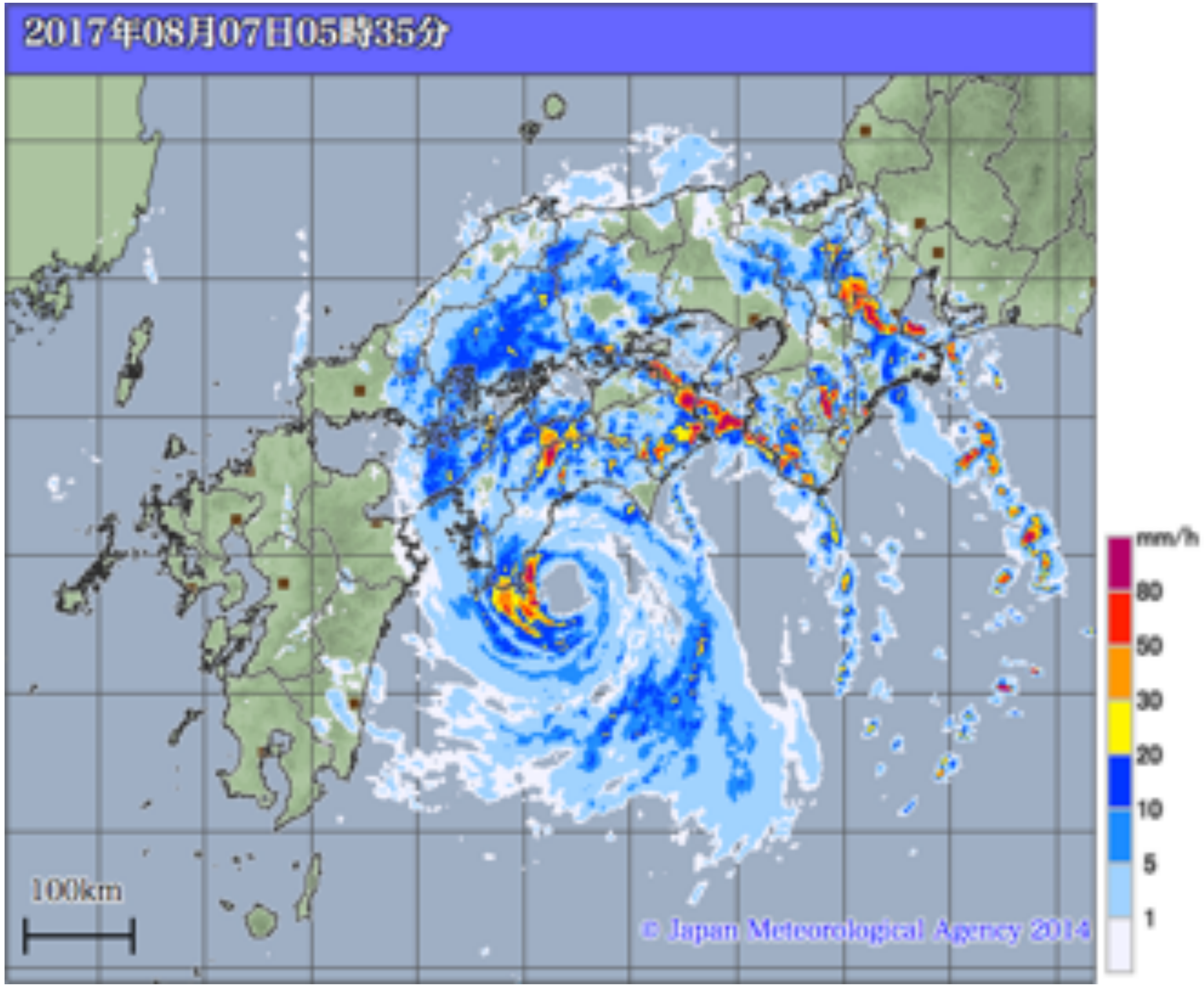
2017年08月07日05時35分
mm/h
80
50
30
20
10
5
1
100km
© Japan Meteorological Agency 2014

AM 05:40

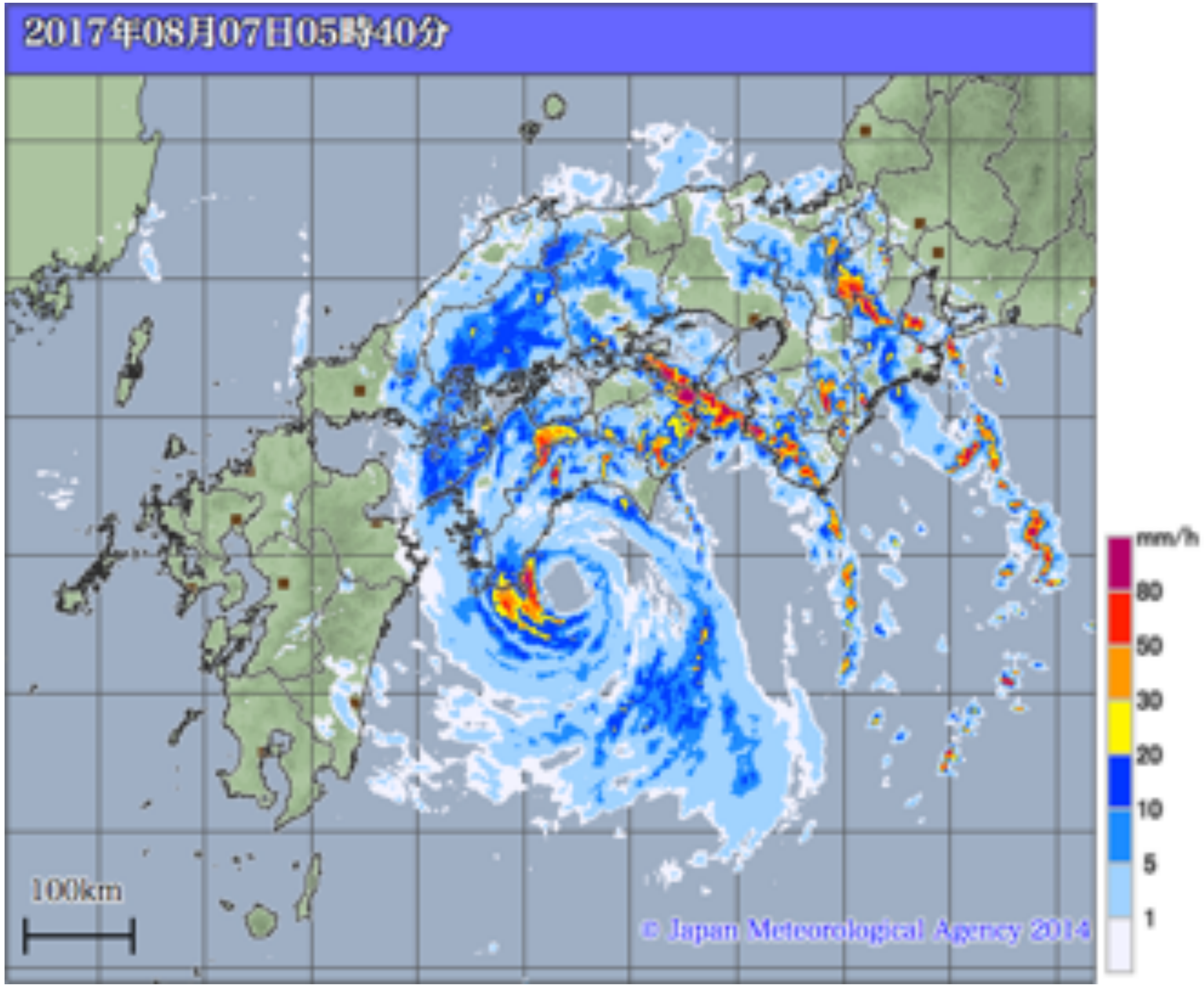
2017年08月07日05時40分
100km
© Japan Meteorological Agency 2014
mm/h
80
50
30
20
10
5
1

AM 05:45

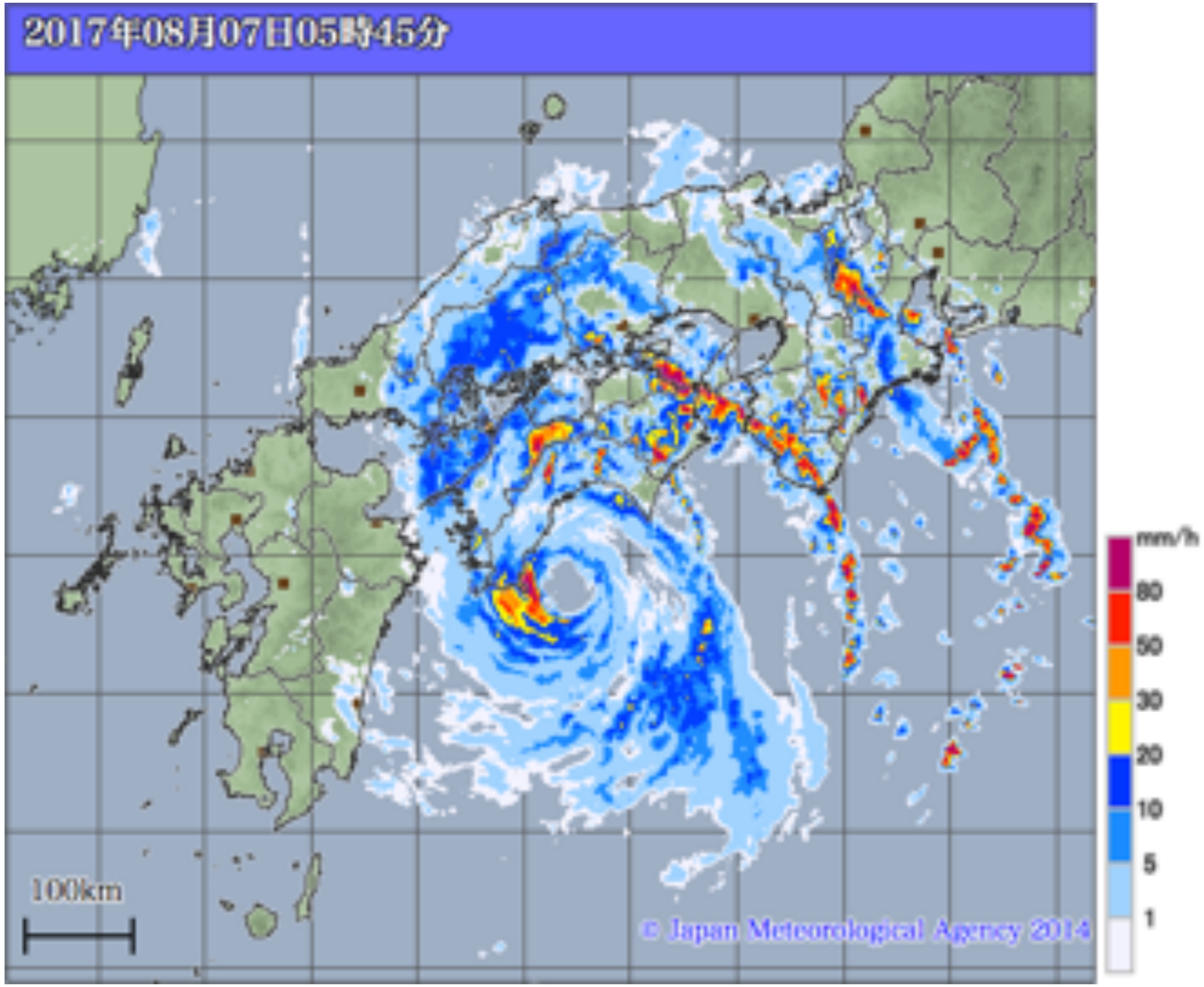
2017年08月07日05時45分
100km
© Japan Meteorological Agency 2014
mm/h
80
50
30
20
10
5
1

AM 05:50

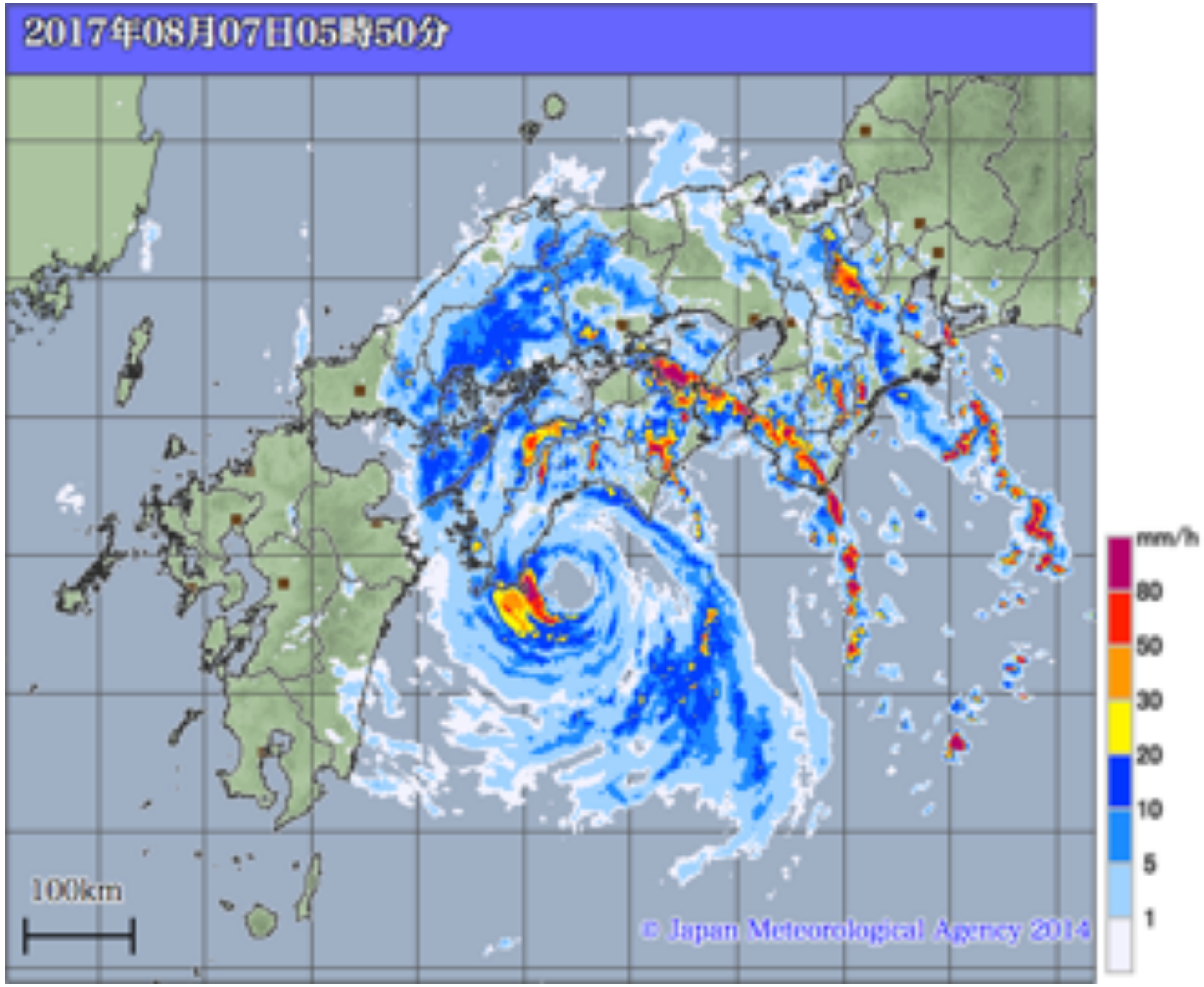
2017年08月07日05時50分
100km
© Japan Meteorological Agency 2014
mm/h
80
50
30
20
10
5
1

AM 05:55

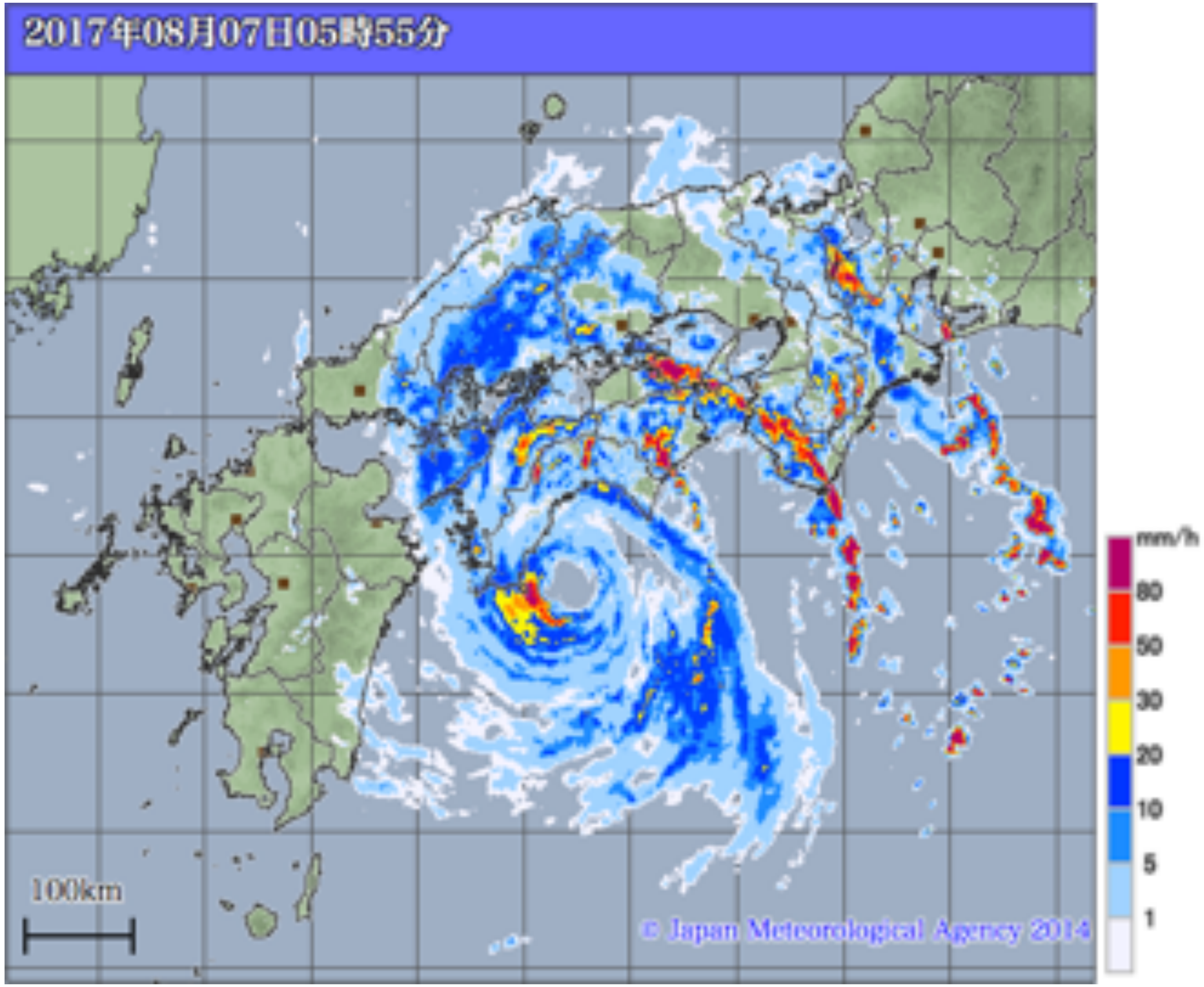
2017年08月07日05時55分
100km
© Japan Meteorological Agency 2014
mm/h
80
50
30
20
10
5
1

AM 06:00

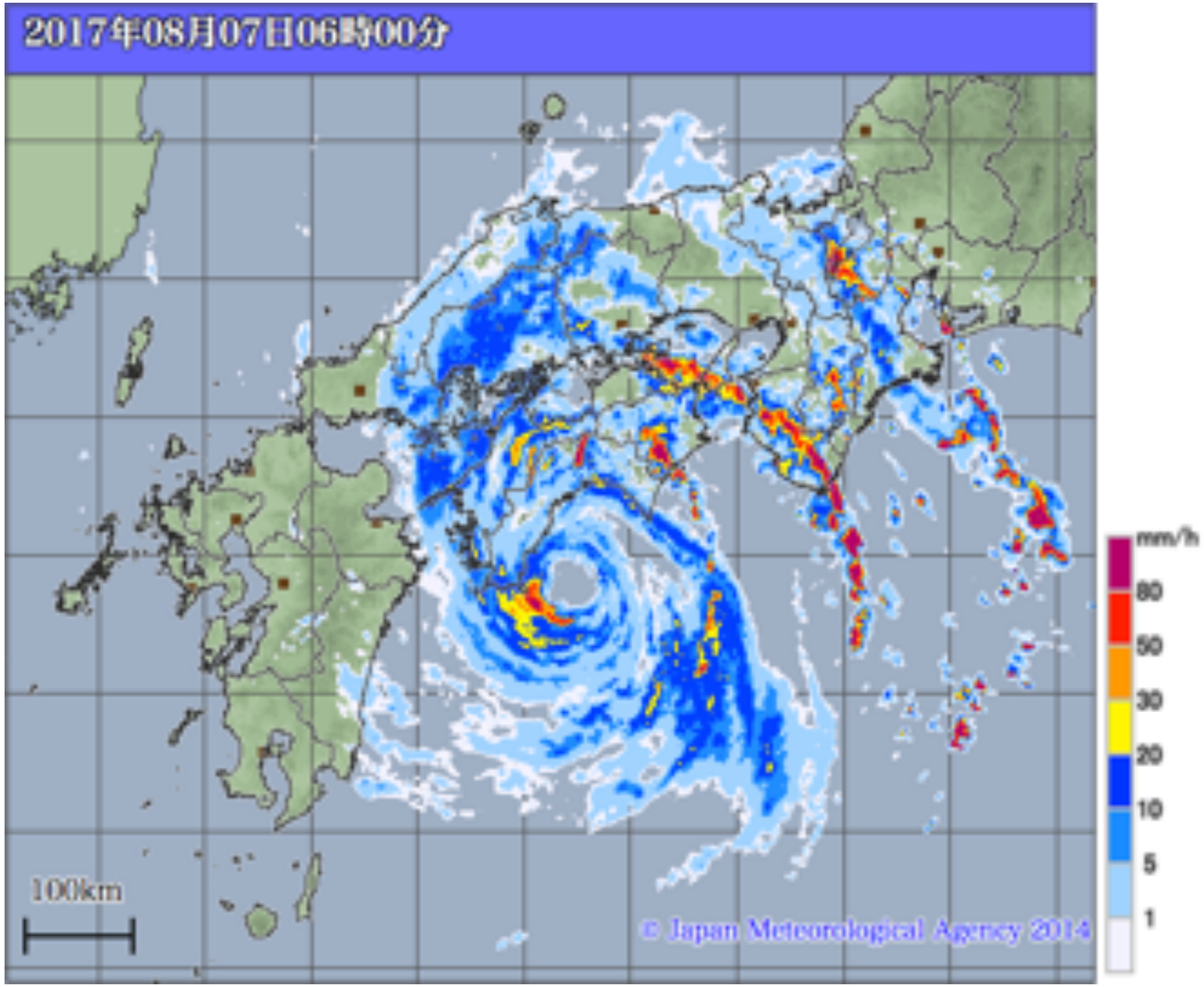
2017年08月07日06時00分
100km
© Japan Meteorological Agency 2014
mm/h
80
50
30
20
10
5
1

AM 06:05

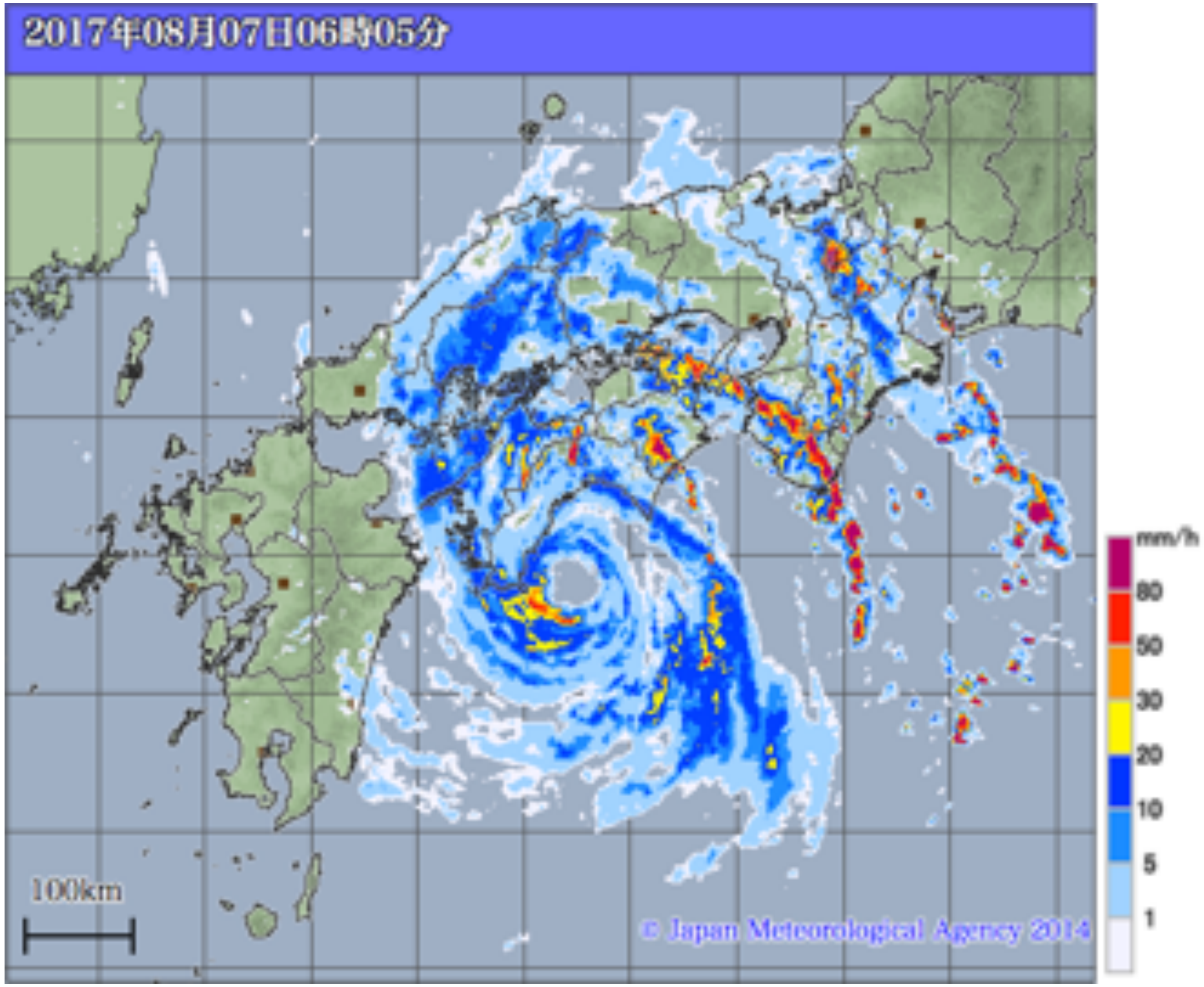
2017年08月07日06時05分
100km
© Japan Meteorological Agency 2014
mm/h
80
50
30
20
10
5
1

AM 06:10

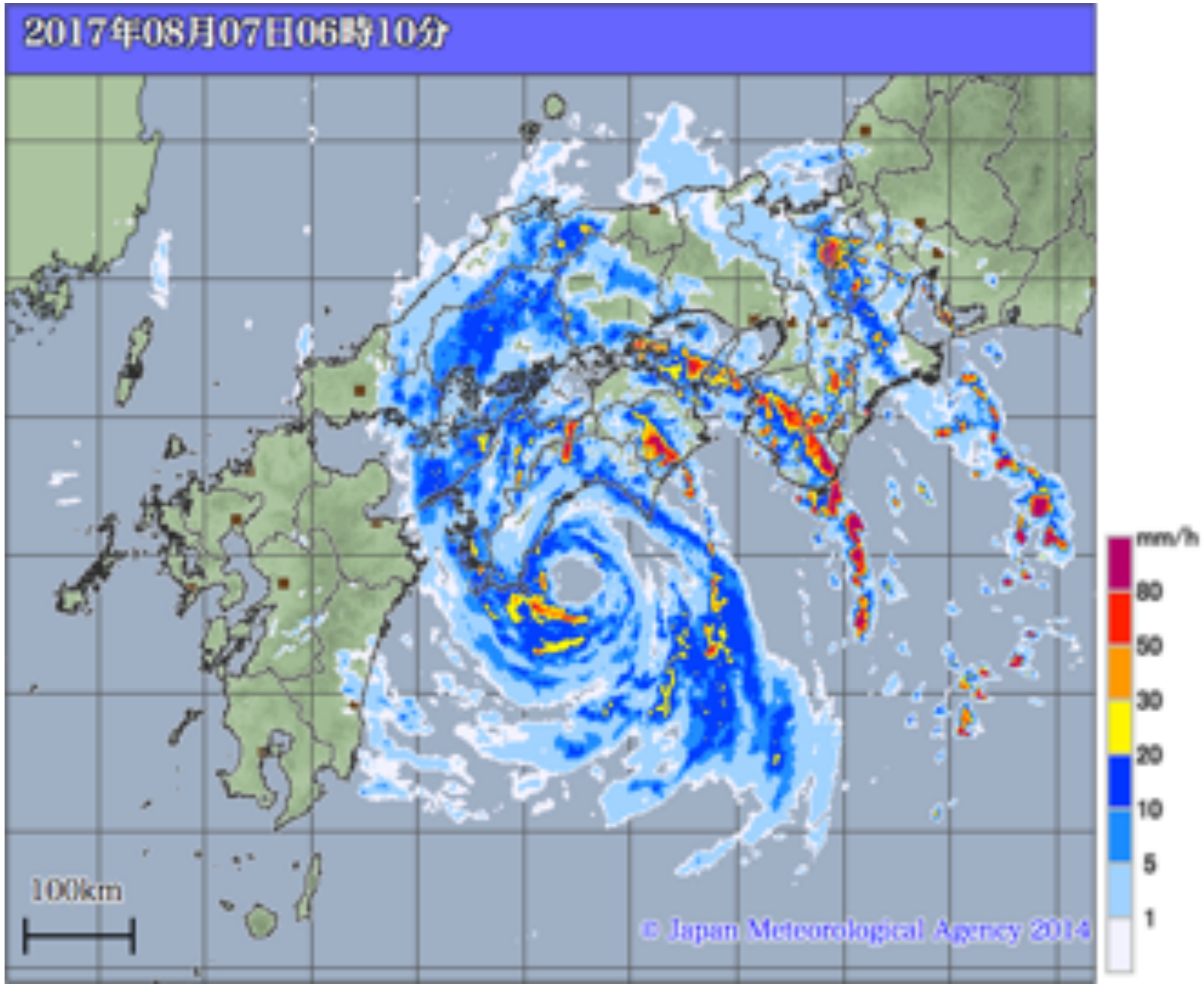
2017年08月07日06時10分
100km
© Japan Meteorological Agency 2014
mm/h
80
50
30
20
10
5
1

AM 06:15

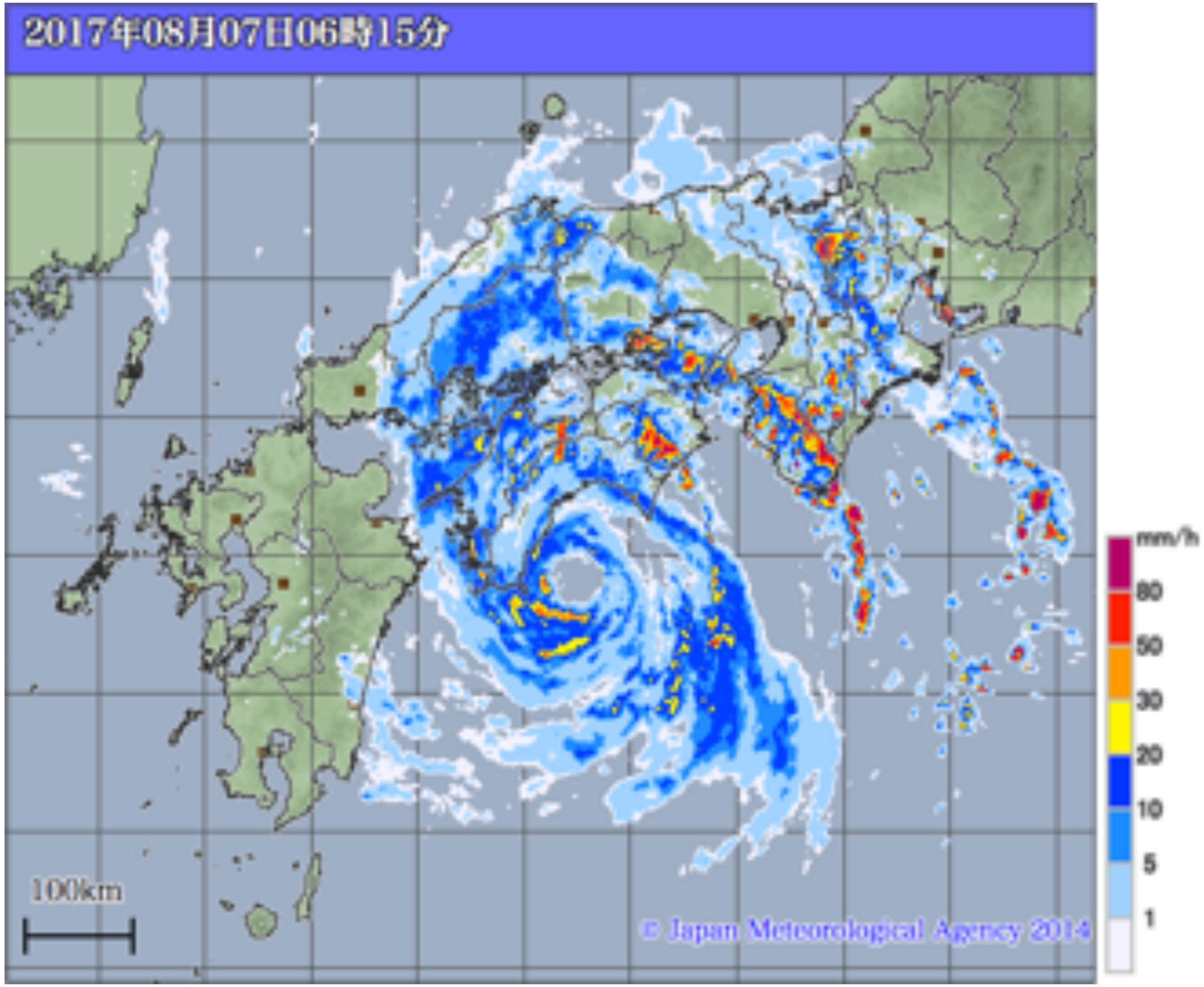
2017年08月07日06時15分
100km
© Japan Meteorological Agency 2014
mm/h
80
50
30
20
10
5
1

AM 06:20

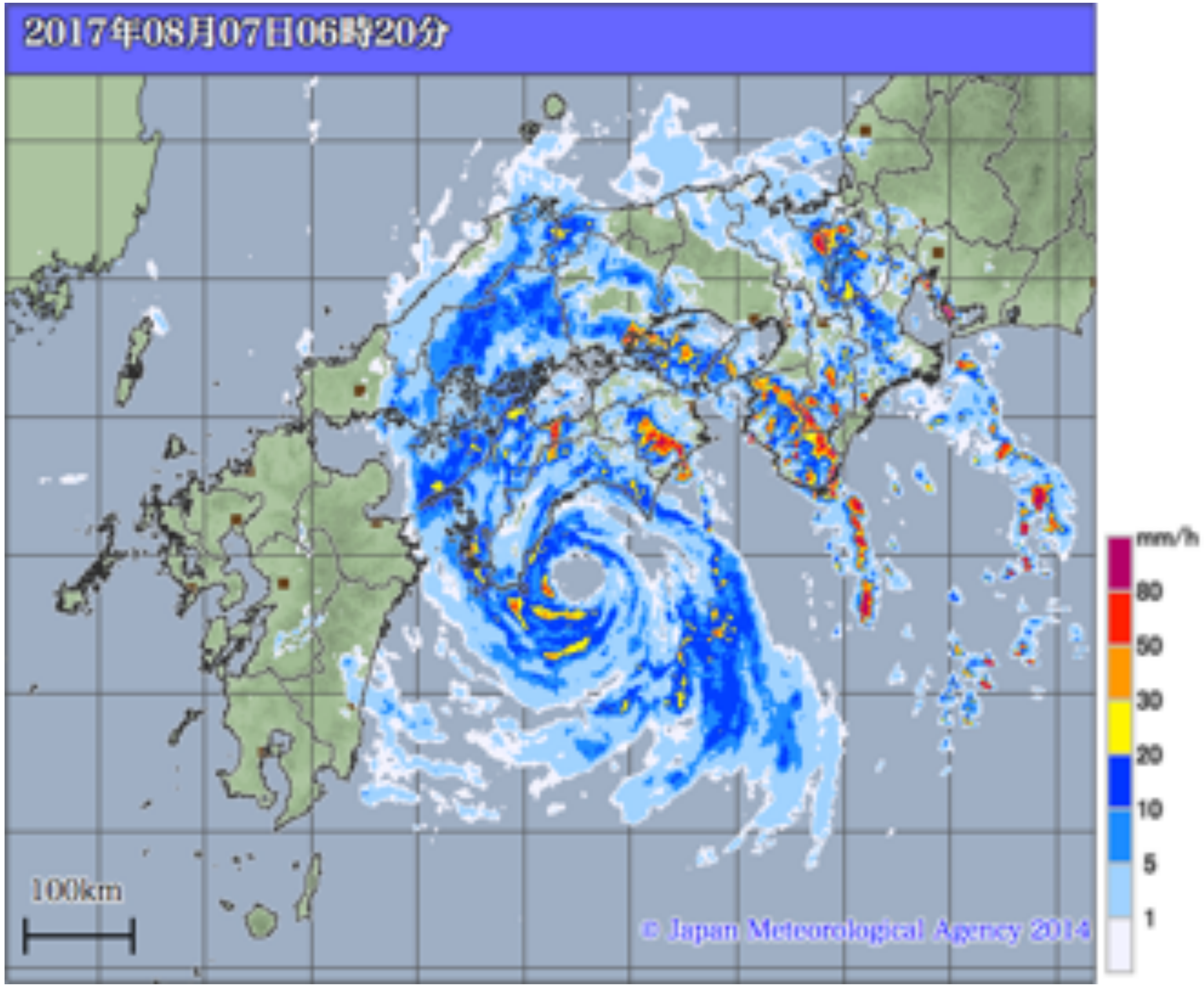
2017年08月07日06時20分
100km
© Japan Meteorological Agency 2014
mm/h
80
50
30
20
10
5
1

AM 06:25

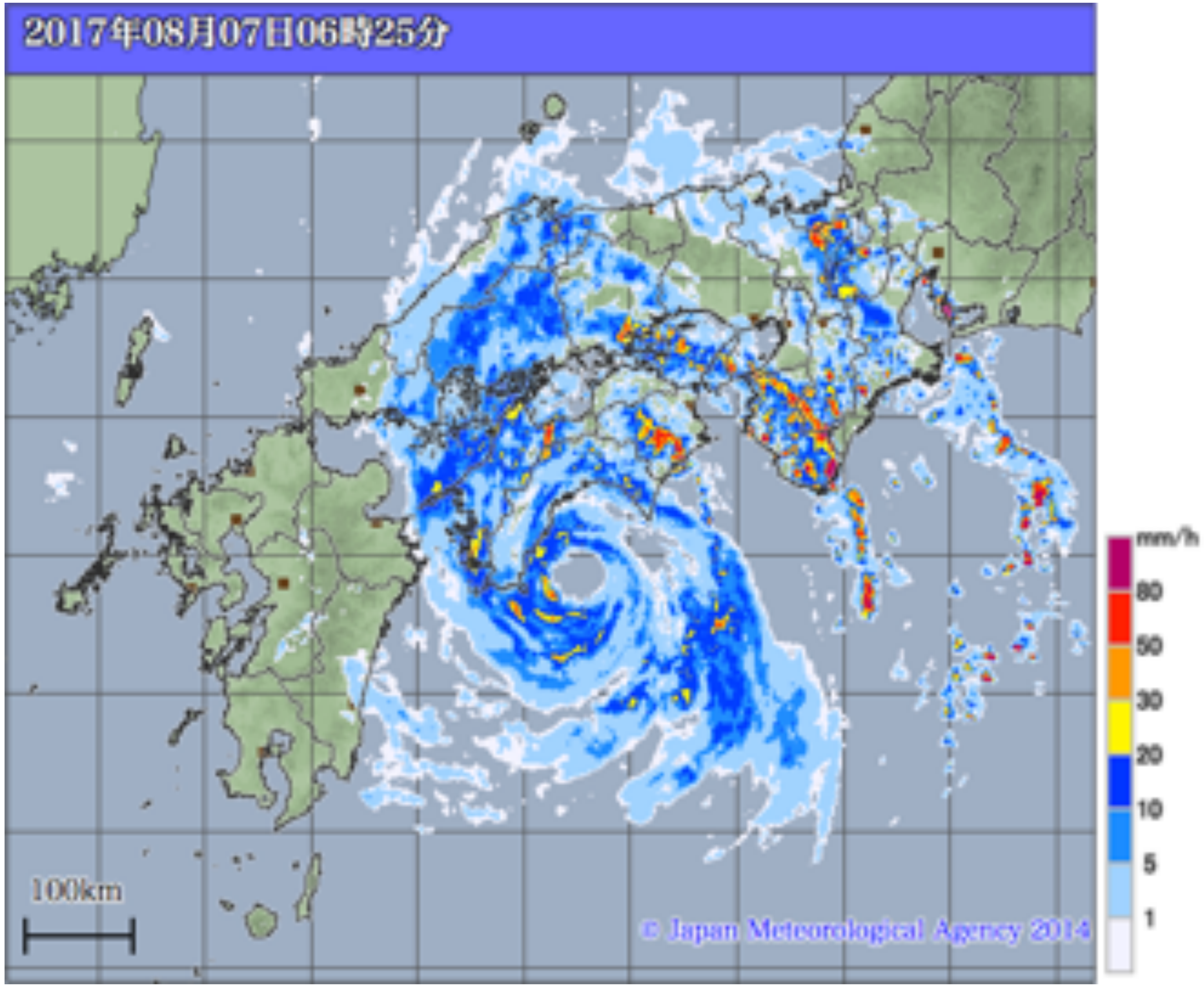
2017年08月07日06時25分
100km
© Japan Meteorological Agency 2014
mm/h
80
50
30
20
10
5
1

AM 06:30

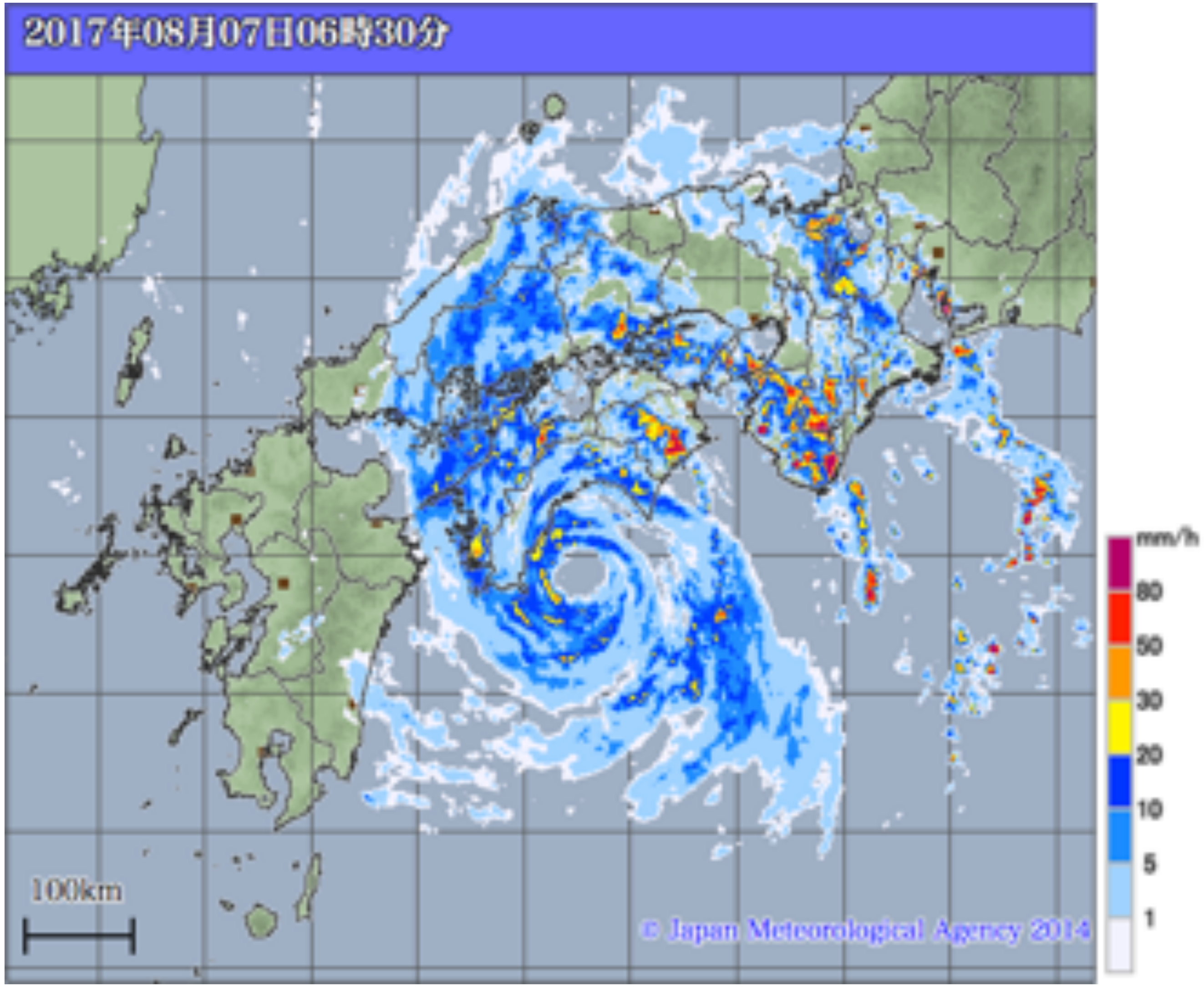
2017年08月07日06時30分
100km
© Japan Meteorological Agency 2014
mm/h
80
50
30
20
10
5
1

AM 06:35

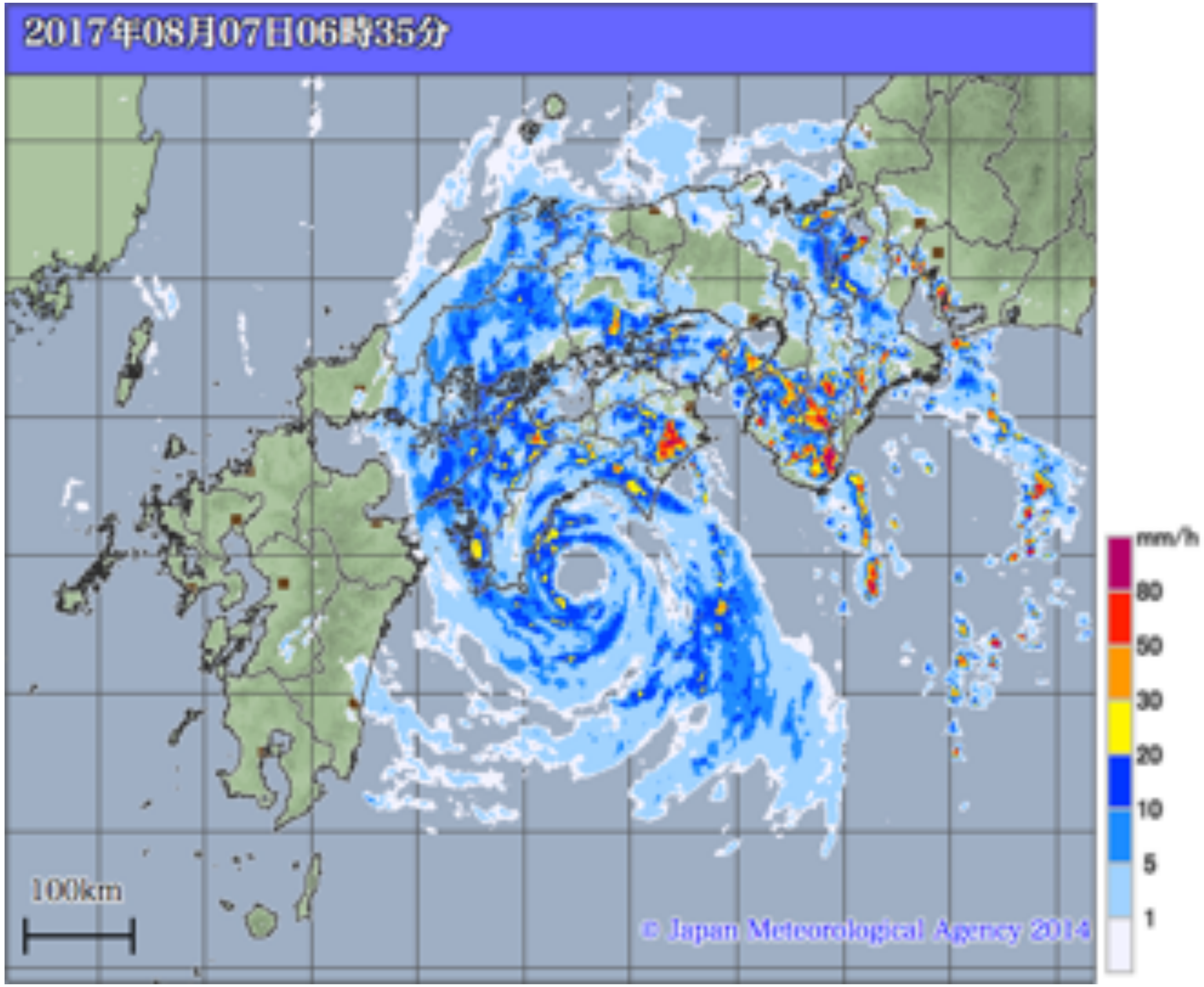
2017年08月07日06時35分
100km
© Japan Meteorological Agency 2014
mm/h
80
50
30
20
10
5
1

AM 06:40

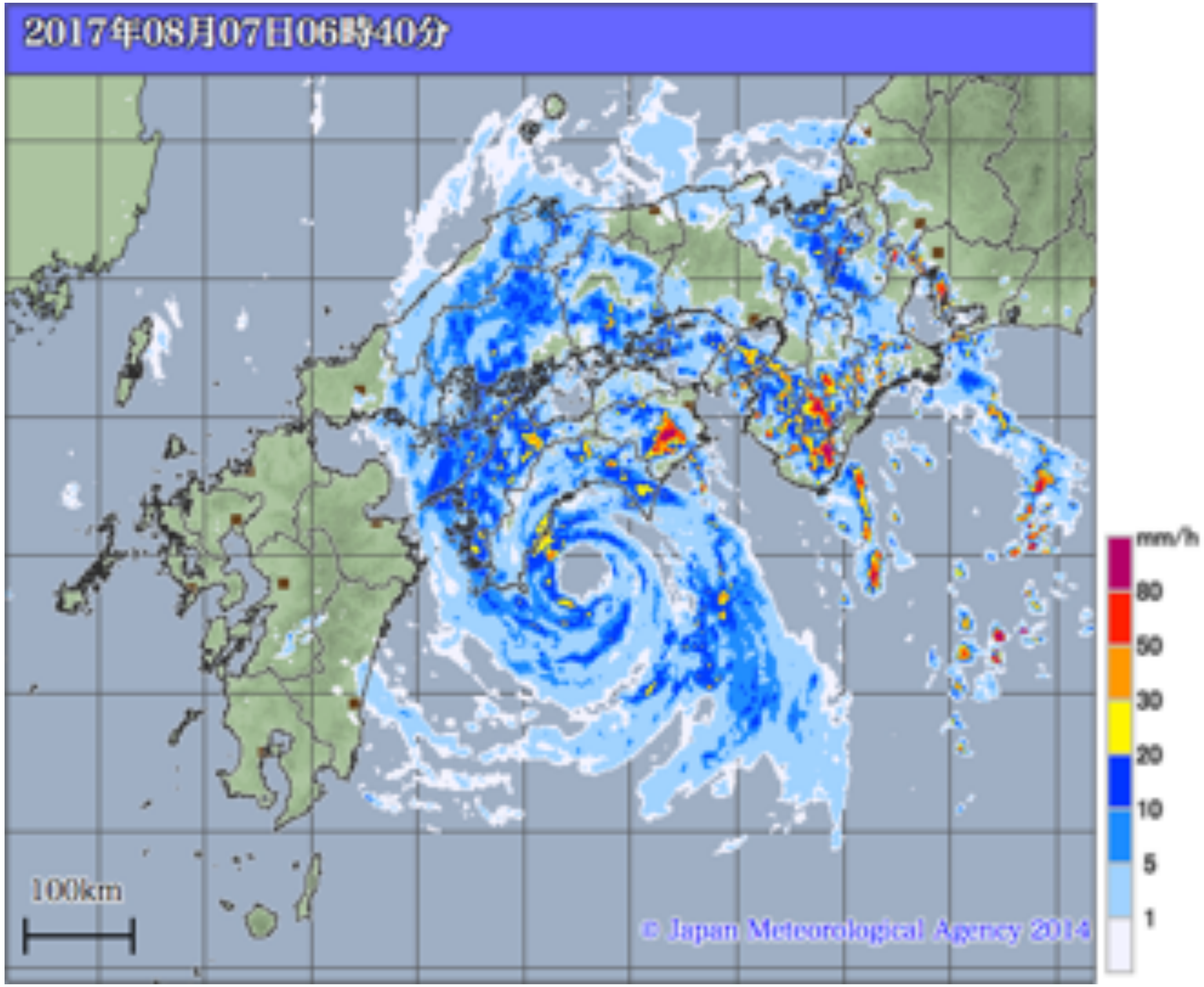
2017年08月07日06時40分
100km
© Japan Meteorological Agency 2014
mm/h
80
50
30
20
10
5
1

AM 06:45

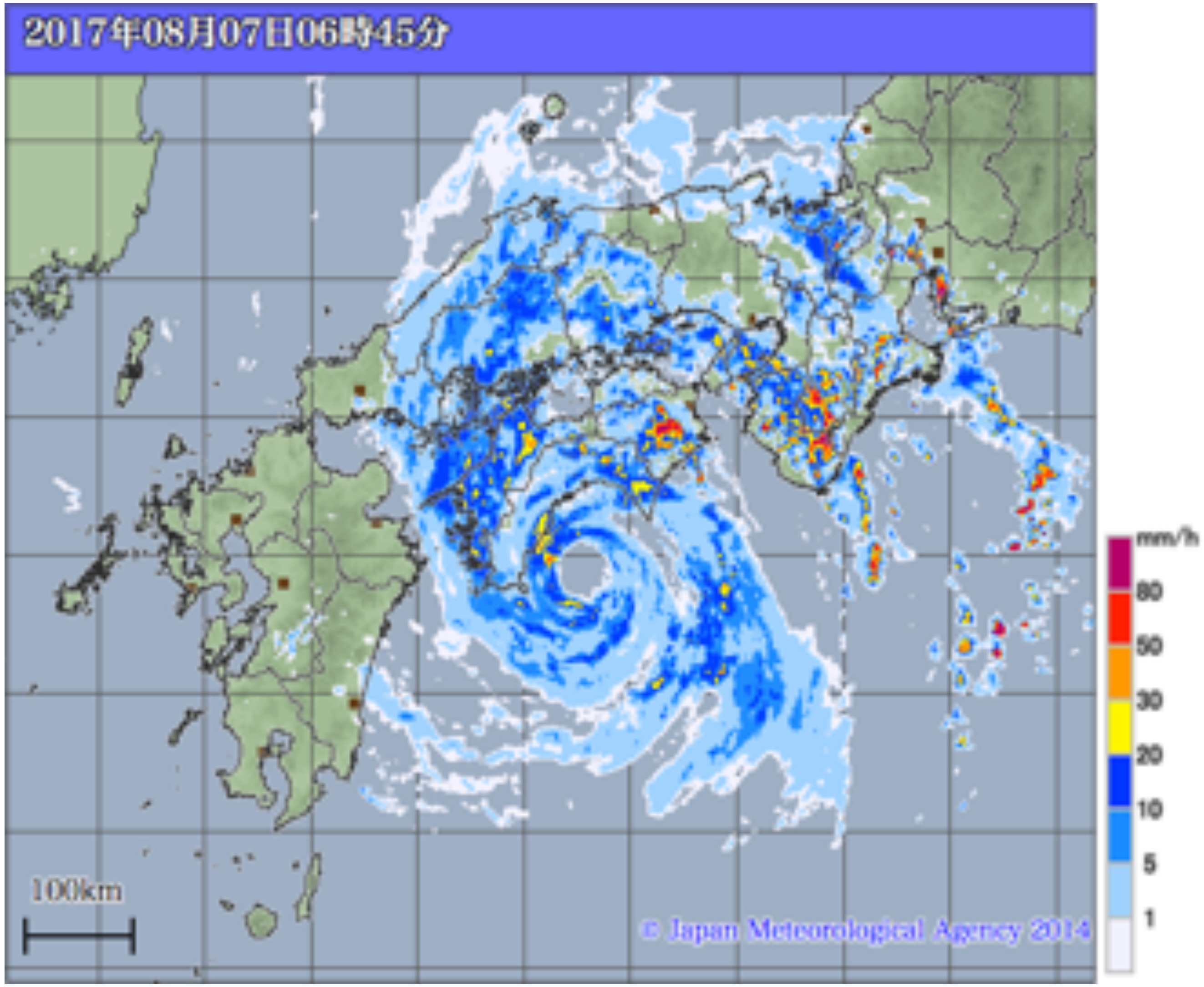
2017年08月07日06時45分
100km
© Japan Meteorological Agency 2014
mm/h
80
50
30
20
10
5
1

AM 06:50

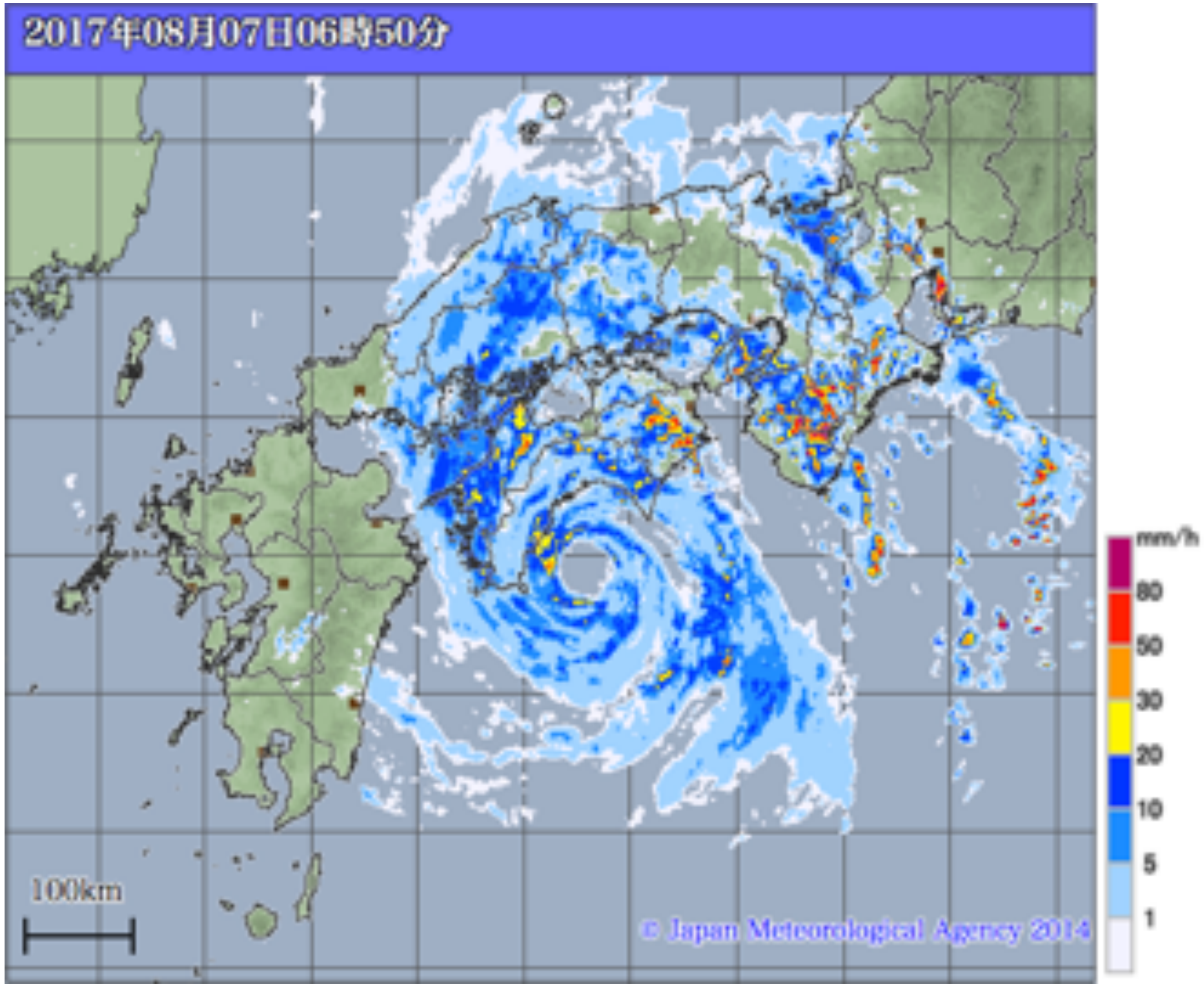
2017年08月07日06時50分
100km
© Japan Meteorological Agency 2014
mm/h
80
50
30
20
10
5
1

AM 06:55

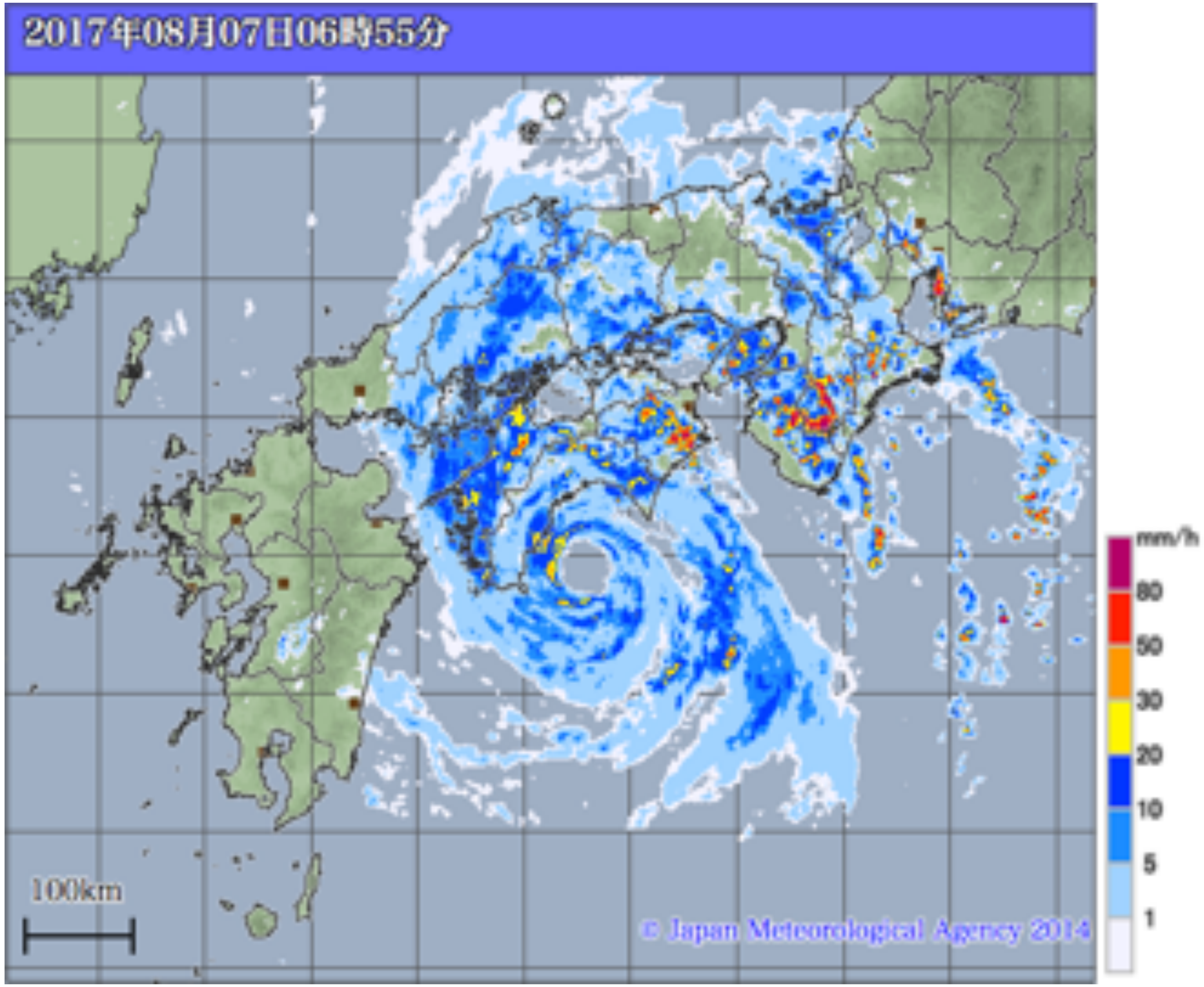

2017年08月07日06時55分
100km
© Japan Meteorological Agency 2014
mm/h
80
50
30
20
10
5
1

AM 07:00

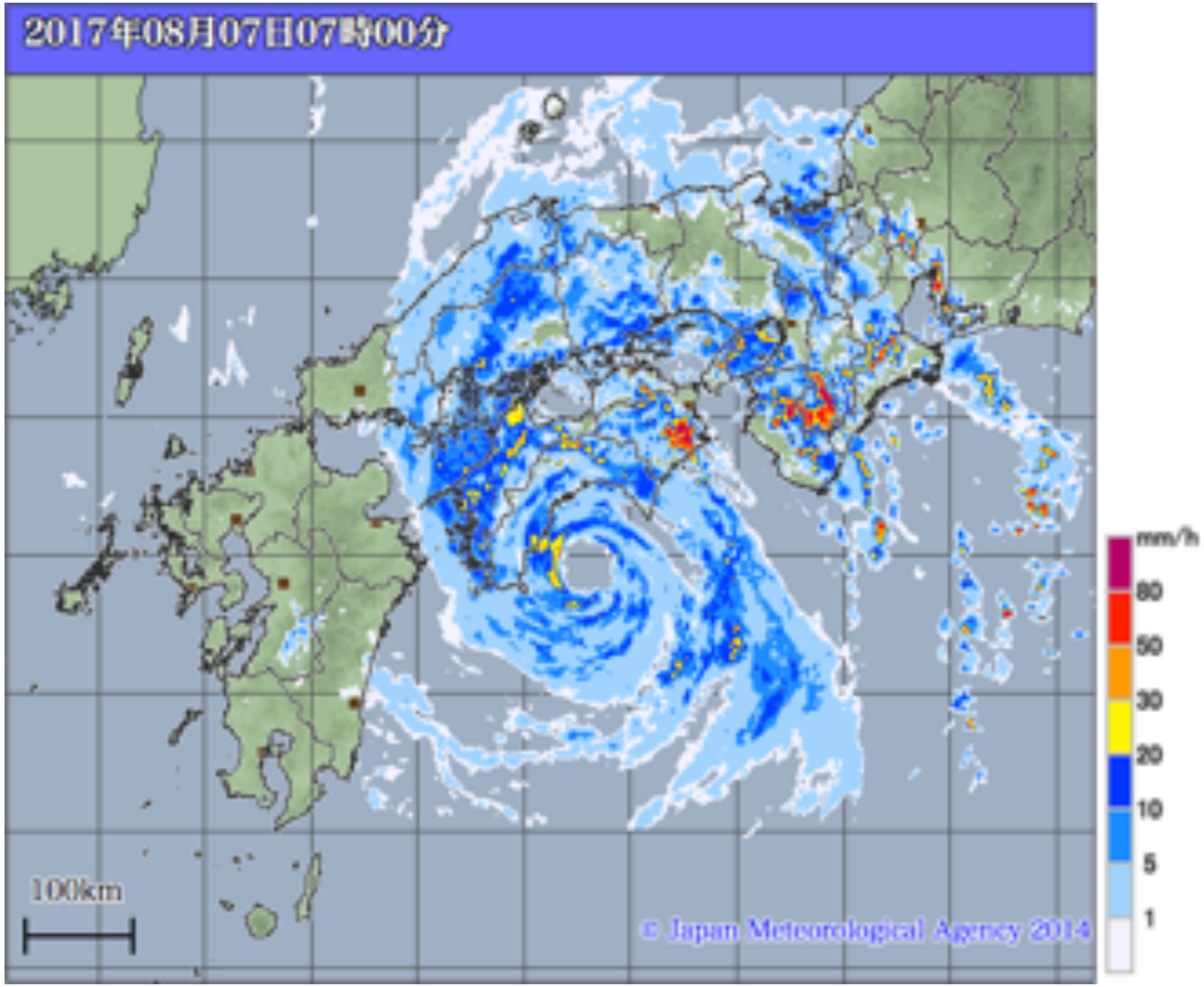

2017年08月07日07時00分
100km
© Japan Meteorological Agency 2014
mm/h
80
50
30
20
10
5
1

Significant layer in real geophysical flow

Layer structures associated with typhoon 5 in 2017

Similar structure

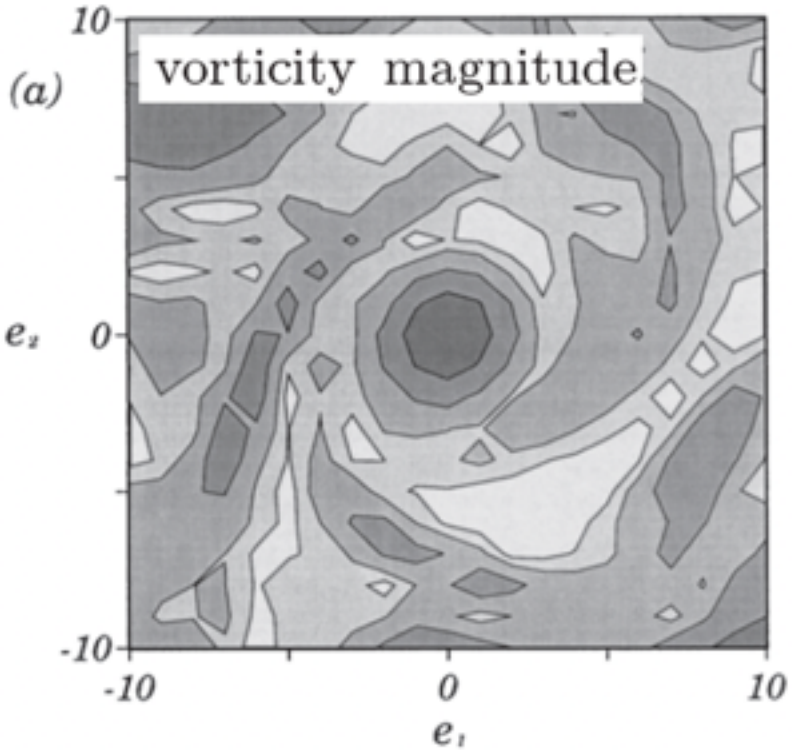

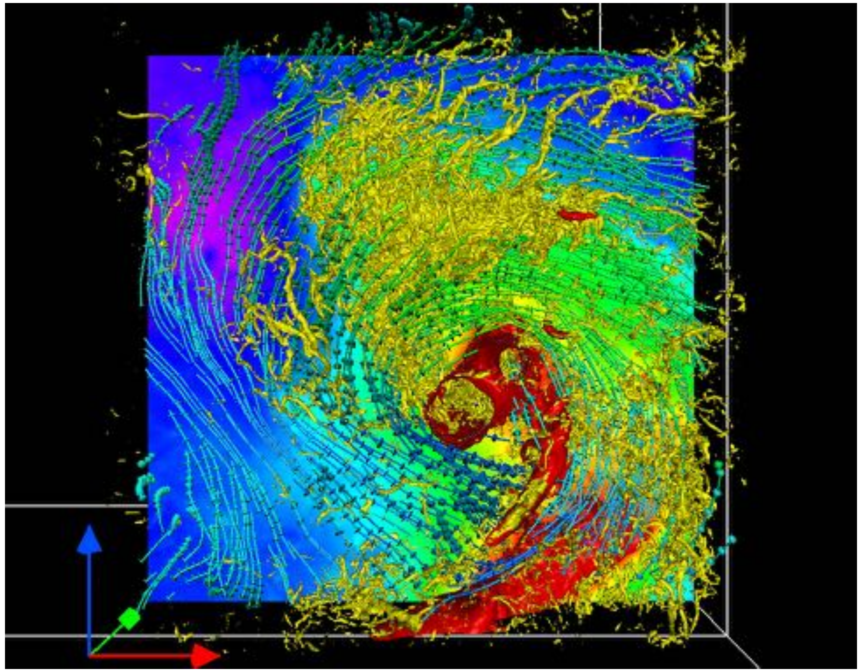

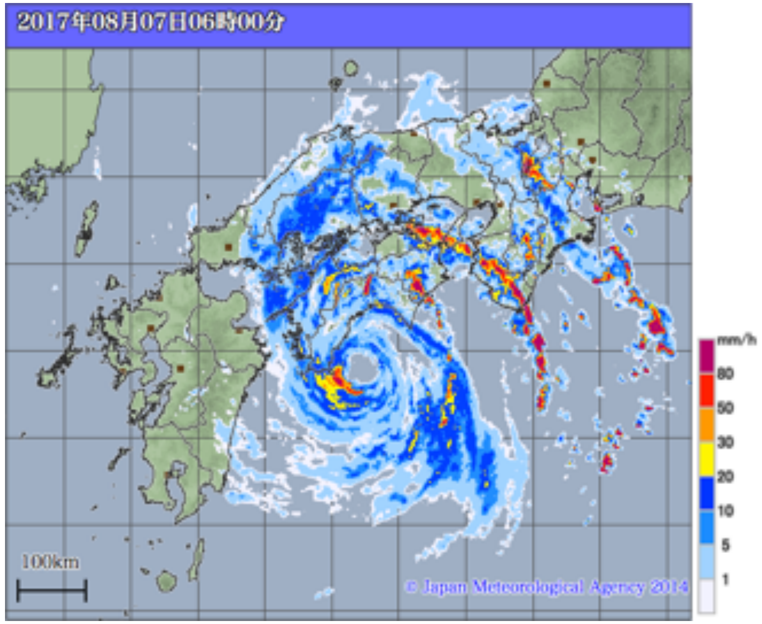

Precipitation

Low pressure core + vortical layer(spiral arms)

Meso-Scale Model (MSM)

Japan Meteorological Agency

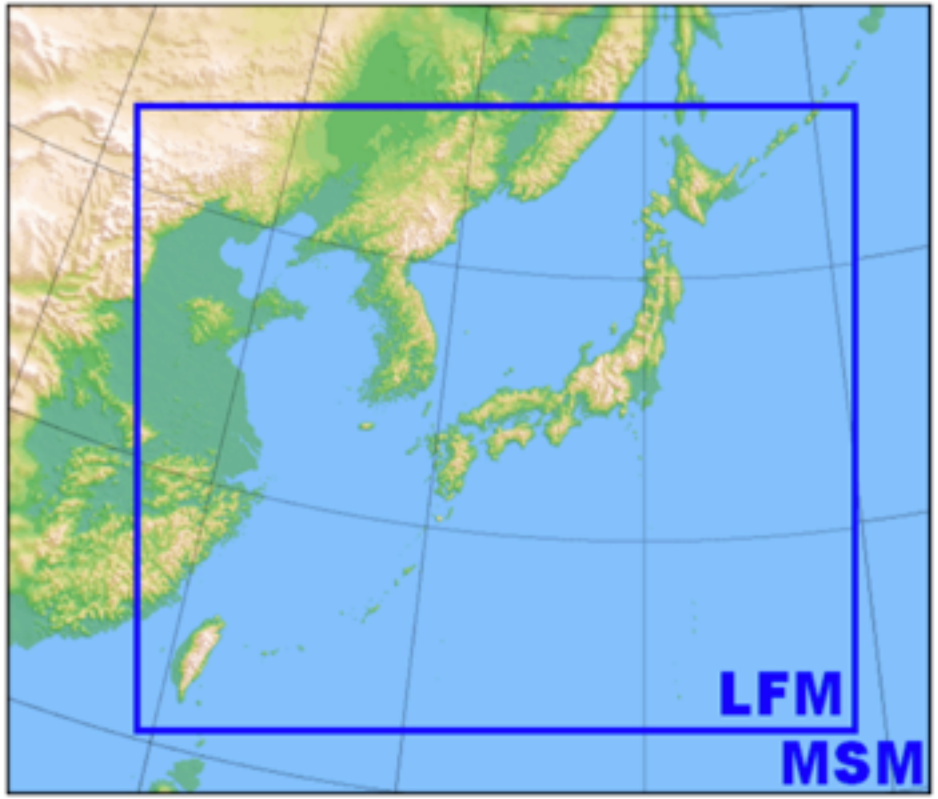

Domains and topography of JMA's NWP models

Purpose: Weather warnings/advisories,
Very short-range forecasts of precipitation

Grid size and/or number of grids: 5 km/817 x 661

Vertical levels/Top: 76/21.8 km

Initial conditions for MSM (every three hours):
Best archived data generated by ensemble-based 4-D variational data assimilation

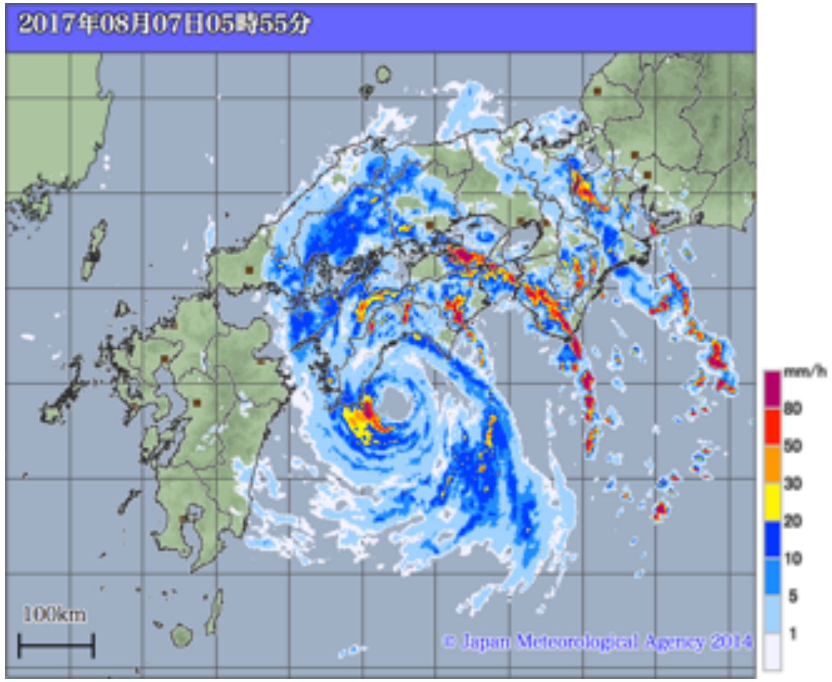

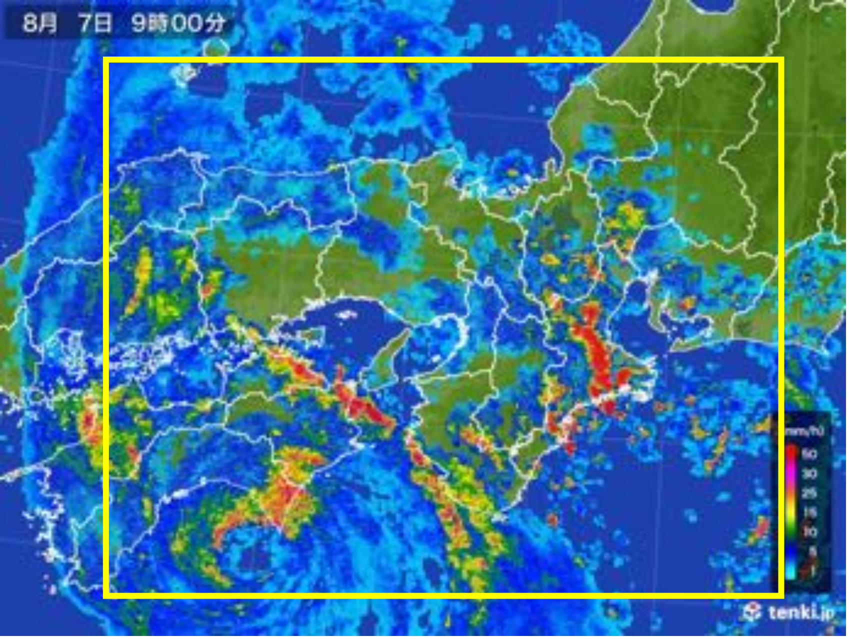

Precipitation

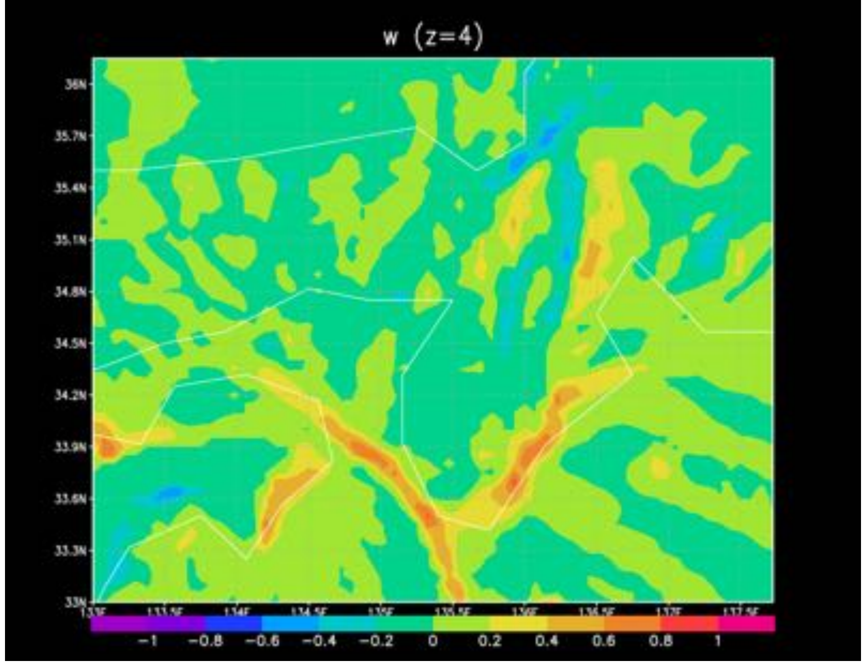

Amplitude of
Vertical velocity

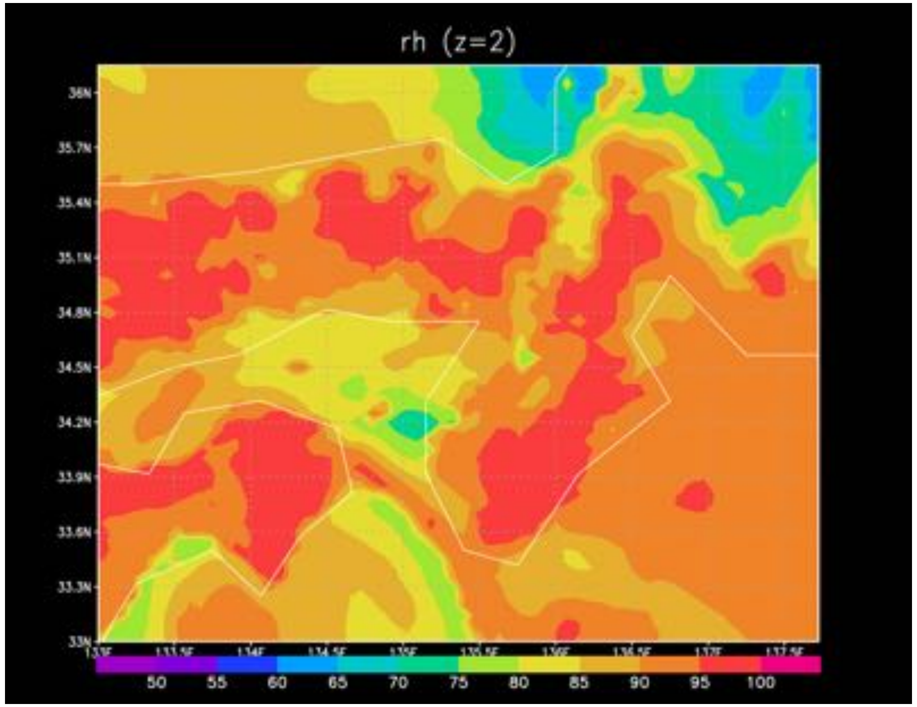

Vapor

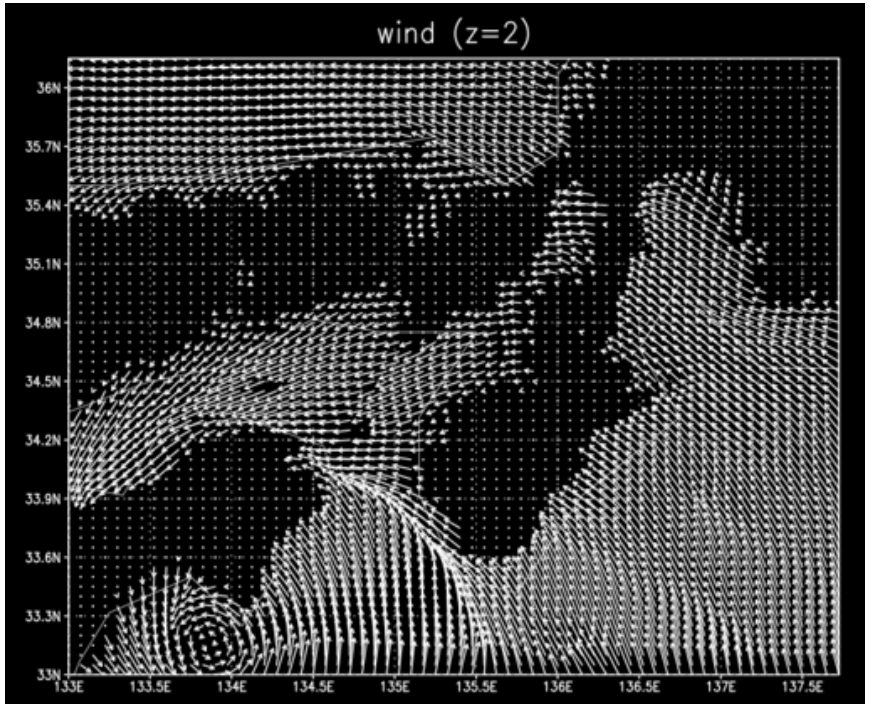

Horizontal
velocity

豊橋市“竜巻”電柱９本倒れる　ケガ人も

ツイートする　シェアする

2017年8月7日 22:28

Tornado in Toyohashi city
Nine power poles toppled　Injured people
(caused by Typhoon No. 5)

Overturned trucks

【台風５号上陸】あすは関東地方を通過か…今後の進路は？

要約

７日午後、愛知県豊橋市で、竜巻とみられる突風が発生し、トラックが横転するなどの被害が出た。市内では子どもなど３人がけがをしている。

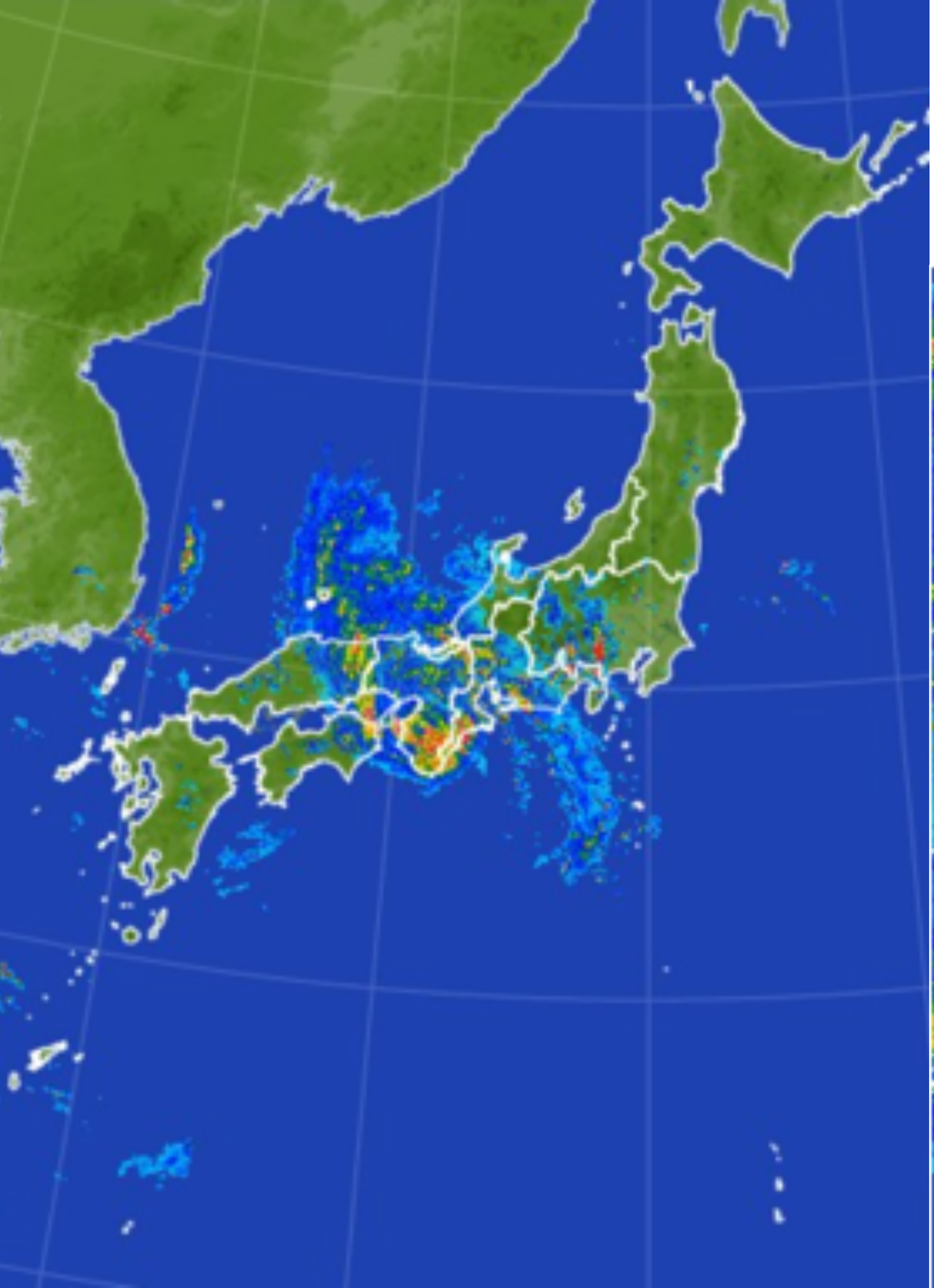

tenki.jp

https://tenki.jp/past/2017/08/07/radar/5/

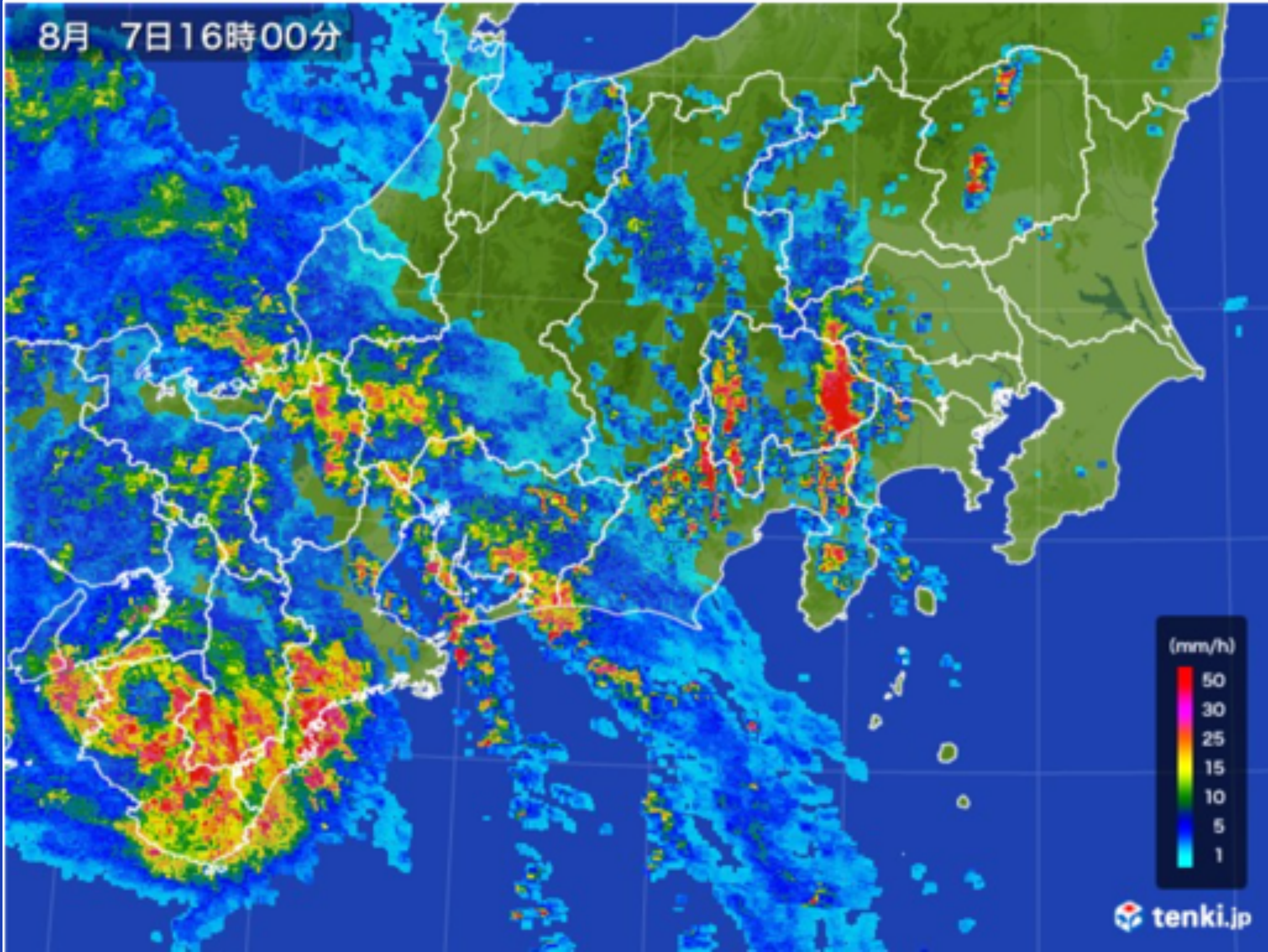

Summary

- We studied vortex cluster structures by visualizing the DNS data of high Re turbulence
  - Thin shear layer studied in detail in FTAC 2013 accompanies a large-scale tube-like low-pressure core
  - The structure is similar to double spirals observed in low Re turbulence (Kida & Miura 2000)
    - The spiral arm in low Re is a vortex layer
    - The spiral arm in high Re is the thin shear layer (a layer-like vortex cluster)
  - The lifetime of the significant layer is less than T.
- In a real geophysical flow, we observed a layer structure similar to that observed in the DNS. Analysis of the MSM data shows the following
    - Observed spiral rainband accompanies a shear layer
    - Generation of the tornado in Toyohashi may relate to the shear layer